

The levamisole-sensitive nicotinic acetylcholine receptor of the potato cyst-nematode *Globodera pallida*

Jessica Manichanh Catherine Marvin

Submitted in accordance with the requirements for the degree of Doctor of Philosophy

The University of Leeds
School of Biology
Faculty of Biological Sciences

September 2015

The candidate confirms that the work submitted is her own and that appropriate credit has been given where reference has been made to the work of others. This copy has been supplied on the understanding that it is copyright material and that no quotation from the thesis may be published without proper acknowledgment.

© 2015 The University of Leeds, Jessica Manichanh Catherine Marvin

Acknowledgements

I would like to thank Professor Urwin for his guidance and support throughout these years. His constant encouragement and feedback has been essential to complete this work, and I will always be grateful for that.

I'd like to thank Dr Catherine Lilley. The value of her impact on my practical work has been immeasurable, and I admire her dedication and attention to detail. I'm also very thankful for her unending patience and kindness.

Thanks to Dr Laura Jones for teaching me about all things worm-y. It's been a pleasure working with you.

I thank the members of the Southampton *C. elegans* Lab and the Electrophysiology lab in INRA, Tours for allowing me to conduct work there.

And thanks to everyone in the Urwin and Kepinski lab for providing such a warm work environment. Even during the long and difficult times of the PhD, I always looked forward to coming into work for the laughter and support. I'll never forget our many essential "extra-curricular" activities that took up far too much of our time and I'll certainly miss the cake!

I'd also like to thank my friends for our essential lunchtime nonsense, Friday drinks, and distracting gossip. It's been great to have such a lovely group of people to go through this with.

Thanks to my family, for always being supportive and understanding at all times. I love you all.

And finally, thanks to Chris for being with me throughout this, and dealing with my grumpiness and stress.

Abstract

The potato cyst nematode *Globodera pallida* costs the UK potato industry over £50 million per annum. In order to invade a host-plant, the infective J2 stage must hatch from eggs within the soil and migrate towards the root system.

Orthologues of *Caenorhabditis elegans* genes involved in neurotransmission were identified in the *G. pallida* and *G. rostochiensis* genome assemblies. The complement of cys-loop ligand-gated ion channel genes was distinct compared to *C. elegans* and other parasitic nematodes. Orthologues of genes encoding subunits which comprise the *C. elegans* levamisole-sensitive nicotinic acetylcholine receptor (*cel-lev-1*, *cel-lev-8*, *cel-unc-29*, *cel-unc-63* and *cel-unc-38*) were searched for, and *cel-lev-1* and *cel-lev-8* orthologues were absent in both *Globodera* spp. Two orthologues were identified for *cel-unc-29* and *cel-unc-38*. This suggested that the composition of the *G. pallida* L-nAChR may differ.

The use of *C. elegans* as a heterologous system to study the expression pattern of *G. pallida* nAChR genes was explored. GFP-expressing lines were created using promoter regions of *gpa-acr-2* and *gpa-unc-63*. Expression was observed in the ventral nerve cord and nerve ring for *pgpa-acr-2*. Expression of *pgpa-unc-63* was variable, but was found in the head and tail region and along the ventral side of the body.

The impact of this distinct complement of cys-loop subunits on anthelmintic sensitivity was demonstrated by the increased resistance of both *G. pallida* and *G. rostochiensis* J2s to levamisole. The EC₅₀ of *G. pallida* and *G. rostochiensis* was 19.7 mM and 5.6 mM respectively, compared to the EC₅₀ of 9 µM for *C. elegans*, representing a 500 – 2000 fold increase in levamisole resistance. This increased resistance to levamisole was associated with an orthologue of *cel-unc-38* identified in *G. pallida*, *gpa-unc-38.1*. Rescue of *C. elegans unc-38(x20)* mutants with *gpa-unc-38.1* restores normal movement suggesting a functional reconstitution of the L-nAChR, but full sensitivity to levamisole is not restored. *Gpa-unc-38.1* was expressed with the remaining four subunits from *C. elegans* in *Xenopus* oocytes to produce a chimeric receptor. The EC₅₀ of the response to acetylcholine and levamisole of the chimeric receptor and the native receptor was comparable and had similar opening responses to different agonists.

Chimeric genes were created to analyse key motifs in *gpa-unc-38.1* that may affect receptor function and levamisole sensitivity. *Gpa-unc-38.1* was necessary for structural reformation of the receptor, but not acetylcholine binding. Removal or addition of a loop B glutamate residue, previously associated with levamisole sensitivity of Cel-UNC-38, did not affect levamisole sensitivity of Cel-UNC-38 or Gpa-UNC-38.1. An amino acid change (I>M) in TM2 of Cel-UNC-38 increased levamisole sensitivity and basal thrashing rate. The reciprocal change (M>I) in Gpa-UNC-38.1 comprised basal

thrashing rescue. The basis of increased levamisole resistance of *gpa-unc-38.1* was not identified, as all *gpa-unc-38.1* chimeric genes retained a higher resistance to levamisole than *cel-unc-38*. This works reveals that the nAChRs of plant-parasitic nematodes have distinct pharmacological characteristics.

Table of contents

1. General Introduction	1
1.1 Nematode evolution and phylogeny.....	1
1.2 Plant-parasitic nematodes.....	3
1.2.1 Ectoparasites	3
1.2.1.1 Migratory	3
1.2.1.2 Sedentary	4
1.2.2 Semi-endoparasites	4
1.2.3 Endoparasites	4
1.2.3.1 Migratory	4
1.2.3.2 Sedentary	4
1.3 Root-knot nematodes	5
1.3.1 Agricultural impact and host range	5
1.3.2 Life-cycle of root-knot nematodes	5
1.3.2.1 Pre-invasion	5
1.3.2.2 Invasion and induction of giant cells.....	6
1.3.2.3 Root-knot nematode reproduction.....	7
1.4 Cyst nematodes	7
1.4.1 Agricultural impact and host range	7
1.4.2 Life-cycle of cyst nematodes.....	8
1.4.2.1 Pre-invasion	8
1.4.2.2 Invasion and induction of syncytia formation	8
1.4.2.3 Reproduction	9
1.5 The need for novel methods of control.....	11
1.5.1 Current social methods.....	11
1.5.2 Nematicide use is reduced	11
1.5.3 Use of resistant crops	11
1.6 <i>Caenorhabditis elegans</i>	12

1.6.1	Food-searching behaviours of <i>C. elegans</i>	12
1.6.2	The use of <i>C. elegans</i> as a model organism	14
1.6.2.1	<i>C. elegans</i> as a model for plant-parasitic nematodes	16
1.6.3	Aspects of the neurobiology of <i>C. elegans</i>	18
1.6.3.1	Musculature and locomotion.....	18
1.6.3.2	Acetylcholine.....	20
1.6.3.3	GABA	20
1.6.3.4	Glutamate	22
1.6.3.5	Serotonin.....	22
1.6.3.6	Dopamine.....	23
1.6.3.7	Octopamine.....	23
1.6.3.8	Tyramine	23
1.6.3.9	Neuropeptides	24
1.7	Cys-loop receptors	24
1.7.1	Cys-loop receptors and anthelmintic drugs	25
1.8	Known aspects of neurobiology in plant-parasitic nematodes.....	27
2.	General Materials and Methods.....	31
2.1	Maintenance of nematodes	31
2.1.1	Maintenance of <i>Globodera pallida</i> populations	31
2.1.2	Collection of cysts from infected soil	31
2.1.3	Hatching of cysts for collection of J2s	31
2.2	<i>C. elegans</i> strains	31
2.2.1	N2.....	31
2.2.2	ZZ20.....	32
2.2.3	DP38.....	32
2.2.4	Maintenance of <i>C. elegans</i> populations	32
2.2.5	Production of NGM-lite media plates.....	32
2.2.6	Cleaning contaminated <i>C. elegans</i> stocks.....	32

2.3	Bacterial strains	33
2.4	Growth media	33
2.4.1	LB media.....	33
2.4.2	SOB media	33
2.5	General solutions composition	33
2.5.1	TE buffer.....	33
2.5.2	M9 buffer	33
2.5.3	TB solution.....	34
2.5.4	DNA Extraction buffer.....	34
2.5.5	Standard DNA quantification	34
2.6	General molecular biology methods	34
2.6.1	Extraction of total RNA	34
2.6.2	Phenol:chloroform extraction of genomic DNA.....	34
2.6.3	Preparation of cDNA.....	35
2.6.4	Preparation of ultra-competent cells	35
2.6.5	Restriction digest.....	35
3.	Identification of orthologous genes from <i>Caenorhabditis elegans</i> in the <i>Globodera pallida</i> and <i>Globodera rostochiensis</i> genomes	36
3.1	Introduction.....	36
3.2	Materials and methods	39
3.2.1	Homology searching and cloning using the <i>Globodera pallida</i> genome assembly	39
3.2.2	Amplification and cloning	39
3.2.3	Quality control of sequences obtained	39
3.2.4	Analysis of transcriptome assembly and unassembled 454 reads	40
3.2.5	Homology searching in the <i>Globodera rostochiensis</i> genome	43

3.2.6	<i>C. elegans</i> sequence	43
3.2.7	Producing alignments and calculating amino acid identity	43
3.2.8	Signal peptide prediction	43
3.2.9	Transmembrane domain prediction.....	43
3.2.10	RaptorX 3D protein modelling	44
3.2.11	Phylogenetic trees	44
3.2.12	Bioassays	44
3.2.12.1	Application of exogenous serotonin to <i>G. pallida</i> J2s.....	44
3.2.12.2	Application of exogenous octopamine to <i>G. pallida</i> J2s.....	44
3.2.13	Product amplification by polymerase chain reaction and product isolation	46
3.2.13.1	Screening for working primer pairs.....	46
3.2.13.2	Gradient PCR for optimisation of amplification.....	46
3.2.13.3	Amplification of products for cloning	46
3.2.13.4	PCR clean-up	46
3.2.13.5	DNA isolation from agarose gel	48
3.2.14	Cloning and sequencing	48
3.2.14.1	A-tailing of PCR products	48
3.2.14.2	Cloning reaction	48
3.2.14.3	Transformation	48
3.2.14.4	Screening of colonies by Colony PCR	48
3.2.14.5	Plasmid preparations	50
3.2.14.6	Sequencing of plasmid inserts	50
3.3	Results.....	51
3.3.1	Acetylcholine genes – metabolism and synthesis.....	51
3.3.1.1	<i>Cel-cha-1</i>	51
3.3.1.2	<i>Cel-unc-17</i>	51
3.3.2	Acetylcholine genes – receptor subunits.....	55
3.3.3	Glutamate genes – synthesis and metabolism	55
3.3.3.1	<i>Cel-eat-4</i>	55

3.3.4 Orthologues of <i>C. elegans</i> glutamate-gated chloride channel subunit genes	55
3.3.4.1 <i>Cel-glc-1</i>	55
3.3.4.2 <i>Cel-glc-2</i>	55
3.3.4.3 <i>Cel-glc-3</i>	56
3.3.4.4 <i>Cel-glc-4</i>	56
3.3.4.5 <i>Cel-avr-14</i>	56
3.3.4.6 <i>Cel-avr-15</i>	57
3.3.4.7 Phylogenetic relationship of cloned subunits of glutamate-gated chloride channels	57
3.3.5 Orthologues of <i>C. elegans</i> genes involved in serotonin synthesis and metabolism	71
3.3.5.1 <i>Cel-tph-1</i>	71
3.3.5.2 <i>Cel-ser-7</i>	71
3.3.5.3 <i>Cel-mod-5</i>	71
3.3.6 Orthologues of <i>C. elegans</i> genes involved in GABA synthesis	72
3.3.6.1 <i>Cel-unc-25</i>	72
3.3.7 Genes involved in dopamine metabolism	72
3.3.7.1 <i>Cel-dat-1</i>	72
3.3.8 Orthologues of <i>C. elegans</i> genes involved in octopamine synthesis	72
3.3.8.1 <i>Cel-tbh-1</i>	72
3.3.9 Expression analysis of identified orthologues at different life-stages of <i>G. pallida</i>	73
3.4 Discussion.....	82
3.4.1 Quality of bioinformatic data sources must be assessed to determine confidence in results	82
3.4.2 Key neurotransmitter synthesis genes are present in the <i>G. pallida</i> and <i>G. rostochiensis</i> genome	83
3.4.3 Some orthologues of <i>C. elegans</i> genes encoding glutamate-gated chloride channels can be found in the <i>G. pallida</i> and <i>G. rostochiensis</i> genomes.....	85
3.4.3.1 Differences in the complement of glutamate-gated chloride channels may affect ivermectin targets.....	86

3.4.4 Gene expression analysis highlights importance of neurotransmitter-related genes at motile life-stages or stages which must respond to hosts	88
3.4.5 Confidence in orthology.....	88
3.4.6 Identification of isoforms.....	89
4. Identification of <i>Globodera pallida</i> orthologues of <i>Caenorhabditis elegans</i> genes that encode nicotinic acetylcholine receptor subunits ...	91
4.1 Introduction.....	91
4.1.1 The structure and function of nAChRs	91
4.1.2 The neuromuscular system is a target for novel anthelmintic discovery	93
4.1.3 Expression analysis and transformation by bombardment.....	93
4.2 Materials and methods	98
4.2.1 Identification of orthologues for other nematodes	98
4.2.2 Analysis of GFP expression regulated by nAChR promoters from <i>G. pallida</i>	98
4.2.2.1 Production of expression vector.....	98
4.2.2.2 Cloning of promoter regions from gDNA	98
4.2.2.3 Production of expression clone	99
4.2.2.4 Gold particle preparation.....	99
4.2.2.5 Preparation of plasmid for bombardment.....	99
4.2.2.6 Preparation of <i>unc-119</i> cultures	100
4.2.2.7 Growth of HB101 as food source for liquid culture	100
4.2.2.8 Microparticle bombardment of <i>unc-119(ed3)</i>	100
4.2.2.9 Selection of positive transformants.....	101
4.2.2.10 Visualization and photography of GFP expression	101
4.3 Results.....	105
4.3.1 Complement of all known nicotinic acetylcholine receptors in <i>G. rostochiensis</i> and <i>G. pallida</i>	105
4.3.2 Orthologues of components of the levamisole-sensitive nicotinic acetylcholine receptor of <i>C. elegans</i>	105
4.3.2.1 Orthologues of <i>cel-lev-1</i> and <i>cel-lev-8</i> could not be identified.....	105

4.3.2.2	Two orthologues of Cel-UNC-29 are present.....	105
4.3.2.3	An orthologue of <i>cel-unc-63</i> is present.....	106
4.3.2.4	Two orthologues of Cel-UNC-38 are present both with differences in key residues	107
4.3.3	The UNC-29 group of nAChR subunits.....	107
4.3.3.1	The <i>acr-2 acr-3</i> operon structure is an example of synteny between the <i>C. elegans</i> , <i>G. pallida</i> and <i>G. rostochiensis</i> genome	108
4.3.3.2	The orthologue of <i>cel-acr-2</i> is present as a full-length gene	108
4.3.3.3	Orthologue of Cel-ACR-3 may lack a signal peptide	108
4.3.4	The UNC-38 group of nAChRs	109
4.3.5	The ACR-8 group of nAChRs	109
4.3.5.1	Orthologues of Cel-ACR-8 and Cel-ACR-12 are present.....	109
4.3.6	nAChR subunit genes are most highly expressed at life stages involved in locomotion or host-sensing.....	109
4.3.7	Phylogeny of genes and in the UNC-38, UNC-29 and ACR-8 groups.....	110
4.3.8	Promoters of nAChRs from <i>G. pallida</i> are functional in <i>C. elegans</i>	110
4.4	Discussion.....	131
4.4.1	<i>G. pallida</i> and <i>G. rostochiensis</i> have fewer members of the ACR-16 group	131
4.4.2	The levamisole-sensitive nicotinic acetylcholine (L-nAChR) receptor of <i>G. pallida</i> and <i>G. rostochiensis</i> is likely to differ from that of <i>C. elegans</i>	131
4.4.2.1	Gpa-ACR-8 is a candidate to replace LEV-8 in the native <i>G. pallida</i> receptor	131
4.4.2.2	Several candidates may replace LEV-1.....	132
4.4.2.3	Gpa-UNC-63 may play an altered role	133
4.4.2.4	Gpa-UNC-29.1 is a good orthologue of Cel-UNC-29, but Gpa-UNC-29.2 may not be functional.....	133
4.4.2.5	Gpa-UNC-38.1 and Gpa-UNC-38.2 lack important determinants of an α -subunit.....	134
4.4.2.6	UNC-38 orthologues in other plant-parasitic nematodes share the same features	135
4.4.3	The TM3-TM4 intracellular loop is generally larger in orthologues identified in plant-parasitic nematodes than in <i>C. elegans</i>	136

4.4.4	Work in other parasitic nematodes can provide insight for potential stoichiometries of the <i>G. pallida</i> receptor	136
4.4.5	The <i>cel-acr-2 cel-acr-3</i> operon found in <i>C. elegans</i> appears to be conserved in <i>G. pallida</i> , but may include <i>gpa-unc-29.1</i>	137
4.4.6	Phylogenetic relations of subunits show that orthologues are the best identified, despite differences in sequence	138
4.4.7	<i>C. elegans</i> as a heterologous system for analysis of <i>G. pallida</i> promoter activity using GFP transcriptional fusions	138
5.	Characterisation of the effect of levamisole in <i>Globodera pallida</i> and <i>Globodera rostochiensis</i>	144
5.1	Introduction.....	144
5.1.1	Determining the effect of levamisole on <i>G. pallida</i> and <i>G. rostochiensis</i> J2s	144
5.1.2	Use of transgenic <i>C. elegans</i> to investigate endogenous genes of <i>G. pallida</i>	144
5.1.3	<i>Xenopus</i> oocytes as a heterologous expression system for investigation of ion channels and receptors	145
5.2	Materials and methods	149
5.2.1	Assessment of effect of levamisole on <i>G. pallida</i> and <i>G. rostochiensis</i> J2s..	149
5.2.1.1	Production of levamisole treatment plates	149
5.2.1.2	Assessment of average speed.....	149
5.2.1.3	Assessment of shrinkage at 2 hours over a range of levamisole concentrations	149
5.2.1.4	Assessment of shrinkage over 20 minutes in response to a high dose of levamisole	151
5.2.1.5	Assessment of shrinkage over 24 hours in response to a low dose of levamisole	151
5.2.2	Heterologous expression of <i>Gpa-unc-38.1</i> in <i>C. elegans</i>	151
5.2.2.1	Production of the <i>Gpa-unc-38</i> and <i>Cel-unc-38</i> line.....	151
5.2.3	Selection of <i>C. elegans</i> worms for use in thrashing assays	151
5.2.3.1	Thrashing assays	152

5.2.4 Expression of <i>gpa-unc-38.1</i> to replace <i>cel-unc-38</i> in the <i>C. elegans</i> receptor in <i>Xenopus</i> oocytes	152
5.2.4.1 Subcloning of <i>gpa-unc-38.1</i> into the oocyte expression vector pTB207	152
5.2.4.2 Preparation of vector for cRNA transcription	152
5.2.4.3 Preparation of cRNAs for injection into <i>Xenopus</i> oocytes	155
5.2.4.4 Preparation of injection mixes	155
5.2.4.5 Storage and preparation of <i>Xenopus</i> oocytes prior to injection	155
5.2.4.6 Injection of <i>Xenopus</i> oocytes with cRNA injection mixture	155
5.2.4.7 Voltage-clamp recordings from injected oocytes	156
5.3 Results.....	158
5.3.1 <i>G. pallida</i> J2s have higher resistance to levamisole than <i>C. elegans</i>	158
5.3.2 <i>G. rostochiensis</i> J2s are less resistant to levamisole than <i>G. pallida</i> , but are more resistant than <i>C. elegans</i>	158
5.3.3 Levamisole induces shrinkage of <i>G. pallida</i> J2s.....	158
5.3.4 Levamisole induces shrinkage of <i>G. rostochiensis</i> J2s.....	158
5.3.5 Treatment of <i>G. pallida</i> J2s with high concentration of levamisole induces shrinkage within a short time period.....	158
5.3.6 Treatment of <i>G. pallida</i> J2s with low concentration of levamisole does not induce shrinkage over 24 hours	159
5.3.7 Gpa-UNC-38.1 is able to rescue the basal thrashing rate of <i>C. elegans unc-38(x20)</i> mutants, but not full sensitivity to levamisole.....	159
5.3.8 Expression of <i>gpa-unc-38.1</i> with <i>C. elegans</i> subunits to produce a chimeric receptor does not alter response to levamisole compared to the native <i>C. elegans</i> receptor	160
5.3.9 Expression of <i>gpa-unc-38.1</i> with <i>C. elegans</i> subunits demonstrates the same pharmacology as the native <i>C. elegans</i> receptor	160
5.4 Discussion.....	174
5.4.1 <i>G. pallida</i> and <i>G. rostochiensis</i> J2s are more resistant to levamisole than <i>C. elegans</i>	174
5.4.2 Analysis of <i>gpa-unc-38.1</i> -rescued <i>C. elegans</i> line suggests <i>gpa-unc-38.1</i> is likely to play a role in this increased resistance	175

5.4.3 Expression of <i>gpa-unc-38.1</i> to replace <i>cel-unc-38</i> in <i>Xenopus</i> oocytes does not support a difference in levamisole binding for <i>gpa-unc-38.1</i>	176
6. Investigation into the significance of key amino acid motif differences between Cel-UNC-38 and Gpa-UNC-38.1	181
6.1 Introduction.....	181
6.1.1 Transformation of <i>C. elegans</i> by microinjection	181
6.1.2 Fate of DNA introduced by microinjection	181
6.1.3 Choice of marker gene.....	182
6.1.4 The use of <i>C. elegans</i> to analyse <i>cel-unc-38</i> and <i>gpa-unc-38.1</i> chimeric genes	183
6.2 Materials and methods	185
6.2.1 Production of chimeric <i>unc-38</i> coding sequences by Spliced Overlap Extension	185
6.2.2 Generation and transformation of constructs.....	185
6.2.3 Preparation of other materials for microinjection.....	186
6.2.4 Production of injection mixture	186
6.2.5 Transformation of <i>C. elegans</i> by microinjection	186
6.2.6 Maintenance of transformed stable lines	187
6.2.7 Analysis of mutant lines rescued by chimeric genes.....	187
6.3 Results.....	194
6.3.1 The YxxCC motif involved in acetylcholine binding.....	194
6.3.1.1 Addition of the YxxCC motif to <i>Gpa-unc-38.1</i> does not affect ability of chimeric genes to rescue basal thrashing or levamisole sensitivity	194
6.3.1.2 Removal of the YxxCC motif from <i>cel-unc-38</i> does not affect ability of chimeric genes to rescue basal thrashing, or affect sensitivity to levamisole.....	195
6.3.2 Investigation into the effect of a glutamate residue in loop B, which may be involved in levamisole sensitivity.....	195
6.3.2.1 Introduction of a glutamate residue in loop B of <i>gpa-unc-38.1</i> does not affect ability of chimeric genes to rescue basal thrashing and does not affect levamisole sensitivity	195

6.3.2.2 Removal of a glutamate residue from loop B of <i>cel-unc-38</i> does not affect ability of chimeric genes to rescue basal thrashing and does not affect levamisole sensitivity	196
6.3.3 Investigation into a single amino acid residue change in transmembrane domain 2 which may affect channel opening properties and levamisole sensitivity.	197
6.3.3.1 A methionine to isoleucine change in the TM2 domain of <i>gpa-unc-38.1</i> affects the ability of the chimeric gene to rescue basal thrashing, but not levamisole sensitivity	197
6.3.3.2 An isoleucine to methionine change in <i>cel-unc-38</i> increases basal thrashing rate and increases levamisole sensitivity.....	198
6.4 Discussion.....	218
6.4.1 Considerations involved in working with transgenic lines of <i>C. elegans</i>	218
6.4.2 Limitations of thrashing assay analysis.....	219
6.4.3 The YxxCC motif is non-essential in both Gpa-UNC-38.1 and Cel-UNC-38 to basal thrashing function of the reconstituted receptor	219
6.4.4 The glutamate residue in loop B of Cel-UNC-38 may not be involved in levamisole sensitivity	220
6.4.5 Amino acid changes in transmembrane domain 2 affect channel opening properties in response to agonist binding	222
6.4.6 The basis of levamisole resistance for Gpa-UNC-38.1 has not been established.....	223
6.4.6.1 Cel-UNC-38 has been defined as an α -subunit, but may not be directly involved in agonist binding	224
7. GENERAL DISCUSSION	229
7.1 Host-seeking is a common and essential behaviour for plant-parasitic nematodes.....	229
7.2 Differences in complement of cys-loop receptors indicate that <i>G. pallida</i> and <i>G. rostochiensis</i> may have distinct pharmacological neuromuscular targets.....	229
7.3 Bioassays and functional experimentation supported a difference in resistance to levamisole and linked it to <i>Gpa-unc-38.1</i>	231
7.4 Motif swaps between <i>Cel-unc-38</i> and <i>Gpa-unc-38.1</i> did not elucidate the basis of levamisole resistance of <i>G. pallida</i>	231

7.5 The levamisole resistance of <i>G. pallida</i>	232
7.5.1 The whole native <i>G. pallida</i> receptor must be considered	232
7.5.2 Other genes that are not nAChRs have also been associated with levamisole resistance	233
7.5.3 Mechanisms of levamisole resistance in animal-parasitic nematodes..	234
7.6 Cys-loop receptors are a diverse class and are the target of many antihelmintics and antiparasitics.....	235
7.7 Alternate splicing and RNA editing further increase diversity of nAChRs ..	236
7.7.1 RNA editing.....	236
7.7.2 Alternate splicing.....	236
7.8 Specificity is key in drug design	237
7.9 <i>C. elegans</i> as a model for plant-parasitic nematodes	238
7.10 Duplications and deletions of cys-loop receptor subunits is common throughout the phylum Nematoda, and leads to the diversity of subunits found	238
7.11 Further directions	240
7.11.1 Further work on nAChRs	240
7.11.2 Further work on other cys-loop receptor members and neurotransmitter synthesis genes	241
7.11.3 Further aspects of gene regulation to be considered	242
7.12 The cys-loop ligand-gated ion channel gene family is a source of potential targets for antihelmintic design	242
8. References	247

List of Figures

Figure 1-1: Cladogram of inferred relationships in the phylum Nematoda	2
Figure 1-2: Life cycle of a cyst nematode.....	10
Figure 1-3: Life-cycle of the <i>C. elegans</i> hermaphrodite at 22 °C.....	13
Figure 1-4: Generation of sinusoidal locomotion in <i>C. elegans</i>	19
Figure 1-5: Schematic of mechanism of acetylcholine release.....	21
Figure 1-6: Schematic of cys-loop receptor subunit structure	26
Figure 3-1: Examples of positive and negative signal peptide prediction outputs generated by SignalP v4.1	45
Figure 3-2: Selection of optimum annealing temperature by gradient PCR	47
Figure 3-3: Vector map of pCR™8/GW/TOPO®	49
Figure 3-4: Amino acid alignment of Cel-CHA-1 with Gpa-CHA-1 and Gro-CHA-1	52
Figure 3-5: Alignment of Cel-UNC-17 with Gpa-UNC-17 and Gro-UNC-17.....	53
Figure 3-6: Structure of <i>unc-17 cha-1</i> operon in <i>C. elegans</i> and <i>G. rostochiensis</i>	54
Figure 3-7: Alignment of Cel-EAT-4 with Gpa-EAT-4 and Gro-EAT-4	58
Figure 3-8: Schematic of residues involved in ivermectin binding identified from X-ray crystal structure.....	59
Figure 3-9: Alignment of Cel-GLC-2 with Gpa-GLC-2 and Gro-GLC-2	61
Figure 3-10: Output from TMHMM prediction server for Cel-GLC-2, Gpa-GLC-2 and Gro-GLC-2	62
Figure 3-11: 3D model of Cel-GLC-2 and Gpa-GLC-2	63
Figure 3-12 : Alignment of Cel-GLC-3 with Gpa-GLC-3 and Gro-GLC-3	64
Figure 3-13: Alignment of predicted amino acid sequence of Cel-GLC-4 with Gpa-GLC-4 and Gro-GLC-4	65
Figure 3-14: Alignment of Cel-AVR-14a with Gpa-AVR-14.1 and Gpa-AVR-14.2	66
Figure 3-15: Alignment of Cel-AVR-14 (isoform a) with Gpa-AVR-14.1 and Gro-AVR-14.1.....	67

Figure 3-16: Alignment of Cel-AVR-14 (isoform a) with Gpa-AVR-14.2 and Gro-AVR-14.2	68
Figure 3-17: 3D models of Cel-AVR-14a, Gpa-AVR-14.1 and Gpa-AVR-14.2	69
Figure 3-18: Phylogeny of glutamate-gated chloride channel subunits identified from <i>G. pallida</i> and <i>G. rostochiensis</i> with <i>C. elegans</i> subunits.....	70
Figure 3-19: Alignment of Cel-TPH-1 with Gpa-TPH-1 and Gro-TPH-1.....	74
Figure 3-20 : Alignment of Cel-SER-7 (isoform b) with Gpa-SER-7 and Gro-SER-7	75
Figure 3-21: Application of exogenous neurotransmitters to <i>G. pallida</i> J2s	76
Figure 3-22: Alignment of Cel-MOD-5 with Gpa-MOD-5 and Gro-MOD-5.....	77
Figure 3-23: Alignment of Cel-UNC-25 with Gpa-UNC-25 and Gro-UNC-25.....	78
Figure 3-24: Alignment of Cel-DAT-1 with Gpa-DAT-1 and Gro-DAT-1	79
Figure 3-25: Alignment of Cel-TBH-1 with predicted amino acid sequence of Gpa-TBH-1 and Gro-TBH-1.....	80
Figure 3-26: Expression of transcripts for identified orthologues over the life-stages of <i>G. pallida</i>	81
Figure 4-1: Schematics of the levamisole-sensitive nicotinic acetylcholine receptor of <i>C. elegans</i>	96
Figure 4-2: Vector map of pGFPexpress	104
Figure 4-3: Alignment of Cel-UNC-29 with Gpa-UNC-29.1 and Gpa-UNC-29.2	113
Figure 4-4: Alignment of Cel-UNC-29 with Gpa-UNC-29.1 and Gro-UNC-29.1.....	114
Figure 4-5: Alignment of Cel-UNC-29 with Gpa-UNC-29.2 and Gro-UNC-29.2.....	115
Figure 4-6: Alignment of Cel-UNC-63 with Gpa-UNC-63 and Gro-UNC-63.....	116
Figure 4-7: Alignment of Cel-UNC-38 with Gpa-UNC-38.1 and Gp-UNC-38.2	117
Figure 4-8: Alignments of Cel-UNC-38 with Gro-UNC-38.1 and Gro-UNC-38.1.....	118
Figure 4-9: Alignments of Cel-UNC-38 with Gpa-UNC-38.2 and Gro-UNC-38.2	119
Figure 4-10: Schematics of the <i>acr-2 acr-3</i> operon in <i>C. elegans</i> and <i>G. pallida</i>	120
Figure 4-11: Alignment of Cel-ACR-2 with Gpa-ACR-2 and Gro-ACR-2	121
Figure 4-12: Alignment of Cel-ACR-3 with Gpa-ACR-3 and Gro-ACR-3	122

Figure 4-13: Alignment of Cel-ACR-6 with Gpa-ACR-6 and Gro-ACR-6	123
Figure 4-14: Alignment of Cel-ACR-8 with Gpa-ACR-8 and Gro-ACR-8	124
Figure 4-15: Alignments of Cel-ACR-12 with Gpa-ACR-12 and Gro-ACR-12	125
Figure 4-16: Phylogenetic tree of relationship between <i>C. elegans</i> , <i>G. pallida</i> and <i>G. rostochiensis</i> nAChR subunits of the UNC-38, UNC-29 and ACR-8 groups.....	126
Figure 4-17: Expression levels of transcripts for identified orthologues of <i>C. elegans</i> genes from the UNC-38, UNC-29 and ACR-8 groups over the life-stages of <i>G. pallida</i>	127
Figure 4-18: Auto-fluorescence of gut granules in N2 worms	128
Figure 4-19: GFP expression of pgpa-acr-2 GFP reporter construct	129
Figure 4-20: GFP expression of pgpa-unc-63 GFP reporter construct	130
Figure 4-21: Phylogenetic tree of relationship between paralogues of UNC-29 identified in <i>G. pallida</i> , <i>G. rostochiensis</i> , <i>H. contortus</i> and <i>C. elegans</i>	140
Figure 4-22: Loops A-C and transmembrane domain 2 of UNC-38 in plant-parasitic nematodes compared to <i>C. elegans</i> , animal-parasitic nematodes and the mouse α -subunit	141
Figure 4-23: Stoichiometries of L-nAChRs in animal-parasitic nematodes deduced by expression in <i>Xenopus</i> oocytes and a starting model for the native <i>G. pallida</i> receptor	142
Figure 5-1: Chemical structure of levamisole	147
Figure 5-2: Image processing steps to determine average speed of <i>G. pallida</i> and <i>G. rostochiensis</i> J2s	150
Figure 5-3: Schematic of a single <i>C. elegans</i> thrash in liquid	154
Figure 5-4: Vector map of pTB207.....	157
Figure 5-5: Effect of levamisole on <i>Globodera pallida</i> J2s	162
Figure 5-6: Effect of levamisole on <i>Globodera rostochiensis</i> J2s	163
Figure 5-7: Effect of a range of levamisole concentrations on J2 length after 2 hours exposure.....	164
Figure 5-8: Effect of high doses of levamisole on <i>G. pallida</i> J2s	165
Figure 5-9: Effect of a low dose of levamisole after 24 hour exposure.....	166

Figure 5-10: Effect of 10 µM levamisole on thrashing rate of <i>C. elegans</i>	167
Figure 5-11: Effect of 50 µM levamisole on thrashing rate of <i>C. elegans</i>	168
Figure 5-12: Effect of 100 µM levamisole on thrashing rate of <i>C. elegans</i>	169
Figure 5-13: Comparison between the lines of thrashing rate after 30 mins exposure to the range of levamisole concentrations	170
Figure 5-14: Dose-response curve for acetylcholine and levamisole on the native and chimeric L-type nAChR receptors	171
Figure 5-15: Examples of current recordings for the full range of concentrations of acetylcholine and levamisole for the native and chimeric L-type nAChR expressed in <i>Xenopus</i> oocytes.....	172
Figure 5-16: Response of the native and chimeric L-type nAChR in response to a panel of nicotinic acetylcholine receptor agonists	173
Figure 5-17: Potential changes caused in acetylcholine binding sites on the L-type nAChR caused by substituting Gpa-UNC-38.1 on different conformations of the native <i>C. elegans</i> receptor	179
Figure 6-1: Schematic of chimeric genes produced by Spliced Overlap Extension	188
Figure 6-2: Schematic of Spliced Overlap Extension PCRs	190
Figure 6-3: Products of Spliced Overlap Extension visualised by agarose gel electrophoresis.....	191
Figure 6-4: Example of suitable hermaphrodite for microinjection and marker gene for selection of transformants	192
Figure 6-5: Vector map of pDEST-myo3.....	193
Figure 6-6: Thrashing rate after 30 mins exposure to a range of levamisole concentrations for <i>Gpa-unc-38.1-H236_I234delinsNYPSCCPGSA</i>	200
Figure 6-7: Effect of 50 µM levamisole on thrashing rate of <i>Gpa-unc-38.1-H236_I234delinsNYPSCCPGSA</i>	201
Figure 6-8: Effect of 100 µM levamisole on thrashing rate of <i>Gpa-unc-38.1-H236_I234delinsNYPSCCPGSA</i>	202
Figure 6-9: Thrashing rate after 30 mins exposure to a range of levamisole concentrations for <i>Cel-unc-38-N234_I242delinsHFFASKNGI</i>	203

Figure 6-10: Effect of 50 μ M levamisole on thrashing rate of <i>Cel-unc-38-N234_I242delinsHFFASKNGI</i>	204
Figure 6-11: Effect of 100 μ M levamisole on thrashing rate of <i>Cel-unc-38-N234_I242delinsHFFASKNGI</i>	205
Figure 6-12: Thrashing rate after 30 mins exposure to a range of levamisole concentrations for <i>Gpa-unc-38.1-Y175_G178delinsFSEN</i>	206
Figure 6-13: Effect of 50 μ M levamisole on thrashing rate of <i>Gpa-unc-38.1-Y175_G178delinsFSEN</i>	207
Figure 6-14: Effect of 100 μ M levamisole on thrashing rate of <i>Gpa-unc-38.1-Y175_G178delinsFSEN</i>	208
Figure 6-15: Thrashing rate after 30 mins exposure over a range of levamisole concentrations for <i>Cel-unc-38-F174_N177delinsYPSG</i>	209
Figure 6-16: Effect of 50 μ M levamisole on thrashing rate of <i>Cel-unc-38-F174_N177delinsYPSG</i>	210
Figure 6-17: Effect of 100 μ M levamisole on thrashing rate of <i>Cel-unc-38-F174_N177delinsYPSG</i>	211
Figure 6-18: Thrashing rate after 30 mins exposure over a range of levamisole concentrations for <i>Gpa-unc-38.1-M302I</i>	212
Figure 6-19: Effect of 50 μ M levamisole on thrashing rate of <i>Gpa-unc-38.1-M302I</i>	213
Figure 6-20: Effect of 100 μ M levamisole on thrashing rate of <i>Gpa-unc-38.1-M302I</i> . ..	214
Figure 6-21: Thrashing rate at 30 mins over a range of levamisole concentrations for <i>Cel-unc-38-I301M</i>	215
Figure 6-22: Effect of 10 μ M levamisole on thrashing rate of <i>Cel-unc-38-I301M</i>	216
Figure 6-23: Effect of 50 μ M levamisole on thrashing rate of <i>Cel-unc-38-I301M</i>	217
Figure 6-24: Schematic of potential effects of addition or removal of the YxxCC motif from <i>gpa-unc-38.1</i> or <i>cel-unc-38</i>	226
Figure 6-25: Schematics of the transmembrane 2 (TM2) region of nAChR subunits ..	227
Figure 7-1: Maximum Likelihood tree of nAChRs and Glutamate-gated chloride channels associated with anthelmintic sensitivity from <i>C. elegans</i> , <i>H. contortus</i> , <i>O. dentatum</i> , <i>A. suum</i> , <i>B. malayi</i> and <i>G. pallida</i> . ..	246

List of tables

Table 1: Summary of <i>C. elegans</i> genes and their roles searched for in initial orthology search.....	41
Table 2: Primers used to amplify full-length products from <i>G. pallida</i> (unless otherwise specified)	42
Table 3: Summary of features of orthologues of glutamate-gated chloride channel subunits cloned from <i>G. pallida</i> and identified in <i>G. rostochiensis</i>	60
Table 4: Summary of nAChR subunits in <i>C. elegans</i>	95
Table 5: Primers used for amplification of nAChR subunit-encoding genes	102
Table 6: Sources for amino acid sequence for subunits of nAChRs identified in other nematode species.....	103
Table 7: Summary of orthologues of <i>C. elegans</i> nAChR genes identified in <i>G. pallida</i> and <i>G. rostochiensis</i>	112
Table 8: Primers used for Spliced Overlap Extension PCRs	189
Table 9: Examples of drugs targeting cys-loop receptors.....	243
Table 10: Complement of genes encoding members of nAChR subunits and glutamate-gated chloride channel subunits in different nematode species.....	244

List of abbreviations

ANOVA	Analysis of variance
µg	micro gram
µm	micro metre
3' UTR	3 prime untranslated region
5-HT	5-hydroxytryptamine
Ach	acetylcholine
ARS	Area Restricted Search
BLAST	Basic Local Alignment Search Tool
BLOSUM62	Block Substitution Matrix
bp	base pairs
RBH	Reciprocal Best hit
CDNA	coding deoxyribonucleic acid
CGC	Caenorhabditis Genetics Center
CO ₂	Carbon Dioxide
°C	Degrees in centigrade
DMSO	Dimethyl sulfoxide
DNA	Deoxyribonucleic acid
dNTP	Deoxynucleotide
Dpi	Days post infection
EC ₅₀	Dose required for 50% of population to be affected by a drug
EMS	Ethyl methanesulfonate
GABA	gamma-Aminobutyric acid
GFP	Green Fluorescent Protein
GPCR	G-Protein Coupled Receptor
iGluR	ionotropic glutamate receptor
J2	Second stage juvenile
J3	Third Stage Juvenile

J4	Fourth Stage Juvenile
kb	kilobase
LB	Lysogeny broth
LGIC	Ligand-gated ion channel
L-nAChR	levamisole-sensitive nicotinic acetylcholine receptor
Mb	megabase
mg	milligram
mins	minutes
ml	millilitres
mM	millimolar
mm	millimetre
mRNA	Messenger ribonucleic acid
nAChR	Nicotinic acetylcholine receptor
NCBI	National Center for Biotechnology Information
NGM	Nematode Growth Media
N-nAChR	nicotine-sensitive nicotinic acetylcholine receptor
ORF	Open reading frame
PCN	potato cyst nematode
PCR	Polymerase chain reaction
PhyML	Maximum Likelihood Phylogeny
PPN	plant-parasitic nematode
RKN	Root Knot Nematode
RNA	Ribonucleic acid
RNA-Seq	RNA sequencing
RPKM	Reads per kilobase per million
rpm	rotations per minute
s	seconds
SEM	Standard Error of the Mean

SOE	Spliced Overlap Extension
SSU rDNA	small-subunit ribosomal DNA
TM	Transmembrane
TMHMM	Transmembrane Hidden Markov Model
μ g	microgram
WTSI	Wellcome Trust Sanger Institute
YFP	Yellow Fluorescent protein

1. General Introduction

Nematodes are roundworms, characterised by their bilateral symmetry and unsegmented body. The phylum Nematoda is large and includes members with diverse morphologies, life-styles, and habitats. More than 23,000 individual species of nematodes have been described (Blaxter 2011), yet it is estimated that the total number of nematode species may be over a million with a large number of these unidentified species present in marine environments (Lambshead and Boucher 2003). The longest known species of nematode *Placenta gigantissima* parasitises the placenta of sperm whales, and can grow to a length of over 8 metres (Gubanov 1951) while the smallest is a marine nematode only 0.08 mm long (Groombridge 1992). Free-living species can feed on bacteria, fungi or other nematodes in the soil and parasitic species are able to parasitise plants, animals or insects. They may inhabit terrestrial or aquatic environments and be able to endure freezing (Wharton and Block 1993), desiccation (Freckman, Mankau and Ferris 1975) or long periods of starvation (Golden and Riddle 1984).

1.1 Nematode evolution and phylogeny

Nematodes are an ancient class of organism. Due to their soft bodies, the age of the nematode phylum is not easy to determine as fossil records are not common. Nevertheless, there is some fossil evidence that dates nematodes as being present 470 million years ago (Baliński, Sun and Dzik 2013) and they are believed to have first appeared during the “Cambrian Explosion” that occurred 600-550 million years ago. Understanding the phylogenetic relationship amongst nematodes to each other is complex, although as increasing amounts of DNA sequencing data have been made available in the last few years, multiple phylogenetic relationships have been drawn (Blaxter *et al.* 1998; Holterman *et al.* 2006; van Megen *et al.* 2009).

These phylogenetic trees support three main subdivisions of the phylum Nematoda, the Enoplia, Dorylaimida and Chromadorea (Figure 1-1). In the most recent phylogenetic trees (Holterman *et al.* 2006; van Megen *et al.* 2009) full-length SSU rDNA sequences from nematodes throughout the phylum were used to generate a phylogenetic tree which hypothesises the further division of these subdivisions into 12 clades.

The Enoplia consist of clade 1, and are predicted to be the most basal of the clades (Holterman *et al.* 2006). Many members of this clade are marine nematodes, although some freshwater nematodes are found here. There are a few examples of ectoparasitic plant-parasitic nematode species. The Dorylaimida comprise clade 2 and contain freshwater and terrestrial nematodes. Some ectoparasitic plant-parasitic nematodes are present in this clade such as the *Xiphinema* and *Longidorus* genera (van Megen *et al.* 2009). The Chromadorea consist of clades 3-12. Clades 3-7 contain predominantly

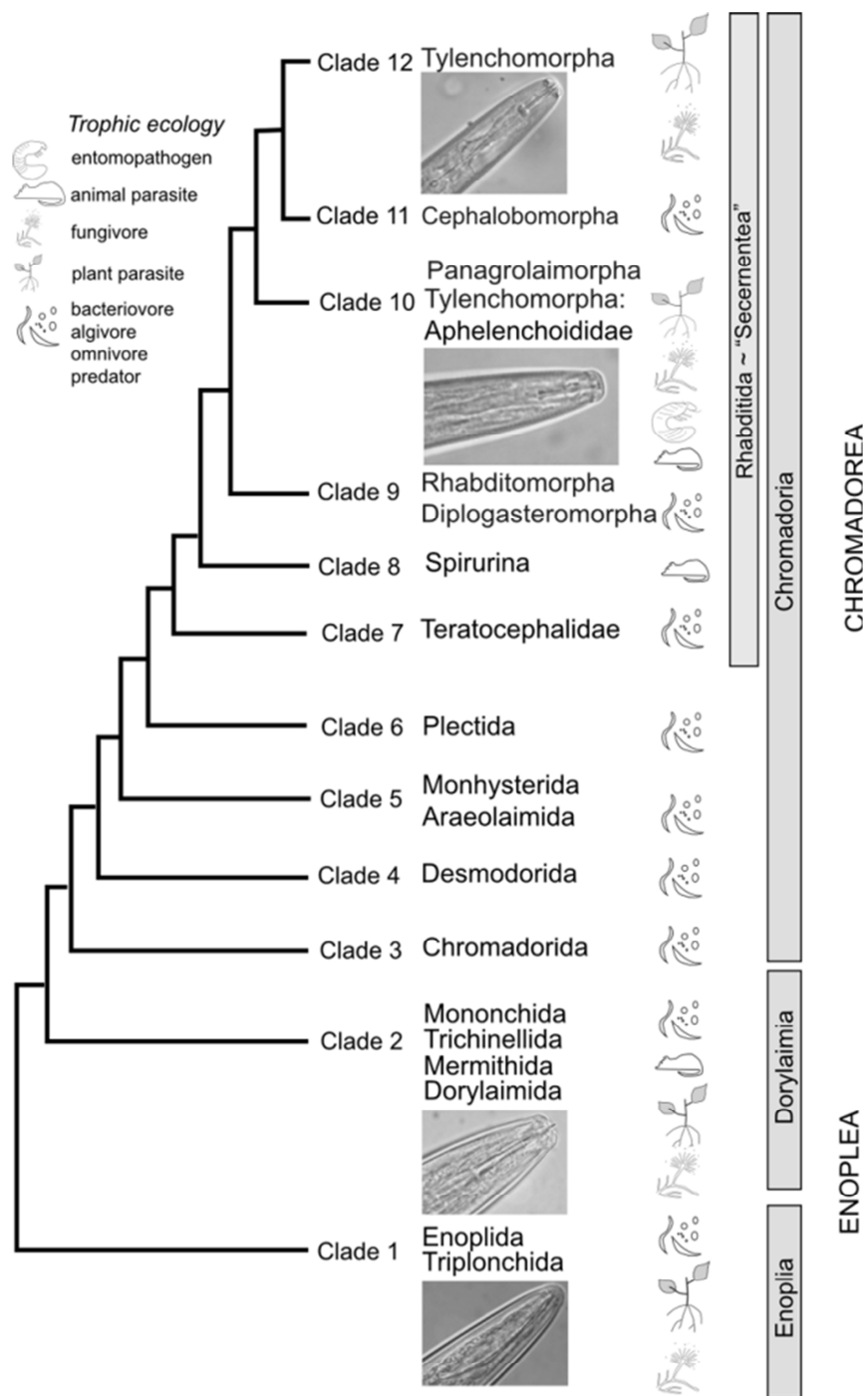


Figure 1-1: Cladogram of inferred relationships in the phylum Nematoda

Relationships derived from Holterman *et al.* (2006) and van Meegen *et al.* (2009). Subdivisions of the phylum Nematoda are indicated at the side. The main feeding strategy within clades is indicated by the icons and key. Main orders in each clade are listed. An image of the feeding apparatus of a representative plant-parasitic nematode is shown for each clade where they are present. Image from Jones *et al.* (2013).

marine nematodes. Clades 9 and 10 contain mainly bacteria feeding nematodes. The Rhabditomorpha, of which the bacterivore *Caenorhabditis elegans* is a member, is in Clade 9. Some animal parasitic nematodes such as *Haemonchus contortus* (9) and *Strongyloides ratti* (10) are present in these clades. Clade 8 contains animal parasites such as *Ascaris suum* and *Loa loa*.

Clade 12 contains the majority of plant-parasitic nematodes. The order Tylenchida is in Clade 12 which contains the sedentary endoparasitic root-knot and cyst nematode species. Migratory endoparasites are found in multiple clades. Clade 10 contains the *Bursaphelenchus* species. Clade 12 contains the *Pratylenchus* and *Radopholus* species which attack the root and *Ditylenchus dipsaci* which attacks stem and bulb tissues. The semi-endoparasitic nematode *Rotylenchulus reniformis* belongs to clade 12.

There is evidence that plant-parasitism has evolved multiple times due to the presence of plant-parasites in multiple clades and may have evolved from ancient fungivorous nematodes. Fungivorous nematodes are only found in the clades which contain plant-parasitic nematodes and in some clades (i.e. 12) it has been demonstrated that fungivorous nematodes are basal to the plant-parasitic nematodes (Holterman *et al.* 2006).

1.2 Plant-parasitic nematodes

Plant-parasitic nematodes are obligate parasites that infect a wide range of plants (Nicol *et al.* 2011). They are among the most damaging pathogens of crops worldwide and are estimated to have an annual economic impact of over \$125 billion dollars globally (Chitwood 2003).

All plant-parasitic nematodes share the common feature of a stylet, which is a hollow needle-like mouthpart. The stylet is involved in a range of behaviours such as exploring the surface of the root preceding invasion, puncturing of plant cells and the uptake of nutrients.

Among the plant-parasitic nematodes, there are three main methods of infecting plants. These are ectoparasitism, semi-endoparasitism and endoparasitism.

1.2.1 Ectoparasites

1.2.1.1 Migratory

Migratory ectoparasites do not enter the root and remain in the soil throughout their life-cycle. They travel along the root surface and feed from cells available from the root surface using the stylet. The length of the stylet affects how deep into the root-tissue the nematode is able to feed. Those with short stylets (15-30 µm long), such as members of the Genus *Tylenchorhynchus* feed on cells which are close to the surface such as epidermal cells and root hair cells. Those with longer stylets, such as members

of the family Longidoridae feed at the root tips from cells deeper within the tissue. They feed from single cells by puncturing them with their stylet, but do not establish permanent feeding sites.

1.2.1.2 Sedentary

Sedentary ectoparasites may feed for several days from a single root cell (cortical or epidermal). The nematode *Criconemella xenoplax* is able to feed on a single cortical cell for up to 8 days (Hussey, Mims and Westcott III 1992).

1.2.2 Semi-endoparasites

Rotylenchulus reniformis nematodes are sedentary semi-endoparasites, which infect over 350 plant species. The females penetrate the root and initiate a feeding site from cells in the endodermis or pericycle, although 2/3 of the body remains outside the root. Males of the species are not parasitic, do not feed and remain in the soil (Robinson *et al.* 1997).

1.2.3 Endoparasites

1.2.3.1 Migratory

Migratory endoparasites enter the root, but do not set up permanent feeding sites. They migrate inter- and intra-cellularly through root-cells feeding and reproducing. Damage caused to the host includes mechanical damage, caused by feeding and migration and the inducement of galling within the root tissue. Three nematode families adopt this feeding strategy. Those in the Pratylenchidae attack below-ground tissues and include the burrowing nematode *Radopholus similis* which infects over 250 plant species in 16 families and *Pratylenchus penetrans* which can reproduce on over 350 hosts. The two other families Anguinidae and Aphelenchoididae attack the above-ground areas of the plants. In the Aphelenchoididae is the pinewood nematode, *Bursaphelenchus xylophilus*, which infects the vascular system of the plant leading to blocked xylem vessels and to pine-wilt disease. *Bursaphelenchus* species associate with beetle hosts, which spread infective juveniles to new trees and provide feeding wounds that facilitate nematode entry (Perry and Moens 2013; Jones *et al.* 2013). The stem and bulb nematodes belong to the family Anguinidae. *Ditylenchus dipsaci* has a wide host range and is a pest on important food crops such as garlic, onion and broad bean as well as ornamental crops such as tulips and narcissus. They enter the plant through stomata or other wounds and feed from parenchyma cells (Duncan and Moens 2013).

1.2.3.2 Sedentary

Nematodes that adopt this feeding strategy are among the most widespread and damaging. These set up long-term (weeks) feeding structures in their host plant, and

induce physiological and genetic changes to produce this specialised feeding structure. They fall into two main categories characterised by either the galling of the roots caused by cell proliferation (root-knot nematodes) or visible cysts on the roots caused by the eruption of gravid adult females through the root tissue (cyst nematodes). Root-knot nematodes and cyst nematodes are further differentiated by method of root invasion and the type of feeding structure that is induced.

1.3 Root-knot nematodes

1.3.1 Agricultural impact and host range

Root-knot nematodes are members of the genus *Meloidogyne* and belong to the order Tylenchida. They are generally able to infect a wide-range of host species (Trudgill 1997) successfully, although some species have narrower host ranges such as *M. naasi* which parasitises grasses and cereals. Most are able to parasitise a wide range of monocotyledonous and dicotyledonous plants. The most economically important species have wide host ranges and are *M. arenaria*, *M. incognita*, *M. javanica* and *M. hapla*. These four species are able to reproduce on important agricultural crops such as rice, wheat, tomato and tobacco. However, between the species there are differences in host range. *M. arenaria* and *M. hapla* reproduce well on groundnut, while *M. incognita* does not. *M. incognita* is able to parasitise cotton whereas the other three species cannot, and *M. javanica* is unable to reproduce on pepper while the other species can. The four species are all able to reproduce on tomato (Sasser 1980; Moens, Perry and Starr 2009).

The effect of root-knot nematode infection in the field can be very damaging. Damage to the root system leads to plants which have reduced shoot growth, wilting and reduction in plant yields. Changes to the root architecture also impact the ability of nutrient uptake, contributing to reduced yields.

1.3.2 Life-cycle of root-knot nematodes

1.3.2.1 Pre-invasion

The eggs of *Meloidogyne* species are enclosed in a gelatinous matrix known as an egg mass that protects them from the soil environment. Hatching of the eggs is triggered generally by temperature-related cues, rather than by specific host-derived cues (Goodell and Ferris 1989), although root diffusate can also stimulate hatching. *M. chitwoodi* J2s hatch in a temperature-dependent manner early in the plant growing season, while unhatched J2s in egg masses at the end of the growing season may be stimulated to hatch by diffusate from host roots (Wesemael, Perry and Moens 2006).

The infective J2 stages, once hatched, are attracted to plant roots and accumulate behind the root cap in the region of cell elongation. General attractants such as CO₂

and amino acids are generated by a growing root and form a gradient in the soil which may act as cues for J2s to follow. CO₂ has been demonstrated to be an attractant for *M. incognita* and *M. javanica* (Rasmann *et al.* 2012) and a pH between 4.5 and 5.4 has also been shown to act as an attractant (Wang, Bruening and Williamson 2009). This chemotaxis towards host roots has been shown to be sufficient for J2s of *M. incognita* and *M. graminicola* to reach host roots by the most efficient method when separated from host-roots by a maze-system. There was also evidence for host-specific cues acting on the J2s as movement towards a host plant was greater than movement towards a non-host plant (Reynolds *et al.* 2011).

1.3.2.2 Invasion and induction of giant cells

Following contact with the root, J2s search for an invasion site. This behaviour is characterised by the rubbing of lips over the epidermal cell surface and the gentle exploratory thrusting of the stylet. At the region of cell elongation, the J2s penetrate the root with a combination of mechanical disruption provided by the thrusting of the stylet and the secretion of cell wall-degrading enzymes to rupture the cell walls. On successful invasion, the nematodes travel intercellularly towards the root-tip until they reach the apex of the meristematic zone and then turn round and migrate back towards differentiating tissue. Here, the nematodes stop moving and initiate formation of their feeding site (Wyss, Grundler and Munch 1992).

The J2 starts feeding from several cells by inserting the stylet, inducing formation of the giant cells. These are specialised feeding structures for root-knot nematodes, and their formation is essential for the J2 to successfully complete its life-cycle. They are initially established from cells of the phloem or parenchyma and each J2 induces and feeds from between 2 – 12 cells. The giant cells are multinucleated as a result of multiple rounds of endomitosis without cytokinesis. The J2 feeds from these cells by withdrawing the cell contents through the stylet and feeding tube.

Secretions from the nematode, injected into the cell through the stylet contain effector proteins which contribute to this reprogramming of the plant cells to produce giant cells. Some candidate effectors have been identified, which allow successful invasion by co-opting cellular processes. Some affect hormone balances within the cell, such as a chorismate mutase, which may act to suppress auxin formation (Doyle and Lambert 2003). Some are localised to the nucleus of giant cells (Jaouannet *et al.* 2012), or have canonical nuclear localisation signals which predict targeting to the nucleus (Huang *et al.* 2003), although the targets of many of these effectors are not known. The targets of some have been identified, such as the effector 16D10 which interacts with the root protein SCARECROW which causes root cell proliferation (Huang *et al.* 2006). These effectors are synthesised in the oesophageal glands of the root knot nematode. Three moults occur in order to reach maturation. During this process the nematode swells and after the final moult the females become pear-shaped and

secrete a gelatinous matrix in which they lay eggs. Male root-knot nematodes follow a different developmental path and become vermiform after the final moult.

1.3.2.3 Root-knot nematode reproduction

The *Meloidogyne* genus has three different modes of reproduction. There are amphimictic species like *M. pinis* and *M. carolinensis* in which male worms fertilise females, and the oocyte undergoes meiosis. This method of reproduction is uncommon in the *Meloidogyne* genus. Some species such as *M. chitwoodi* and most populations of *M. hapla* reproduce by facultative meiotic parthenogenesis in which, if males are present, amphimictic reproduction occurs. In the absence of males, the pro nucleus and polar body of the oocyte fuse and the embryo develops. Most species of *Meloidogyne* reproduce by obligate mitotic parthenogenesis and these include the most economically damaging root-knot nematodes *M. incognita*, *M. arenaria*, *M. javanica* and some populations of *M. hapla*. Although males are present in these species, they play no role in reproduction and their number is affected by environmental state.

The parthenogenic nature of many *Meloidogyne* species may be a result of hybridization between two ancient RKN genomes resulting in polyploidisation. This results in a high background of genetic diversity within *Meloidogyne* species, which is thought to account for the broad host-range of many *Meloidogyne* species as it can provide variability in order to overcome plant defences. In contrast, the amphimictic species have narrower host ranges (Castagnone-Sereno 2006; Castagnone-Sereno 2002; Chitwood and Perry 2009).

1.4 Cyst nematodes

1.4.1 Agricultural impact and host range

The most economically damaging cyst nematodes belong to the genera *Heterodera* and *Globodera*. Cyst nematodes typically have a narrower host range than *Meloidogyne* species and each species can only reproduce on a small range of crops. *Globodera pallida* and *G. rostochiensis* can reproduce on potato, tomato and eggplant whilst wheat, barley, oat and maize are hosts for *H. avenae* and *filipjevi*. *H. glycines* reproduces on soybean and other legume varieties, although it can also reproduce on other non-leguminous weeds. *H. schachtii* has a wide host range for a cyst nematode, and is able to infect plants such as broccoli, chickpea and spinach (Turner and Subbotin 2013).

Despite the reduced host-range of cyst nematode species, many important crops have a cyst nematode species which is able to infect them. The economic loss associated with cyst nematode infection is high. 9% of potato crop yield losses worldwide have been estimated to be due to potato cyst nematodes (Perry and Moens 2013). The

potato cyst nematode, *G. pallida*, causes yield losses of over £50 million per annum to the UK potato industry. Potato cyst nematode has been found in 65% of potato growing fields in the UK, of which 67% of the nematodes were *G. pallida* (Minnis *et al.* 2002) and the remaining *G. rostochiensis*.

1.4.2 Life-cycle of cyst nematodes

1.4.2.1 Pre-invasion

As cyst nematodes tend to have a more limited host-range, their hatching is triggered by specific host-derived cues. This hatching response to host-derived cues varies between cyst nematode species. While *G. pallida* and *G. rostochiensis* are dependent on host-derived cues for hatching, *H. schachtii* with a wider host range hatches well in the absence of host-derived cues. *Globodera pallida* in particular requires root-exudates of potato to induce a hatching response (Den Nijs and Lock 1992). While host-derived cues are required for hatching, temperature also affects hatching. Two potato cyst nematode species *G. pallida* and *G. rostochiensis* have different optimal hatching temperatures (16°C and 20°C) (Turner and Subbotin 2013).

The eggshell of cyst nematode J2s protects against environmental conditions. Within the eggshell, the J1 undergoes the first moult to a J2. In its quiescent state, the J2 is partially dehydrated and metabolically inactive. In response to hatching cues, the permeability of the eggshell changes to allow rehydration of the J2, which becomes metabolically active. The J2s uses the stylet to perforate the eggshell until a slit is produced through which it exits the egg.

Host-derived cues may also be attractants for cyst nematodes as diffusate from host-roots tends to attract infective J2s (Reynolds *et al.* 2011). Specific compounds which have been highlighted include δ-aminobutyric acid and L-glutamic acid for *G. pallida*, and α-aminobutyric and L-glutamic acid for *G. rostochiensis* (Rasmann *et al.* 2012).

1.4.2.2 Invasion and induction of syncytia formation

The J2s initiate root invasion near to the tips of the roots. The stylet is used to rupture the epithelial cell walls by thrusting. The J2 enters the cortical cells and migrates intracellularly towards the vascular cylinder. During this intracellular migration, the stylet is used to rupture cell walls and aid the J2's movement through the cells of the root.

Upon reaching the vascular cylinder, the J2 selects a cell to initiate formation of the feeding site by piercing it with the stylet. The stylet may be withdrawn and a new cell selected several times, before a suitable cell is found (Wyss and Zunke 1986; Wyss and Grundler 1992). The syncytium is formed from enlarged root cells caused by the

breakdown of cell walls between neighbouring cells and has a dense granular cytoplasm. Endoreduplication leads to increased number of nuclei and there is an increase in the number of ribosomes and mitochondria. The J2 feeds from this cell by withdrawing the cell contents through the stylet and a specialised feeding tube structure that forms at the stylet tip.

Nematode effectors are injected into the cell via this stylet that trigger a plethora of changes in gene expression which facilitate syncytium formation. A Cellulose Binding Protein (CBP) identified in *H. schachtii* interacts with a cell wall modifying enzyme pectin methylesterase and is involved in the restructuring of cell wall architecture (Hewezi *et al.* 2008). Host genes such as expansins (Wieczorek *et al.* 2006) and endo- β -1,4-glucanases are also found to be upregulated in syncytia, and are required for successful infection and expansion of the cells (Karczmarek *et al.* 2008). Effectors also act to suppress host defences. The Hs4F01 gene of *H. schachtii* interacts with an *Arabidopsis* oxygenase, which has been shown to be involved in pathogen susceptibility previously (Patel *et al.* 2010). A chorismate mutase gene identified in *G. pallida* may also have a role in reducing plant defence response, or in altering auxin levels (Jones *et al.* 2003). More putative effectors have been identified in cyst nematodes such as *G. pallida*, although the function of most is not yet known. They can be observed by GFP fusions accumulating in the nucleus and cytoplasm (Thorpe *et al.* 2014).

The J2 feeds from the syncytial cell for approximately 7 days before moulting to a J3. This is the last stage at which the male cyst nematode will feed, although the female continues to feed. After the final moult to J4 stage, the female nematode enlarges and the posterior end erupts from the root. The vermiform adult male develops within the J4 cuticle, before emerging from the root (Turner and Subbotin 2013; Lilley, Atkinson and Urwin 2005).

1.4.2.3 Reproduction

Cyst nematodes reproduce amphimictically. Sex determination occurs towards the end of the J2 stage and there is evidence that this is dependent on aspects of the status of the syncytium such as nutrient availability. More females develop under environmentally favourable conditions (Grundler, Betka and Wyss 1991), while a high proportion of males develop under conditions such as high infestation levels (Trudgill 1967). The adult male locates the female on the root, likely by responding to sex pheromones (Riga *et al.* 1996) in order for fertilization to occur. After fertilisation, the female nematode becomes gravid and polyphenol oxidases tan the cuticle to produce the cyst, which contains the fertilised eggs (Awan and Hominick 1982).

The life-cycle of a cyst nematode is summarised in Figure 1-2.

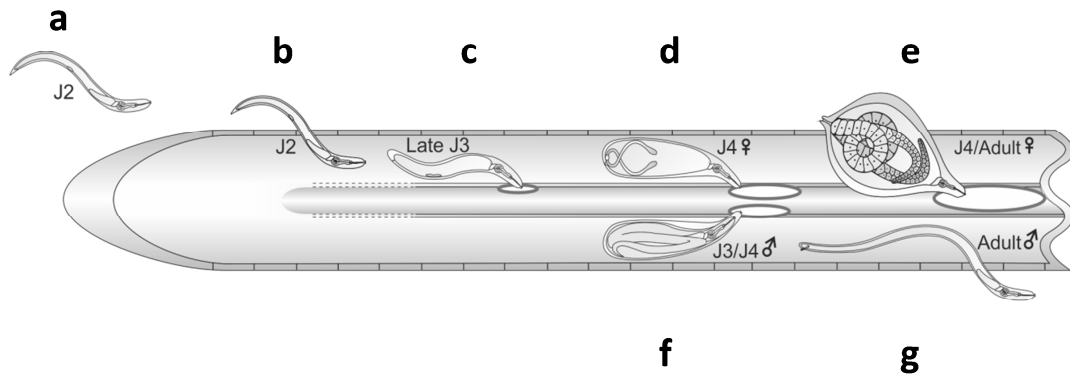


Figure 1-2: Life cycle of a cyst nematode

The life cycle of a cyst nematode such as *G. pallida*.

- a) Eggs hatch from the soil as migratory J2 stages. Hatching is triggered by sensing of host-derived cues under favourable conditions.
- b) The J2 enters the root and migrates intracellularly towards the vascular cylinder. A cell is selected for initiation of the feeding site. Sex is determined towards the end of the J2 stage.
- c) The J2 moults to the J3 stage. The syncytium is induced and the nematode feeds and begins to swell.
- d) The final moult to the J4 stage occurs. The ovaries of the female develop.
- e) Eggs develop within the female body wall, tanning by phenol oxidases occur to produce the toughened cyst.
- f) Male worms develop as a vermiform inside the J4 cuticle.
- g) Adult male worms leave the root and fertilise eggs within the females.

Adapted from Lilley, Atkinson and Urwin (2005).

1.5 The need for novel methods of control

1.5.1 Current social methods

Nematode infection in fields is often overlooked as symptoms of infection can be similar to those of abiotic stresses such as drought. As a result, nematode infection is frequently not controlled as it is not identified.

Crop rotation can be used to control nematodes. However, for cyst nematodes such as *G. pallida* long crop rotation periods are required in order to reduce cyst nematode populations due to the highly protective cyst (Kerry, Barker and Evans 2002). Decline rates of *G. pallida* in the field are <30% per year resulting in a recommended rotation time of between 8 and 14 years (Trudgill *et al.* 2003). Although the eggs of *Meloidogyne* species do not have a toughened protective coating, crop rotations for control of *Meloidogyne* species requires the growth of host-species that *Meloidogyne* cannot proliferate on. As most *Meloidogyne* species have a wide-host range, selection of suitable crops for crop rotations can be difficult. Crop rotation also entails an economic cost, as often less profitable crops are used. Use of trap crops to control *Meloidogyne* species is being investigated. In this model, plants which induce *Meloidogyne* hatching and invasion, but are unsuitable hosts in which to complete the nematode life cycle are used (Melakeberhan *et al.* 2006).

1.5.2 Nematicide use is reduced

Nematicides have been used in the past to control nematodes, but many relied upon nematicides are now becoming phased out due to environmental concerns. Fumigants are used to treat the soil by mixing nematicidal compounds into the air spaces between the soil particles. The fumigant methyl bromide is no longer used in most countries due to its classification as an ozone depleting compound (Ristaino and Thomas 1997). The carbamate Aldicarb targeted chemoreception, but has been banned due to its effect in off-target organisms. The producer of Aldicarb, BayerCrop Sciences, plans to end distribution by the end of 2017.

New research in the areas of control focuses on novel manufactured nematicides such as fluensulfone (Kearn *et al.* 2014) and monepantel (Rufener *et al.* 2010) and nematicides derived from biological sources like garlic extracts (Danquah *et al.* 2011). However, it has been estimated that unless a nematicide is able to reduce the population of nematodes in a field by over 90%, a sufficient number will remain for the population levels to rebound to problematic levels (Trudgill *et al.* 2003).

1.5.3 Use of resistant crops

Crops resistant to nematode infection have also been produced using traditional breeding techniques. The *Mi-1* gene of tomato (introgressed from a wild tomato

relative) confers resistance to the root-knot nematodes *M. incognita*, *M. arenaria* and *M. javanica* (Vos *et al.* 1998). Some commercial cultivars of potato which carry the H1 resistance gene are fully resistant against *G. rostochiensis* (Bakker *et al.* 2004). The *Hero* gene confers high resistance of tomato to *G. rostochiensis* and partial resistance to *G. pallida* (Ernst *et al.* 2002).

Development and breeding of resistant lines is time-consuming and expensive. Resistance genes which are effective in one host-plant, may not be effective in another making the use of identified resistance genes more limited. For example, transgenic potato lines expressing the tomato *Hero* gene were not resistant to potato cyst nematodes (Sobczak *et al.* 2005). Additionally, resistance genes are often over-come in time due to high-selection pressures on the parasite. Growth of potato cultivars resistant to *G. rostochiensis* has additionally had the unintended side-effect of increasing *G. pallida* populations due to reduced competition (Minnis *et al.* 2002).

Genetic engineering of resistance is also part of ongoing research, although there is still considerable resistance against GM crops, particularly in Europe. However, it is critical that new avenues for nematode control are continually being investigated.

1.6 *Caenorhabditis elegans*

C. elegans is a free-living bacterivore found in soil environments. Wild populations of *C. elegans* have been found associated with composting material (Dolgin, Felix and Cutter 2008). The *C. elegans* worm is translucent and as an adult ~1 mm in length. The life-cycle (Figure 1-3) is fast and the nematode develops from egg to sexually mature adult in three days, although adults can live for several weeks (Brenner 1974). Before reaching maturity, there are four larval stages and four moults that occur in the life-cycle. Under unfavourable environmental conditions such as starvation or overcrowding the worm may enter a dauer stage after the second moult. These are developmentally arrested, and metabolically less active stages which can survive for weeks until conditions become favourable for continued development (Cassada and Russell 1975).

The adult hermaphrodite contains 959 somatic cells; the lineage of each has been studied in detail. Thousands of worms can easily be propagated within a week on agar plates seeded by *E. coli* as an individual self-fertilising hermaphrodite can lay over 300 eggs (Brenner 1974). There are two *C. elegans* sexes, although males in the population are rare (under 0.1%) (Ward and Carrel 1979).

1.6.1 Food-searching behaviours of *C. elegans*

C. elegans has distinct behaviours in the way it responds to and seeks food. As a simple model, a *C. elegans* worm on a lawn of bacteria will primarily adopt dwelling behaviours, where it will move slowly and remain in a restricted area. It may

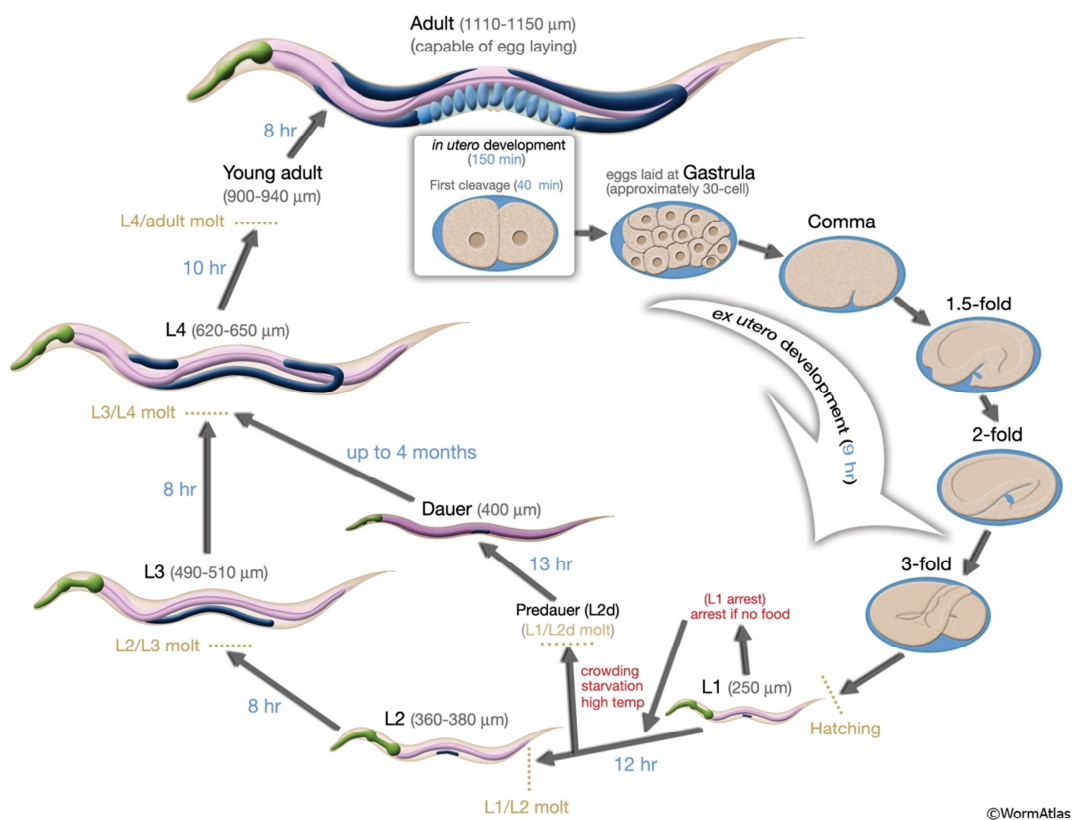


Figure 1-3: Life-cycle of the *C. elegans* hermaphrodite at 22 °C

Diagram shows the different life-stages of *C. elegans* and duration of the life-stage at 22 °C. The conditions under which L1 larval arrest and dauer formation can be induced are shown in red. Development of the reproductive system is shown in blue, the pharynx in green and the intestine in purple. Length of the worm at each stage is given in µm. Diagram from Altun and Hall (2005)

sometimes switch to roaming behaviours, where it will move more quickly over the lawn. If the worm is moved from a bacterial lawn to a plate without bacteria, the behaviour changes to rapid movement punctuated with turns mediated either by reversals followed by a directional change or omega turns (Croll 1975). This behaviour is known as Area Restricted Search (ARS). During the 30 minutes following the worm being moved from food, the number of reversals steadily decreases and the behaviour changes to a dispersal based behaviour. On encountering a new food source, the worm will slow its speed in a behaviour known as enhanced slowing. These changes in response to food serve to help *C. elegans* locate food sources in an environment where food is likely to be disrupted in discrete units (e.g. bacterial colonies around rotting fruit). In the presence of bacteria, behaviours which may lead to leaving the food are suppressed. If the food runs out, the local area is searched first and then the worm leaves to find new bacterial sources (Bargmann 2006).

1.6.2 The use of *C. elegans* as a model organism

C. elegans was the first multicellular organism for which the full genome was sequenced (Consortium 1998) and this is now completed to a high degree of confidence (Chen *et al.* 2005a). Although more genomes of plant-parasitic and other parasitic nematodes have been sequenced and published (Opperman *et al.* 2008; Cotton *et al.* 2014; Abad *et al.* 2008; Laing *et al.* 2013; Jex *et al.* 2011; Ghedin *et al.* 2007) in the last few years, *C. elegans* is still considered an excellent model on which to base research of other nematode species.

C. elegans was popularised as a model organism by Sydney Brenner in the 1960s. Initial study of the worm employed forward genetics and induced mutations by ethyl methanesulphonate (EMS) in order to characterise aberrant phenotypes, such as those which caused deviations in locomotion (Brenner 1974). Developments in RNAi technology employed reverse genetics to target specific genes, and analyse the phenotype caused by disruption of gene function (Fire *et al.* 1998).

Microinjection allows transformation of *C. elegans* by injection of DNA into the gonads of a young hermaphrodite. The injected DNA forms large extrachromosomal arrays which can become stably inherited. A selectable marker e.g. *rol-6* or *gfp* allows positive selection of transformants (Mello *et al.* 1991). Microparticle bombardment has also been developed to create transgenic lines of *C. elegans*. Plasmid DNA is coated onto gold beads, and bombarded into large populations of *C. elegans* to generate lines in which the transforming DNA has been integrated into the genome (Praitis *et al.* 2001). In recent years, CRISPR-Cas9 technology has allowed specific targeting of genomic sequence to create insertions, mutations or deletions in the genomic copies of specific genes (Friedland *et al.* 2013). As *C. elegans* populations are predominantly self-fertilising hermaphrodites which can produce 300-350 offspring per day, the

maintenance and propagation of mutant strains is very simple, as they can be generated from a single worm.

The *C. elegans* community is large and collaborative and many resources have been made available online. The full genome sequence is publicly available on Wormbase. The genome is 100 Mb in size and contains over 19,000 predicted genes collated with associated data that is available on Wormbase. The ORFeome project provides validated predicted gene models, and integrates it with the *C. elegans* genome sequence and provides open reading frames of *C. elegans* genes in vectors to facilitate expression in bacteria (Chen *et al.* 2004). Studies on the effect of RNAi on more than 86% of *C. elegans* genes have been done systematically and the results have been integrated onto the Wormbase database (Kamath *et al.* 2003). Microarray data is also available, detailing changes in gene expression of *C. elegans* in response to different growth conditions, developmental stages and in different mutants (Kim *et al.* 2001b). Additionally SAGE (Serial Analysis of Gene Expression) has also yielded information about changes in gene expression over different life-stages and in different conditions (Jones *et al.* 2001). High-throughput yeast-two-hybrid screen has also yielded information about protein-protein interactions in *C. elegans*, and an interactome for many proteins is available (Li *et al.* 2004). The expression patterns of many *C. elegans* genes are available online, generated from a promoterome which used the expression pattern of GFP driven by promoters of interest to highlight where particular genes are expressed (Dupuy *et al.* 2004). This is all available, organised by gene name on the Wormbase site with links to the supporting literature.

The *Caenorhabditis* genetics centre (CGC) produces and distributes mutant strains to *C. elegans* researchers. Over 3,000 mutant strains of *C. elegans* are available to academic institutes free of charge, or for a small fee to industrial institutes.

The physical features of *C. elegans* and the amount of genetic resources, databases and research papers has made *C. elegans* a very popular model organism. It has been used in biomedical studies to investigate human diseases, despite the very wide evolutionary gap between the nematode worm and human biology. Despite this, the worm still has many features that are shared in the mammalian body such as muscle, intestine, reproductive system, glands and a nervous system. It has found uses as a model for anticancer drugs (Hara and Han 1995) and in the development of treatments for depression (Dempsey *et al.* 2005), among many other examples in the pharmaceutical world (Kaletta and Hengartner 2006). Much of the information and techniques used to produce the *C. elegans* genome sequence were subsequently used to aid the human genome project (Blaxter 2011).

1.6.2.1 *C. elegans* as a model for plant-parasitic nematodes

C. elegans can be maintained in the laboratory environment using simple materials and techniques. For these reasons, *C. elegans* is an attractive model for plant-parasitic nematodes. In contrast, plant-parasitic nematodes are obligate parasites which require their host-species to complete their life-cycle. The life-cycles are comparatively long (4-5 weeks) and require the time to grow the host plants and the space in which to keep them. There have been no reported instances of the production of transgenic lines of plant-parasitic nematodes, although there has been some success at creating transformants for some other parasitic nematodes (Li *et al.* 2006; Grant *et al.* 2006). However, the time and space required to generate and maintain such mutant lines would make such a task unfeasible. The molecular techniques available for plant-parasitic nematodes are more limited than those for *C. elegans*. RNAi has been used to knockdown target genes in some plant-parasitic nematode species (Urwin, Lilley and Atkinson 2002; Chen *et al.* 2005b) and in some animal-parasitic species (Aboobaker and Blaxter 2003), however this effect is transient.

Despite the different life-styles of *C. elegans* and parasitic nematodes, they are likely to have broadly the same body structure, development, reproduction and responses to stimuli. In comparisons between the nervous system of *A. suum* and *C. elegans* the structure of the nervous system has been shown to be very similar despite the hypothesised species divergence time of 500 million years (Jorgensen 2005; White *et al.* 1986). All nematodes have the requirement to sense and migrate towards food sources or hosts, and the molecular mechanisms underpinning these behaviours are likely to be shared. The dauer larval stage of *C. elegans* and the infective juvenile stages of parasitic nematodes had been thought to be functionally homologous as both are long-lived, non-aging and non-feeding. However, metabolism in *C. elegans* dauer larvae and soybean cyst nematodes *H. glycines* J2s has been shown to be dissimilar. Additionally only 22% of dauer-enriched genes are conserved in *H. glycines*, and only 41% of these are expressed at the same analogous time point as in the dauers (Elling *et al.* 2007). Furthermore, an orthologue of *daf-7* in the parasitic nematode *Parastonyloides trichosuri*, a gene that controls entry into dauer development in *C. elegans*, was unable to rescue *daf-7* *C. elegans* mutants. It seems likely that the parasitic infective stages are either not functionally identical to the *C. elegans* dauers, or evolutionary distance has changed many pathways (Crook, Grant and Grant 2010).

C. elegans can be used as a model for plant-parasitic nematodes in two main ways. Information obtained from *C. elegans* may be applied directly to plant-parasitic nematodes or it may be used as an expression system in which the gene from the parasite is expressed and its function probed.

The mode of action of many of the anthelmintic drugs has been elucidated in *C. elegans* before the parasite which they target. The molecular targets of ivermectin

(Dent *et al.* 2000), levamisole (Lewis *et al.* 1980) and monepantel (Kaminsky *et al.* 2008) along with many others were first characterised in *C. elegans*. It has also been used as a method of high-throughput screen for potential anthelmintic drugs (Taylor *et al.* 2013; Katiki *et al.* 2011). The roles of certain families of proteins have been characterised first in *C. elegans* and from this, their role in parasitic nematodes inferred. For example, a cathepsin L protease was demonstrated to be essential for embryonic development of *C. elegans* (Hashmi *et al.* 2002) and this role was shown to be functionally conserved in the parasite *H. contortus* (Britton and Murray 2002).

C. elegans may also be used as an expression system in which to express genes from parasitic species in order to investigate their function. By expressing homologues of *C. elegans* genes identified in a parasitic nematode, the function of the parasitic gene can be determined if it is able to rescue the equivalent mutant strain of *C. elegans* (Glendinning *et al.* 2011). This allows the likely role of genes from parasites to be studied further, such as the characterisation of the *tub-1* gene encoding β-tubulin from *H. contortus* and its role in benzimidazole resistance (Kwa *et al.* 1995). It has also been used in vaccine develop against parasites such as *H. contortus* in order to express *H. contortus* derived antigens (Roberts *et al.* 2013). Expression patterns of genes from parasitic nematodes can also be analysed by the generation of promoter:GFP or LacZ fusions from the parasitic nematode, which are then transformed into *C. elegans*. The promoter region of an acetylcholinesterase gene, *gpa-ace-2* from *G. pallida* has been used to drive GFP expression in *C. elegans* in specific neurons. *Gpa-ace-2* was also able to rescue the *C. elegans* acetylcholinesterase mutants (Costa *et al.* 2009). The promoter region of a GAPDH gene from *G. rostochiensis* has been used to drive GFP expression in the body wall muscle of *C. elegans*. (Qin *et al.* 1998) The expression pattern of GFP is likely to be similar to where the gene is expressed in the parasite.

The new era of genome sequencing is beginning to provide more completed genome sequences for parasitic nematode species. The 959 Nematode Genomes project aims to collate all the ongoing genome sequencing work on nematodes (Kumar, Schiffer and Blaxter 2012). A similar resource also exists for nematode transcriptome data (Elsworth, Wasmuth and Blaxter 2011). Including *C. elegans*, 21 genomes have been recently sequenced and of these 16 are parasitic nematode genomes (Rödelsperger, Streit and Sommer 2013). This increase allows for a new field of comparative genomics highlighting aspects of parasitic nematodes.

C. elegans as the organism in which functions have been ascribed to most genes, has a fundamental role in this. Comparisons of newly sequenced parasitic genomes can allow orthologues between the species to be identified, and can highlight expansions or reductions in gene families which may be indicative of the switch to a parasitic lifestyle. Parasitic genomes can also be compared to each other to determine which, if any, are the core genes for parasitism (Sommer and Streit 2011). This has also

highlighted the role of Horizontal Gene Transfer in nematodes, which may have had implications on the evolution of parasitism (Dieterich and Sommer 2009).

1.6.3 Aspects of the neurobiology of *C. elegans*

The adult hermaphrodite *C. elegans* contains 302 neurons and over 7000 synapses. The nervous system makes up roughly one third of the animal (White *et al.* 1986). These neurons are separated into two distinct and independent systems; the larger somatic system that consists of the 282 neurons in the body of the worm and the smaller pharyngeal system of 20 neurons that controls the pharynx. The two networks are connected by a pair of RIP interneurons allowing signalling between the two neuronal systems. The neurons of *C. elegans* can be functionally grouped into 4 categories: motor neurons that connect onto muscular tissue, sensory neurons that mostly have ciliated ends for sensing, interneurons which receive signals and pass on signals to other neurons and polymodal neurons that have more than one function. The synapses connecting the neurons are primarily chemical and signal via the use of neurotransmitters. Additionally, gap junctions that mediate electrical signalling between cells are found between muscle cells and between neurons (White *et al.* 1986).

The neurotransmitters used at the chemical synapses are acetylcholine, γ -Aminobutyric acid (GABA), glutamate, dopamine, serotonin, tyramine, octopamine, and neuropeptides. They are involved in all aspects of *C. elegans* neurobiology controlling locomotion, food-seeking behaviours, pharyngeal pumping and egg-laying. The annotation of neurotransmitter roles has been achieved through investigation of the behavioural changes of mutants in which synthesis or perception of the neurotransmitters has been decreased. Application of exogenous neurotransmitter and the change in behavioural responses has also been used to elucidate their role. Through methods like these the involvement of neurotransmitters in particular behaviours can be elucidated.

1.6.3.1 Musculature and locomotion

The body wall muscle of *C. elegans* is obliquely striated, as is all nematode muscle studied so far. In contrast, vertebrate muscle is cross striated. 95 rhomboid-shaped body wall muscle cells line the body wall muscle of the adult hermaphrodite. 75 motor neurons innervate the body wall muscles, leading to the sinusoidal locomotion pattern observed on solid media. Sinusoidal locomotion is controlled by cholinergic B-type (forward locomotion) and A-type (backward locomotion) as well as GABAergic D-type neurons. Rhythmic co-ordination between contractions of body wall muscle on one side of the body, accompanied by relaxation on the other side drives this sinusoidal movement. In forward locomotion, alternating excitation of dorsal and ventral muscle

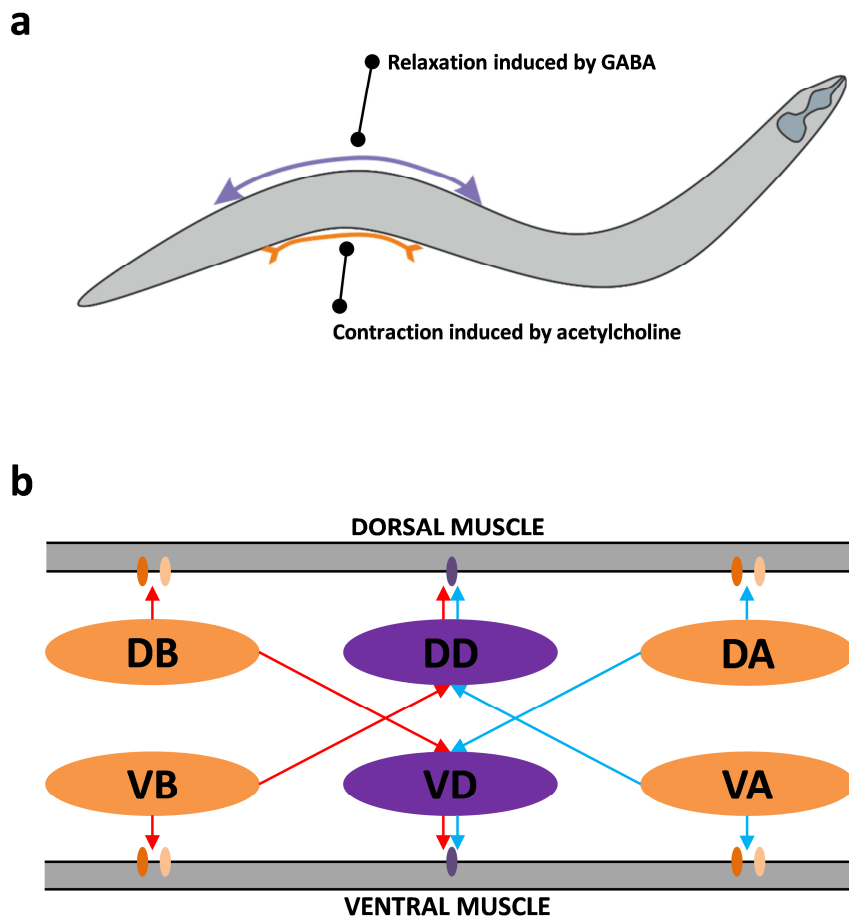


Figure 1-4: Generation of sinusoidal locomotion in *C. elegans*

a) Basic principle of sinusoidal locomotion in *C. elegans*. Contraction on one side of the worm is induced by acetylcholine and relaxation on the other side of the worm is induced by GABA.

b) Neurons that control this behaviour. In forward locomotion (red), DB and VB neurons trigger acetylcholine receptors in the body wall muscle, and trigger GABA release from DD and VD neurons on the alternate side of the wall triggering a GABA receptor. In backward locomotion (blue), DA and VA neurons trigger acetylcholine receptors and DD and VD neurons.

is mediated by the DB and VB neurons respectively, which then elicit relaxation on the opposite side of the worm via the VD or DD neuron. Contraction of the body wall muscle is mediated by two acetylcholine receptors (contraction), and a GABA receptor (relaxation) at the neuromuscular junction (Richmond and Jorgensen 1999) (Figure 1-4).

1.6.3.2 Acetylcholine

Acetylcholine is the major excitatory neurotransmitter acting at neuromuscular junctions. 120 of the 302 neurons in the hermaphrodite nervous system are cholinergic and they are primarily motor neurons. It has roles in feeding, egg-laying and locomotion. The mechanism of acetylcholine release from the synapse is shown in Figure 1-5. Acetylcholine is loaded into vesicles by a synaptic vesicle acetylcholine transporter UNC-17 (Alfonso *et al.* 1993). The vesicles then dock with the cell membrane and are primed for Ca^{2+} dependent fusion. On fusion with the membrane, acetylcholine is released into the synaptic cleft and activates acetylcholine receptors on the post-synaptic membrane. Continued activation is prevented by the action of acetylcholinesterase that breaks down acetylcholine and removes it from the synaptic cleft. The resulting choline is then taken up again to the presynaptic cleft by a choline transporter CHO-1 (Okuda *et al.* 2000). CHA-1 resynthesises acetylcholine by the acetylation of choline (Rand and Russell 1985). Mutants in *cha-1* and *unc-17*, which are impaired in acetylcholine synthesis, are uncoordinated in movement, as acetylcholine is required for generation of smooth body movement. Pharyngeal pumping is also slowed as the MC neuron that stimulates pharyngeal pumping is activated by acetylcholine. *Null* mutants of *cha-1* and *unc-17* are lethal (Alfonso *et al.* 1993).

The largest class of acetylcholine receptors in *C. elegans* are the nicotinic acetylcholine receptors (nAChRs). These are cys-loop receptors which will be discussed in more detail in 1.7. In addition to these, there are also G-protein coupled receptors, expressed primarily in the head and pharyngeal muscle.

1.6.3.3 GABA

GABA in *C. elegans* is an inhibitory neurotransmitter and primarily acts at the neuromuscular synapses to affect the body movements which mediate locomotion and head movements during foraging (McIntire *et al.* 1993). UNC-25 is a glutamic acid decarboxylase and essential for GABA synthesis. Mutations in *unc-25* abolish GABA transmission. The animals shrink in size, and their movements are uncoordinated e.g. display exaggerated head movements during foraging (McIntire, Jorgensen and Horvitz 1993). *Unc-47* encodes a transporter which loads GABA into vesicles in the presynaptic neuron (McIntire *et al.* 1997). GABA is cleared from the synaptic cleft by active transport mediated by GABA transporter SNF-11 (Jiang *et al.* 2005).

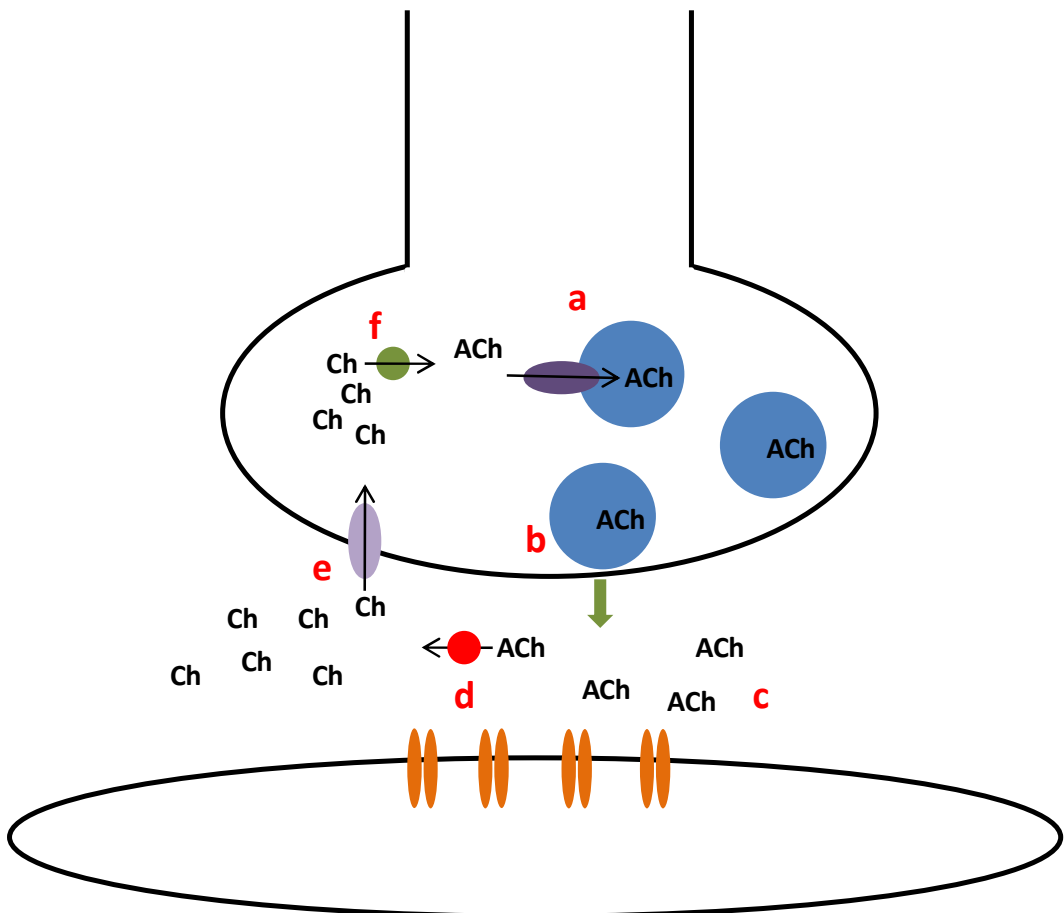


Figure 1-5: Schematic of mechanism of acetylcholine release

- a) Acetylcholine is loaded into vesicles by UNC-17.
- b) Vesicles dock at the presynaptic membrane.
- c) Vesicles fuse with the membrane and acetylcholine is released into the synaptic cleft and activates acetylcholine receptors on the post-synaptic membrane.
- d) Removal of acetylcholine from the synaptic cleft by breakdown catalysed by acetylcholinesterase.
- e) Uptake of choline by choline transporter CHO-1.
- f) Synthesis of acetylcholine by CHA-1.

There are two classes of GABA receptors. The GABA_A receptors belong to the cys-loop family. The *unc-49* gene encodes three different subunits of the GABA_A receptor via alternate splicing. An additional receptor, EXP-1 has also been identified which provides an excitatory role for GABA during defecation (Schuske, Beg and Jorgensen 2004). The GABA_B receptor is a GPCR that is a heterodimer of two subunits.

1.6.3.4 Glutamate

Glutamate mediates rapid excitatory synaptic signalling and is involved in locomotion, the perception of the environment and feeding activity (Hills, Brockie and Maricq 2004). Mutants of *eat-4*, a vesicular glutamate transporter which mediates release of glutamate into the synapse, are deficient in glutaminergic signalling, and are abnormal in the pharyngeal pumping responsible for feeding (Lee *et al.* 1999).

The primary receptors for glutamate are the ionotropic glutamate receptors (iGluRs), a class of heteromeric ligand-gated ion channels. At least 10 genes encoding subunits of iGluRs exist in *C. elegans* (Brockie and Maricq 2002). The subunit encoded by *glr-1* appears to be involved in many aspects of nematode biology as mutants for this gene do not demonstrate the typical backing away response to nose touch (Hart, Sims and Kaplan 1995). *Glr-1* and *glr-2* also appear to be involved in the onset of area-restricted search, which increases turning rate after an encounter with food to remain in an area where more food is likely to be encountered (Hills, Brockie and Maricq 2004).

In addition to the iGluRs, there is a small family of glutamate-gated chloride channels which appear to be unique to invertebrates and were first identified by their sensitivity to the anthelmintic paralysing drug ivermectin.

1.6.3.5 Serotonin

Serotonin modulates behaviour in response to food and egg laying (Sawin, Ranganathan and Horvitz 2000). Serotonin signalling is involved in the enhanced slowing response that food deprived animals demonstrate when encountering a bacterial lawn. Pharyngeal pumping is triggered and increased by serotonin and egg laying is promoted. *Bas-1* and *cat-4*, both involved in serotonin biosynthesis, demonstrate that serotonin is important in this enhanced slowing response as mutations in these genes abolish this response (Sawin, Ranganathan and Horvitz 2000). *Tph-1* encodes a tryptophan hydroxylase that catalyses a rate limiting step in serotonin biosynthesis. Mutants in this gene do not accumulate serotonin and are not able to respond to the presence of food (Sze *et al.* 2000).

Four receptors for serotonin have been identified: MOD-1 is a serotonin gated chloride channel, and SER-1, SER-4 and SER-7 are G-protein coupled receptors. Mutants in *ser-7* show various differing responses to food such as irregular pharyngeal pumping

(Hobson *et al.* 2006). MOD-5 is the reuptake transporter which clears serotonin from the synaptic cleft after release (Ranganathan *et al.* 2001).

1.6.3.6 Dopamine

In *C. elegans*, dopamine is involved in modulating locomotion in response to environmental cues, and learning particularly in food-seeking behaviours (Hills, Brockie and Maricq 2004; Sawin, Ranganathan and Horvitz 2000). Dopamine is proposed to have a role in slowing in the presence of food. It has a role in the area-restricted search behaviour, which is triggered by encountering food and keeps worms in an area where it is likely to encounter food again by increasing the number of high-angled turns. Mutations in *cat-2*, which encodes a tyrosine hydroxylase that synthesises dopamine, are deficient in this behaviour. Application of exogenous dopamine was also shown to be sufficient to increase the number of high-angled turns (Hills, Brockie and Maricq 2004). Additionally, dopamine is involved in the basal slowing response when a worm encounters food and slows its locomotion rate. Mutations in *cat-2* completely abolished this basal slowing response. The application of exogenous dopamine is sufficient to restore this response in *cat-2* mutants (Sawin, Ranganathan and Horvitz 2000). *Dat-1*, the reuptake transporter for dopamine, is necessary for thrashing behaviour in liquid (McDonald *et al.* 2007).

Four dopamine receptors have been identified in *C. elegans* (DOP1-DOP4) and are G-protein coupled receptors (Chase, Pepper and Koelle 2004; Suo, Sasagawa and Ishiura 2002; Suo, Sasagawa and Ishiura 2003).

1.6.3.7 Octopamine

Octopamine has a limited role in *C. elegans* neurobiology and is possibly involved in signalling starvation and low-food situations. Starvation triggers changes in gene expression such as the activation of CREB, cAMP response element-binding protein. CREB induces gene expression from genes containing a cAMP responsive element. The starvation-triggered induction of CREB expression was demonstrated to be dependent on SER-3, an octopamine receptor and TBH-1, a putative dopamine β -hydroxylate, which converts tyramine to octopamine (Suo, Kimura and Van Tol 2006). It has also been shown to be necessary to trigger the loss of body fat in *C. elegans* (Noble, Stieglitz and Srinivasan 2013). SER-6, OCTR-1 and SER-3 have been proposed to form octopamine receptors (Mills *et al.* 2012).

1.6.3.8 Tyramine

Tyramine is only present in low abundance in *C. elegans*. There is evidence that it may also have a role in signalling starvation. Application of exogenous tyramine inhibits pharyngeal pumping, which may be a food-deprivation response (Alkema *et al.* 2005). A gene encoding a receptor SER-2, has been identified (Rex and Komuniecki 2002).

1.6.3.9 Neuropeptides

Neuropeptides are short sequences of amino acids (4-20 amino acids in length) that either act directly at the synapse, or modulate synaptic activity in co-ordination with other neurotransmitters. Over 250 neuropeptides have been detected in *C. elegans* and there is evidence to show that they are involved in all aspects of *C. elegans* neurobiology. Over 113 genes in *C. elegans* are known to encode neuropeptides which give rise to the 250 neuropeptides detected by posttranslational modification (Li 2005).

Proneuropeptides are packed into dense core vesicles in the endoplasmic reticulum and kinesins are required for the vesicles' movement and neuropeptide release. Processing of the proneuropeptides occurs within these dense core vesicles to produce mature neuropeptides (Jacob and Kaplan 2003). Four propeptide convertases are involved in this process KPC-1, EGL-3, KPC-3 and KPC-4 (Thacker and Rose 2000). Fewer different mature neuropeptides were detected by mass-spectrometry in *C. elegans egl-3* mutants than in the wild-type N2 (Husson *et al.* 2006), showing the role of these propeptide convertases in production of these neuropeptides. Behavioural effects of mutations in *egl-3* include defects in egg-laying and impaired response to external stimuli (Kass *et al.* 2001).

The sheer number of different individual neuropeptides and the possibility of overlap in function make individual functions difficult to ascribe although some roles are beginning to be assigned. For example, *fhp-1* appears to be involved in locomotion. Mutants in *fhp-1* demonstrate hyperactivity and a more exaggerated waveform during movement (Nelson, Rosoff and Li 1998).

1.7 Cys-loop receptors

The cys-loop ligand-gated ion channels (cys-loop LGICs) are found in both vertebrates and invertebrates. They are likely to have evolved from an ancient bacterial counterpart, which may have acted in a chemosensory capacity (Tasneem *et al.* 2004). *C. elegans* has the largest known superfamily of cys-loop LGIC subunits in which over 102 members of this family have been identified and are involved in neurotransmission.

Cys-loop LGICs fall broadly into two categories - those which are cation permeable such as the serotonin and nicotinic acetylcholine receptors (nAChRs) and anion-permeable such as those gated by GABA and glutamate. There is also a class of cys-loop LGIC gated by acetylcholine which are cation selective. Some classes of cys-loop receptors seem to be unique to invertebrates such as those gated by glutamate and serotonin. Many of the putative cys-loop LGICs identified in *C. elegans*

have not yet been characterised, such as those belonging to the *ggr-1* group and the *ggr-3* group.

Cys-loop LGICs comprise five subunits forming a pentameric ring around a central channel pore. The receptors may be homomeric (consist of the same repeated subunit) or heteromeric (contain up to five different subunits). Different stoichiometries and combinations of subunits in heteromeric receptors can yield differing pharmacological properties and differing channel properties. This leads to a high diversity of potential receptors.

Each subunit consists of three main domains, the extracellular domain, the transmembrane domain and the intracellular domain. The extracellular domain contains the cys-loop after which the class of proteins is named. This is two cysteine residues forming a disulphide bond, and separated by 13 amino acids. The extracellular domain also contains various loops, which are involved in forming the ligand binding pocket. When arranged in the pentameric structure, the ligand binding site is between the interfaces of two subunits. In a homomeric receptor, there will be five identical ligand-binding subunits. In a heteromeric receptor, there will be fewer ligand binding sites as not all subunits will have ligand binding residues. A minimum of two ligand binding sites is believed to be required for efficient opening of the receptor (Rayes *et al.* 2009). The transmembrane domain consists of four membrane spanning α -helices. The second of these transmembrane helices is involved in lining the channel pore. The amino acid residues that face the channel pore affect ion selectivity and channel opening times. The third and fourth transmembrane domains are important for structural reasons. The intracellular M3-M4 loop is thought to be involved in the assembly of the receptor, targeting and trafficking and may also contain phosphorylation targets that may alter channel properties (Thompson, Lester and Lummis 2010).

On the binding of two ligands to the ligand binding domain, the extracellular domain moves and this movement is transduced to the second transmembrane region. Movement of this second transmembrane domain opens the channel.

1.7.1 Cys-loop receptors and anthelmintic drugs

The nAChRs and glutamate-gated chloride channels have attracted the most interest, as they are common targets for anthelmintic drugs (Jones and Sattelle 2008). GABA-gated cys-loop receptors have also been the target for new anthelmintic drugs, such as piperazine. As glutamate-gated chloride channels are unique to invertebrates, and the family of nAChRs is much larger in nematodes, they have been a common target for design of anthelmintic drugs.

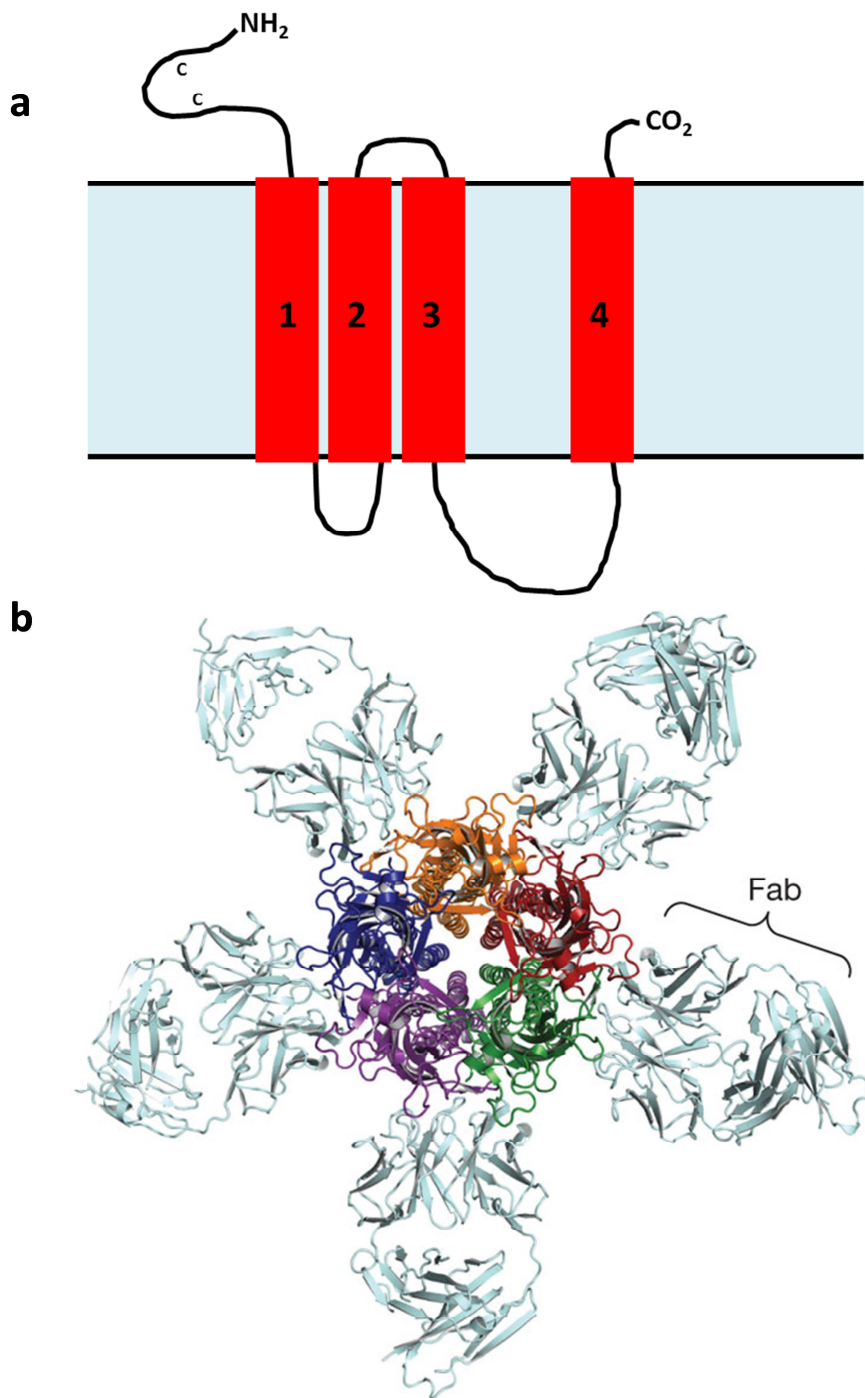


Figure 1-6: Schematic of cys-loop receptor subunit structure

a) The basic structure of a cys-loop receptor. The N-terminal extracellular domain contains the cys-loop and ligand binding loops. Four membrane spanning regions are present. The intracellular domain between M3 and M4 is the longest internal loop. b) X-ray structure of assembled cys-loop receptor (glutamate-gated chloride channel) arranged in a pentameric structure. Coloured units represent the cys-loop receptor subunits. Grey subunits represent fab fragment used to stabilise structure for X-ray crystallography. Diagram from Hibbs and Gouaux (2011).

The glutamate-gated chloride channels are the targets of the anthelmintic ivermectin. Discovered in the 1970s, it has been used extensively since to treat human-infecting and animal-infecting nematodes, as well as other parasites such as mites and ticks. In *C. elegans* ivermectin targets body-wall muscle, but causes paralysis of the pharynx more potently. Genes encoding subunits of the glutamate-gated chloride channels in *C. elegans* are *glc-1*, *glc-2*, *glc-3*, *avr-14*, *avr-15* and a putative channel *glc-4*.

Avr-14 and *avr-15* can each be alternatively spliced to produce two different subunit configurations. Due to this range of different subunits it is not yet established what configuration of subunits each glutamate-gated chloride channel exists in, and how many multiple forms of the receptor there may be (Yates, Portillo and Wolstenholme 2003). Co-expression of *glc-1* and *glc-2* in *Xenopus* oocytes yields a functional ivermectin sensitive-channel (Cully *et al.* 1994), although as *glc-2* expression appears to be restricted to the pharynx (Laughton, Lunt and Wolstenholme 1997) this association may not occur as a native glutamate-gated channel.

There is evidence that the subunits contribute different amounts of ivermectin sensitivity. The subunits *glc-1*, *avr-14* and *avr-15* are associated with susceptibility to ivermectin. A mutation in just one of these is not sufficient to cause ivermectin resistance - all three must be mutated before full resistance is achieved (Dent *et al.* 2000). *Avr-15* is expressed in the pharynx and is required for the regulation of pharyngeal pumping and for the sensitivity of the pharyngeal muscle to ivermectin (Dent, Davis and Avery 1997). Ivermectin was also found to bind to and activate GLC-3 when expressed in *Xenopus* oocytes (Horoszok *et al.* 2001) and this subunit may also play a role in forming ivermectin sensitive glutamate-gated chloride channels.

The nicotinic acetylcholine receptors present in the body-wall muscle are targets for anthelmintic drugs. Levamisole is a widely used anthelmintic, particularly used in veterinary applications to treat farm animals for nematode infection. ACR-16 forms a homomeric cys-loop receptor sensitive to nicotine, but insensitive to levamisole (Touroutine *et al.* 2005). The levamisole-sensitive nicotinic acetylcholine receptor of *C. elegans* is the main excitatory receptor at the neuromuscular junction and is comprised of the subunits LEV-1, LEV-8, UNC-29, UNC-38 and UNC-63 (Boulin *et al.* 2008; Lewis *et al.* 1980). Binding of levamisole to this receptor induces paralysis of the worm. A newly identified anthelmintic monepantel targets ACR-23, also present in the body-wall muscle (Rufener *et al.* 2013). Other nicotinic acetylcholine receptors are expressed in the neurons of *C. elegans*, such as the neuronal receptor comprised of UNC-63, UNC-29, ACR-12, ACR-2 and ACR-3 (Jospin *et al.* 2009).

1.8 Known aspects of neurobiology in plant-parasitic nematodes

In comparison to *C. elegans*, little is currently known about the neurobiology of plant-parasitic nematodes.

Studies in which exogenous neurotransmitters have been applied to the J2s of *M. hapla* and *H. glycines* have revealed there to be likely receptors for the biogenic amines in plant-parasitic nematodes as they are observed to affect nematode behaviours such as locomotion and stylet thrusting (Masler 2008; Masler 2007). Acetylcholine is likely to have a role, due to the effect that acetylcholinesterase inhibitors have on plant-parasitic nematodes. Application of acetylcholinesterase inhibitors initially increases body movement, and then causes a cessation of activity indicating that acetylcholine is building up at the neuromuscular junction, leading ultimately to paralysis (Wright, Birtle and Roberts 1984). Genes encoding acetylcholinesterases have been cloned from *M. incognita* and *G. pallida* (Costa *et al.* 2009; Laffaire *et al.* 2003). The roles of glutamate and GABA remain less well characterised (Holden-Dye and Walker 2011).

The neuropeptides are the best studied aspects of the neurobiology of plant-parasitic nematodes. They have roles in locomotion and are expressed in pharyngeal neurons and nerves surrounding the sensory apparatus, indicating a role in host-seeking behaviours (Kimber *et al.* 2001). Five *fip* genes so far have been cloned from *G. pallida* (Kimber and Fleming 2005) and 19 *fip* and 21 *nlp* genes have been identified from *M. incognita* (Abad *et al.* 2008). *In situ* hybridisation experiments in *G. pallida* allowed the expression patterns of these *fip* genes to be examined, in order to elucidate their role. *Gpfip-6* was expressed in the circumpharyngeal and perianal ring, although the interneurons identified were involved in many processes making a role difficult to ascribe. *Gpfip-12* is expressed in neurons innervating the muscles in the body wall, and is likely to have a role in locomotion. *Gpfip-14* is expressed in motor neurons around the head of *G. pallida*, and in nerves which receive input from the amphids. This suggests that *Gpfip-14* may have a role in responding to environmental cues and may be involved in host-seeking behaviour. *Gpfip-1* is expressed in the motor neurons in the retrovesicular ganglion, suggesting a role in the coordination of movement (Kimber and Fleming 2005). In *M. incognita* and *M. minor*, five genes encoding FLPS were identified using RACE PCR, designated *miflp-1*, *miflp-7*, *miflp-12*, *mmfip-12* and *miflp-14*. A combination of immunoreactivity and *in situ* hybridisation showed expression of these *fip* genes in the circumpharyngeal nerve ring, pharyngeal nerves and ventral nerve cord. These locations imply a role in locomotion and responding to sensory cues (Johnston *et al.* 2010)

The genome sequences of *M. incognita* and *M. hapla* have allowed comparison to *C. elegans*, identifying potential receptors for acetylcholine, serotonin and potential GPCR (Abad *et al.* 2008; Opperman *et al.* 2008). In *M. hapla* and *M. incognita*, 147 and 108 genes for GPCRs have been identified respectively.

The receptors that are targets for anthelmintic drugs (e.g. levamisole and ivermectin) have not yet been studied in detail in plant-parasitic nematodes and little is known about them.

Objective

The overall objective of this work is to investigate aspects of the neurobiology of *Globodera pallida* that may reveal potential selective targets for control of the potato cyst nematode. Analysis of cys-loop receptors involved in neurotransmission and associated mechanisms of sensitivity and resistance to anthelmintics will be facilitated by the wealth of data and resources available for *Caenorhabditis elegans* compared to plant parasitic nematodes. The complement of genes encoding cys-loop receptors in *Globodera* spp. will be defined and functional studies will provide insight into their roles in mediating observed behaviours and sensitivity to anthelmintics.

2. General Materials and Methods

2.1 Maintenance of nematodes

2.1.1 Maintenance of *Globodera pallida* populations

Globodera pallida (Pa 2/3) population Lindley was originally obtained from the James Hutton Institute. Nematodes were cultured on susceptible potato plants (*Solanum tuberosum* cv. Desiree) in a glasshouse growing in an equal mix of sand/loam. Cysts were stored in dry soil at 4°C.

2.1.2 Collection of cysts from infected soil

Cysts of *G. pallida* were extracted from the soil using the Fenwick canning method (Fenwick 1940). Briefly, infected soil was washed through a wide mesh sieve into a Fenwick can. Dense soil debris settled to the bottom, while the lighter cysts floated and were washed through a column of three different meshes (500 µm, 150 µm and 63 µm). Cysts were collected in the 150 µm mesh sieve, and washed into a fast flow filter paper (Whatman, UK) in a funnel with the end sealed. The mixture was allowed to stand for a few minutes then the water was released, leaving the cysts stranded in a ring around the top of the filter paper. The cysts were then collected using fine tweezers into a microcentrifuge tube containing water under a (stereo-binocular microscope).

2.1.3 Hatching of cysts for collection of J2s

Cysts were prepared for hatching by a bleaching method (Heungens *et al.* 1996) using a modified 20 ml syringe with the end cut off and replaced by a 30 µm nylon mesh. Cysts were put in the syringe, and washed in 5 ml of 100 % ethanol for 30 seconds. The cysts were then treated with 10 ml 1% hypochlorite solution for 12 minutes or until sufficient numbers of the cysts had lightened in colour and broken open to release eggs. The cysts were then washed in 5 ml of autoclaved tap water five times before the disrupted cysts and eggs were transferred to a ring with 30 µm mesh at the bottom, and placed in 10 ml of sterile tap water in a hatching jar. The eggs were then left to hatch at 20°C in darkness for three days before J2s were collected from the liquid outside the mesh on the fourth day. Collections of J2s were continued daily over five days, replacing the water taken each time. The collected J2s were stored at 10°C in water if not used immediately.

2.2 *C. elegans* strains

2.2.1 N2

Genotype: *C. elegans* wild-type; var. Bristol wild-type isolate. Available from the *Caenorhabditis* Genetics Centre (<https://www.cbs.umn.edu/research/resources/cgc>)

2.2.2 ZZ20

Genotype: *unc-38(x20)* I – deletion in third exon of *unc-38* gene. Phenotype: uncoordinated movement and levamisole resistance. Available from the *Caenorhabditis* Genetics Centre (<https://www.cbs.umn.edu/research/resources/cgc>)

2.2.3 DP38

Genotype: *unc-119 (ed3)* – mutagenised by EMS. Phenotype: uncoordinated, dauer defective. Available from the *Caenorhabditis* Genetics Centre (<https://www.cbs.umn.edu/research/resources/cgc>)

2.2.4 Maintenance of *C. elegans* populations

All *C. elegans* strains were maintained on NGM-lite media plates seeded with *Escherichia coli* (strain: OP50) at 20°C in the dark. 10 worms were transferred onto fresh plates approximately every 3-5 days to maintain a healthy population.

2.2.5 Production of NGM-lite media plates

1 L of NGM media contained 1.5 g NaCl, 4 g Peptone, 3 g KH₂PO₄, 0.5 g K₂HPO₄ and 20 g Agar. This was autoclaved, allowed to cool, and then cholesterol added to a final concentration of 8 µg/ml. Nystatin was added to a final concentration of 10 µg/ml. 10 ml of media was poured into 5 cm petri dishes and allowed to set. 50 µl of an overnight culture of *E. coli* (strain: OP50) was spread onto each plate and allowed to grow for two days at 20°C. For some experiments, which required a faster growing strain, *E. coli* (strain: HB101) was used.

2.2.6 Cleaning contaminated *C. elegans* stocks

If necessary due to bacterial or fungal infection of *C. elegans* stocks, a bleaching method was used to sterilise the affected lines. Contaminated plates containing gravid adults were washed with 4 ml sterile water into 15 ml polypropylene tubes. 0.5 ml 5 M NaOH and 0.5 ml bleach (10 % sodium hypochlorite) was added. The tube was shaken vigorously every 2 minutes for 10 minutes to dissolve adult carcasses and release eggs. The tube was centrifuged for 30 seconds at 1300 x g. Liquid was aspirated to 0.1 ml and sterile water added to 5 ml. The tube was centrifuged again, and aspirated to 0.1 ml. The cleaned pellet of eggs was pipetted onto the edge of a clean NGM-lite plate with *E. coli* OP50 lawn. The plate was checked for healthy hatched larvae after 24 hours, which were moved to fresh NGM-lite plates seeded with *E. coli* OP50.

2.3 Bacterial strains

Host strain	Routine use	Genotype
<i>E. coli</i> DH5α	Ultra-competent cells for cloning	F-, endA1, glnV44, thi-1, recA1, relA1, gyrA96, deoR, nupG, Φ80dlacZΔM15, Δ(lacZYA-argF)U169, hsdR17(rK- mK+), λ-
<i>E. coli</i> DB3.1	Propagating vectors containing ccdB operon	F- gyrA462 endA1 glnV44 Δ(sr1-recA) mcrB mrr hsdS20(rB-, mB-) ara14 galK2 lacY1 proA2 rpsL20(Smr) xyl5 Δleu mtl1
<i>E. coli</i> OP50	Food-source for <i>C. elegans</i>	Ura-
<i>E. coli</i> HB101	Food-source for <i>C. elegans</i>	F- mcrB mrr hsdS20(rB- mB-) recA13 leuB6 ara-14 proA2 lacY1 galK2 xyl-5 mtl-1 rpsL20(Smr) glnV44 λ-

2.4 Growth media

2.4.1 LB media

10 g NaCl, 10 g tryptone, 5 g yeast extract were added to 1 L ELGA water and autoclaved. 1 % bacteriological agar was added to make LB agar. Antibiotics were added at the following concentrations if required: Carbenicillin (100 µg/ml); spectinomycin (100 µg/ml); kanamycin (50 µg/ml).

2.4.2 SOB media

1.25 g yeast extract, 5 g tryptone, 0.146 g NaCl, 47 mg KCl, 0.508 g MgCl₂, 2.5 ml of 1M MgSO₄ in 250 ml deionised water. Solution was autoclaved.

2.5 General solutions composition

2.5.1 TE buffer

10 mM Tris HCL, 1 mM EDTA pH 8.0. Solution was autoclaved.

2.5.2 M9 buffer

3 g KH₂PO₄, 6 g Na₂HPO₄, 5 g NaCl in 1 L deionised water. Solution was autoclaved. After cooling, 1 ml of 1M MgSO₄ was added.

2.5.3 TB solution

0.302 g PIPES, 0.22 g CaCl₂, 1.86 g KCl in 80 ml deionised water. KOH or HCl was used to adjust pH to 6.7. 1.09 g of MnCl₂·4H₂O was added and the volume adjusted to 100 ml. Solution was then filter-sterilised with 0.45 µm filter.

2.5.4 DNA Extraction buffer

0.1 M NaCl, 10 mM Tris pH8, 10 mM EDTA, 1% SDS, 1% 2-Mercaptoethanol, 100 µg/ml proteinase K

2.5.5 Standard DNA quantification

When required, DNA was quantified using a Nanodrop 1000.

2.6 General molecular biology methods

2.6.1 Extraction of total RNA

Total RNA was extracted from whole frozen J2s using the Qiagen RNeasy Plant Mini kit, following the manufacturer's instructions. A sterile plastic homogeniser was used to thoroughly disrupt J2 tissue in 50 µl of ice-cold RLT buffer. 400µl of RLT buffer was added to the sample and the sample was placed in a QIAshredder spin column in order to remove undisrupted nematodes and other debris. Ethanol was added to the cleared supernatant, and the sample applied to a RNeasy spin column. A 20 minute DNase I digestion was performed to remove genomic DNA. The column was then washed with RW1 and RPE buffers. RNA was eluted from the column in 30 µl RNase-free water and stored at -80°C. Concentration and purity of RNA samples was determined using a Nanodrop spectrophotometer.

2.6.2 Phenol:chloroform extraction of genomic DNA

Extraction of genomic DNA was carried out using phenol:chloroform. Frozen J2s were homogenised in 300 µl extraction buffer. The volume was made up to 750 µl and 100 µl of 10% SDS was added, mixed by inversion and incubated at 65 °C for 10 minutes. 250 µl 5M potassium acetate was added, mixed by inversion and incubated on ice for 20 minutes. Debris was removed by centrifugation at 14,500 rpm for 20 minutes. The supernatant was removed to a fresh microfuge tube, and 0.5 ml isopropanol added, mixed by inversion, and incubated at -20 °C overnight to allow precipitation of DNA. The tube was centrifuged at 14,500 rpm for 15 min and the supernatant discarded. The remaining DNA pellet was resuspended in 100 µl of 50 mM Tris, 10 mM EDTA pH8. Debris was removed by centrifugation at 14,500 rpm for 5 min and supernatant transferred to a fresh microfuge tube. Equal volume of phenol:chloroform was added, and the mixture vortexed and centrifuged for 5 min. The upper aqueous phase was transferred to a fresh microfuge tube and 10 µl of 3M sodium acetate and 200 µl

ethanol was added. DNA was allowed to precipitate for 10 min. DNA was pelleted by centrifugation. Ethanol was removed, and the pellet washed with 0.5 ml of 70 % ethanol. The tube was centrifuged for 5 min, and ethanol removed. The pellet was air-dried for 15 min to allow all ethanol to evaporate. DNA pellet was redissolved in 50 μ l TE buffer and stored at -20 °C.

2.6.3 Preparation of cDNA

cDNA was prepared from total RNA using the protocol provided by the manufacturers (Superscript II Reverse Transcriptase, Invitrogen). Approximately 500 ng of total RNA was added to 1 μ l anchored oligodT primers, 1 μ l of 10 mM dNTPs and sterile, distilled water up to 12 μ l. This was incubated at 65°C for 5 minutes and then quick-chilled on ice. 4 μ l of 5x First Strand Buffer and 2 μ l of 0.1M DTT was added and incubated at 42°C for 2 minutes. 1 μ l of Superscript II Reverse Transcriptase (200 units) was then added and the mixture was incubated at 42°C for 50 minutes, followed by a 15 minute incubation at 70°C to inactivate the reaction. This produces single stranded cDNA complementary to the mRNA population as the oligodT primers anneal to the poly (A)+tails.

2.6.4 Preparation of ultra-competent cells

Ultra-competent cells for use in all cloning were prepared following the protocol described in (Inoue, Nojima and Okayama 1990). DH5 α bacterial cells were streaked onto LB agar plates, and cultured overnight at 37 °C. 10 – 12 single colonies were transferred to 2x 250 ml SOB medium in 1L flask and grown at 19 °C with vigorous shaking until an OD₆₀₀ of 0.5 was reached (24 - 36 hrs). Flasks were placed on ice for 10 min, and then the suspension was centrifuged at 4000 x g for 10 min at 4 °C. Cells were resuspended in 80 ml ice-cold TB solution and stored on ice for 10 min. The suspension was then centrifuged again at 4000 rpm for 10 min at 4 °C. The cell pellet was then resuspended in 20 ml ice-cold TB solution and 1.4 ml thawed DMSO was added. 100 μ l of the cells were aliquoted into microfuge tubes and snap-frozen in liquid nitrogen. Cells were stored at -80 °C until required for use.

2.6.5 Restriction digest

Routine restriction digests were performed in 20 μ l total volume. 1 μ g of plasmid DNA was used with 1 μ l of selected restriction enzyme(s). The appropriate buffer was selected as per recommendation from the manufacturer. The reaction was routinely incubated at 37 °C for 3 hrs.

3. Identification of orthologous genes from *Caenorhabditis elegans* in the *Globodera pallida* and *Globodera rostochiensis* genomes

3.1 Introduction

C. elegans has been used as a model organism for many parasitic-nematodes, despite the differences in lifestyles. *C. elegans* is free-living in the soil, while other parasitic nematodes have many different diverse lifestyles including animal-infecting and plant-infecting nematodes, which are specific to different hosts. Despite these differences in lifestyles, *C. elegans* remains a popular model organism to guide both genomic studies and drug-based studies on parasitic-nematodes.

The molecular basis of action of many popular anthelmintics has been discovered first in *C. elegans* such as the molecular basis of ivermectin resistance (Dent *et al.* 2000; Cully *et al.* 1994), rather than within the parasitic nematode that is the intended target. Ivermectin is typically used to treat both human and animal infecting nematodes and has been credited with controlling devastating nematode diseases such as river blindness, caused by *Onchocerca volvulus*. *C. elegans* remains at the core of research regarding anthelmintic drugs due to the intractability of transformation and laboratory maintenance of many parasitic nematodes. It remains a valuable resource for investigating increasing incidences of ivermectin resistance in nematode populations (Geary 2005).

With the reducing cost of genome sequencing technology allowing the full genome sequences of many parasitic nematodes to be analysed, *C. elegans* remains at the forefront of comparative genomics for newly sequenced nematode species. Of particular interest is the diversity of subunits for known targets of anthelmintic drugs, and other neuromuscular targets. Comparisons of the newly sequenced nematode genome, with the *C. elegans* genome and the wealth of functional data behind it, allows areas of interest to be highlighted due to the under or overrepresentation of orthologues in the parasitic genome due to duplications or losses that have occurred during the evolutionary timeline.

Comparison to the genome of the ruminant-infecting nematode *Haemonchus contortus* has identified 5,937 orthology groups between *C. elegans* and *H. contortus* and highlighted a number of orthology groups in which *H. contortus* has a significant expansion in number of members. Included in this are the glutamate-gated chloride channel subunits, where two genes *hco-glc-5* and *hco-glc-6* are present in the *H. contortus* genome but absent in the *C. elegans* genome (Laing *et al.* 2013). *Hco-glc-6* is likely to be involved in ivermectin sensitivity of *H. contortus*. Expression of *hco-glc-6* in ivermectin insensitive *C. elegans* mutants was able to restore ivermectin sensitivity

(Glendinning *et al.* 2011). Other targets identified by comparative genomics may guide further research.

In the genome sequence of the animal-infecting nematodes *Brugia malayi* and *Trichinella spiralis*, a reduction in the number of genes encoding glutamate-gated chloride channels subunits was found, following a general trend of a reduction in number of cys-loop type subunits in these species (Williamson, Walsh and Wolstenholme 2007).

The *G. pallida* genome was sequenced recently in partnership with the Wellcome Trust Sanger Institute. A number of other plant-parasitic nematode genomes have also been published such as the root-knot nematodes *Meloidogyne incognita* (Abad *et al.* 2008) and *M. hapla* (Opperman *et al.* 2008), although the *G. pallida* genome was the first sequenced for a cyst-nematode. The draft sequence was completed in late 2013, although earlier iterations of the data set have been available from 2012. A mixture of 454, Illumina and Sanger sequencing were used to produce the *G. pallida* genome. In addition to the genome sequence, transcriptome data sets were produced at different significant life-stages of the *G. pallida* life-cycle: J2s, females 7 dpi (days post infection), 14 dpi, 21 dpi, 28 dpi and 35 dpi and males. This allowed examination of the expression levels of genes at different life-stages indicating changes in the suite of genes required at pre-parasitic and parasitic stages. This expression level was quantified for each life-stage. The number of RNA-seq reads per gene model is counted and normalised by RPKM (reads per kilobase per million) to account for the increased likelihood of longer transcripts having more transcripts matched to their region (Cotton *et al.* 2014).

As an addition to the *G. pallida* sequencing project, a draft genome sequence of *G. rostochiensis* was produced. Transcriptome data were also produced for the J2 and sedentary female life-stages of *G. rostochiensis*. As technology and methodology had improved since the assembly of the *G. pallida* genome, and the *G. rostochiensis* population used for sequencing had lower genetic diversity (Bendezu *et al.* 1998) in the UK, this genome assembly proved to be a useful comparison and checkpoint for research in *G. pallida*.

In this chapter, the focus is on key aspects of the neurobiology of *G. pallida* and *G. rostochiensis*. As with previous work on other parasitic-nematodes, *C. elegans* has been used to guide this work allowing comparisons to be made and conclusions about the expansion or reduction in members of orthologue groups to be drawn. The genes encoding the key enzymes involved in the biosynthetic pathways of neurotransmitters, as well as key genes encoding subunits for known and potential targets of anthelmintic drugs are the focus of this chapter. Here the best orthologues of *C. elegans* genes are identified in *G. pallida* and *G. rostochiensis* and differences between the species are identified.

Aims

- Identify best orthologues for a variety of neurotransmitter related genes
- Highlight areas of difference between *C. elegans* and *G. pallida*

3.2 Materials and methods

3.2.1 Homology searching and cloning using the *Globodera pallida* genome assembly

The *Globodera pallida* genome assembly, located on the WTSI (Wellcome Trust Sanger Institute, available at <https://www.sanger.ac.uk/resources/downloads/helminths/globodera-pallida.html>) was used for primary orthology searching. A list of genes, and their roles, that were searched for are found in Table 1. The BLAST server on the WTSI site allowed identification of potential homologues to *C. elegans* proteins used as the initial search query. Protein sequences were used in TBLASTN searches against the *G. pallida* genome assembly (scaffolds) (May 2012) database. Positive hits provided location of the identified gene on the most current genome assembly. The April 2012 assembly was viewed on Gbrowse, and checked visually to identify issues with the computer generated predicted gene models. As predicted gene models were often unclear or incorrect, several primers were often designed per gene in order to amplify full-length product. Sites of primer design were selected to be upstream of the predicted initiating methionine, and downstream of the predicted stop codon and within areas of gene expression. A list of primers used to amplify final full-length products is found in Table 2.

3.2.2 Amplification and cloning

Genes were amplified and cloned as detailed in sections 3.2.13 and 3.2.14.

3.2.3 Quality control of sequences obtained

Upon cloning and sequencing, in order to determine if a potential orthologue of a *C. elegans* gene had been obtained, the Reciprocal Best Hits (RBH) method was used. The translated sequence was used in a reciprocal BLASTP search against the *C. elegans* protein database located at NCBI (<http://blast.ncbi.nlm.nih.gov/Blast.cgi?PAGE=Proteins>). If the original *C. elegans* gene used to find this potential orthologue also had the lowest e-value in this search, the *G. pallida* gene obtained was considered to be a potential orthologue for this *C. elegans* gene and given the name *gpa-genename*. If a different *C. elegans* gene was returned with the lowest e-value, and this gene matched the *G. pallida* gene with a lower e-value, the identity of the cloned *G. pallida* gene was revised to be an orthologue of this. If multiple potential orthologues were identified in *G. pallida* and both potential orthologues returned the same RBH in the *C. elegans* database, both these genes were considered potential orthologues and given the names *gpa-genename.1* and *gpa-genename.2*.

To determine if a full-length clone had been obtained, the translated amino acid sequence of the product was checked for features to confirm the identity of the gene and confirm if it was full-length. The presence of a signal peptide was searched for in

proteins known to be targeted to the membrane (See 3.2.8). Additionally, the number of transmembrane domains was predicted (See 3.2.9) for membrane-spanning proteins and compared against the known number for similar proteins in the NCBI database. An alignment between the amino acid sequences of the *C. elegans* and *G. pallida* proteins was used to identify potential gaps or variations in sequence. Interpro was also used in some circumstances to identify key domains associated with proteins of interest (<http://www.ebi.ac.uk/interpro/>).

3.2.4 Analysis of transcriptome assembly and unassembled 454 reads

In some cases, the assembled genome visible on Gbrowse had limitations which only became apparent at a later date. Such issues included: unassembled portions of genes absent from the gene model, but present on other contigs; misassembly errors where a portion of a gene had been repeated obscuring the true sequence and instances where whole genes had either not been predicted (but were present in the assembly) or had been omitted from the assembly entirely.

In order to identify genes where small portions (e.g. the start or end) were missing, the original unassembled 454 reads could be used to assemble the gene manually. TBLASTN searches were conducted on the *G. pallida* unassembled 454 reads database located at WTSI (<https://www.sanger.ac.uk/resources/downloads/helminths/globodera-pallida.html>) using the closest known sequence to the start or end of the gene. The resulting 454 reads were then used to assemble the gene manually, using several rounds of TBLASTN to identify more up or downstream sequence.

The unmapped transcriptome assembly for the J2 life-stage could be mined. This was a *de novo* J2 transcriptome assembly produced alongside the *G. pallida* genome (Cotton *et al.* 2014). This assembly could be searched using command-line BLAST tools available from NCBI (http://blast.ncbi.nlm.nih.gov/Blast.cgi?CMD=Web&PAGE_TYPE=BlastDocs&DOC_TYPE=Download). A searchable database was produced on a local computer drive using .fasta files containing transcriptome data. TBLASTN searches were then carried out via command-line input to identify orthologues present in the transcriptome assembly. This method highlighted several genes which were completely absent in the final genome assembly.

Genes	Role
<i>cel-glc-1; cel-glc-2; cel-glc-3; cel-avr-14; cel-avr-15</i>	Subunits of glutamate-gated chloride receptors; target of ivermectin
<i>cel-mod-5; cel-ser-7</i>	Involved in serotonin signalling
<i>cel-tph-1</i>	Involved in serotonin biosynthesis
<i>cel-eat-4</i>	Glutamate transporter
<i>cel-dat-1</i>	Involved in dopamine biosynthesis
<i>cel-unc-25</i>	Involved in GABA biosynthesis
<i>cel-cha-1; cel-unc-17</i>	Involved in acetylcholine biosynthesis
<i>cel-tbh-1</i>	Involved in octopamine biosynthesis

Table 1: Summary of *C. elegans* genes and their roles searched for in initial orthology search

Gene	Primer Sequence
<i>gpaavr-14.1</i>	F: CCTCCGACTCGTGGAAAATCC R: GCCATTACATCAAATAGACG
<i>gpaavr-14.2</i>	F: GCCAAAATGTCTTCGGC R: GATCAGCAACACTATGAAATGATC
<i>gpa-cha-1</i>	F: AAAGGGGAATGAACGAGGAG R: TGTGCTTCTATAGTTTCATTG
<i>gpa-dat-1</i>	F: GATGCCACGATTGTTCAAT R: CTTCTACAACAGCACATCGC
<i>gpa-eat-4</i>	F: GATCACAGATGCATTCTTCAAG R: AGAGAGTATCCAAATGATCAG
<i>gpa-glc-2</i>	F: AAATTTTGTGCCGTTTG R: TAACATTTGCCAATTATTG
<i>gpa-glc-3</i>	F: GTGACCCGTCTCGGACACGCA R: TGGCCGTCGTATGGTTAGATG
<i>gpa-glc-4</i> (did not produce product)	F: CCTCCGGCGATGCTTACC R: CGGCTTCATTGGCGAACTC
<i>gpa-mod-5</i>	F: GACGAGAACACGACCACG R: CGCTTTCTTCTAAAGGTGC
<i>gpa-ser-7</i>	F: GTTCAGGCCATGCCAAAT R: CGGTAGTTGCCAACGC
<i>gpa-tph-1</i>	F: GTAAAAATGGCTCCGGCATG R: CACTCAATTAGTTGAAATAG
<i>gpa-unc-17</i>	F: ATGGCGCAATGTTTAAATGAC R: GCTAACAAATAAGCGAGGTT
<i>gpa-unc-25</i>	F: AAGCACACGACGAGCAGTGAC R: TTGTCCCGCGCAATTTCGTC

Table 2: Primers used to amplify full-length products from *G. pallida* (unless otherwise specified)

3.2.5 Homology searching in the *Globodera rostochiensis* genome

The *G. rostochiensis* genome was used as both comparison and checkpoint for orthologues identified in *G. pallida*. These two species are closely related, although the *G. rostochiensis* population in the UK is less genetically diverse than the *G. pallida* population. Sequencing of the *G. rostochiensis* genome followed the sequencing of *G. pallida*.

Following sequencing and gene prediction, the genome data and transcriptome data could be accessed. Translated sequences of *C. elegans* genes were used in BLAST searches (powered by Badger (Elsworth, Jones and Blaxter 2013) available at <http://globodera.bio.ed.ac.uk/search/species>) to identify potential orthologues of these genes. The RBH method was used to check potential orthologues. The gene model was then viewed on the genome browser Apollo (Lewis *et al.* 2002) (available at <http://apollo.nematodegenomes.org/apollo-1.0.4-RC3/sequences>) and as manually curated based on information available from transcriptome data; available *C. elegans* data and known sequences of cloned *G. pallida* genes.

3.2.6 *C. elegans* sequence

C. elegans sequences were identified from the NCBI protein database (<http://www.ncbi.nlm.nih.gov/>). In cases where multiple isoforms of the *C. elegans* protein were available, the longest was selected. Uniprot (UniProt 2015) was used to annotate amino acid sequence, if reviewed information was available.

3.2.7 Producing alignments and calculating amino acid identity

Alignments between amino acid sequences was performed using the multiple-sequence alignment tool Clustal Omega, found at <http://www.ebi.ac.uk/Tools/msa/clustalo/> (Sievers *et al.* 2011). This alignment was visualised in Jalview (downloadable from <http://www.jalview.org/download>). Amino acid identity between pairs was determined within Jalview by the Needleman and Wunsch methodology of pairwise alignments and a BLOSUM62 matrix (Waterhouse *et al.* 2009).

3.2.8 Signal peptide prediction

SignalP V4.1 was used to predict presence of signal peptides (Petersen *et al.* 2011). Translated cDNA to amino acid sequence was used. SignalP is available at <http://www.cbs.dtu.dk/services/SignalP/>. Examples of output from the program showing a positive and negative result can be seen in Figure 3-1.

3.2.9 Transmembrane domain prediction

The presence and number of transmembrane domain regions was predicted using TMHMM Server V2.0 (Krogh *et al.* 2001). Phobius was also used as a comparison as a

different prediction model is used and models may vary (Käll, Krogh and Sonnhammer 2007). TMHMM is available at <http://www.cbs.dtu.dk/services/TMHMM-2.0/> and Phobius is available at <http://phobius.sbc.su.se/>.

3.2.10 RaptorX 3D protein modelling

3D models of protein structure were generated by the webserver RaptorX (<http://raptorgx.uchicago.edu/>). RaptorX predicts secondary and tertiary structures of amino acid chain by incorporating sequence-based model prediction alongside sequence-based alignment models. The algorithm produces a p-value indicating the likelihood of the model generated being a result of a random string of amino acids. P-values of less than 10^{-3} are indicative of good models (Peng and Xu 2011).

3.2.11 Phylogenetic trees

Phylogenetic relationships were drawn from Clustal Omega aligned sequence using TOPALI v2.5 (PhyML, WAG substitution model, bootstrap value: 500) (Milne *et al.* 2009) and visualised using FigTree (Rambaut 2009). Topali v2.5 is available to download at <http://www.topali.org/> and FigTree is available to download at <http://tree.bio.ed.ac.uk/software/figtree/>

3.2.12 Bioassays

3.2.12.1 Application of exogenous serotonin to *G. pallida* J2s

20 J2s were added in 90 µl water on a glass slide. 10 µl of 62.5 mM serotonin (treated) or 10 µl water (control) was added. After 10 minutes J2s were observed for stylet thrusting under 40 x magnification. Individual J2s were observed for 60 secs and number of stylet thrusts counted.

3.2.12.2 Application of exogenous octopamine to *G. pallida* J2s

Speed of J2s was assessed as described in 5.2.1.2, except plates were made to contain 50 mM octopamine (treated) or M9 (control). Speed was assessed after four hour exposure and 24 hour exposure.

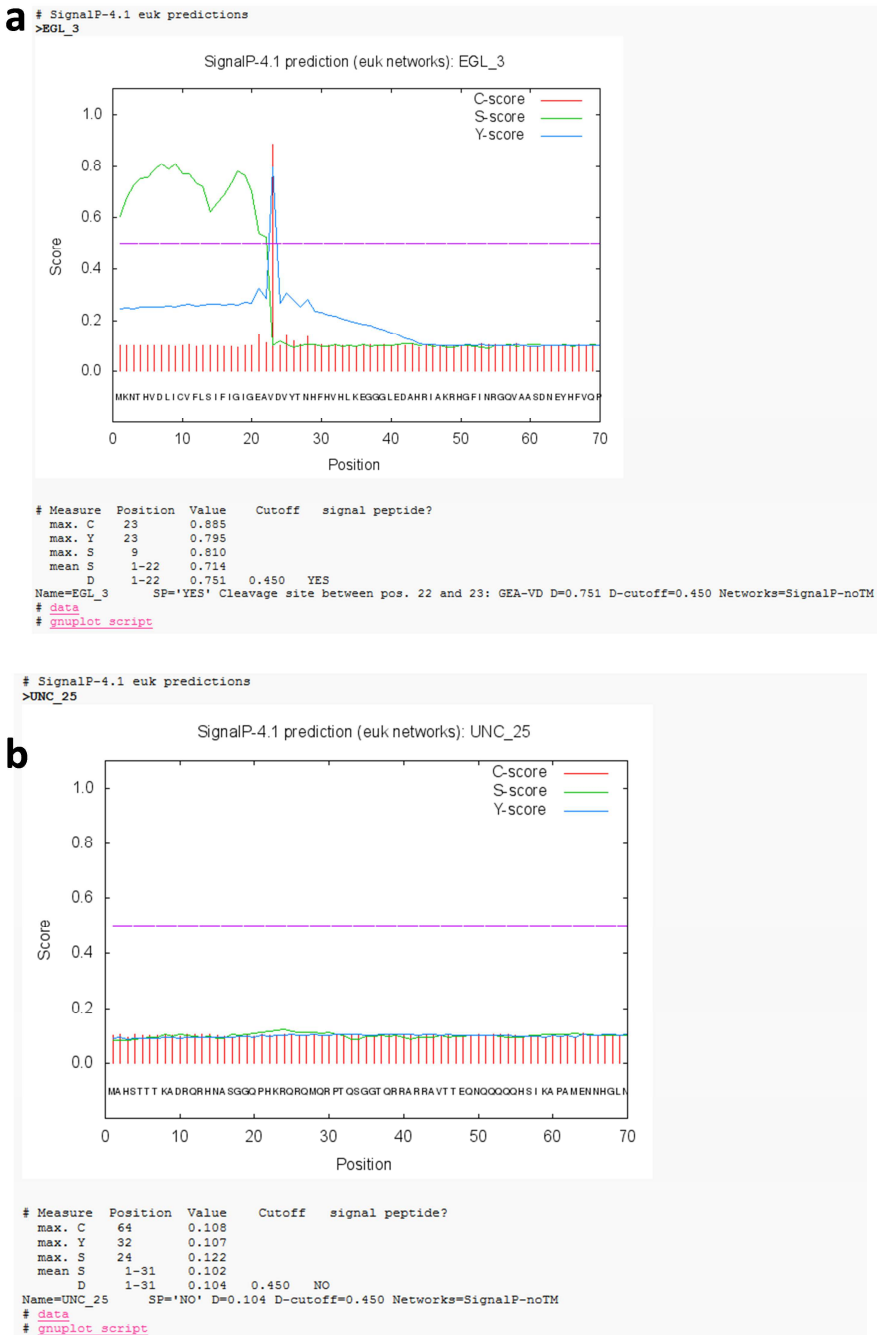


Figure 3-1: Examples of positive and negative signal peptide prediction outputs generated by SignalP v4.1

a) Output for amino acid sequence (EGL-3) with a positive signal peptide prediction. Cleavage site is predicted between amino acid residues 22 and 23. b) Output for negative signal peptide (UNC-25) prediction. C score predicts probability of the signal peptide cleavage site, the S score predicts signal peptide sequence and the Y score combines both C and S score to determine maximum likely signal peptide cleavage location.

3.2.13 Product amplification by polymerase chain reaction and product isolation

3.2.13.1 Screening for working primer pairs

PCR was conducted using a total reaction volume of 50 µl containing 0.2 mM of each dNTP, 1 µM each of the forward and reverse primer; MgCl₂ at 2 mM, 1 unit of Platinum Taq (Invitrogen), the appropriate buffer and template cDNA. The thermocycling program was conducted on a Biorad Thermocycler (T100) and comprised of an initial denaturing step at 94°C for 2 min, 30 steps of denaturing at 94°C for 30 secs, annealing at 55°C for 1 minute, and an extension at 72°C for 3 min (1 min/kb of amplified product). A final extension step of 10 min at 72°C was used. PCR products (5 µl) were analysed by agarose gel electrophoresis.

3.2.13.2 Gradient PCR for optimisation of amplification

The annealing temperature can affect the successful amplification of the correct PCR product. A master mix totalling 90 µl with the same protocol as in 3.2.13.1 was used for each primer combination and 10 µl was pipetted into an 8-strip PCR tube. The thermocycler was used on the same settings as in 3.2.13.1, except the annealing temperature was set to perform a gradient across the plate. Annealing temperatures used were 50°C, 51.0°C, 52.9°C, 55.7°C, 59.1°C, 62.0°C, 63.8°C and 65°C. The PCR products were analysed by gel electrophoresis and the optimum annealing temperature chosen. An example of gradient PCR is shown in Figure 3-2.

3.2.13.3 Amplification of products for cloning

Products for cloning were prepared as 3.2.13.1 with the exception that the enzyme used was Platinum Taq Hi-Fidelity (Invitrogen) which has a proof-reading component. Extension temperature was 68°C. Products were analysed by gel electrophoresis.

3.2.13.4 PCR clean-up

PCR reactions yielding a single product were cleaned using a QIAquick PCR Purification Kit to removed unincorporated nucleotides and primers. 5 volumes of buffer PB was added to the PCR sample. pH of the solution was assessed by a colour indicator. If required, 10 µl of 3 M sodium acetate was added to bring the solution to an efficient pH for DNA binding. The mixture was added to a QIAquick spin column to bind DNA, and centrifuged for 30 sec. The flow-through was removed, and the membrane was washed by addition of 0.75 ml PE buffer. Flow-through was removed, and the column centrifuged again for 1 min to remove excess PE buffer from the membrane. DNA was eluted in 30 µl EB buffer and stored at -20 °C.

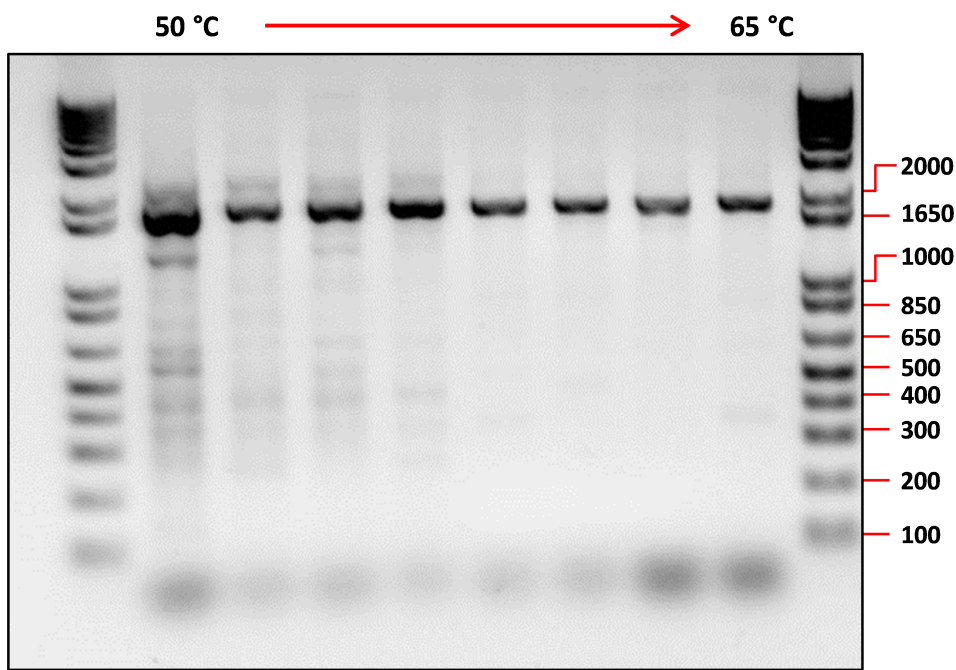


Figure 3-2: Selection of optimum annealing temperature by gradient PCR

A reduction in non-specific amplification of undesired bands is seen as annealing temperature increases. Good amplification of the desired product (1.8 kb) without non-specific amplification is seen at an annealing temperature of 62 °C and above.

3.2.13.5 DNA isolation from agarose gel

PCR reactions yielding multiple products required isolation of the correct product size. Products were separated by gel electrophoresis and the correct product size excised from the gel. DNA extraction from the gel slice was carried out using the Qiagen Gel Extraction Kit. 3 times volume of QG buffer was added to the gel slice, and solubilised at 50 °C. The mixture was then added to a QIAquick column for DNA binding. The column was centrifuged for 30 sec and the flow-through discarded. 0.75 buffer PE was added to wash the column, and centrifuged again. The flow-through was discarded and the column centrifuged to remove excess PE from the membrane. DNA was eluted in 30 µl EB buffer and stored at -20 °C.

3.2.14 Cloning and sequencing

3.2.14.1 A-tailing of PCR products

Purified PCR product was used in an A-tailing reaction to ensure maximum number of A-tailed PCR products for TOPO TA cloning. For each product, a 10 µl reaction was set up with 0.2 mM dATP, 5 units of Biotaq red (Bioline, UK), 2 mM MgCl₂, the appropriate buffer, and PCR product up to 10 µl. This was incubated at 72°C for 30 minutes.

3.2.14.2 Cloning reaction

pCR™8/GW/TOPO® TA Cloning® kit (Invitrogen) (Figure 3-3) was used to clone freshly amplified PCR products following the protocol stated by the manufacturer. Briefly, 4 µl of the freshly A-tailed PCR product was used in a cloning reaction along with 1 µl salt solution and 1 µl of cloning vector. The cloning reaction was allowed to proceed for 10 minutes at room temperature before being placed on ice.

3.2.14.3 Transformation

2 µl of the cloning reaction were added to One-Shot® *E. coli* competent cells (Invitrogen) on ice. The cells were heat-shocked in a water-bath at 42°C for 30 seconds before 250 µl of LB media at room-temperature was added to each transformation. The cells were allowed to recover at 37°C for 1 hour in an incubator shaking at 200 rpm. Cells were then plated out onto LB-agar containing spectinomycin (Sigma) at 100 µg/ml and allowed to dry under a Bunsen burner for 15 minutes. Plates were then incubated at 37°C overnight.

3.2.14.4 Screening of colonies by Colony PCR

Selection of colonies containing plasmids with the correct insert in the correct orientation was achieved by PCR analysis using the M13F (-20) primer as the forward primer, and the gene-specific reverse primer. A pipette tip was touched briefly to an individual colony, and the bacteria re-suspended in 20 µl of autoclaved ELGA water.

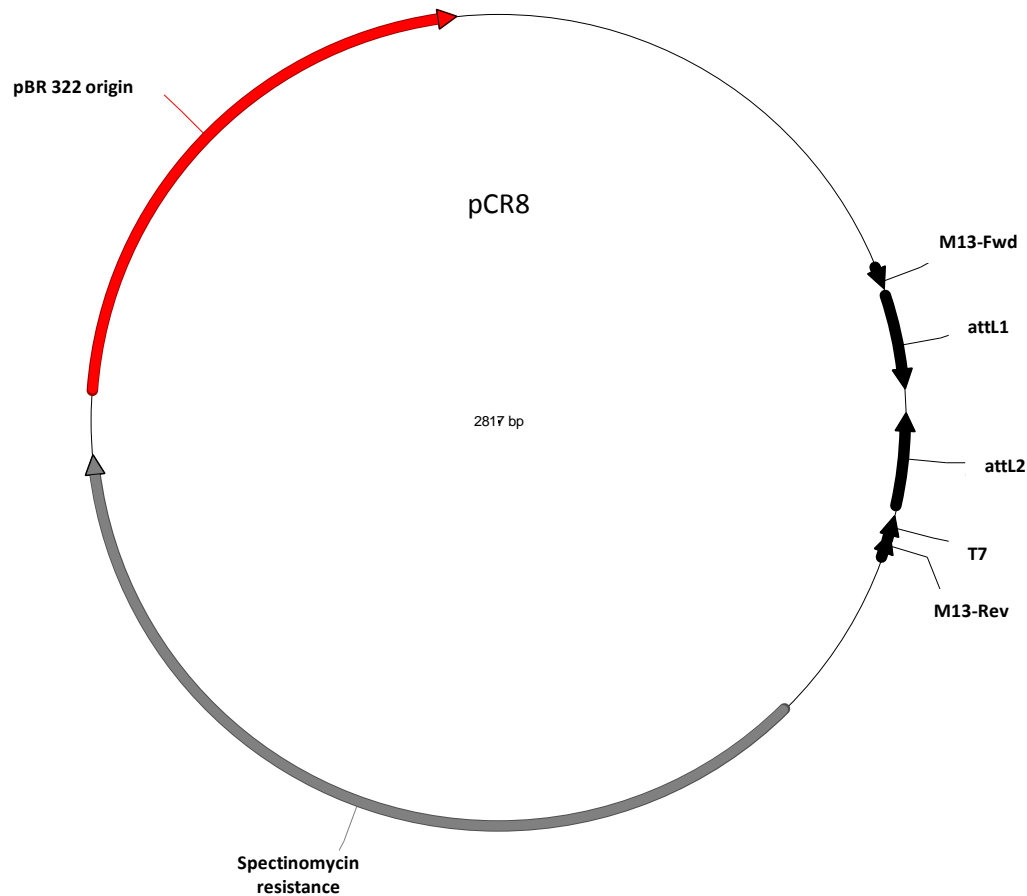


Figure 3-3: Vector map of pCR™8/GW/TOPO®

pCR™8 was used for gene cloning. The plasmid contains a spectinomycin resistance gene for antibiotic selection. The plasmid is provided by the manufacturer linearised at the attL1 and attL2 sites with Topoisomerase I covalently linked to the ends. M13 F, M13 R and T7 primers can be used to sequence the insert.

A master mix per primer pair was produced that comprised of 0.4 mM of each dNTP, 1 µl of both the forward and reverse primer, 10 µM MgCl₂ at 2 mM, the appropriate buffer and 2 units of BIOTAQ red (Bioline) per 20 µl of reaction. 1 µl of the bacterial suspension was added to 19 µl of the master mix. The amplification reaction was carried out by an initial denaturing step at 94°C for 10 min to break open the bacterial cells. 25 steps of denaturing at 94°C for 30secs, annealing at 55°C for 30 secs, then extension at 72°C for 90 secs (30 secs/kb of amplified product) followed. The PCR product was analysed by gel electrophoresis allowing positive colonies to be identified.

3.2.14.5 Plasmid preparations

Colonies identified as per 3.2.14.4 were grown in 5 ml LB broth with 100µg/ml spectinomycin at 37 °C overnight. To extract plasmid, 3 ml of the culture was used and prepared with the QIAprep Spin Miniprep Kit (Qiagen) according to manufacturer's instructions. Briefly, 3 ml of cultured colonies was centrifuged at 6800 x g to pellet bacterial cells. The supernatant was discarded and 250 µl of buffer P1 with RNase A was added. The bacterial cells were resuspended and 250 µl of buffer P2 was added and mixed. 350 µl of buffer N3 was added, mixed and centrifuged for 10 minutes at 17,900 x g. The supernatant was transferred to a QIAprep spin column and centrifuged for 30 secs to bind DNA. The QIAprep spin column was washed with 500 µl of PB buffer, centrifuged and the flow-through discarded. 750 µl of PE buffer was added and centrifuged for 60 seconds and the flow-through discarded. The column was centrifuged for an additional 60 seconds to remove all traces of PE buffer. Plasmid DNA was eluted in 50 µl EB buffer.

3.2.14.6 Sequencing of plasmid inserts

Sequencing of plasmid insert was carried out by Beckmann Coulter Genomics, UK using the M13F and M13R primers. A minimum of three clones were sequenced for each gene. Sequencher 5.2.2 (Gene Codes) was used to analyse sequencing results.

3.3 Results

Unless specified otherwise, all *G. pallida* genes discussed in this section have been cloned and sequenced from cDNA, while data from *G. rostochiensis* is bioinformatic, although manually curated. In this section, orthologues of the *C. elegans* gene (*cel-genename*) identified as the best match in *G. pallida* and *G. rostochiensis* are given the nomenclature *gpa-genename* and *gro-genename* respectively. The translated amino acid sequence is used to assess features of the protein. Percentage amino acid identity is given as those which match exactly, but does not take into account positives (which are amino acids which share similar characteristics). Percentage identity between the orthologous *G. pallida* gene and the *G. rostochiensis* gene is typically over 90%.

3.3.1 Acetylcholine genes – metabolism and synthesis

Genes involved in the synthesis and metabolism of acetylcholine were identified and cloned from *G. pallida* and identified in *G. rostochiensis*.

3.3.1.1 *Cel-cha-1*

Cha-1 encodes a choline acetyltransferase which synthesises acetylcholine. The orthologue of Cel-CHA-1 found in *G. pallida* shared 40% identity with Cel-CHA-1 and in *G. rostochiensis*, 42% amino acid identity was shared with Cel-CHA-1. This low percentage identity is likely due to an expanded region of 73 amino acids in *G. pallida* and *G. rostochiensis* genes which shares no homology to Cel-CHA-1 located between position 185 and 186 of the Cel-CHA-1. Potential residues involved in enzyme function can be identified in the *G. pallida* sequence such as co-factor binding and proton acceptor sites (Alfonso *et al.* 1994) (Figure 3-4).

3.3.1.2 *Cel-unc-17*

Cel-unc-17 is a synaptic acetylcholine transporter. The best orthologue identified in *G. pallida* and *G. rostochiensis* shared 63% and 58% amino acid identity with Cel-UNC-17 respectively. As Cel-UNC-17 is a membrane bound transporter, TMHMM was used to predict the number of transmembrane domains. Cel-UNC-17 has 12 transmembrane domains, and in Gpa-UNC-17, 12 transmembrane domains are predicted by TMHMM. Predicted N-glycosylation sites (Alfonso *et al.* 1993) from Cel-UNC-17 are present (Figure 3-5).

In *C. elegans* *cel-cha-1* and *cel-unc-17* are in an operon structure with *cel-cha-1* directly downstream of *cel-unc-17* (Rand 1989). In both *G. pallida* and *G. rostochiensis*, this operon-like structure seems to be maintained, although evidence could not be found of the shared untranslated exon (Figure 3-6).

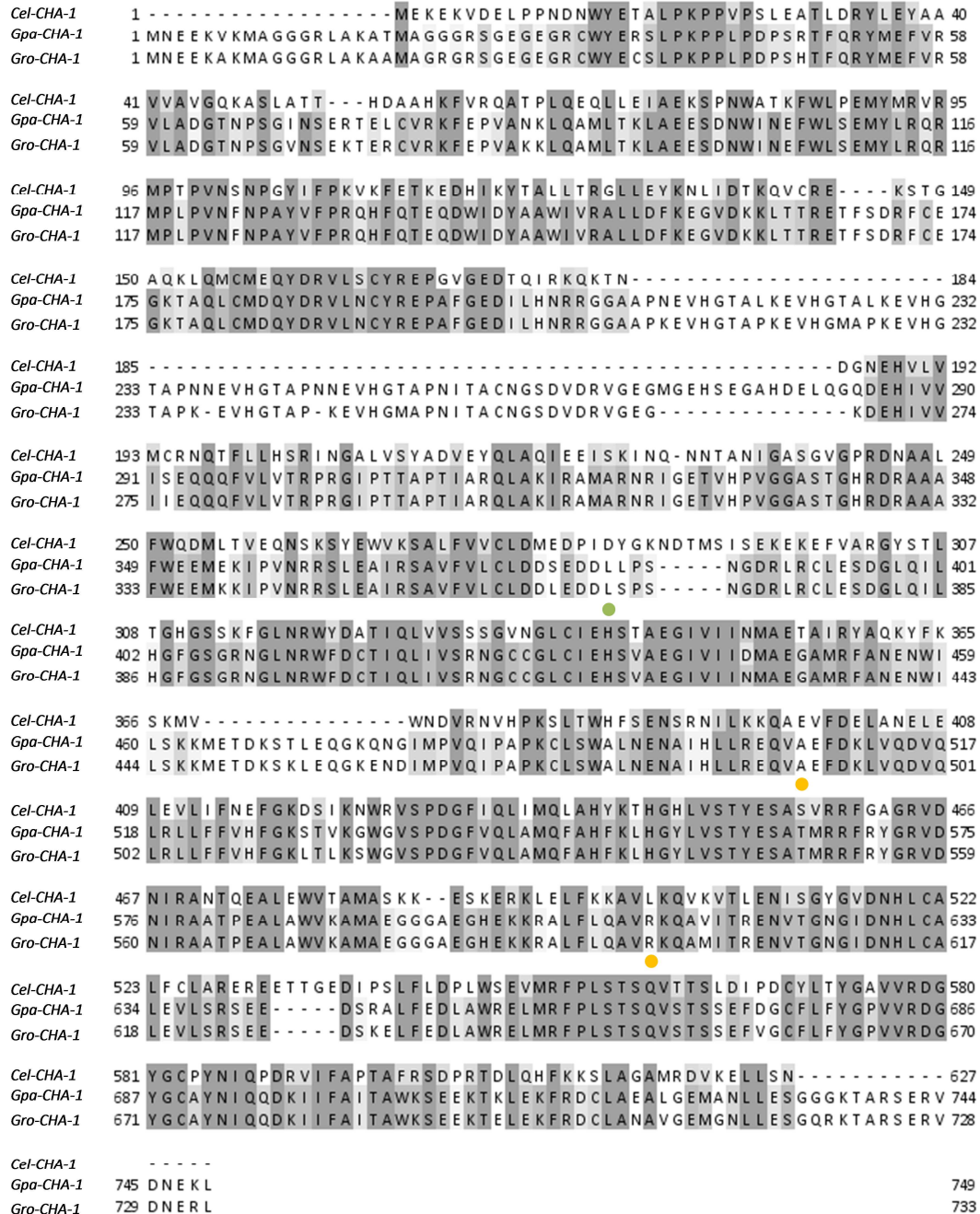


Figure 3-4: Amino acid alignment of Cel-CHA-1 with Gpa-CHA-1 and Gro-CHA-1

Green circle indicates proton acceptor site. Orange circle indicates residues involved in cofactor binding.

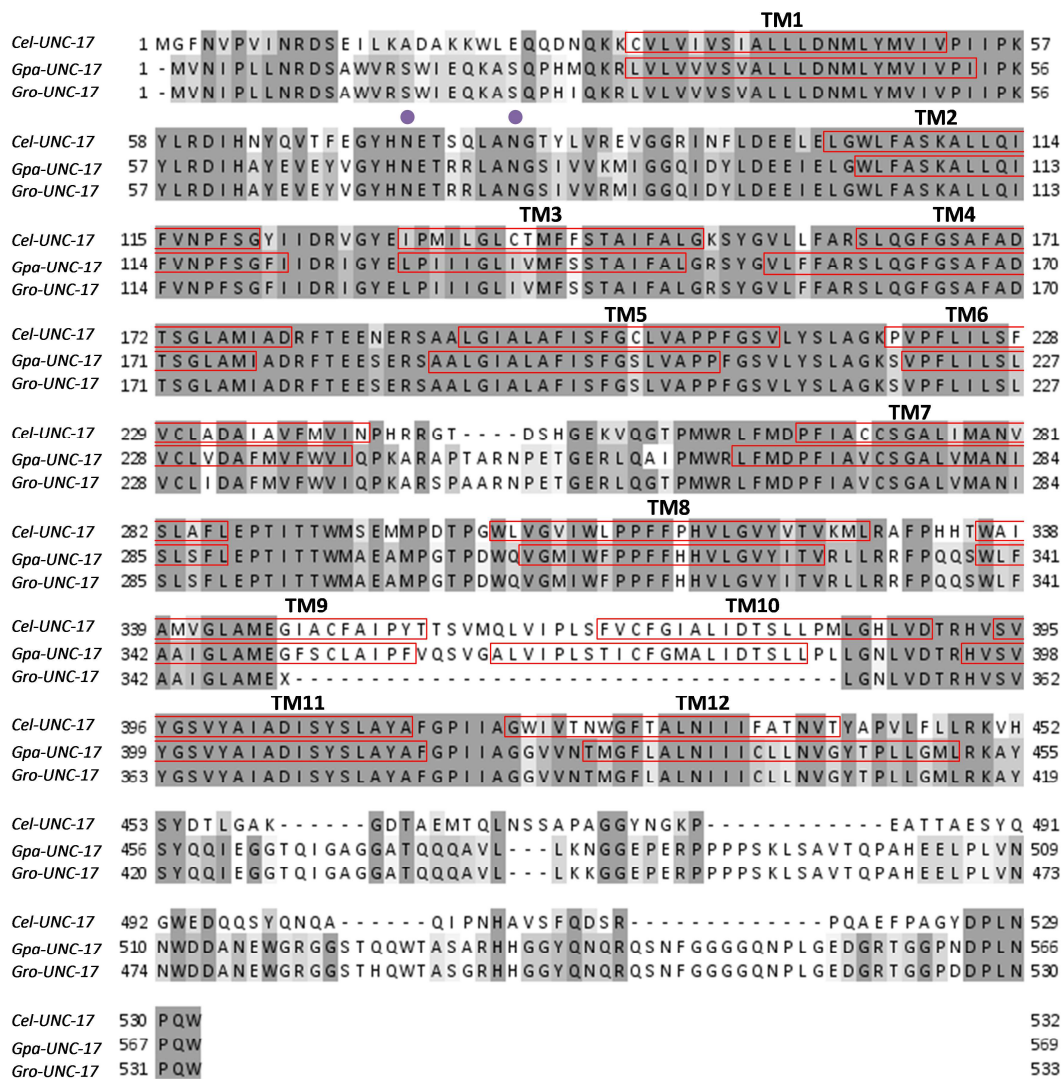
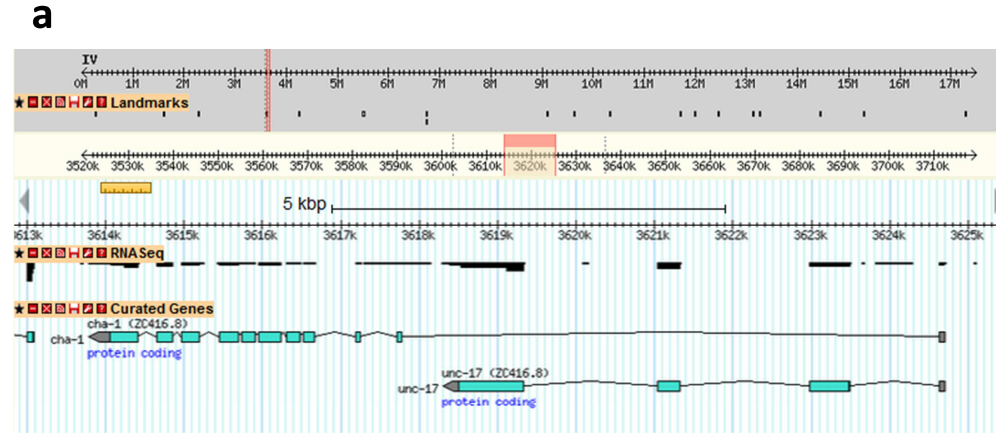


Figure 3-5: Alignment of Cel-UNC-17 with Gpa-UNC-17 and Gro-UNC-17

Red boxes indicate transmembrane regions from Cel-UNC-17 (confirmed in Uniprot database) and Gpa-UNC-17 (predicted). Purple circles indicate possible glycosylation sites.



b

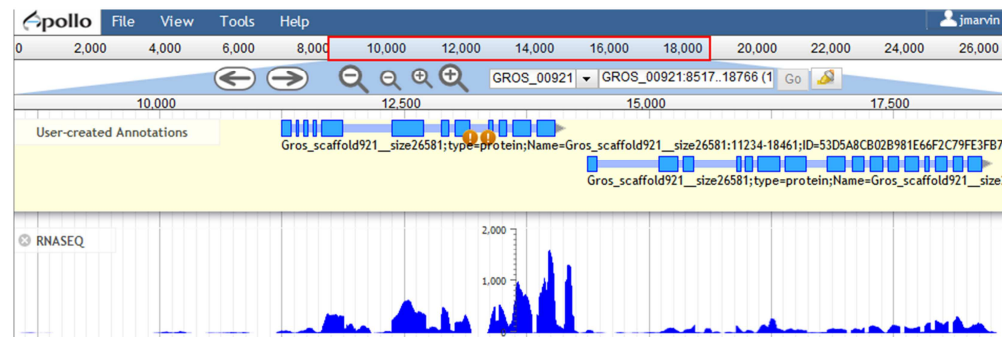


Figure 3-6: Structure of *unc-17 cha-1* operon in *C. elegans* and *G. rostochiensis*

a) *cel-unc-17 cel-cha-1* operon as viewed on *C. elegans* Gbrowse. The genes are orientated right to left. Shown is RNAseq data (black bars) representing expression levels. “Curated genes” shows gene structure. Black lines are introns, blue boxes are translated exons. The shared grey box in the two gene models is the shared untranslated exon. b) *gro-unc-17 gro-cha-1* operon model as viewed on Apollo for *G. rostochiensis*. The genes are orientated left to right. Shown is RNAseq data (dark blue peaks) and gene structure. Grey lines are introns and blue boxes are exons. There is no evidence of a shared untranslated exon and RNAseq data does not support this as a possibility.

3.3.2 Acetylcholine genes – receptor subunits

Investigation of genes encoding subunits of nicotinic acetylcholine receptors will be covered in detail in Chapter 4.

3.3.3 Glutamate genes – synthesis and metabolism

3.3.3.1 *Cel-eat-4*

Cel-eat-4 encodes a vesicular glutamate transporter. Orthologues of this gene were identified and cloned in *G. pallida* and identified in *G. rostochiensis*. The amino acid identity shared between Gpa-EAT-4 and Cel-EAT-4 is 63%, and between Gro-EAT-4 and Cel-Eat-4 is 62%.

Cel-EAT-4 is a membrane bound transporter and in *C. elegans* is reported to have 12 transmembrane domains (Lee *et al.* 1999). Phobius analysis of the translated sequence of *gpa-eat-4* predicts 12 transmembrane domains as expected (Figure 3-7).

3.3.4 Orthologues of *C. elegans* glutamate-gated chloride channel subunit genes

These genes encode subunits of glutamate-gated chloride channels, which may be homomeric or heteromeric. Some members of this gene family present in *C. elegans* are absent in *G. pallida* and *G. rostochiensis*, and some seem to have undergone duplication. Members of this class of genes should contain both a signal peptide for targeting to the secretory pathway towards their site in the plasma membrane, and four transmembrane spanning domains (Thompson, Lester and Lummis 2010). The amino acid sequences were also examined for presence of extracellular loops; residues involved in glutamate binding and residues involved in ivermectin binding as identified from X-ray crystal structures of Cel-GLC-1 (Hibbs and Gouaux 2011). A schematic of these residues is shown in (Figure 3-8). The details of shared percentage identity and presence of signal peptides, transmembrane domains and receptor-type features are summarised in Table 3.

3.3.4.1 *Cel-glc-1*

An orthologue of *Cel-glc-1* is absent in both *G. pallida* and *G. rostochiensis* genome assemblies. The transcriptome assemblies available were also searched for a *cel-glc-1* without an orthologue being detected.

3.3.4.2 *Cel-glc-2*

There is a long region of low sequence homology between TM3 and TM4 of the orthologue of Cel-GLC-2 in *G. pallida* and *G. rostochiensis*. Both Gpa-GLC-2 and Gro-GLC-2 are 133 amino acids longer than Cel-GLC-2 due to this expanded region

between TM3 and TM4. All extracellular loops can be identified in Gpa-GLC-2, as well as key residues in glutamate binding. Some residues involved in ivermectin binding can be identified in Cel-GLC-2 and Gpa-GLC-2 (Figure 3-9).

TMHMM analysis of Gpa-GLC-2 and Gro-GLC-2 predicts five transmembrane regions for each, where Cel-GLC-2 contains four. This additional transmembrane region coincides with the expanded region of Gpa-GLC-2 and Gro-GLC-2 (Figure 3-10). However, 3D modelling of the amino acid sequence by RaptorX predicts a long intracellular TM3-TM4 loop rather than an additional transmembrane domain. For comparison, the predicted model of Cel-GLC-2 has a much shorter TM3-TM4 loop (Figure 3-11).

3.3.4.3 *Cel-glc-3*

There is a long region of low sequence homology between TM3 and TM4 of the orthologue of Cel-GLC-3 in *G. pallida* and *G. rostochiensis*. Modelled by RaptorX, the prediction is for a long intracellular TM3-TM4 loop. Features characteristic of a glutamate-gated chloride subunit are identified in Gpa-GLC-3 and Gro-GLC-3. Most residues involved in ivermectin binding can be identified in Gpa-GLC-3 (Figure 3-12).

3.3.4.4 *Cel-glc-4*

Cel-glc-4 encodes a putative glutamate-gated chloride channel in *C. elegans*. Orthologues for this putative gene could be identified in *G. pallida* from transcriptome data and in *G. rostochiensis*, but were not cloned. Between TM3 and TM4 there is a region of low sequence homology. Analysis of the amino acid sequence identifies glutamate binding residues and some residues which may play a role in ivermectin binding. However, a highly conserved arginine residue in Loop G that is linked to glutamate binding (Lynagh *et al.* 2015) is absent in the predicted amino acid sequence for Gpa-GLC-4 and Gro-GLC-4 (Figure 3-13).

3.3.4.5 *Cel-avr-14*

Two orthologues of *cel-avr-14* were identified and cloned from *G. pallida* and identified in *G. rostochiensis*. These are separate genes, rather than different isoforms of the same gene. These genes have been termed *gpa/gro-avr-14.1* and *gpa/gro-avr-14.2*. The percentage identity between Gpa-AVR-14.1 and Gpa-AVR-14.2 is 41% (Figure 3-14).

In Gpa-AVR-14.1, there is a region of low amino acid sequence identity between TM3 and TM4. Features of a glutamate gated chloride channel subunit are present in the predicted amino acid sequence. Most residues involved in ivermectin binding are present. No signal peptide is detected by SignalP for either Gpa-AVR-14.1 or Gro-AVR-14.1. This may coincide with an expansion in the amino acid sequence for

Gpa-AVR14.1 and Gro-AVR14.1 at the N-terminal region. There are possible residues in this region which suggest a signal peptide may have been lost at some point in time (Figure 3-15).

A second orthologue to *celavr-14* was identified from the *G. pallida* transcriptome and was cloned. In RBH searches to the *C. elegans* protein database, the highest match was *celavr-14* so this gene was considered to be a second orthologue in *G. pallida* and termed *gpaavr-14.2*. This orthologue was also identified in *G. rostochiensis*. Five transmembrane domains are predicted by TMHMM. One region is towards the N-terminal end of the amino acid chain, which may actually indicate a signal peptide. However, SignalP does not predict a signal peptide for Gpa-AVR-14.2 or Gro-AVR-14.2 (Figure 3-16).

3D modelling of the two identified orthologues produces two different structures. Both have longer TM3-TM4 intracellular loops than Cel-AVR-14. Gpa-AVR-14.2 is predicted to have additional helical structures in the extracellular domain (Figure 3-17).

3.3.4.6 *Celavr-15*

An orthologue of *celavr-15* is absent in both the *G. pallida* and *G. rostochiensis* genome assemblies. Transcriptome databases were also searched for a *celavr-15* orthologue without success.

3.3.4.7 Phylogenetic relationship of cloned subunits of glutamate-gated chloride channels

The relationship between the cloned subunits of glutamate-gated chloride channels from *G. pallida*, the identified subunits from *G. rostochiensis* and the *C. elegans* subunits is described by a maximum likelihood phylogenetic tree. The outgroup used was the sequence of an ancestral glutamate-gated chloride channel identified from the sea slug *Aplysia californica*.

Orthologues identified cluster together, with *G. pallida* and *G. rostochiensis* being more closely related to each other than to the *C. elegans* subunits. Gpa-AVR-14.2 clusters with Cel-AVR-14, and Gpa-AVR-14.1 and Gro-AVR14.1 but is more distantly related (Figure 3-18).

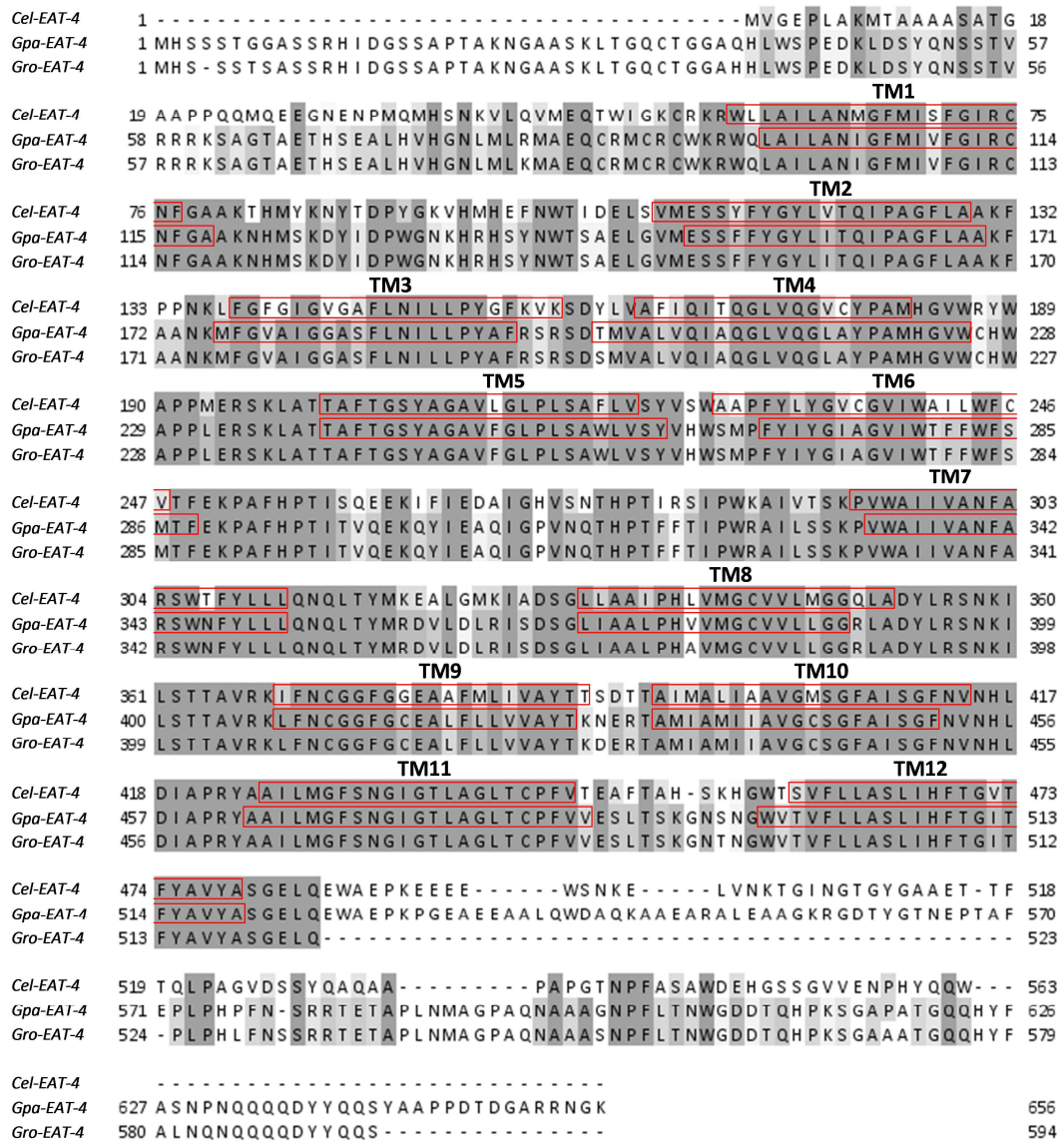


Figure 3-7: Alignment of Cel-EAT-4 with Gpa-EAT-4 and Gro-EAT-4

Red boxes indicate transmembrane regions for Cel-EAT-4 (confirmed in Uniprot database) and Gpa-EAT-4 (estimated by Phobius).

TM1

Ce¹-GLC-2: FSYYLVQLYAPTTMIVIVSWVSFWI
Ce¹-GLC-1: FSFYLLQLYIPSCMLVIVSWVSFWI
Gpa-AVR-14.1: FSYYLLQLYIPSCMLVIVSWVSFWL

M2-M3 Loop

Ce¹-GLC-2: LPPVSYVK
Ce¹-GLC-1: LPPVSYIK
Gpa-AVR-14.1: LPPVSYTK

TM2

Ce¹-GLC-2: HSTAGRVALGVTTLLTMTTMQSAINAK
Ce¹-GLC-1: TAIPARVTLGVTLLTMTAQSAGINSQ
Gpa-AVR-14.1: DSVPARVTLGVTLLTMTTQS^YSGINAK

TM3

Ce¹-GLC-2: VVDVWLGACQTFVFGALLEYAFVSYQDSV
Ce¹-GLC-1: AIDVWIGACMTFIFCALLEFALVNHIANA
Gpa-AVR-14.1: AVDVWIGVCMAFIFGALLEFALVNIAARK

Figure 3-8: Schematic of residues involved in ivermectin binding identified from X-ray crystal structure

The residues involved in ivermectin binding have been shown by x-ray structure analysis of crystallised Cel-GLC-1. Residues highlighted in grey are involved in van der Waal interactions with ivermectin. Residues highlighted in yellow are involved in hydrogen bonding with ivermectin. Involvement of residues from Gpa-AVR-14.1 is inferred from Cel-GLC-1 data. Figure adapted from Hibbs and Gouaux 2011

Gene name (<i>gpa/gro</i>)	Percentage ID Ce to Gpa	Percentage ID Ce to Gr	Signal Peptide prediction	Transmembrane prediction	Receptor features
Glc-1	no orthologue identified	no orthologue identified	-	-	-
Glc-2	50%	51%	Cleavage between residues 21 and 23	5 predicted (not supported by 3D model)	Cys-loop present Extracellular loops present
Glc-3	56%	57%	Cleavage between residues 32 and 33	4 predicted	Cys-loop present Extracellular loops present
Glc-4	60%	61%	Cleavage between residues 23 and 24	4 predicted	Cys-loop present Extracellular loops present
Avr-14.1	61%	62%	None predicted	4 predicted	Cys-loop present Extracellular loops present
Avr-14.2	45%	51%	None predicted	5 predicted (additional coiled in extracellular domain)	Cys-loop present Extracellular loops present
Avr-15	No orthologue identified	No orthologue identified	-	-	-

Table 3: Summary of features of orthologues of glutamate-gated chloride channel subunits cloned from *G. pallida* and identified in *G. rostochiensis*

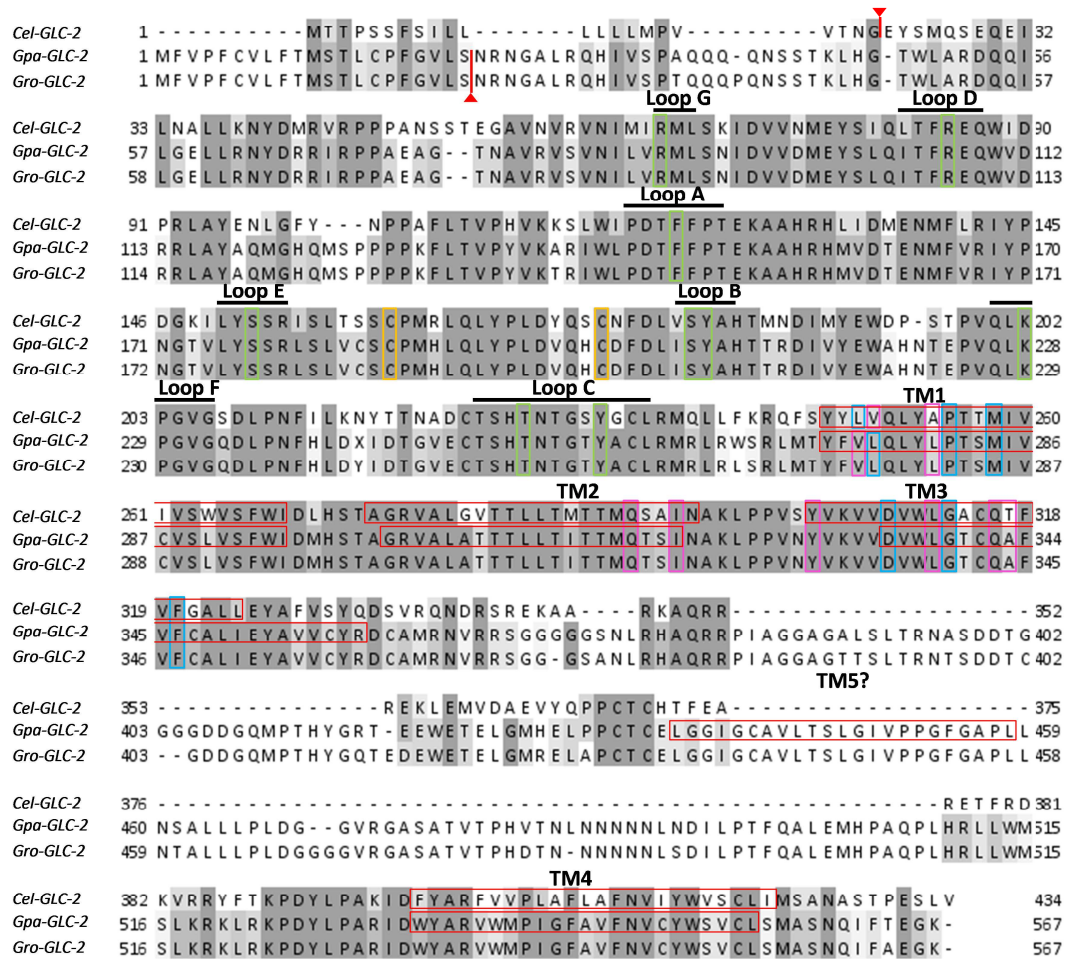


Figure 3-9: Alignment of Cel-GLC-2 with Gpa-GLC-2 and Gro-GLC-2

Red arrows indicate signal peptide cleavage sites. Black lines indicate the different extracellular loops presents. Orange boxes indicate paired cysteines of a cys-loop receptor. Red boxes indicate predicted transmembrane regions. Green boxes indicate residues involved in glutamate binding. Blue boxes indicate residues involved in ivermectin binding, that match consensus. Pink boxes indicate residues in positions that may interact with ivermectin, but do not fit consensus.

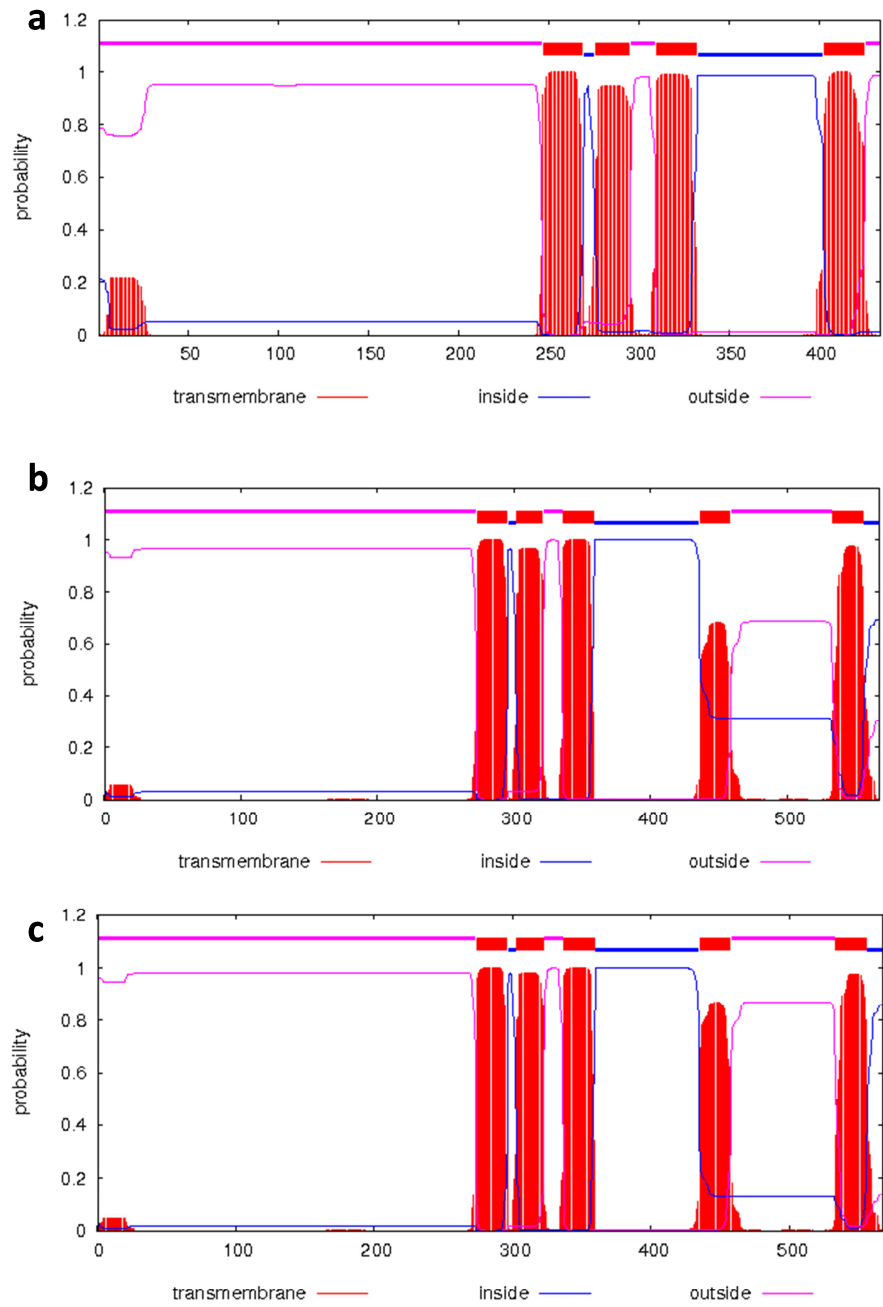


Figure 3-10: Output from TMHMM prediction server for Cel-GLC-2, Gpa-GLC-2 and Gro-GLC-2

a) Prediction for Cel-GLC-2 predicts four membrane spanning domains. b-c) predictions for Gpa-GLC-2 and Gro-GLC-2 predict five transmembrane regions, with an additional transmembrane region predicted between amino acids 400 – 500.

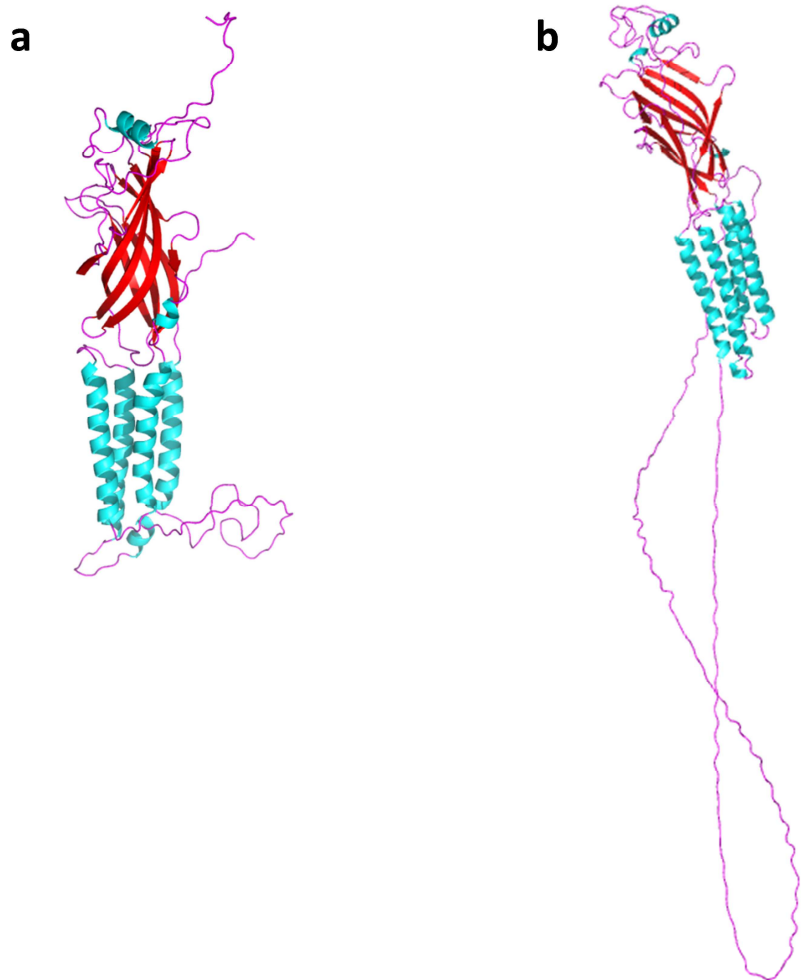


Figure 3-11: 3D model of Cel-GLC-2 and Gpa-GLC-2

a) 3D model of Cel-GLC-2 as built by RaptorX. Template is based on PDB: 3rhwA. P-value for model 1.47^{e-15} . b) 3D model of Gpa-GLC-2 as built by RaptorX. Template based on PDB: 3rhwA. P-value for model 1.01^{e-15} . Protein models are coloured by secondary structure: α helix (turquoise), β sheet (red) and loops (pink). Cel-GLC-2 and Gpa-GLC-2 share the same overall features, although the TM3-TM4 intracellular loop is elongated in Gpa-GLC-2. A fifth transmembrane domain for Gpa-GLC-2 is not predicted by the model.

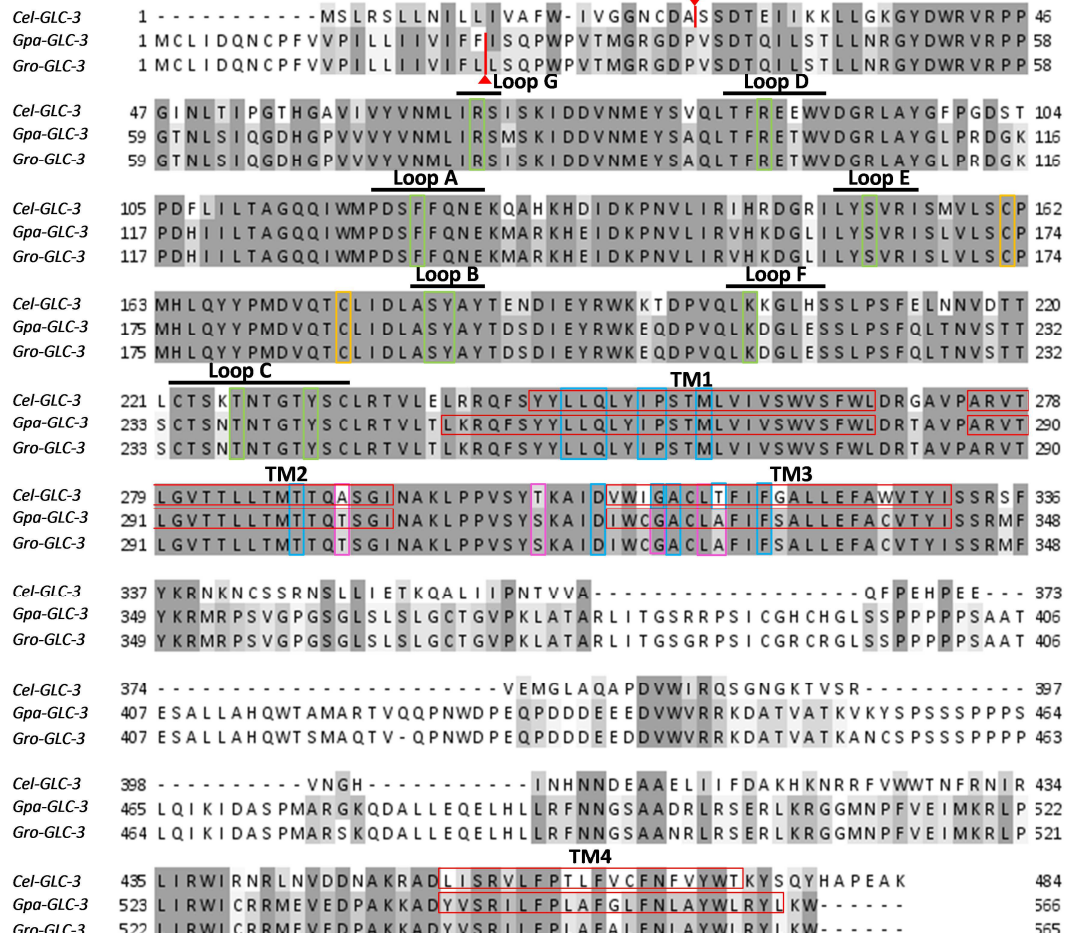


Figure 3-12 : Alignment of Cel-GLC-3 with Gpa-GLC-3 and Gro-GLC-3

Red arrows indicate signal peptide cleavage sites. Black lines indicate the different extracellular loops presents. Orange boxes indicate paired cysteines of a cys-loop receptor. Red boxes indicate predicted transmembrane regions. Green boxes indicate residues involved in glutamate binding. Blue boxes indicate residues involved in ivermectin binding, that match consensus. Pink boxes indicate residues in positions that may interact with ivermectin, but do not fit consensus.

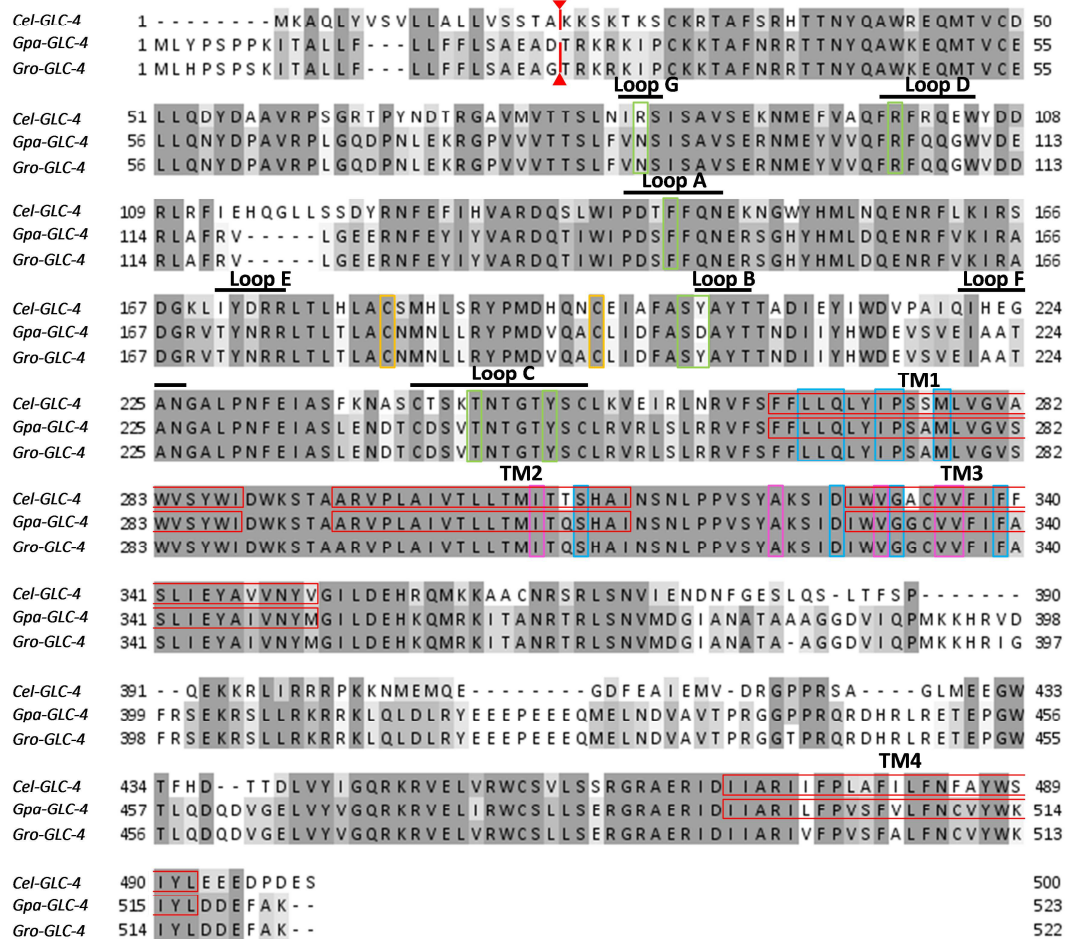


Figure 3-13: Alignment of predicted amino acid sequence of Cel-GLC-4 with Gpa-GLC-4 and Gro-GLC-4

Red arrows indicate signal peptide cleavage sites identified. Black lines indicate the different extracellular loops presents. Orange boxes indicate paired cysteines of a cys-loop receptor. Red boxes indicate predicted transmembrane regions. Green boxes indicate residues involved in glutamate binding. Blue boxes indicate residues involved in ivermectin binding, that match consensus. Pink boxes indicate residues in positions that may interact with ivermectin, but do not fit consensus.

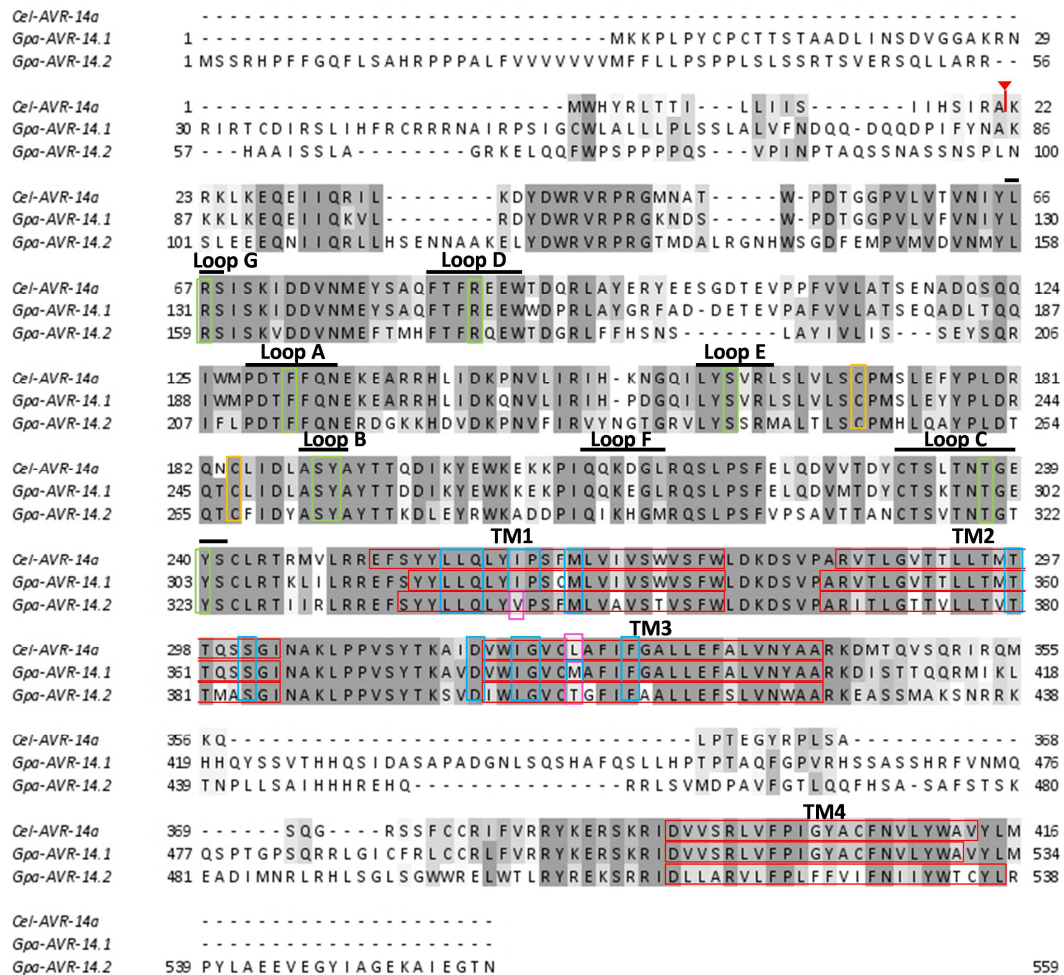


Figure 3-14: Alignment of Cel-AVR-14a with Gpa-AVR-14.1 and Gpa-AVR-14.2

Red arrows indicate signal peptide cleavage sites identified. Black lines indicate the different extracellular loops presents. Orange boxes indicate paired cysteines of a cys-loop receptor. Red boxes indicate predicted transmembrane regions. Green boxes indicate residues involved in glutamate binding. Blue boxes indicate residues involved in ivermectin binding, that match consensus. Pink boxes indicate residues in positions that may interact with ivermectin, but do not fit consensus.

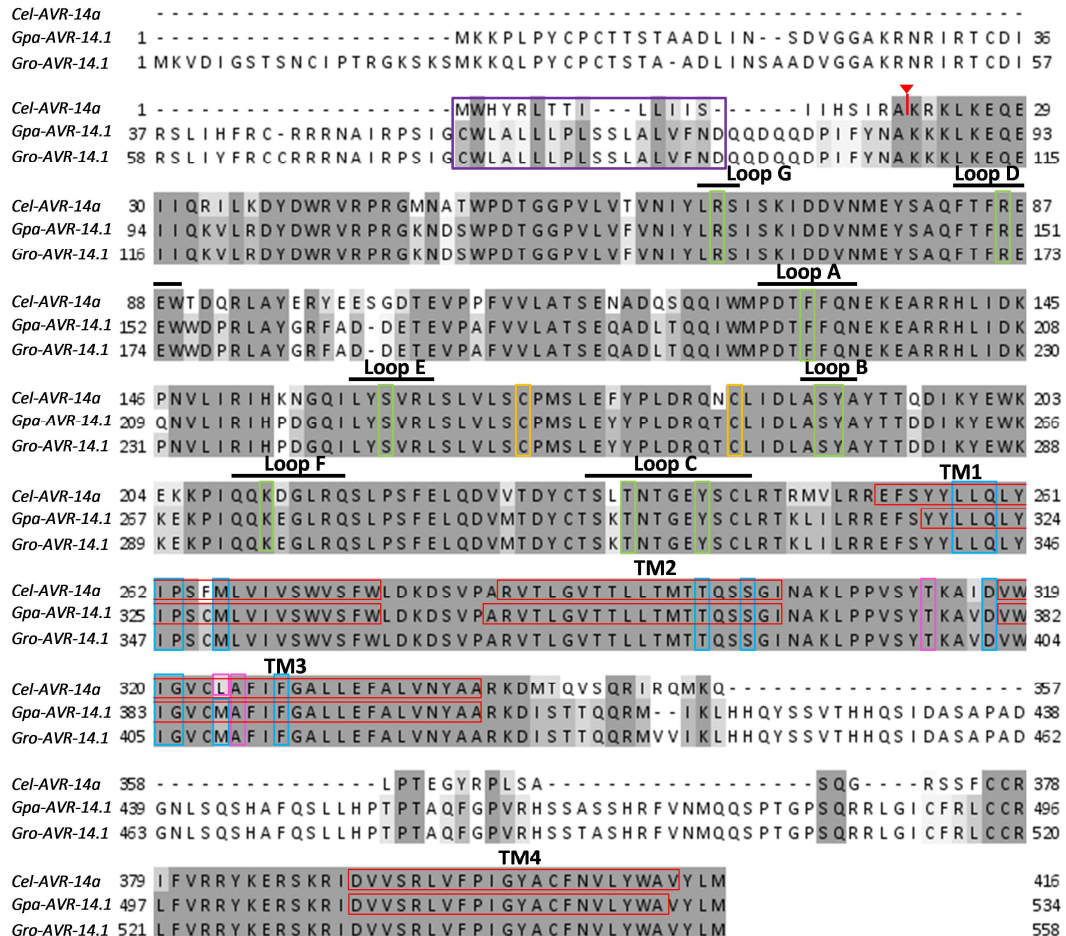


Figure 3-15: Alignment of Cel-AVR-14 (isoform a) with Gpa-AVR-14.1 and Gro-AVR-14.1.

Red arrows indicate signal peptide cleavage sites identified. The purple box indicates region of sequence similarity with the Cel- AVR-14 signal peptide. Black lines indicate the different extracellular loops presents. Orange boxes indicate paired cysteines of a cys-loop receptor. Red boxes indicate predicted transmembrane regions. Green boxes indicate residues involved in glutamate binding. Blue boxes indicate residues involved in ivermectin binding, that match consensus. Pink boxes indicate residues in positions that may interact with ivermectin, but do not fit consensus.

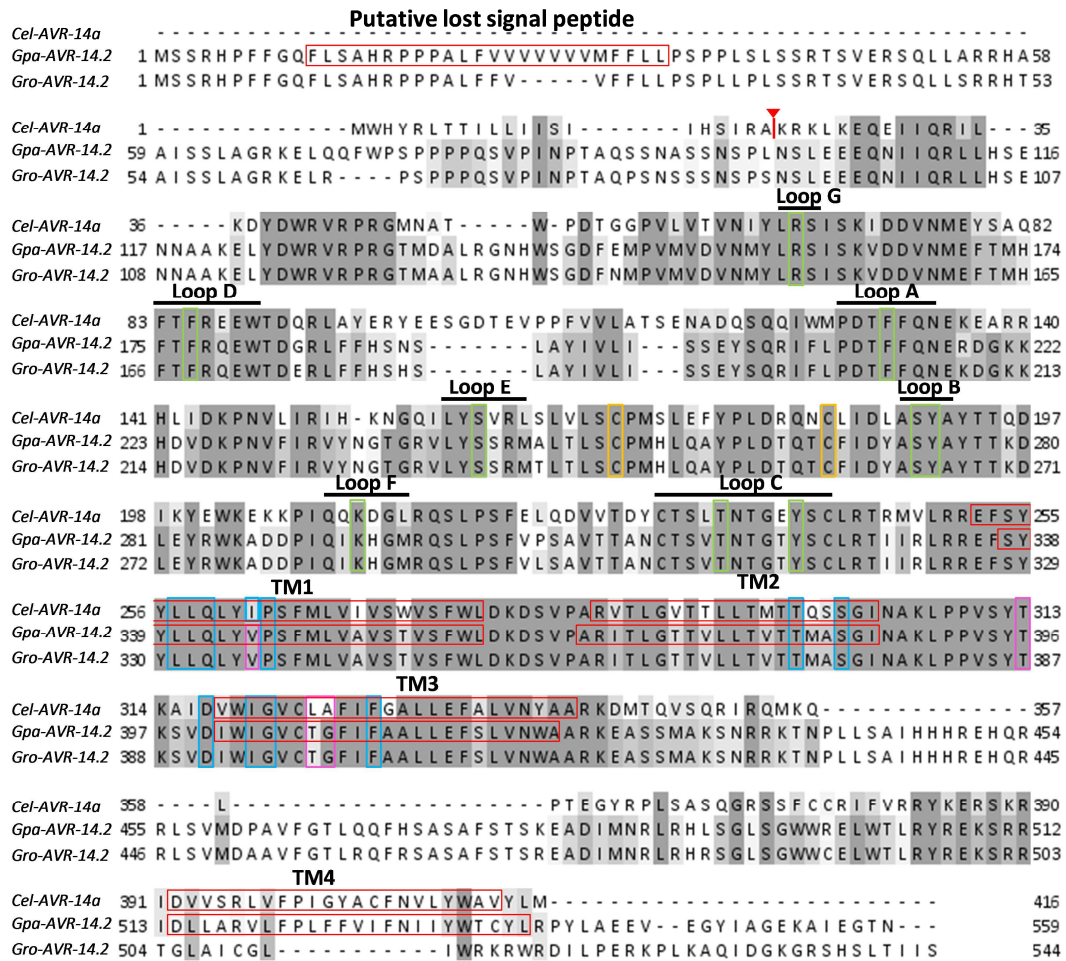


Figure 3-16: Alignment of Cel-AVR-14 (isoform a) with Gpa-AVR-14.2 and Gro-AVR-14.2

Red arrows indicate signal peptide cleavage sites identified. Labelled red box indicates predicted transmembrane region towards N-terminal end, but is a possible lost signal peptide. Black lines indicate the different extracellular loops presents. Orange boxes indicate paired cysteines of a cys-loop receptor. Red boxes indicate predicted transmembrane regions. Green boxes indicate residues involved in glutamate binding. Blue boxes indicate residues involved in ivermectin binding, that match consensus. Pink boxes indicate residues in positions that may interact with ivermectin, but do not fit consensus.

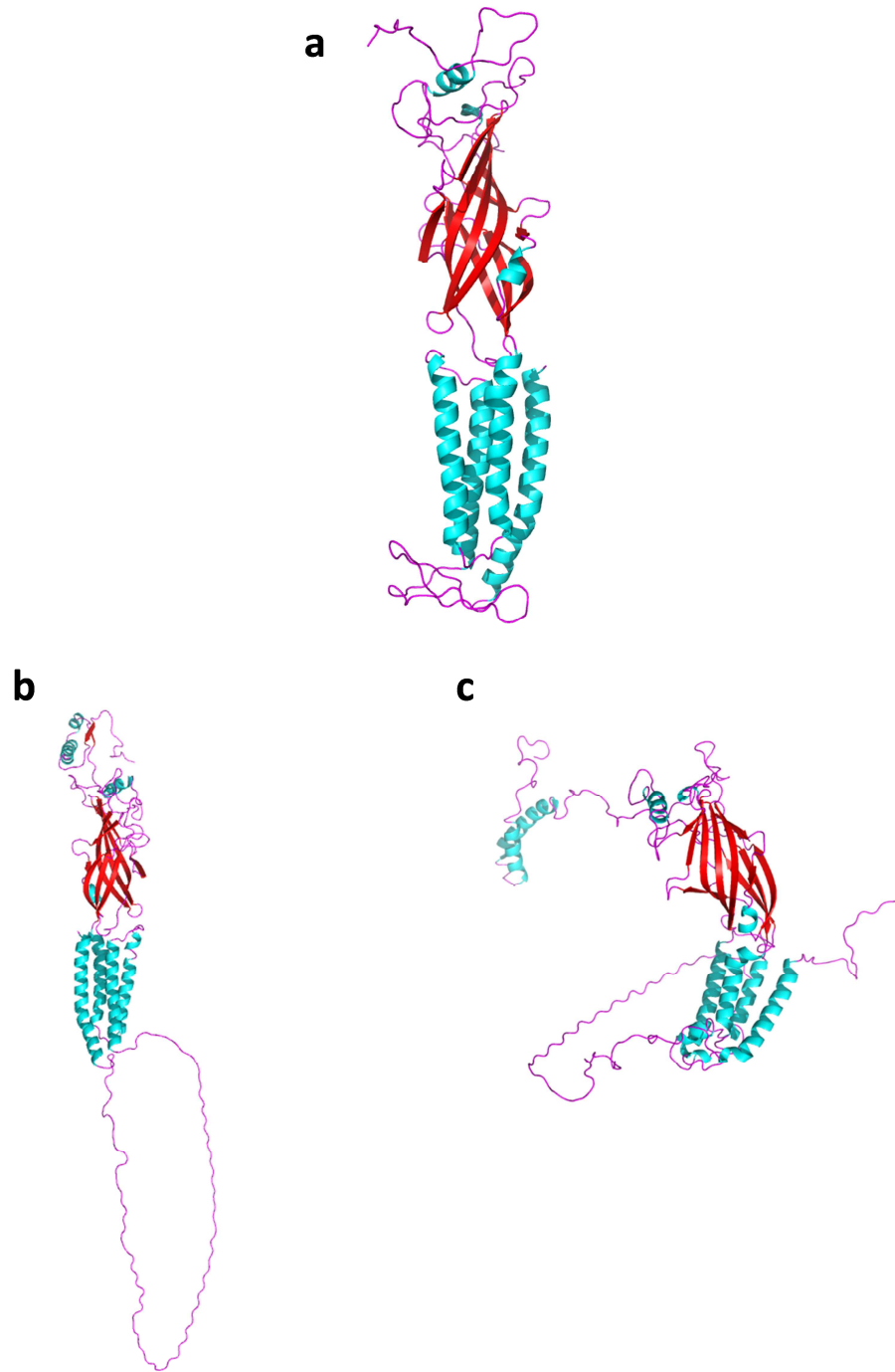


Figure 3-17: 3D models of Cel-avr-14a, Gpa-avr-14.1 and Gpa-avr-14.2

a) 3D model of Cel-avr-14a as built by RaptorX. Template is based on PDB: 4.43^{e-16}. P-value for model 1.47^{e-15}. b) 3D model of Gpa-avr-14.1. Template: 3rhwA. P-value 1.37^{e-15} c) 3D models of Gpa-avr-14.2. Template: 3rhwA. P-value 5.92^{e-15}. Protein models are coloured by secondary structure: α helix (turquoise), β sheet (red) and loops (pink). Gpa-avr-14.1 and Gpa-avr-14.2 differ from Cel-avr-14a and each other. TM3-TM4 region is elongated in both Gpa models.

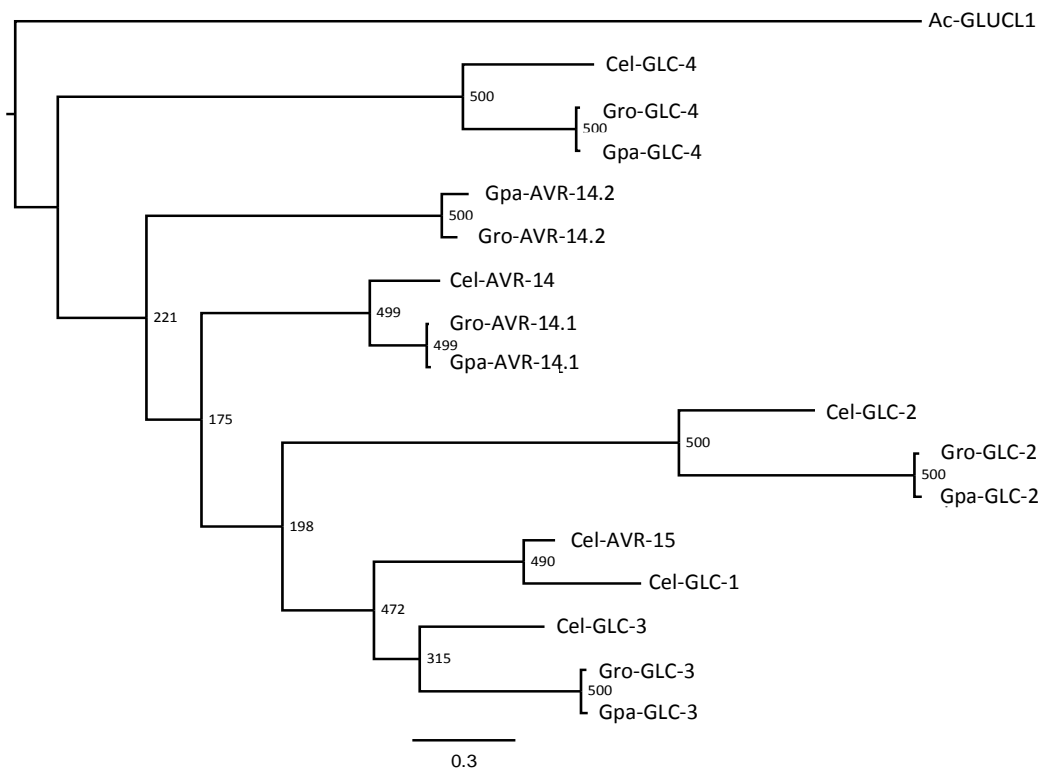


Figure 3-18: Phylogeny of glutamate-gated chloride channel subunits identified from *G. pallida* and *G. rostochiensis* with *C. elegans* subunits

Maximum likelihood phylogeny using predicted protein alignment of glutamate-gated chloride channel subunits. Bootstrap values for 500 iterations labelled on nodes. Scale bar represents average number of substitutions per site. Subunits cluster by orthology groups rather than species.

3.3.5 Orthologues of *C. elegans* genes involved in serotonin synthesis and metabolism

3.3.5.1 *Cel-tph-1*

Cel-tph-1 encodes a tryptophan hydroxylase that catalyses the rate-limiting step in serotonin biosynthesis. Percentage identity between Cel-TPH-1 and Gpa-TPH-1 is 66% and between Cel-TPH-1 and Gro-TPH-1 is 66%.

Known cofactor binding sites present in Cel-TPH-1 are present in Gpa-TPH-1 (UniProt 2015) (Figure 3-19).

3.3.5.2 *Cel-ser-7*

Application of exogenous serotonin stimulates stylet thrusting of *G. pallida* J2s (Figure 3-21a). Serotonin-induced stylet thrusting is accompanied by cessation of movement in liquid. This response indicates that receptors present for serotonin are present in *G. pallida*.

An orthologue for *cel-ser-7*, which encodes a serotonin receptor, was identified. Percentage identity between Cel-SER-7 isoform b and Gpa-SER-7 is 40%, and between Cel-SER-7 isoform b and Gro-SER-7 is 40%.

A signal peptide is predicted for Gpa-SER-7 and Gro-SER-7. However, SignalP does not predict a signal peptide for Cel-SER-7. Cel-SER-7 is known to contain seven transmembrane domains (Hobson *et al.* 2003). TMHMM predicts seven transmembrane domains for Gpa-SER-7.

PKC phosphorylation sites have been predicted in Cel-SER-7, which can take place at serine or threonine residues. Two of these potential phosphorylation sites are present in Gpa-SER-7, and three are present in Gro-SER-7. A PKA phosphorylation site was also predicted in Cel-SER-7, but a serine or threonine is not present in Gpa-SER-7 in this position (Hobson *et al.* 2003)(Figure 3-20).

3.3.5.3 *Cel-mod-5*

Cel-mod-5 encodes a serotonin transporter present on neurosecretory neurons responsible for reuptake of serotonin from the synaptic cleft.

The percentage identity between Cel-MOD-5 and Gpa-MOD-5 is 58% and between Cel-MOD-5 and Gro-MOD-5 is 57%. There is a conserved aspartate residue present in serotonin and dopamine transporters (Ranganathan *et al.* 2001), which can be identified in Gpa-MOD-5.

TMHMM model predicts 12 transmembrane domains for both Gro-MOD-5 and Gpa-MOD-5 which is characteristic of this type of transporter (Figure 3-22).

3.3.6 Orthologues of *C. elegans* genes involved in GABA synthesis

3.3.6.1 *Cel-unc-25*

Cel-unc-25 encodes a glutamic acid decarboxylase, involved in the synthesis of GABA. Percentage identity between Cel-UNC-25 and Gpa-UNC-25 is 70%, and between Cel-UNC-25 and Gro-UNC-25 is 68%.

The NPHK tetrapeptide which binds the pyridoxal phosphate cofactor and is characteristic of glutamic acid decarboxylases, can be identified in Gpa-UNC-25 (Jin *et al.* 1999) (Figure 3-23).

3.3.7 Genes involved in dopamine metabolism

3.3.7.1 *Cel-dat-1*

Cel-dat-1 encodes a dopamine transporter responsible for reuptake of dopamine from the synaptic cleft (Jayanthi *et al.* 1998). Percentage identity between Cel-DAT-1 and Gpa-DAT-1 is 63%, and between Cel-DAT-1 and Gro-DAT-1 is 63%. The amino acid sequence contains the conserved aspartate residue common to dopamine and serotonin transporters (Ranganathan *et al.* 2001).

This class of transporter has 12 transmembrane domains. Both Gro-DAT-1 and Gpa-DAT-1 are predicted 12 transmembrane domains by the TMHMM; however the location of the predicted transmembrane domain regions differs between Cel-DAT-1 and Gpa-DAT-1 (Figure 3-24).

3.3.8 Orthologues of *C. elegans* genes involved in octopamine synthesis

3.3.8.1 *Cel-tbh-1*

Cel-tbh-1 encodes a tyramine β-hydroxylase and is involved in the synthesis of octopamine (Alkema *et al.* 2005). A potential orthologue of *tbh-1* was identified in *G. pallida*, but could not be cloned. An orthologue of *tbh-1* was also identified in *G. rostochiensis*. The orthologues as identified from bioinformatic data had low percentage identity to Cel-TBH-1 with percentage identity to Gpa-TBH-1 being 31% and to Gro-TBH-1 being 33% (Figure 3-25). The predicted amino acid sequence obtained is not predicted a signal peptide, while Cel-TBH-1 has a signal peptide. However, analysis by Interpro both identifies it as a tyramine β-hydroxylase and identifies key domains in the predicted Gpa-TBH-1 sequence, which are present in Cel-TBH-1 such as the DOMON domain, involved in extracellular adhesion (Aravind 2001).

G. pallida J2s were exposed to 50 mM octopamine to determine if exogenous application of the neurotransmitter caused an effect. After 24 hours exposure, octopamine treated J2s moved significantly faster than control worms (Figure 3-21b).

3.3.9 Expression analysis of identified orthologues at different life-stages of *G. pallida*

Expression data obtained from RNASeq results from life-stages show that the genes identified are most highly expressed in the eggs, J2s and males. Expression level in sedentary stages is low (Figure 3-26) apart from for *gpa-dat-1*. Expression of *gpa-tbh-1* remains low throughout although is slightly elevated during the sedentary life stages.

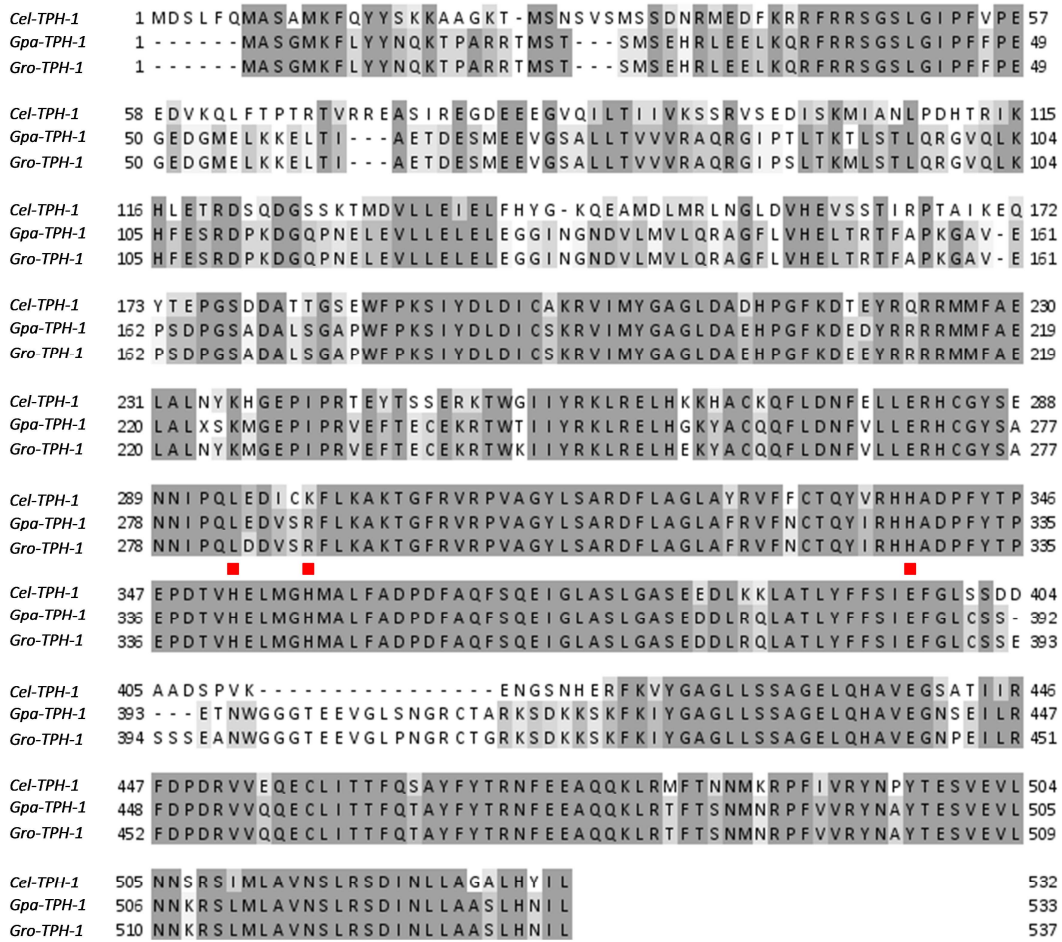


Figure 3-19: Alignment of Cel-TPH-1 with Gpa-TPH-1 and Gro-TPH-1

Red squares indicate known cofactor binding sites in Ce-TPH-1

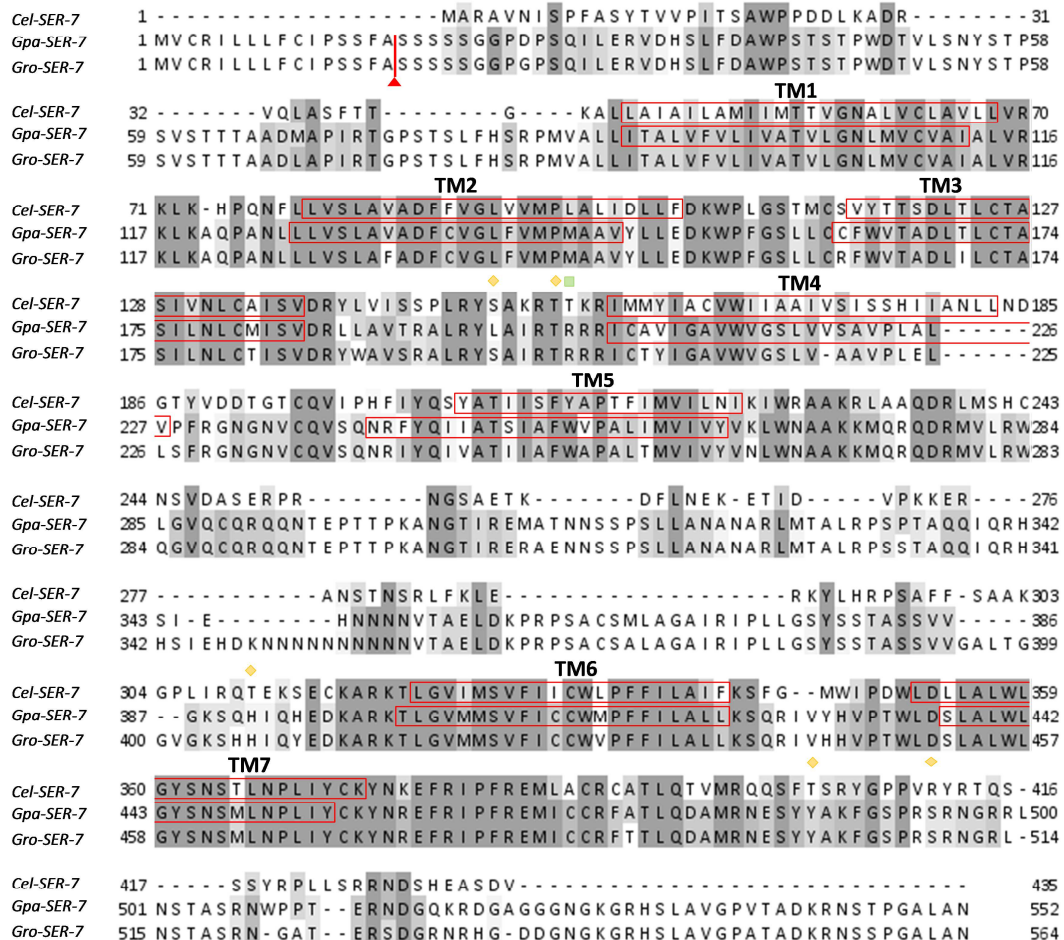


Figure 3-20 : Alignment of Cel-SER-7 (isoform b) with Gpa-SER-7 and Gro-SER-7

Red arrows indicate cleavage site of signal peptide identified by SignalP. Red boxes indicate transmembrane domain regions. Yellow diamonds indicate potential PKC phosphorylation sites. Green squares indicate potential PKA phosphorylation sites.

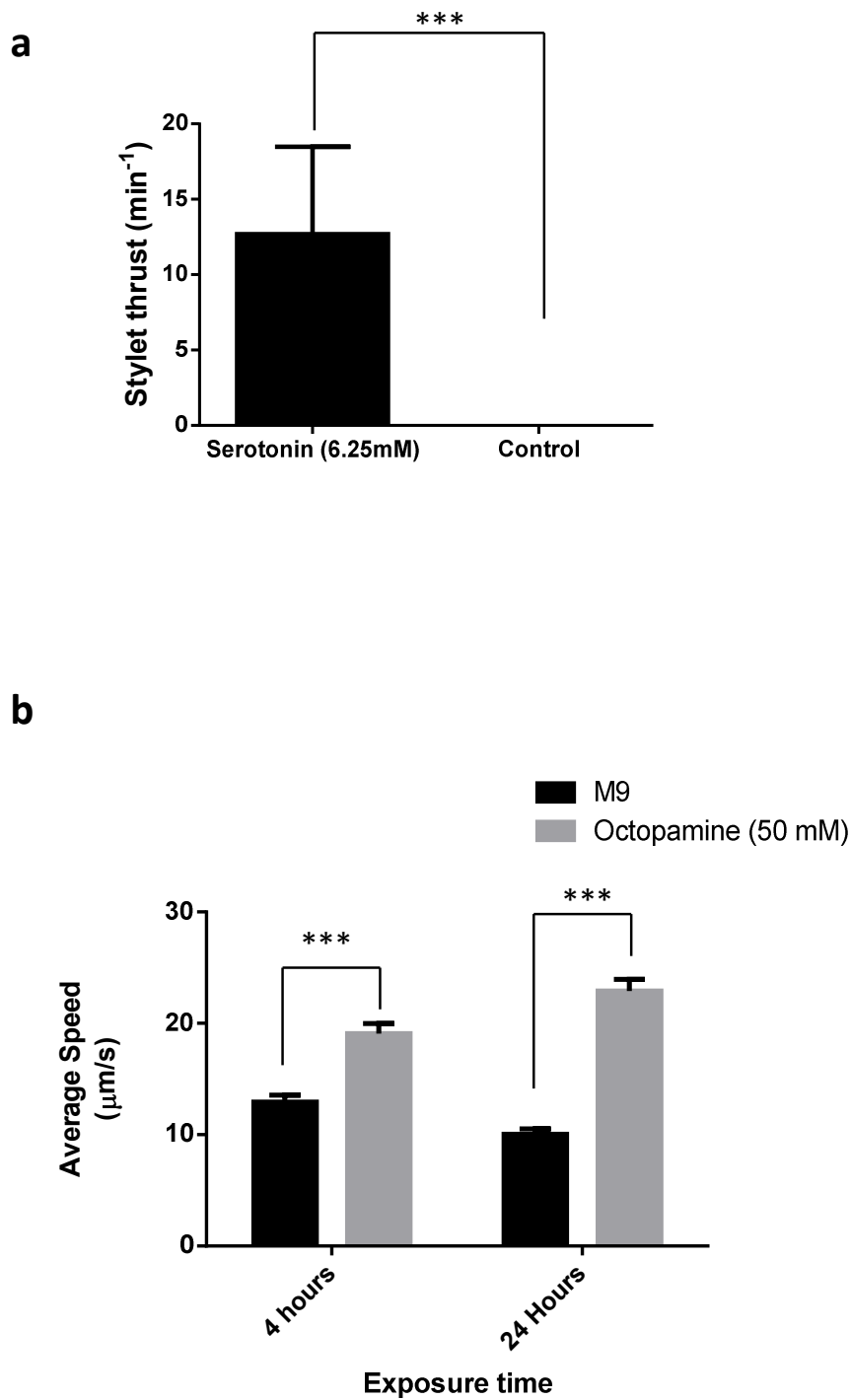


Figure 3-21: Application of exogenous neurotransmitters to *G. pallida* J2s

a) Application of 6.25 mM serotonin to *G. pallida* J2s stimulates stylet thrusting. In the absence of serotonin, J2s do not stylet thrust (ANOVA, $p = <0.001$) b) Application of octopamine to *G. pallida* J2s increases speed of movement at 4 hours and 24 hours exposure. (Two-way ANOVA, $p < 0.001$). Error bars represent SEM.

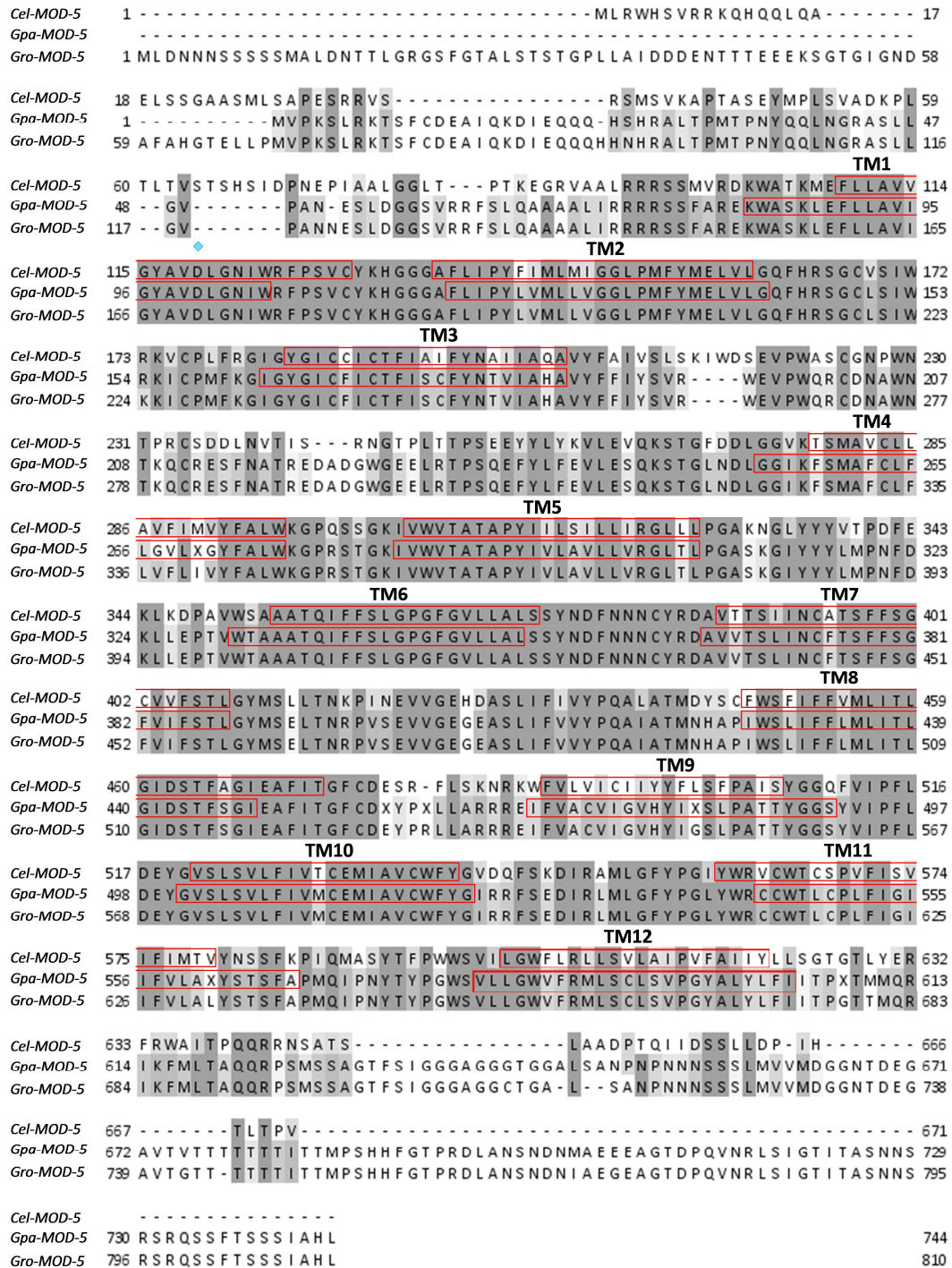


Figure 3-22: Alignment of Cel-MOD-5 with Gpa-MOD-5 and Gro-MOD-5

Red boxes indicate transmembrane regions. Blue diamond indicates a conserved aspartate residue common to serotonin and dopamine transporters.

<i>Cel-UNC-25</i>	- - - - -	
<i>Gpa-UNC-25</i>	- - - - -	
<i>Gro-UNC-25</i>	1 MAH S T T K A D R Q R H N A S G G Q P H K R Q R Q M Q R P T Q S G G T Q R R A R R A V T T E Q N Q Q Q Q H S	57
<i>Cel-UNC-25</i>	1 - - - - -	M S S A A A D E S D A V L E N L I A K E I L P - Q T G N
<i>Gpa-UNC-25</i>	1 M Q N N H G Q H Q L E L N Q Q S T S N E G G Q E D G E Q S L M N G - P N K A K K E M V D C F A T D L F P H N L Q G	56
<i>Gro-UNC-25</i>	58 I K A P A M E N N H G L N Q Q S T S N E V G Q E D G E Q S L M N G - P N K A K N E M V D L F A T D L F P H N L Q G	113
<i>Cel-UNC-25</i>	28 W E G T E E F L N R I V Q V L I - - - - -	L K Y I K D Q N D R D Q K I L E F H H P D
<i>Gpa-UNC-25</i>	57 W E H T Q Q Q F L E A I V H I L L N - - - - -	Y I R E E N D R S T K V L E F H Q P E
<i>Gro-UNC-25</i>	114 W E H T Q Q Q F L E A I V Q I L L N Y I R E E N D R S T X L E A I V Q I L L N Y I R E E N D R S T K V L E F H Q P E	170
<i>Cel-UNC-25</i>	64 K M Q M L M D L S I P E K P E S L L K L V K S C E D V L R L G V R T G H P R F F N Q I S C G L D L V S M A G E W L	120
<i>Gpa-UNC-25</i>	93 E M A Q L I D L H I P K E P I K L G E L L H S C Y N V L R L G V R T G H P R F F N Q I S C G L D L V A M A G E W L	149
<i>Gro-UNC-25</i>	171 E M A Q L I D L H I P R E P I K L G E L L H S C Y N V L R L G V R T G H P R F F N Q I S C G L D L V A M A G E W L	227
<i>Cel-UNC-25</i>	121 T A T A N T N M F T Y E I A P V F I L M E K S V M A R M W E A V G W D P E K A D G I F A P G G A I A N L Y A M N A	177
<i>Gpa-UNC-25</i>	150 T A T S N T N M F T Y E I S P V F I L M E K E V T Q R M V E L I G W P - N G G D A V F S P G G A I A N M Y A M N A	205
<i>Gro-UNC-25</i>	228 T A T S N T N M F T Y E I S P V F I L M E K E V T Q R M I E L I G W P - N G G D A V F S P G G A I A N M Y A M N A	283
<i>Cel-UNC-25</i>	178 A R H Q L W P R S K H L G M K - D I P T L C C F T S E D S H Y S I K S A S A V L G I G A D Y C F N I P T D K N G K	233
<i>Gpa-UNC-25</i>	206 A R H Y H F P R A K P L G M T T G M P T L C C F T S E D S H Y S I K S A S A V L G I G A D N C F N I A V D D Q A R	262
<i>Gro-UNC-25</i>	284 A R H Y H F P R A K S L G M T A G M P T L C C F T S E D S H Y S I K S A S A V L G I G A D N C F N I A V D D Q A R	340
<i>Cel-UNC-25</i>	234 M I P E A L E A K I I E C K K E G L T P F F A C C T A G S T V Y G A F D P L E R V A N I C E R H K L W F H V D A A	290
<i>Gpa-UNC-25</i>	253 M I P E A L E E C I I K C K D E G L H P F F V C A T A G T T V Y G A W D P I P Q I A D I C N R H K L W L H V D A A	319
<i>Gro-UNC-25</i>	341 M I P E A L E E C I I K C K D E G L H P F F V C A T A G T T V Y G A W D P I P Q I A D I C K R H K L W L H V D A A	397
<i>Cel-UNC-25</i>	291 W G G G M L L S P E H R Y K L A G I E R A N S V T W N P H K L M G A L L Q C S A C L F R Q D G L L F Q C N Q M S A	347
<i>Gpa-UNC-25</i>	320 W G G G L L L S P E H R H K L S G I E K A N S V T W N P H K L M G A L L Q C S A C F V R Q E G L L F Q T N Q M S A	376
<i>Gro-UNC-25</i>	398 W G G G L L L S P E H R H K L S G I E K A N S V T W N P H K L M G A L L Q C S A C F V R Q E G L L F Q T N Q M S A	454
<i>Cel-UNC-25</i>	348 D Y L F Q Q D K P Y D V S F D T G D K A I Q C G R H - - N D V F K L W L M W K S K G M E G Y R Q Q I N K L M D L A	402
<i>Gpa-UNC-25</i>	377 D Y L F Q Q D K P Y D V S Y D T G D K A M Q C G R H - - N D I F K L W L M W R S K G M E G Y R H Q I N R L M D L A	431
<i>Gro-UNC-25</i>	455 D Y L F Q Q D K P Y D V S Y D T G D K A M Q C V S I P G D Q K H G L W L M W R S K G M E G Y R R Q I N R L M E L A	511
<i>Cel-UNC-25</i>	403 N Y F T R R I K E T E G F E L I I E N P E F L N I C F W Y V P S K I R - - N L E P A E M R A R L E K I A P K I K A G	458
<i>Gpa-UNC-25</i>	432 N Y F T A K I K R T E G Y E M V V D D P E F L N I C F W Y V P P S M R R E M D H K E K M A R L E K I A P K I K A R	488
<i>Gro-UNC-25</i>	512 D Y F T V K I K N T E G Y E M V V D D P E F L N I C F W Y V P P S M R R A M E H K E K M A R L E K I A P K I K A R	568
<i>Cel-UNC-25</i>	459 M M Q R G T T M V G Y Q P D K Q R P N F F R M I I S N Q A I T R E D L D F L I K E I V D I G E S L E	508
<i>Gpa-UNC-25</i>	489 M M E R G T T M V G Y Q P D K Q R P N F F R M I I L S N P A I R E A D D L D F L I D E I V T L A K D L -	537
<i>Gro-UNC-25</i>	569 M M E R G T T M V G Y Q P D K Q R P N F F R M I I L S N P A I R E V D L D F L I D E I V T L A K D L -	617

Figure 3-23: Alignment of Cel-UNC-25 with Gpa-UNC-25 and Gro-UNC-25

Yellow box indicates the NPHK tetrapeptide characteristic of a glutamic acid decarboxylase.

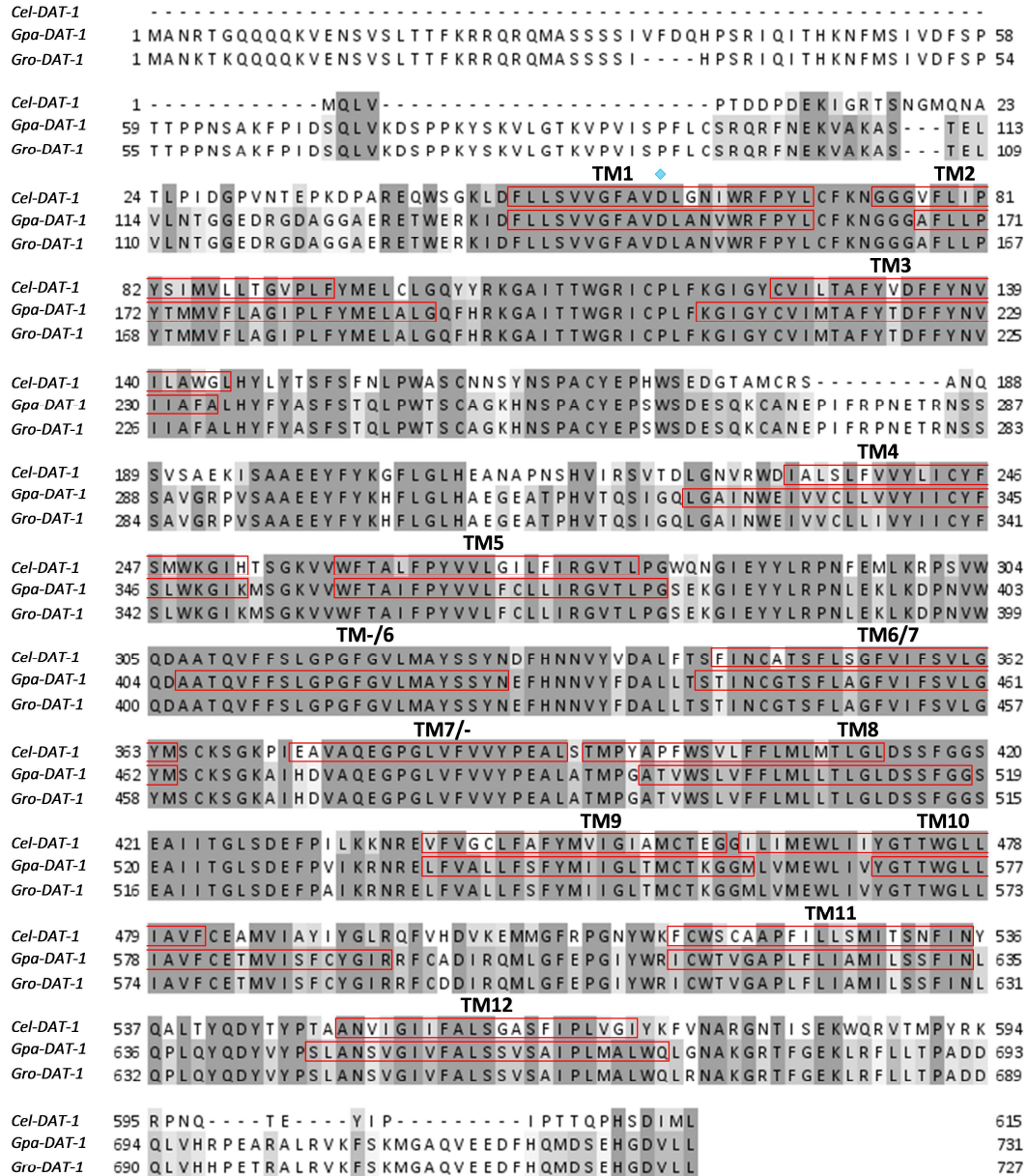


Figure 3-24: Alignment of Cel-DAT-1 with Gpa-DAT-1 and Gro-DAT-1

Transmembrane domain regions are indicated by red boxes. The transmembrane domains for Cel-DAT-1 are confirmed, whereas the transmembrane domain regions for Gpa-DAT-1 are predicted. The blue diamond indicates the presence of an aspartate residue common to serotonin and dopamine receptors.

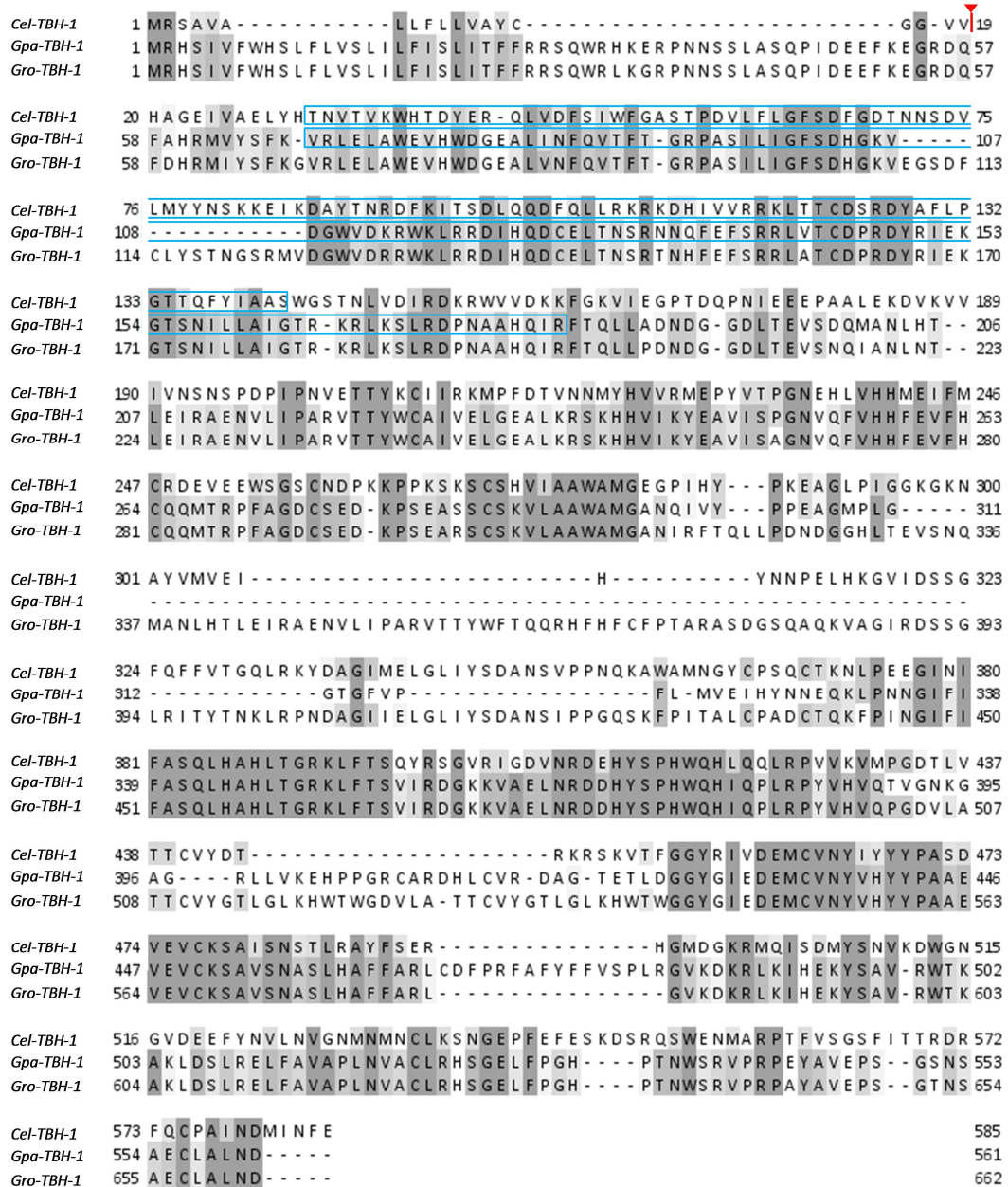


Figure 3-25: Alignment of Cel-TBH-1 with predicted amino acid sequence of Gpa-TBH-1 and Gro-TBH-1

Red arrow indicates signal peptide cleavage site. Blue box highlights the DOMON domain for Cel-TBH-1 (Uniprot) and Gpa-TBH-1 (as predicted by InterPro).

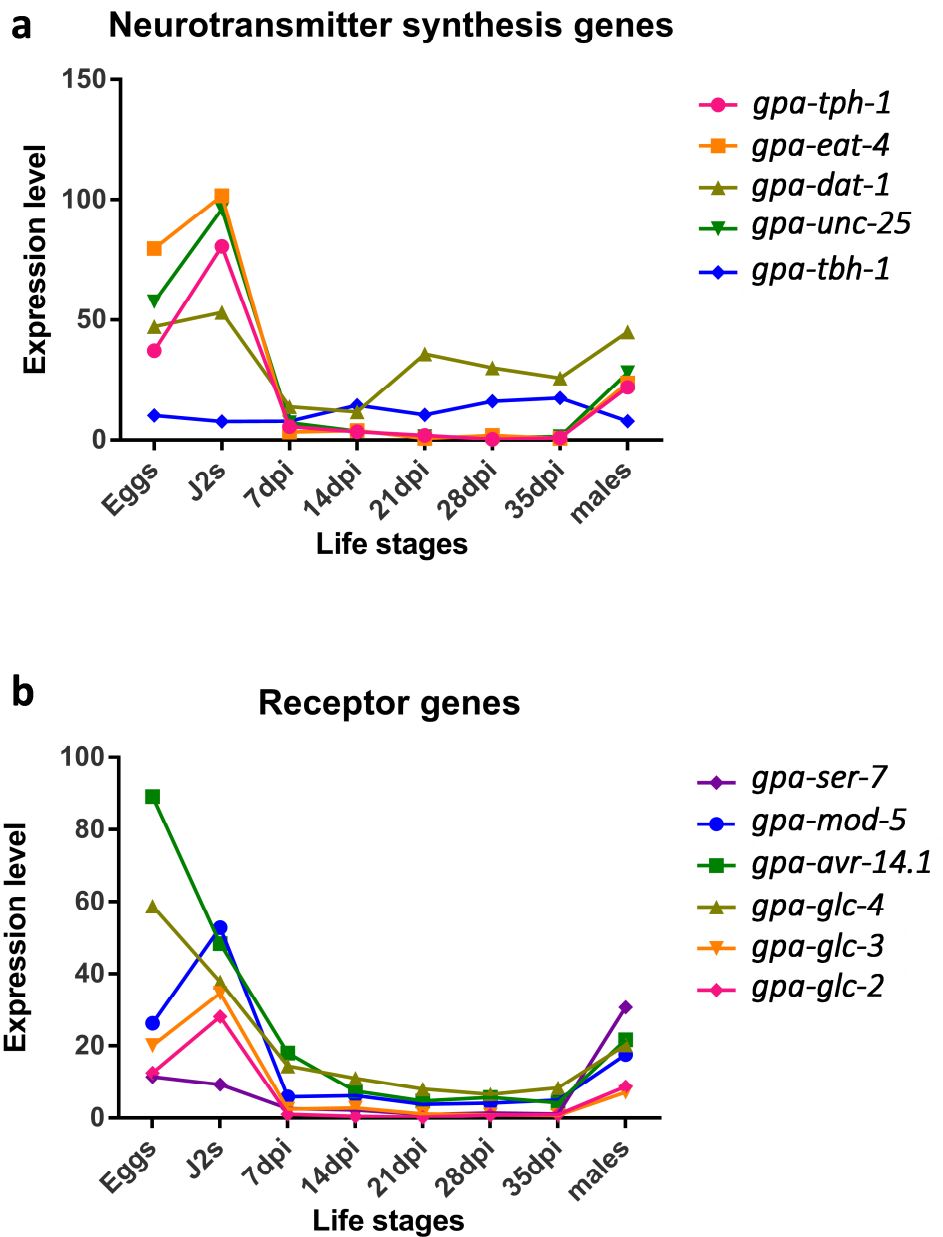


Figure 3-26: Expression of transcripts for identified orthologues over the life-stages of *G. pallida*

Expression in the eggs, the motile stages (J2s and males) and sedentary stages (7-35 dpi females) for a) the neurotransmitter synthesis genes b) the genes encoding subunits of glutamate-gated chloride channels.

3.4 Discussion

3.4.1 Quality of bioinformatic data sources must be assessed to determine confidence in results

Potential orthologues of *C. elegans* genes have been identified and cloned for *G. pallida* for all but two of the genes searched for in this chapter. The genome assembly of *G. rostochiensis* has acted as a valuable extra resource for this work. Due to the reduced genetic diversity of *G. rostochiensis* in the UK (Bendezu *et al.* 1998) compared to *G. pallida* the genome assembly produced was more robust. This allowed a second set of orthologues to *C. elegans* genes to be identified using bioinformatic methods alone in *G. rostochiensis* with a higher degree of confidence in the data set.

It is important to assess the quality of source data when searching for orthologues of genes by purely bioinformatic methods. Many sources of error can be introduced in the production of a genome sequence. The DNA collected must be of good quality and free from contamination. Due to variation between individuals, and as the individual DNA of one plant-parasitic nematode was not sufficient to sequence a genome, it helps to have a source of DNA with low allelic variation. The production of inbred lines prior to DNA collection to reduce variability can be helpful.

The choice of sequencing technology is also important, and sequencing technology is improving rapidly as time progresses. Sanger sequencing led the field of sequencing for over 25 years (Sanger, Nicklen and Coulson 1977), but next-generation sequencing has made improvements in speed, cost and accuracy. Next-generation sequencing methods include Roche 454 sequencing (generates up to 800 bp reads), Illumina HiSeq sequencing (150bp) and Pacific Biosciences (up to 5 kb) (Ekblom and Wolf 2014). Choice of sequencing technology impacts the coverage required (typically shorter reads require a deeper sequencing coverage to ensure enough overlapping sequence for genome assembly) and impacts choice of assembly algorithm downstream as algorithms differ between short-read assembly and long-read assembly. The ease of assembly is also affected by presence of repetitive sequences and highly variable regions at any stage can complicate final assembly. In these cases, the repetitive sequences may be incorporated erroneously into the assembly. If sequencing has not been conducted to an appropriate depth, large amounts of sequence data may be omitted from the final assembly. Preassembly, the sequencing data can be checked for low-quality reads and contaminating sequence from other organisms.

Genes are then predicted by gene prediction programs such as Augustus. Modelling genes is complex, and must take into account large introns present in eukaryotic genomes, and the ability to determine the start and end of genes. The production of transcriptome data mapped onto an assembled genome can provide information about the quality of gene model prediction, particularly the accuracy of mapping

intron-exon boundaries. The biological role of predicted genes can be annotated through databases such as gene ontology (GO) terms which yields functional information, but such methods are likely to miss novel genes which may be of particular interest in parasitic genomes, such as effector genes. Comparison to a closely related species can aid genome annotation, as well as manual annotation by trained researchers.

In the case of the *G. pallida* genome assembly, many practical hurdles had to be overcome. The *G. pallida* populations in the UK are very genetically diverse. As *G. pallida* must be cultured on potato plants, and each female nematode may be fertilised by multiple males, the production of inbred lines would have been difficult and time-consuming. Although all material for the *G. pallida* genome originated from an individual field site, there was clearly high genetic diversity in the starting material. To produce enough genetic material for DNA sequencing, a strategy known as Whole Genome Amplification (WGA) was initially used, this unfortunately introduced a large number of inverted repeats into the starting material after amplification. As sequencing occurred over several years in which the technology was improving, three different types of reads generated by different sequencing technologies was incorporated into the final pool to be assembled which may have complicated assembly (Cotton *et al.* 2014).

Without knowledge of the quality of a genome assembly, and the processes that have led to the final assembly, it is hard to determine how much trust to place in orthology searching that relies solely on bioinformatic methods. If a gene is not identified in an assembled genome, its absence cannot be confirmed without analysing other data sources. If a gene model predicts a truncated form of the gene, the gene model may have mispredicted gene structure or it could be the result of assembly error.

As *G. pallida* and *G. rostochiensis* are closely related, any absences in orthologues for *C. elegans* genes can be stated with confidence as they have not been found in two genome assemblies, and at least two sets of transcriptome data.

3.4.2 Key neurotransmitter synthesis genes are present in the *G. pallida* and *G. rostochiensis* genome

Previous work in this field has also indicated that the same major neurotransmitters are present and play a major role in nematodes across the clade. This is substantiated by the genome data as key enzymes involved in the synthesis and metabolism of neurotransmitters have been identified and cloned in *G. pallida* and identified bioinformatically in *G. rostochiensis* indicating that the same neurotransmitters are likely to be present and active between *C. elegans* and both *Globodera* spp.

Acetylcholinesterase-inhibitors disrupt chemoreception in *G. pallida* and *H. glycines* (Winter, McPherson and Atkinson 2002) and genes encoding acetylcholinesterases, involved in the removal of acetylcholine from the synaptic cleft, have been identified in *M. incognita*, *M. javanica* (Piotte *et al.* 1999) and *G. pallida* (Costa *et al.* 2009). Here, genes encoding two key enzymes involved in the production of acetylcholine (*cha-1*) and the loading of acetylcholine into vesicles (*unc-17*) have been identified.

Exogenous application of serotonin to J2s of plant-parasitic nematodes causes behavioural changes. The stimulation of stylet thrusting is a behavioural change common to *M. incognita*, *H. glycines* (Masler 2008) and *G. pallida* (Figure 3-21a). In *G. pallida* this increased stylet thrusting is accompanied by the cessation of worm movement, and may possibly indicate that serotonin signalling is involved in the invasion process. Here, a gene encoding a key enzyme in the synthesis of serotonin (*gpa-tph-1*) has been identified along with the post-synaptic receptor (*gpa-ser-7*) and the reuptake transporter present on the neurosecretory neuron (*gpa-mod-5*) (Ranganathan *et al.* 2001). Although there are discrepancies between Cel-SER-7 and Gpa-SER-7, primarily the presence of a predicted signal peptide in Gpa-SER-7, but not in Cel-SER-7, serotonin is able to activate a receptor as demonstrated by the response of *G. pallida* J2s to exogenous serotonin. The absence of a signal peptide in Cel-SER-7 may be a result of a false-negative prediction by SignalP or that Cel-SER-7 is targeted to the membrane by other mechanisms, such as by signals within the first transmembrane domain which has been shown to target Type II receptors.

Dopamine has been detected by glyoxylic acid fluorescence in *G. rostochiensis* J2s (Sharpe and Atkinson 1980) and has been detected in homogenates of *M. incognita* J2s by HPLC analysis (Stewart, Perry and Wright 2001). Dopamine may be involved in different roles, as exogenous application of dopamine to *H. glycines* at 5 mM stimulates body movement, but at 50 mM inhibits it. This inhibition of movement caused by 50 mM dopamine is also observed in *M. incognita*. In this chapter, a gene encoding a dopamine reuptake transporter (*dat-1*) has been identified.

Putative GABA receptors have been identified in *G. pallida* (Cotton *et al.* 2014), although the role of this neurotransmitter is not well explored in plant-parasitic nematodes. Here the enzyme involved in the synthesis of GABA has been identified, indicating that GABA is present in *G. pallida*.

Exogenous application of octopamine increases movement of *H. glycines* at 5 mM, and *M. incognita* at 5 mM and 50 mM (Masler 2008). This indicates that a pathway for octopamine recognition is likely to exist in plant-parasitic nematodes, and that octopamine is likely to be used as a neurotransmitter in the nervous system. The orthologue identified for an enzyme involved in octopamine synthesis TBH-1 had low identity to Cel-TBH-1 and could not be cloned, although Interpro analysis showed the sequence contained the DOMON domain associated with this enzyme-type (Aravind

2001), suggesting that despite the low sequence identity, the orthologue identified in *G. pallida* is likely to be functional. Furthermore, exogenous application of 50 mM octopamine to *G. pallida* J2s had a stimulatory effect after 24 hours exposure (Figure 3-21b) indicating that a receptor for octopamine is likely to exist, and that octopamine functions in the nervous system of *G. pallida*.

3.4.3 Some orthologues of *C. elegans* genes encoding glutamate-gated chloride channels can be found in the *G. pallida* and *G. rostochiensis* genomes

Orthologues for the *C. elegans* genes (*cel-glc-1*, *cel-glc-2*, *cel-glc-3*, *cel-glc-4*, *cel-avr-14* and *cel-avr-15*) encoding glutamate-gated chloride channels were searched for in the *G. pallida* genome and *G. rostochiensis* assembly. Orthologues for *cel-glc-1* and *cel-avr-15* could not be identified in the *G. pallida* genome assembly. Unassembled reads and transcriptome data were also examined for any evidence of orthologues of *cel-glc-1* and *cel-avr-15* that had not been processed into the main genome assembly. Once the *G. rostochiensis* genome assembly could be accessed, and was found to lack orthologues of *cel-glc-1* or *cel-avr-15* their absence in *Globodera* spp. could be stated with more confidence. Orthologues of *cel-glc-1* and *cel-avr-15* are also absent in *B. malayi* and *T. spiralis* (Williamson, Walsh and Wolstenholme 2007).

Orthologues for *cel-glc-2*, *cel-glc-3*, *cel-glc-4* and two orthologues of *cel-avr-14* could be identified in both *G. pallida* and *G. rostochiensis*. Coding sequences of most of these genes were cloned from *G. pallida* and the predicted amino acid sequences examined for features common to glutamate-gated chloride channels. A clone of *gpa-glc-4* could not be obtained, so the amino acid sequence of this is derived from the *G. pallida* transcriptome and the *G. rostochiensis* genome. Unless the *G. rostochiensis* gene differed significantly from the *G. pallida* gene, statements made about the *G. pallida* gene apply equally to the *G. rostochiensis* gene.

Features of a glutamate-gated chloride subunit are present in all predicted amino acid sequences. Four membrane spanning domains and extracellular loops A-F are present and residues known to be involved in glutamate binding are identified in all orthologues (Hibbs and Gouaux 2011). The cysteine pair separated by 13 conserved amino acids that characterises the cys-loop class of receptor (Thompson, Lester and Lummis 2010) is also present in all orthologues.

Two orthologues of *cel-avr-14* have been identified. *Gpa-avr-14.1* is more closely related to *cel-avr-14* than *gpa-avr-14.2*, although the predicted amino acid sequence of *gpa-avr-14.2* also has all features that mark a glutamate-gated chloride channel. *Gpa-avr-14.1* is predicted to lack a signal peptide, and although the N-terminal end of *Gro-avr-14.1* is longer no signal peptide is predicted. It may be that this subunit is not targeted to the membrane in *G. pallida* that it reaches the membrane by other mechanisms or that signal peptide prediction by SignalP is not infallible.

The predicted amino acid sequence of *gpa-avr-14.2* is also not predicted to have a signal peptide. However, TMHMM predicts five transmembrane spanning domains rather than the four typical for this subunit type. The additional transmembrane domain occurs close to the N-terminal end of the amino acid sequence and may itself function as a signal peptide, as both signal peptides and transmembrane domains share similar features.

The orthologues of *cel-glc-4* identified in *G. pallida* and *G. rostochiensis* lack a key arginine residue in Loop G, which is replaced by an asparagine. In an R76N mutation affecting the loop G arginine of Cel- AVR-14, the channel did not activate in response to glutamate when expressed in *Xenopus* oocytes (Lynagh *et al.* 2015). As the orthologue has not been cloned from either *G. pallida* or *G. rostochiensis*, the amino acid sequence cannot be confirmed. However, the presence of this residue change in both genome assemblies increases the likelihood of this being the genuine sequence.

One feature common to the predicted amino acid sequences of all orthologues of glutamate-gated chloride subunits cloned in *Globodera* spp. is an extension in the amino acid sequence between TM3 and TM4. This is typically an expansion of ~100 amino acid residues with little sequence homology to the *C. elegans* protein. In the predicted amino acid sequence for *gpa-glc-2*, this expanded region is predicted to include a fifth transmembrane region not present in Cel-GLC-2, although modelling by RaptorX does not support the presence of a fifth transmembrane domain (Figure 3-11). However, whether or not this predicted transmembrane region occurs *in vivo* has not been confirmed. Modelling of Gpa- AVR-14.1 and Gpa- AVR-14.2 also shows an extended TM3-TM4 loop (Figure 3-17). This region between TM3 and TM4 is an intracellular loop, which may be involved in aspects which affect receptor function such as desensitisation or aggregation (Lo *et al.* 2008; Kracun *et al.* 2008) as shown in other members of the cys-loop family.

3.4.3.1 Differences in the complement of glutamate-gated chloride channels may affect ivermectin targets

Ivermectin sensitivity in *C. elegans* is linked to the genes encoding Ce-GLC-1, Ce- AVR-15 and Ce- AVR-14. As orthologues for *cel-glc-1* and *cel-avr-15* could not be identified, the possible contribution of the identified *cel-avr-14* orthologues, and the remaining subunits, were investigated. *G. pallida* J2s are sensitive to ivermectin as they become paralysed upon exposure therefore the absence of *cel-glc-1* and *cel-avr-15* has not affected sensitivity. However, *cel-avr-15* is linked to the high sensitivity of the *C. elegans* pharynx to ivermectin (Dent, Davis and Avery 1997) and the efficacy of ivermectin to starve *C. elegans* at low doses of ivermectin (Dent *et al.* 2000). As *G. pallida* J2s are non-feeding, and do not stylet thrust, the effect of ivermectin on stylet thrusting was not investigated. As serotonin induces stylet thrusting of *G. pallida* J2s, the effect of ivermectin on serotonin-induced stylet thrusting could be examined.

In *C. elegans*, mutation of *celavr-14*, *celglc-1* and *celavr-15* together is required for high ivermectin resistance (Dent *et al.* 2000).

It is likely that the orthologues of *celavr-14* identified in *G. pallida* mediate sensitivity to Ivermectin. The residues involved in ivermectin binding have been identified by X-ray crystal structure in a homomeric pentamer of Cel-GLC-1 (Hibbs and Gouaux 2011), and the predicted *G. pallida* orthologues were investigated for the presence of these residues (Figure 3-8).

Gpa-AVR-14.1 shares most of the amino acid residues involved in ivermectin binding with Cel-GLC-1, although there is no isoleucine at position 376. This residue is also a threonine in Cel-AVR-14, which is known to have a role in ivermectin sensitivity. There Alanine replaces threonine at position 388, although again this is present in Cel-AVR-14. From study of these residues it seems likely that Gpa-AVR-14.1 is able to bind ivermectin as effectively as Cel-AVR-14 and may play a role in sensitivity of *G. pallida* to Ivermectin. Similarly, Gpa-AVR-14.2 shares the same residues associated with ivermectin sensitivity as Cel-AVR-14.

However, it is unclear which of these residues is essential for ivermectin binding. Cel-GLC-2 homomers are insensitive to ivermectin when expressed in *Xenopus* oocytes (Cully *et al.* 1994), though it shares some of the residues highlighted in ivermectin sensitivity. These residues are shared by Gpa-GLC-2 suggesting that Gpa-GLC-2 would have a similar sensitivity to ivermectin as Cel-GLC-2. Although *celglc-3* has not been linked genetically to ivermectin sensitivity in *C. elegans*, when the subunit is expressed in *Xenopus* oocytes, a homomeric receptor sensitive to ivermectin is formed (Horoszok *et al.* 2001). The predicted amino acid sequence of Cel-GLC-3 shares most of the residues associated with ivermectin sensitivity, and those are mostly present in Gpa-GLC-3 as well. From sequence alone it is hard to predict how Gpa-GLC-3 affects ivermectin sensitivity, but it may have a role.

Information about Cel-GLC-4 is still relatively sparse, although examination of the amino acid sequence suggests that a similar amount of ivermectin associated residues are present as for Cel-GLC-2, leading to a conclusion that it may not play a significant role in ivermectin sensitivity. These residues are also shared by Gpa-GLC-4.

As there is little information about the stoichiometry and location of these different channels in native *C. elegans*, it is difficult to draw too many conclusions from the channels that are present and which residues are present within them. It is unknown which are expressed in the same neurons and therefore whether homomeric or heteromeric receptors are formed. This would also affect ivermectin binding as it binds between subunits (Hibbs and Gouaux 2011).

3.4.4 Gene expression analysis highlights importance of neurotransmitter-related genes at motile life-stages or stages which must respond to hosts

Analysis of gene expression over different life-stages (Figure 3-26) shows that generally these orthologues identified in *G. pallida* are most highly expressed at life-stages that are non-parasitic and require either motility or response to host cues (Den Nijs and Lock 1992). Eggs must be able to hatch in response to host-derived cues, and J2s must be able to locate and move towards a suitable host. The males of *G. pallida* are motile, and must seek the sedentary female within the root. There is some indication that dopamine may be involved in the maintenance of parasitism, as *gpa-dat-1* expression remains elevated at 21 dpi. It may be expected that, as *cel-eat-4* is involved in pharyngeal pumping and feeding in *C. elegans* (Lee *et al.* 1999) and that during the sedentary parasitic stages, *G. pallida* must feed, expression of *gpa-eat-4* would remain high throughout parasitism. However, expression of *gpa-eat-4* is low during these sedentary stages. *Gpa-tbh-1* expression is generally low throughout, although expression is slightly higher in the sedentary stages.

3.4.5 Confidence in orthology

It can be difficult to establish orthology with confidence from bioinformatic data alone. Several methods have been used to determine that the orthologue identified in *G. pallida* and *G. rostochiensis* is the best possible.

The Reciprocal Best Hits (RBH) system can be robust, particularly when the species are closely related. However, using this methodology may lead to missing other orthologues when gene duplication leads to two genes being potential orthologues (Gabaldón 2008) such as with *gpa-avr-14.1* and *gpa-avr-14.2*.

To confirm if these orthologues identified in *G. pallida* are likely to share the same function as in *C. elegans*, more experimentation would be required. The ability of the *G. pallida* version of the gene to complement *C. elegans* mutants of the same gene and rescue the mutant phenotype would be a good way to prove functional orthology. Indeed, *gpa-tph-1*, *gpa-ser-7* and *gpa-eat-4* have been used to rescue the respective *C. elegans* mutants to a near wild-type phenotype, indicating that the *G. pallida* genes are able to function in the same role (Anna Crisford, unpublished). In the absence of similar data for the rest of the orthologues identified here, the amino acid sequence can be searched to identify known features common to proteins of that function. Here, the use of signal peptide and transmembrane predictions provide evidence for the targeting of the protein, its location in the cell, and the number of any transmembrane domains. Additionally some enzymes have cofactor binding sites and other motifs which identify them as members of particular enzyme classes.

Some *C. elegans* genes have very specific expression patterns. For example, *cel-eat-4* is expressed weakly in the extrapharyngeal nervous system and strongly in the pharynx (Lee *et al.* 1999). The expression of the glutamate-gated channel subunit *cel-glc-2* is restricted solely to the metacorpus of the pharynx (Laughton, Lunt and Wolstenholme 1997). Analysis of the expression patterns of the *G. pallida* orthologues would allow further inferences to be made about their function.

3.4.6 Identification of isoforms

Many of the *C. elegans* genes discussed in this chapter are known to encode different protein isoforms, produced by differential splicing of the mRNA transcripts. To date, no evidence for different isoforms of *G. pallida* orthologues has been found but this has not yet been investigated extensively.

Summary

- Key genes involved in neurotransmitter synthesis, metabolism and transduction are present in *G. pallida* and *G. rostochiensis*
- *G. pallida* and *G. rostochiensis* have a different complement of glutamate-gated chloride channel subunits than *C. elegans*

4. Identification of *Globodera pallida* orthologues of *Caenorhabditis elegans* genes that encode nicotinic acetylcholine receptor subunits

4.1 Introduction

More than 30 genes in *C. elegans* encode subunits of nicotinic acetylcholine receptors, leading to a predicted large diversity of nicotinic acetylcholine receptors in nematodes (Jones and Sattelle 2004; Jones *et al.* 2007). They are involved in behaviours such as locomotion, chemosensation and egg-laying (Kim *et al.* 2001a). They are divided into five main groups by sequence homology and are named after the first member of the group to be identified. A summary of *C. elegans* nicotinic acetylcholine receptor subunits can be found in Table 4.

The exact roles of many of these genes have not yet been characterised, and many do not have a clear phenotype in mutagenesis experiments. However, roles can be inferred from expression pattern of particular genes. The roles of some are beginning to be elucidated. *Cel-acr-12* is expressed exclusively in neurons and loss of *cel-acr-12* affects the balance between relaxation and contraction that drives locomotion in *C. elegans* (Pettrash *et al.* 2013; Gottschalk *et al.* 2005). *Cel-acr-2* is also expressed exclusively in the neurons (Philbrook, Barbagallo and Francis 2013). *Cel-eat-2* is expressed in the pharyngeal muscle and mutants of *cel-eat-2* are deficient in pharyngeal pumping, indicating that *cel-eat-2* is involved in feeding behaviours (McKay *et al.* 2004). *Cel-acr-23* is expressed in body-wall muscle and is the target of the antihelmintic monepantel (Rufener *et al.* 2013). *Cel-acr-5* and *cel-acr-15* are involved in nicotine-induced locomotory behaviours, and were found to influence this behaviour in the neurons rather than in the muscle (Sellings *et al.* 2013). Mutations in *cel-deg-3* lead to degeneration of certain neurons and *cel-des-2* is necessary for the *cel-deg-3* mutant phenotype (Treinin *et al.* 1998).

4.1.1 The structure and function of nAChRs

nAChR subunits all belong to the cys-loop ligand-gated ion channel class. Each subunit characteristically has four transmembrane spanning domains rich in hydrophobic amino acids (TM1-4). TM2 of each subunit contributes towards the lining of the central pore and determines ion selectivity. The intracellular loop between TM3 and TM4 is involved in localisation of the receptor and helps to modulate receptor function (Jones and Sattelle 2004). A cys-loop in the long N-terminal region is characterised by the presence of two cysteine residues separated by 13 amino acids (Corringer, Le Novere and Changeux 2000). Subunits are further defined as α or non- α . α -subunits are characterised by the presence of an YxxCC motif towards the N-terminus, while non-alpha subunits lack this motif (Lewis *et al.* 1980; Kao *et al.* 1984; Lukas *et al.* 1999).

A single type of α -subunit may form a pentamer, producing a homomeric receptor. *Acr-16* forms a homomeric receptor, and is present in body-wall muscle. Expression of this single subunit with the required ancillary factors is sufficient to generate a functional receptor in *Xenopus* oocytes (Touroutine *et al.* 2005). Heteromeric receptors are formed when more than one subunit type forms the pentamer. With the number of nAChR subunits encoded in the *C. elegans* genome, the interacting partners that produce different heteromeric receptors is not clearly defined. As heteromeric receptors consisting of different combinations of nAChR subunits are likely to have different pharmacological characteristics, they are also likely to play different biological roles. There is also overlap between the different types of heteromeric receptors formed, with some subunits being present in more than one subtype of heteromeric receptor. The composition of some of these receptors has been elucidated. A neuronal receptor comprising Cel-ACR-12, Cel-ACR-2, Cel-ACR-3, Cel-UNC-63 and Cel-UNC-38 has been identified (Jospin *et al.* 2009), although Cel-ACR-12 has also been identified as a member of a separate receptor type present in the GABAergic neurons that drive relaxation of body-wall muscle (Petrash *et al.* 2013). The nAChR present in body-wall muscle that is the target of levamisole comprises Cel-UNC-38, Cel-UNC-63, Cel-UNC-29, Cel-LEV-1 and Cel-LEV-8 (Fleming *et al.* 1997; Towers *et al.* 2005; Lewis *et al.* 1980). These five genes, along with genes encoding ancillary factors necessary for receptor assembly, are sufficient to produce functional receptors when expressed in *Xenopus* oocytes (Boulin *et al.* 2008). Heteromeric receptors may consist of a mix of α and non- α -subunits.

Acetylcholine binds in a pocket formed between the positive face of an α -subunit and the negative face of a complementary subunit, which can be α or non- α . Much of the structural understanding of receptor binding came from work conducted on the acetylcholine binding protein, found in the snail *Lymnaea stagnalis* (Brejc *et al.* 2001). This protein lacks the transmembrane and intracellular domains of nAChRs, but is homologous to the extracellular binding domain (Smit *et al.* 2001). Other work in *Mus musculus* (mouse) nAChRs demonstrates that the binding pocket forms between the principal face of an α -subunit and the negative face of another subunit. The α -subunit is comprised of three loops (A-C). From loop A, residues W⁸⁶ and Y⁹³ contribute to ligand binding; loop B, residues W¹⁴⁹, Y¹⁵¹, D¹⁵² and G¹⁵³ and loop C, residues Y¹⁹⁰, C¹⁹², C¹⁹³ and Y¹⁹⁸ (Arias 2000; Corringer, Le Novere and Changeux 2000). These residues are generally well conserved in nematode α -subunits, although there is some variation in Loop B (Figure 4-1b).

The negative face contributes four loops (D-F). from loop D, residues W⁵⁵ and E⁵⁷ contribute to forming the complementary face; loop E, residues L¹⁰⁹, S¹¹¹, C¹¹⁵, I¹¹⁶, Y¹¹⁷ and from Loop F, residues F¹⁷², D¹⁷⁴ and E¹⁸³ (Arias 2000; Corringer, Le Novere and

Changeux 2000). These complementary face residues interacting with acetylcholine appear to be less well conserved in nematode nAChRs. Studies on the nematode binding pocket identify residues W⁵⁵ and Q⁵⁷ as important in loop D and A¹¹⁹ in Loop E of UNC-63 and W⁵⁵ in loop D and V¹¹⁷ in Loop E of Cel-UNC-29 or Cel-LEV-1 (Bartos *et al.* 2009; Hernando *et al.* 2012). Loop F has not been modelled due to its sequence variation, so little is known about contribution of residues from this loop (Figure 4-1c)

4.1.2 The neuromuscular system is a target for novel anthelmintic discovery

Many anthelmintic drugs, such as pyrantel, levamisole and DMPP target the neuromuscular system, and it is an attractive target for novel anthelmintic discovery. Targeting the neuromuscular system allows paralysis to be induced in the parasite, which inhibits its ability to reach the host organism, and may lead to starvation. As there seems to be high diversity in the number of nAChRs in the different species of the phylum Nematoda, study of this group of receptor may allow novel targets to be identified. A summary of nAChRs identified in parasitic nematodes can be found in Holden-Dye *et al.* (2013). The nAChR complement in plant-parasitic nematodes has not been studied in detail, although some attention has been given to the neuromuscular targets for disrupting *fip* gene signalling (Kimber and Fleming 2005).

The levamisole-sensitive nicotinic acetylcholine receptor (L-nAChR) is the most studied of these nAChRs and is one of three acetylcholine receptor types in body wall muscle of *C. elegans* (Jones and Sattelle 2004; Rufener *et al.* 2013; Touroutine *et al.* 2005). It is a heteromeric receptor comprising Cel-LEV-1, Cel-LEV-8, Cel-UNC-38, Cel-UNC-63 and Cel-UNC-29 (Lewis *et al.* 1980; Boulin *et al.* 2008). The anthelmintic levamisole targets this receptor by binding to and activating the receptor. It acts to paralyse the worm by prolonged activation of the muscle, leading to uncoordinated movement and ultimately hyper-contraction and paralysis of the worm. Mutation of any one of *cel-unc-38*, *cel-unc-29* or *cel-unc-63* leads to an uncoordinated phenotype and increased levamisole resistance in *C. elegans*, showing that they are essential for receptor formation and function. Mutation of *cel-lev-1* or *cel-lev-8* also confers partial resistance to levamisole, although they are non-essential to receptor formation (Towers *et al.* 2005; Culetto *et al.* 2004; Fleming *et al.* 1997). The precise arrangement of the subunits is not known, although potential arrangements as proposed in the literature are shown in Figure 4-1a.

4.1.3 Expression analysis and transformation by bombardment

Information about the expression patterns of genes can provide insight into their roles. Different nAChR subunits as members of different receptors, and are expressed in different locations within the nervous system. Expression pattern analysis may allow identification of which nAChR subunits are part of the same receptor and allow their role to be elucidated. *C. elegans* has been used as a heterologous expression system to

analyse spatial expression of plant-parasitic nematode genes using promoter-GFP fusions (Qin *et al.* 1998; Costa *et al.* 2009). In this chapter, the possibility of using promoters of the *G. pallida* nAChRs, in a similar way to infer spatial expression was explored.

DNA transformation by microparticle bombardment is a method used to transform *C. elegans* and produces integrative transformants (Praitis *et al.* 2001). DNA is coated onto gold particles which are bombarded into worms using a “gene gun” producing transformants. Selection of transformants is mediated by the rescue of the mutant phenotype of the bombarded nematode strains. The *unc-119(ed3)* strain is typically used, which are severely uncoordinated, unable to form dauer larvae and dumpy in appearance (Maduro and Pilgrim 1995). The bombarded construct contains the *unc-119* gene to facilitate rescue of the *unc-119(ed3)* phenotype and provide a method for identifying transformants. The construct also contains the promoter region of interest upstream of the coding region of GFP. Unlike microinjection, an alternate transformation method, bombardment generates low-copy transformants reducing the possibility of observed GFP expression being due to high copy numbers of a transgene.

In this chapter, an overall bioinformatic survey of nAChRs in the *G. pallida* and *G. rostochiensis* genomes assemblies has been undertaken. Expansions or reductions in members of particular groups in comparison to *C. elegans* have been considered together with the impact that any such changes may have on the efficacy of anthelmintics.

nAChR subunit	Group	Type	Comments
Cel-UNC-38	UNC-38	α	Part of Lev-sensitive receptor (Fleming et al. 1997)
Cel-ACR-6	UNC-38	α	(Mongan et al. 1998)
Cel-UNC-63	UNC-38	α	Part of Lev-sensitive receptor (Culetto et al. 2004)
Cel-UNC-29	UNC-29	non-α	Part of Lev-sensitive receptor (Fleming et al. 1997)
Cel-ACR-2	UNC-29	non-α	Operon with acr-3 (Squire et al. 1995)
Cel-ACR-3	UNC-29	non-α	Operon with acr-2
Cel-LEV-1	UNC-29	non-α	Part of Lev-sensitive receptor (Fleming et al. 1997)
Cel-ACR-8	ACR-8	α	(Mongan et al. 1998)
Cel-LEV-8	ACR-8	α	(Mongan et al. 1998)
Cel-ACR-12	ACR-8	α	(Mongan et al. 1998)
Cel-ACR-16	ACR-16	α	(Ballivet et al. 1996)
Cel-ACR-7	ACR-16	α	(Mongan et al. 1998)
Cel-ACR-9	ACR-16	non-α	(Mongan et al. 1998)
Cel-ACR-10	ACR-16	α	(Mongan et al. 1998)
Cel-ACR-11	ACR-16	α	(Mongan et al. 1998)
Cel-ACR-14	ACR-16	non-α	(Mongan et al. 1998)
Cel-ACR-15	ACR-16	α	(Mongan et al. 1998)
Cel-ACR-19	ACR-16	α	(Mongan et al. 2002)
Cel-ACR-21	ACR-16	α	(Mongan et al. 2002)
Cel-EAT-2	ACR-16	non-α	(McKay et al. 2004)
Cel-DEG-3	DEG-3	α	Operon with des-2 (Treinin et al. 1998)
Cel-ACR-5	DEG-3	α	(Mongan et al. 1998)
Cel-ACR-17	DEG-3	α	(Mongan et al. 1998)
Cel-ACR-18	DEG-3	α	(Mongan et al. 1998)
Cel-ACR-20	DEG-3	α	(Mongan et al. 1998)
Cel-ACR-23	DEG-3	α	(Mongan et al. 1998)
Cel-DES-2	DEG-3	α	Operon with deg-3 (Treinin et al. 1998)
Cel-ACR-24	DEG-3	α	Predicted

Table 4: Summary of nAChR subunits in *C. elegans*

Adapted from Wormbook. Subunits are categorised by group. Each group is named after the first member that was identified for it.

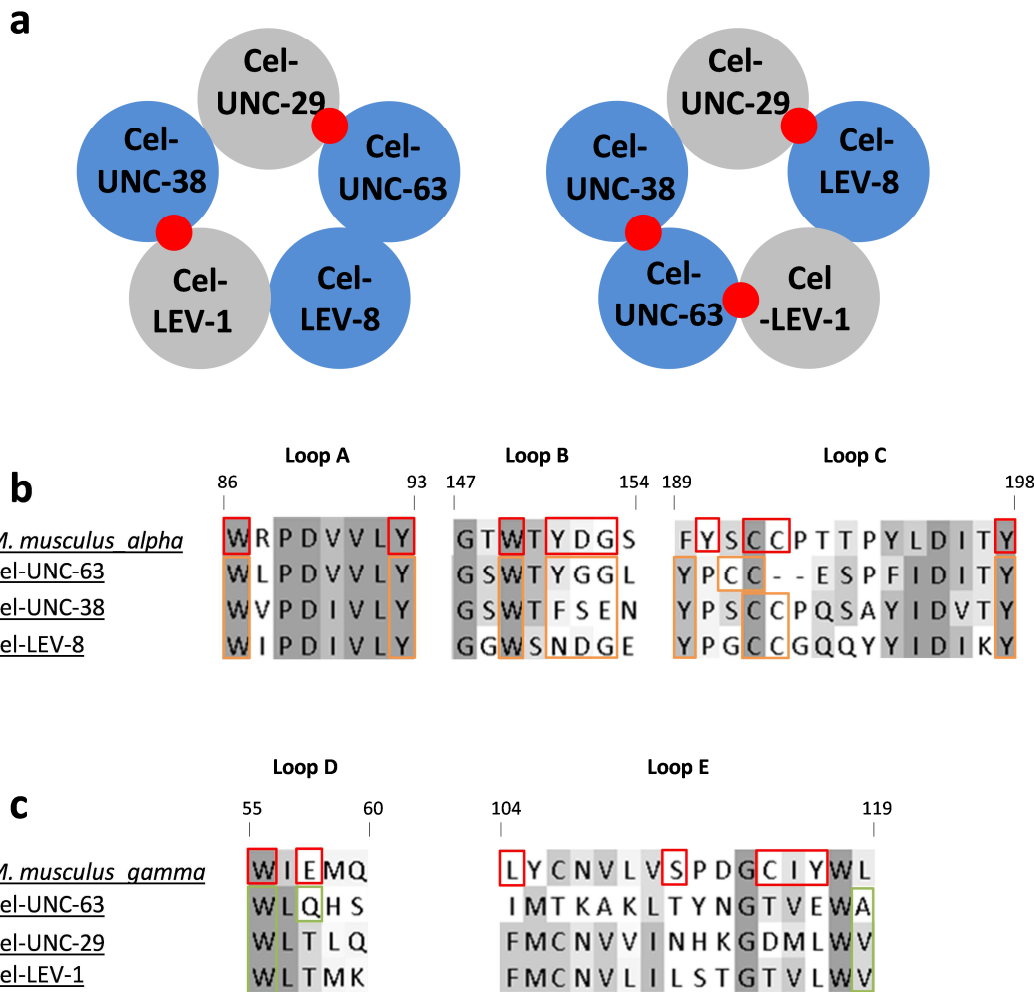


Figure 4-1: Schematics of the levamisole-sensitive nicotinic acetylcholine receptor of *C. elegans*

a) Two schematics representing possible conformations of the *C. elegans* L-nAChR. Blue circles represent α -subunits, grey subunits represent non- α . Red circles represent inferred acetylcholine binding pocket. b) Residues from an α -subunit provide the principal face of the acetylcholine binding site with Loops A-C. Red boxes highlight residues involved in the *M. musculus* receptor and orange indicate equivalent residues in *C. elegans* subunits. Numbering is for the *M. musculus* α -subunit. c) Residues involved in providing the complementary faces of the acetylcholine binding site with Loops D and E. Red boxes highlight residues involved in *M. musculus* γ subunit and green boxes highlight residues from *C. elegans* subunits identified as being involved by modelling. Loop F is not shown as it could not be effectively modelled. Numbering is for the *M. musculus* γ subunit.

Aims

- Investigate nicotinic acetylcholine receptor subunits of *G. pallida*
- Identify differences which may affect diversity of receptors in *G. pallida*

4.2 Materials and methods

All methods used for gene cloning and sequence analysis are described in 3.2. A table of primers used for cloning is found in Table 5.

4.2.1 Identification of orthologues for other nematodes

Sequences of *C. elegans* genes or proteins were obtained from Wormbase (Wormbase 2009). *Meloidogyne incognita* genes were identified from the *M. incognita* genome at http://www.inra.fr/meloidogyne_incognita/sequencing. *Meloidogyne hapla* sequences were obtained from Wormbase. *Ascaris suum* and *H. contortus* sequences were obtained from the NCBI database. *Bursaphelenchus xylophilus* sequences were obtained from <http://www.genedb.org/Homepage/Bxylophilus>. Sequences of *R. reniformis*, *Nacobbus aberrans*, *H. schachtii* and *H. avenae* were obtained from preliminary transcriptome databases produced within this laboratory.

Accession numbers for amino acid sequences used that are publically available are found in Table 6.

4.2.2 Analysis of GFP expression regulated by nAChR promoters from *G. pallida*

4.2.2.1 Production of expression vector

An expression vector for this work was constructed to include the *cbr-unc-119* gene, multiple restriction enzyme cloning sites and the coding region of GFP. The vector pPD95_75 (Addgene plasmid #1494) was selected for the backbone. *Caenorhabditis briggsae unc-119* and its promoter region were obtained from the vector pPK719 (Addgene 38149). The *C. briggsae* orthologue of the *cel-unc-119* cassette was selected due to its shorter length than *cel-unc-119*. The *cbr-unc-119* and promoter cassette was digested from pPK719 using restriction enzymes Sall and XbaI (NEB) in accordance with manufacturer's recommendations. Vector pPD95_75 was digested with the same enzymes under the same conditions. Ligation reaction was carried out at a 4 (insert) to 1 (vector) ratio in a 20 µl reaction as follows: T4 DNA ligase (NEB) (1 µl), vector (as calculated), insert (as calculated), 10x T4 Ligase buffer (2 µl), nuclease-free water (to 20 µl). Ligation was conducted at 4°C for 16 hours. 2 µl of the ligation reaction was then transformed as described in 3.2.14.3. Plasmid DNA prepared from individual colonies was screened for the insert by restriction digest (Sall and XbaI) and confirmed by 3.2.14.6 (using M13R primer). This vector was termed GFPexpress. A restriction map of the vector can be seen in Figure 4-2.

4.2.2.2 Cloning of promoter regions from gDNA

Promoter regions of *gpa-acr-2* and *gpa-unc-63* were cloned from gDNA of *G. pallida*. A total of 2kb upstream sequence from the initiating methionine (or to the end of an upstream gene) was selected as the promoter region to produce a transcriptional

fusion. The promoter region was amplified as described in 3.2.13.3, and cloned into the pCR™8 vector as described in 3.2.14.2. Primers used for *pgpa-acr-2* were: F: AATTGCCCTTCCTCTCCA and R: GCCCAACGATACTGCTGGAGAC and for *pgpa-unc-63* were: F: GTATTGGACTGAAGGTACTC and R: AAACTTAAATGTTTTGGAC. The cloned promoter region was sequenced as described in 3.2.14.6. Appropriate restriction enzymes were selected for cloning into the expression vector and primers were designed with restriction sites tagged onto the end. The restriction enzymes XbaI and KpnI were used for both constructs.

4.2.2.3 Production of expression clone

Products produced in 4.2.2.2 were cloned into pGFExpress (produced in 4.2.2.1) by restriction enzyme cloning as described in the previous sections. Restriction enzyme digestions were conducted as per manufacturer's instructions. Positive clones were selected by colony PCR (3.2.14.4) using the gene-specific forward and GFP-REVchk primer (CAAATTTCTGTCAGTGGAG).

4.2.2.4 Gold particle preparation

1 ml 70% ethanol was added to 30 mg gold particles (Sigma) and vortexed for 5 mins to suspend the particles. The particles were settled for 15 mins, then pulsed in a microcentrifuge to pellet. The supernatant was removed by pipetting then 70% ethanol was added, the tube vortexed for 1 min, settled for 1 min then pulsed in a centrifuge and the supernatant removed. This process was repeated a further two times. The pellet was resuspended in 500 µl sterile 50% glycerol. This preparation of gold particles was kept at 4 °C for up to 1 month.

4.2.2.5 Preparation of plasmid for bombardment

The expression clone produced in 4.2.2.3 was prepared for bombardment. 18 µl (minimum concentration 400 ng/µl) of each expression clone was linearised. 2.5 µl Apal (NEB), 3.5 µl buffer and 11 µl Elga water was added to the plasmid, and digested at 37°C for 2 hours. On the day of bombardment, the gold beads prepared in 4.2.2.4 were vortexed for 20 mins. For each construct to be bombarded, 70 µl of gold bead suspension was added to a non-stick 1.5 ml microfuge tube. The linearised expression clone was added to the gold beads, which were kept in suspension on a vortex mixer throughout the process. Two aliquots of 150 µl 2.5 M CaCl₂ and 112 µl of 0.1 M Spermidine were added drop-wise to the tube. The tube was then vortexed for 5 mins and then pulsed in the centrifuge. The supernatant was removed by pipetting and the gold beads resuspended in 800 µl of 70% ethanol. The tube was pulsed again, the supernatant removed and the gold beads resuspended in 70 µl 100% ethanol. After this point, the tube was vortexed constantly to keep the beads in suspension until used for bombardments.

4.2.2.6 Preparation of *unc-119* cultures

The *unc-119 (ed3)* strain was used for microparticle bombardments. The phenotype of this line is uncoordinated movement, “dumpy” appearance and inability to survive dauer formation (Maduro and Pilgrim 1995).

Unc-119 (ed3) worms were grown on 5 cm NGM-lite plates seeded with *E. coli* (HB101) for 2 weeks until mainly L1/L2s were present on the plates. These were used to start a liquid culture containing approximately 50,000 worms. 50 ml of M9 buffer was used, to which was added 150 µl 1M MgSO₄, 300 µl 0.5M CaCl₂, 50 µl cholesterol (final concentration 8 µg/ml), 500 µl antibiotic mix (penicillin/streptomycin/neomycin final concentration 5/5/10 µg/ml), 50 µl Nystatin (final concentration 10 µg/ml) and 3 ml of HB101 food source. The worms were grown at 18 °C at 200 rpm, checked daily and additional *E. coli* added if appropriate, until the majority had reached the young adult life-stage.

4.2.2.7 Growth of HB101 as food source for liquid culture

HB101 was grown in 1.4 L cultures of Superbroth media (15.68 g K₂HPO₄, 2.89 g KH₂PO₄, 15 g bacto-tryptone, 30 g yeast extract, 10 ml 50% glycerol, 1.4 L distilled water – autoclaved). A 5 ml overnight culture of HB101 was inoculated into a 2 L flask containing 1.4 L Superbroth and grown at 37 °C for approximately 24 hours at 150 rpm. The culture was divided between 12 x 250 ml centrifuge bottles and centrifuged at 4 °C and 8000 x g for 8 mins. Each *E. coli* pellet was resuspended in 6 ml M9 by shaking at 200 rpm for 15 minutes. The resulting suspension was transferred to a 15 ml sterilin tube and frozen at -20 °C. When required, this was defrosted and used as a food source for liquid cultures of *C. elegans*.

4.2.2.8 Microparticle bombardment of *unc-119(ed3)*

Liquid cultures containing young adults (as cultured in 4.2.2.6) were poured into 50 ml Polypropylene tubes and allowed to settle at room temperature for 10 mins. Older worms (young adults) would settle to the bottom of the tube during this time and were collected for use in bombardments. The supernatant was transferred to a fresh tube and transferred to ice where the younger worms were allowed to settle for 20 minutes. The younger worms were collected and stored in order to set up subsequent liquid cultures of *C. elegans*. 1 ml of young adult *C. elegans* was applied between seven target regions on a 9 cm NGM-lite plate seeded with *E. coli* (HB101). The prepared DNA from 4.2.2.5 was applied evenly between seven macrocarrier discs (Bio-Rad) which had previously been cleaned by dipping in isopropanol. The macrocarrier discs were loaded into the bombardment compartment with a stopping screen and rupture disc (1350 psi, Bio-Rad). The hepta-adaptor (PDS100/ HE system, Bio-Rad) was secured inside the chamber, and all components were aligned so that the gas acceleration tube was

directly above a macrocarrier disc and worm target. The Biolistics system used was PDS-1000-HE Biolistic® Particle Delivery System. A vacuum inside the chamber was established (27 inHg) and a shot was fired. 1 ml M9 buffer was applied to each bombarded plate, and the nematodes left to recover for 1-2 hours. Subsequently, 4 ml of M9 buffer was used to wash worms from the bombarded plate and distribute them evenly across 8 seeded 9 cm NGM-Lite plates.

4.2.2.9 Selection of positive transformants

Bombarded worms were allowed to starve for 4-5 weeks at 20°C before selection. A section of NGM-lite seeded with HB101 was placed face-up on the starved lawn of each bombardment plate and left for 16 hours. Transformed worms will have survived dauer formation and will move like wild-type (fast and coordinated) and will congregate on the new source of food. Non-transformed uncoordinated worms will not be able to reach the new food source. Four transformed worms from each plate were taken and transferred individually to a 5 cm seeded NGM-lite plate.

4.2.2.10 Visualization and photography of GFP expression

Transformed worms were mounted on 4% agarose pads and immobilised with 25 mM sodium azide. A coverslip was applied and sealed with varnish. For each line, approximately 15 worms were observed and representative images of GFP expression taken. For all lines, a 5s exposure time was used to capture images. Leica Leitz DMRB binocular microscope with GFP filters were used for visualisation. Images were captured with QCapture Pro 6 software.

Gene	Primer Sequence
<i>gpa-acr-12</i>	F: GCGATGATTGCCATTGCCA R: CCATTCAATTATTCCGCCGTT
<i>gpa-acr-2</i>	F: GCTCAAATTGGTTATTGTCC R: GCGCTTTAATTGGGACAGAA
<i>gpa-acr-3</i>	F: GGCGACGGATGAAAAGAA R: CTTTCCCCAATTTCGCGC
<i>gpa-acr-6</i>	F: GTTTGGGAATGCCTTCC R: GCGGGTGTAACTCAAAA
<i>gpa-acr-8</i>	F: AATGCCTCGGGGCTTGC R: GGGTAAGCAATCACAGAATG
<i>gpa-unc-29.1</i>	F: GGTTACAATTCTGATCCAA R: GTTCGATTAAAACAATTGGT
<i>gpa-unc-29.2</i>	F: TCGGTTCAAATGATTGACAACG R: GGTAAACGCCAAGAAAACGT
<i>gpa-unc-38.1</i>	F: CTGATGGTCTATCACCGGAA R: GGTATATGCAAACAATATGCTT
<i>gpa-unc-38.2</i>	F: AGAAACAATTGGCGCGAAGT R: GTTGCAGTTTACCCAGTA
<i>gpa-unc-63</i>	F: TGCCGCTTATGCCGACC R: CAACAAACAAATCGAATAATGCG

Table 5: Primers used for amplification of nAChR subunit-encoding genes

Gene	Species	Accession Number	Source
<i>cel-unc-38</i>	<i>C. elegans</i>	WP:CE24908	Wormbase
<i>bbr-unc-38</i>	<i>C. briggsae</i>	CAP37493	NCBI
<i>mha-unc-38</i>	<i>M. hapla</i>	MhA1_Contig1335.frz 3.fgene2	http://www.wormbase.org/species/m_hapla#043--10
<i>min-unc-38</i>	<i>M. incognita</i>	Minc17141	http://www6.inra.fr/meloidogyne_incognita/Meloidogyne
<i>asu-unc-38</i>	<i>A. suum</i>	ABS95448	NCBI
<i>hco-unc-38</i>	<i>H. contortus</i>	HCOI01939400.t1	NCBI
<i>ode-unc-38</i>	<i>O. dentatum</i>	AFY08299	NCBI
<i>cel-acr-2</i>	<i>C. elegans</i>	WP:CE07380	Wormbase
<i>cel-acr-3</i>	<i>C. elegans</i>	WP:CE28345	Wormbase
<i>cel-lev-1 isoform a</i>	<i>C. elegans</i>	WP:CE24888	Wormbase
<i>cel-unc-29</i>	<i>C. elegans</i>	WP:CE13451	Wormbase
<i>cel-acr-6</i>	<i>C. elegans</i>	WP:CE46851	Wormbase
<i>cel-unc-63</i>	<i>C. elegans</i>	WP:CE30706	Wormbase
<i>cel-acr-12</i>	<i>C. elegans</i>	WP:CE29334	Wormbase
<i>cel-acr-8</i>	<i>C. elegans</i>	WP:CE36679	Wormbase
<i>acetylcholine receptor subunit alpha precursor</i>	<i>M. musculus</i>	NP_031415	NCBI
<i>acetylcholine receptor subunit gamma precursor</i>	<i>M. musculus</i>	NP_033734	NCBI

Table 6: Sources for amino acid sequence for subunits of nAChRs identified in other nematode species

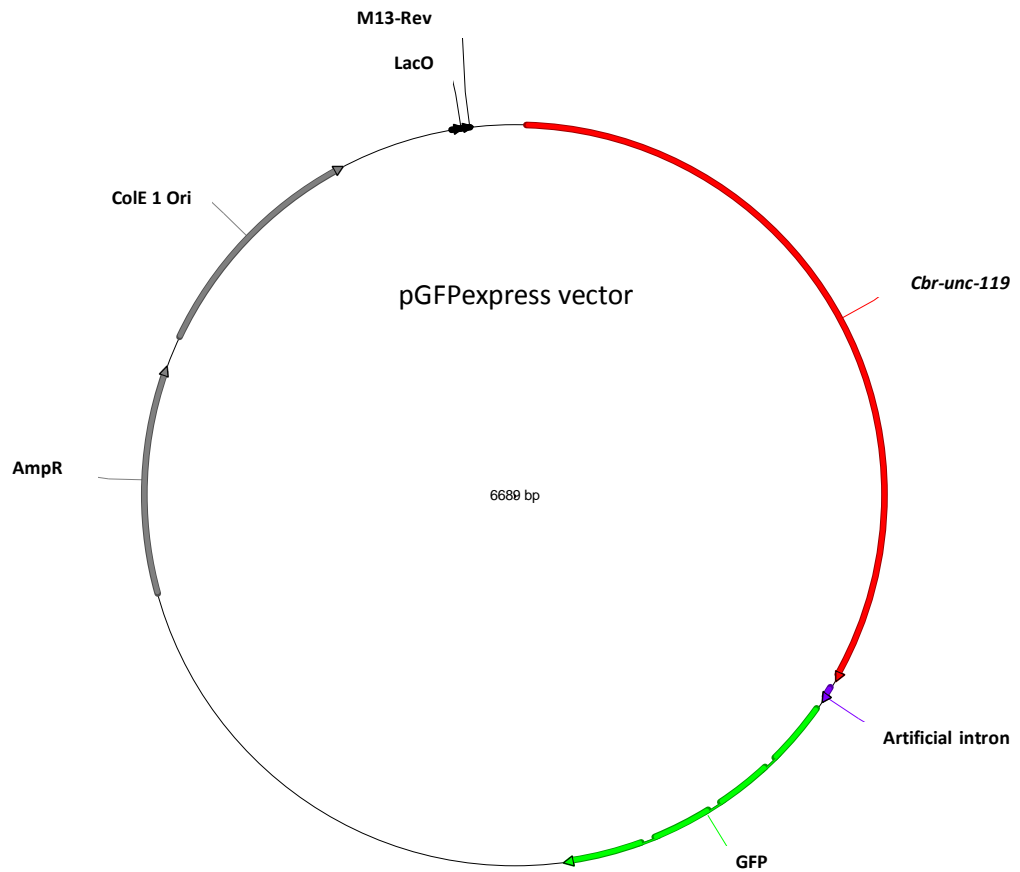


Figure 4-2: Vector map of pGFPexpress

Expression vector contains the *cbr-unc-119* gene and its promoter region and terminator and the coding region for GFP. A multiple cloning site is present upstream of GFP to allow insertion of a promoter region. Other restriction sites present facilitate linearisation of the vector. The vector also contains an ampicillin resistance gene.

4.3 Results

4.3.1 Complement of all known nicotinic acetylcholine receptors in *G. rostochiensis* and *G. pallida*

Orthologues of genes known to encode nicotinic acetylcholine receptors in *C. elegans* (*cel-genename*) were searched for in the genome assemblies of *G. pallida* and *G. rostochiensis*. In order to identify possible novel nAChR genes, all genes with features of a cys-loop receptor were analysed.

There is a reduction in orthologues of the ACR-16 group, with orthologues for only four of the ten members of this group having orthologues in *G. pallida* and *G. rostochiensis*. Orthologues for most members of the DEG-3 group could be identified, except for *cel-acr-23* and *cel-acr-18*.

Orthologues of the genes (*cel-unc-29*, *cel-unc-63*, *cel-unc-38*, *cel-lev-1* and *cel-lev-8*) that comprise the levamisole-sensitive nicotinic acetylcholine receptor were of particular interest. Multiple orthologues were found for some genes, whilst other genes do not have orthologues in the two *Globodera* species. All other members of the UNC-38, UNC-29 and ACR-8 groups have identified orthologues in *G. pallida* and *G. rostochiensis* (Table 7).

The members of the UNC-38, UNC-29 and ACR-8 groups were selected for further analysis, and were cloned from *G. pallida*. Bioinformatic data has been used throughout this chapter for the *G. rostochiensis* orthologues. Genes identified in *G. pallida* and *G. rostochiensis* were termed *gpa-genename* and *gro-genename* respectively. The loops and cys-loop characteristic of this subunit class were present in the predicted amino acid sequence of all cloned genes.

4.3.2 Orthologues of components of the levamisole-sensitive nicotinic acetylcholine receptor of *C. elegans*

4.3.2.1 Orthologues of *cel-lev-1* and *cel-lev-8* could not be identified

Orthologues of *cel-lev-1* and *cel-lev-8* were not identified in *G. pallida* or *G. rostochiensis* in any of the databases available for searching. This included transcriptome data and unassembled 454 reads to allow for the possibility that the genes may not have been assembled correctly into the finalised genome assemblies.

4.3.2.2 Two orthologues of Cel-UNC-29 are present

Two orthologues for *cel-unc-29* were identified in both *G. pallida* and *G. rostochiensis*. Both genes were identified as good candidates for *cel-unc-29* and both returned *cel-unc-29* as the best hit using the RBH method. There is 66% identity between the predicted amino acid sequences of the two orthologues of *cel-unc-29* cloned for

G. pallida (Figure 4-3). These two orthologues are also identified in *G. rostochiensis*. As it is not clear due to lack of functional testing if both these genes are functional orthologues of *cel-unc-29*, or if they are paralogues of each other, the terminology *gpa-unc-29.1* and *gpa-unc-29.2* has been adopted.

Between Cel-UNC-29 and Gpa-UNC-29.1, the identity is 68% and between Cel-UNC-29 and Gro-UNC-29.1 the identity is 67%. A signal peptide cleavage site between amino acids 24 and 25 and four transmembrane domains are identified. Cel-UNC-29 is a non- α -subunit, and may contribute as the negative face of the binding pocket. Residues involved in forming the negative face are present (Figure 4-4)

Between Cel-UNC-29 and Gpa-UNC-29.2, identity is 68%. Between Cel-UNC-29 and Gro-UNC-29.2, the identity is 67%. However, the start of this gene is unclear. A clone from cDNA generates an amino acid product that is not predicted to encode a signal peptide. There is another methionine at residue 19 in the amino acid chain that, if taken to be the initiating methionine, does result in a signal peptide being predicted for Gpa-UNC-29.2, which is the case for Gro-UNC-29.2 as well. Additionally, for both Gpa-UNC-29.2 and Gro-UNC-29.2, only three transmembrane domains are predicted in the correct positions. A fourth transmembrane domain is predicted at the N-terminus of the amino acid chain, but this is potentially a signal peptide and is not in an expected position for a transmembrane domain in this class of protein. Characteristics of a non- α -subunit were identified (Figure 4-5).

4.3.2.3 An orthologue of *cel-unc-63* is present

Amino acid identity between Cel-UNC-63 and Gpa-UNC-63 is 65%. And between Cel-UNC-63 and Gro-UNC-63 the amino acid identity is 66%. There are some differences between the sequence of the cloned *gpa-unc-63* and the *gro-unc-63* which has been bioinformatically identified. The main difference is in the predicted N-terminal amino acid sequence. The gene model in *G. rostochiensis* predicts 50 additional amino acids at the start of the protein sequence. It is not clear which prediction is correct or if these genes differ between *G. pallida* and *G. rostochiensis*. A signal peptide is not predicted for either Gpa-UNC-63 or Gro-UNC-63. Four transmembrane domains are predicted for both Gpa-UNC-63 and Gro-UNC-63. There is a region of amino acids approximately 100 amino acids into Gpa-UNC-63 and Gro-UNC-63 which may indicate a residual signal peptide (Figure 4-6)

Cel-UNC-63 is an α -subunit. Residues involved in forming the principal binding site were identified in the sequence of Gpa-UNC-63 and Gro-UNC-63. Cel-UNC-63 has been hypothesised to contribute to the negative face of the binding pocket in some arrangements of the receptor, and most residues involved in binding the complementary face were also identified. However the alanine at position 119 in Cel-UNC-63 is replaced by a threonine in Gpa-UNC-63 and Gro-UNC-63.

4.3.2.4 Two orthologues of Cel-UNC-38 are present both with differences in key residues

Two orthologues of *cel-unc-38* were cloned from *G. pallida* and these were also identified in the genome of *G. rostochiensis*. The identity between the two orthologues identified in *G. pallida* is 54% (Figure 4-7).

The first orthologues identified for each species were termed *gpa-unc-38.1* and *gro-unc-38.1*. The amino acid identity between Cel-UNC-38 and Gpa-UNC-38.1 is 56% and between Cel-UNC-38.1 and Gro-UNC-38.1 the amino acid identity is 57%. A signal peptide cleavage site is predicted between amino acids 23 and 24 in Gpa-UNC-38.1 and Gro-UNC-38.1. Four transmembrane domains are predicted.

Cel-UNC-38 is an α -subunit. However, there are key differences in the amino acid sequence of Gpa-UNC-38.1 and Gro-UNC-38.1. In Loop A, where in Cel-UNC-38 a tyrosine residue is involved in acetylcholine binding, an isoleucine is present in both Gpa-UNC-38.1 and Gro-UNC-38.1. Loop B also differs in amino acid sequence between Cel-UNC-38 and Gpa-UNC-38. In particular, the YxxCC motif that defines α -subunits is absent from Loop C of Gpa-UNC-38 and Gro-UNC-38. The equivalent of Y¹⁹⁸ is present in Loop C (Figure 4-8)

A second orthologue of *cel-unc-38* was also identified. The amino acid identity between Cel-UNC-38 and Gpa-UNC-38.2 is 58%. Between Cel-UNC-38 and Gro-UNC-38.2 the identity is 55%, although some data is missing for the sequence of Gro-UNC-38.2 in the second transmembrane domain region, due to incomplete genome assembly. A signal peptide cleavage site between amino acids 21 and 22 and four transmembrane domains are predicted.

The tyrosine involved in binding in loop A is present. The loop B region differs from Cel-UNC-38, although the glutamate residue of loop B is predicted to be present in *G. rostochiensis*, but not in *G. pallida*. In Loop C, the tyrosine (Y¹⁹⁰) of the YxxCC motif is present, but the vicinal cysteines are absent. The equivalent of Y¹⁹⁸ in Loop C is absent (Figure 4-9).

In both *cel-unc-38* orthologues identified from the plant-parasitic nematodes these variations in amino acid identities at key positions may have an impact on agonist binding.

4.3.3 The UNC-29 group of nAChR subunits

In *C. elegans*, the UNC-29 group comprises Cel-UNC-29, Cel-LEV-1, Cel-ACR-2 and Cel-ACR-3. Orthologues of *cel-unc-29* and *cel-lev-1* are discussed above. The orthologues of the remaining members were cloned from *G. pallida*, and identified in *G. rostochiensis* and were analysed further.

4.3.3.1 The *acr-2 acr-3* operon structure is an example of synteny between the *C. elegans*, *G. pallida* and *G. rostochiensis* genome

Cel-acr-2 and *cel-acr-3* in *C. elegans* are found in an operon-like structure with *cel-acr-3* located approximately 280 bp downstream of *cel-acr-2* (Figure 4-10b) (Baylis et al. 1997). *G. pallida* and *G. rostochiensis* orthologues for both *cel-acr-2* and *cel-acr-3* have been identified. A similar gene order and distance is present in both *G. pallida* and *G. rostochiensis*, although the distance between *gpa-acr-2* and *gpa-acr-3* is approximately 100 bp shorter. In the genome assemblies of both species the orthologues of *cel-acr-2* and *cel-acr-3* are predicted as a single gene. In both *G. pallida* and *G. rostochiensis*, *gpa/gro-unc-29.1* is located approximately 400 bp downstream of *gpa/gro-acr-3* (Figure 4-10c). In *C. elegans*, an unrelated gene *cel-nas-11*, is located downstream of *cel-acr-3*. It may be that the *gpa/gro-unc-29.1* is also in an operon with *gpa/gro-acr-2* and *gpa/gro-acr-3* in *G. pallida* and *G. rostochiensis*.

4.3.3.2 The orthologue of *cel-acr-2* is present as a full-length gene

Between Cel-ACR-2 and Gpa-ACR-2 the amino acid identity was 51%, and between Cel-ACR-2 and Gro-ACR-2 the amino acid identity was 49%. A signal peptide cleavage site was predicted between position 20 and 21 in both *G. pallida* and *G. rostochiensis* and four transmembrane domains are predicted (Figure 4-11). Cel-ACR-2 is a non- α -subunit and the sequence of Gpa-ACR-2 contains sequences associated with contributing to the complementary face of the acetylcholine binding pocket.

4.3.3.3 Orthologue of Cel-ACR-3 may lack a signal peptide

The percentage identity between Cel-ACR-3 and Gpa-ACR-3 or Gro-ACR-3 was 58% and 60% respectively. Four transmembrane regions were predicted. A signal peptide could not be identified in Gpa-ACR-3 (Figure 4-12). *Gpa-acr-2* and *gpa-acr-3* is predicted as a single gene in *G. pallida*, but primers designed to amplify this whole region did not produce a product. Primers were then designed to amplify *gpa-acr-2* and *gpa-acr-3* separately based on homology to *cel-acr-2* and *cel-acr-3*. On analysis, sequence contributing to the beginning of *gpa-acr-3* could be found at the end of the *gpa-acr-2* clone. Additionally, at the beginning of the *gpa-acr-3* clone, the end of *gpa-acr-2* could be found. This allowed the region between *gpa-acr-2* and *gpa-acr-3* to be concatenated. Homology between Gpa-ACR-3 and Cel-ACR-3 was high at the N-terminal end, although Gpa-ACR-3 lacked a signal peptide. Multiple stop codons are found between the end of Gpa-ACR-2 and the beginning of Gpa-ACR-3 with no evidence of a signal peptide (Figure 4-10a). Bioinformatic analysis of the region between *gro-acr-2* and *gro-acr-3* in the *G. rostochiensis* genome assembly also yielded the same presence of stop codons and absence of a signal peptide.

Cel-ACR-3 is a non- α -subunit. The sequence of Gpa-ACR-3 contains the residues associated with forming the complementary face of acetylcholine binding pocket (Figure 4-12).

4.3.4 The UNC-38 group of nAChRs

In *C. elegans*, the UNC-38 group comprises Cel-UNC-38, Cel-UNC-63 (discussed above) and Cel-ACR-6. An orthologue for the remaining member of this group *cel-acr-6* was cloned from *G. pallida* and identified in *G. rostochiensis*. Percentage identity between Cel-ACR-6 and Gpa-ACR-6 was 45%, and between Cel-ACR-6 and Gro-ACR-6 the percentage identity was 44%. A signal peptide cleavage site is predicted between positions 24 and 25 and four transmembrane regions are predicted (Figure 4-13). Cel-ACR-6 is an α -subunit. The sequences of Gpa-ACR-6 and Gro-ACR-6 contain all the residues associated with providing the positive face of the acetylcholine binding pocket.

4.3.5 The ACR-8 group of nAChRs

The *C. elegans* ACR-8 group comprises Cel-ACR-8, Cel-LEV-8 and Cel-ACR-12. An orthologue of Cel-LEV-8 was not found. *Gpa-acr-8* and *Gpa-acr-12* were cloned from *G. pallida* and identified in *G. rostochiensis*.

4.3.5.1 Orthologues of Cel-ACR-8 and Cel-ACR-12 are present

Percentage identity between Cel-ACR-8 and Gpa-ACR-8 was 54% and between Cel-ACR-8 and Gro-ACR-8 was 53%. A signal peptide cleavage site is predicted between position 25 and 26 and four transmembrane domains are predicted (Figure 4-14). Cel-ACR-8 is an α -subunit. The sequence of Gpa-ACR-8 and Gro-ACR-8 contain the same residues associated with providing the positive face of the acetylcholine binding pocket as Cel-ACR-8.

The percentage identity between Cel-ACR-12 and Gpa-ACR-12 was 57% and between Cel-ACR-12 and Gro-ACR-12 was 56%. A signal peptide cleavage site is predicted between position 21 and 22 and four transmembrane domains are predicted (Figure 4-15). Cel-ACR-12 is an α -subunit. The sequences of Gpa-ACR-12 and Gro-ACR-12 mostly contain the same residues associated with providing the positive face of the acetylcholine binding pocket as Cel-ACR-12, however the equivalent residue of Y¹⁹⁸ in Cel-ACR-12 is a phenylalanine residue in Gpa-ACR-12 and Gro-ACR-12.

4.3.6 nAChR subunit genes are most highly expressed at life stages involved in locomotion or host-sensing

Expression data obtained from RNASeq from life-stages of *G. pallida* show that the nAChR subunit genes identified are most highly expressed in the eggs, J2s and males. Expression in sedentary stages is generally low, although *gpa-acr-8* expression remains

relatively high at 7dpi (Figure 4-17). The expression of *gpa-acr-2* and *gpa-acr-3* is shown together as gene prediction algorithms predicted this as a single large gene. Expression data for *gpa-unc-38.2* was unavailable, as this was not predicted in the initial gene prediction sets.

4.3.7 Phylogeny of genes and in the UNC-38, UNC-29 and ACR-8 groups

A phylogenetic tree was generated from *C. elegans*, *G. pallida* and *G. rostochiensis* subunits from these groups in order to demonstrate that the orthologues identified in *G. pallida* and *G. rostochiensis*, cluster with their predicted *C. elegans* orthologue and within their predicted group. Gpa-UNC-29.1 and Gpa-UNC-29.2 are predicted to share a common ancestor, and possibly result from gene duplication. Gpa-UNC-38.1 and Gpa-UNC-38.2 are also predicted to share a common ancestor (Figure 4-16).

4.3.8 Promoters of nAChRs from *G. pallida* are functional in *C. elegans*

As composition of the L-nAChR of *G. pallida* is likely to differ from that of *C. elegans*, a method was sought to analyse the expression pattern of nAChR genes identified in *G. pallida* in order to determine where in the nervous system they are expressed. Due to an absence of transgenic techniques for *G. pallida*, the use of *C. elegans* as a heterologous system to analyse the expression pattern of GFP regulated by promoter regions of nAChRs from *G. pallida* was explored.

Successful transformants were generated for the promoter regions of *gpa-acr-2* and *gpa-unc-63*. As *cel-acr-2* is part of the neuronal nAChR (Jospin *et al.* 2009) and *cel-unc-63* is part of the muscle nAChR (Boulin *et al.* 2008), the promoter regions of orthologues of these genes from *G. pallida* were selected to examine the difference in their expression patterns.

GFP expression from all transgenic reporter lines was low, indicated by the low-level of GFP fluorescence. The auto-fluorescence observed in the gut of the N2 controls is not GFP expression, and is probably due to the presence of gut granules (Coburn and Gems 2013). For reference, auto-fluorescence of untransformed worms is shown in Figure 4-18.

In contrast, GFP expression of lines carrying *pgpa-acr-2* from *G. pallida* was observed along the ventral nerve cord and in the region around the pharyngeal bulb (nerve ring). This expression was observed at all life stages, but was particularly clear in the younger worms (L1-L3s) (Figure 4-19a). When the nematode is orientated with the vulva facing upwards, faint GFP expression can be seen across the ventral nerve cord punctuated with distinct clusters of GFP expression. Very faint extensions across to the dorsal side of the body can be seen which may be the commissures which link the ventral nerve cord to the dorsal cord (Figure 4-19b). This pattern of GFP expression in the *pgpa-acr-2* line was consistent across worms and lines examined.

The GFP expression of the *pgpa-unc-63* line was more variable between individual worms observed. In some, GFP expression was clustered around the pharyngeal bulb (Figure 4-20a). In others, GFP expression is observed along the ventral side of the body and in two paired points in the tail region (Figure 4-20b). It is difficult to determine if the expression of GFP in the *pgpa-unc-63* line is in the ventral nerve cord or in the body wall muscle. The differences observed in expression of *pgpa-unc-63*:GFP did not correlate with different life-stages.

nAChR subunit	Group	Type	In <i>G. pallida</i> ?	In <i>G. rostochiensis</i> ?
Cel-UNC-38	UNC-38	α	Y (2)	Y (2)
Cel-ACR-6	UNC-38	α	Y (1)	Y (1)
Cel-UNC-63	UNC-38	α	Y (1)	Y (1)
Cel-UNC-29	UNC-29	non-α	Y (2)	Y (2)
Cel-ACR-2	UNC-29	non-α	Y (1)	Y (1)
Cel-ACR-3	UNC-29	non-α	Y (1)	Y (1)
Cel-LEV-1	UNC-29	non-α	N	N
Cel-ACR-8	ACR-8	α	Y (1)	Y (1)
Cel-LEV-8	ACR-8	α	N	N
Cel-ACR-12	ACR-8	α	Y (1)	Y (1)
Cel-ACR-16	ACR-16	α	Y (1)	Y (1)
Cel-ACR-7	ACR-16	α	N	N
Cel-ACR-9	ACR-16	non-α	N	N
Cel-ACR-10	ACR-16	α	N	N
Cel-ACR-11	ACR-16	α	N	N
Cel-ACR-14	ACR-16	non-α	N	N
Cel-ACR-15	ACR-16	α	N	N
Cel-ACR-19	ACR-16	α	Y (1)	Y (1)
Cel-ACR-21	ACR-16	α	Y (1)	Y (1)
Cel-EAT-2	ACR-16	non-α	Y (1)	Y (1)
Cel-DEG-3	DEG-3	α	Y (1)	Y (1)
Cel-ACR-5	DEG-3	α	Y (1)	Y (1)
Cel-ACR-17	DEG-3	α	Y (1)	Y (1)
Cel-ACR-18	DEG-3	α	N	N
Cel-ACR-20	DEG-3	α	Y (1)	Y (1)
Cel-ACR-23	DEG-3	α	N	N
Cel-DES-2	DEG-3	α	Y (1)	Y (1)
Cel-ACR-24	DEG-3	α	Y (1)	Y (1)

Table 7: Summary of orthologues of *C. elegans* nAChR genes identified in *G. pallida* and *G. rostochiensis*

Number in brackets indicates the number of orthologues found in each species.

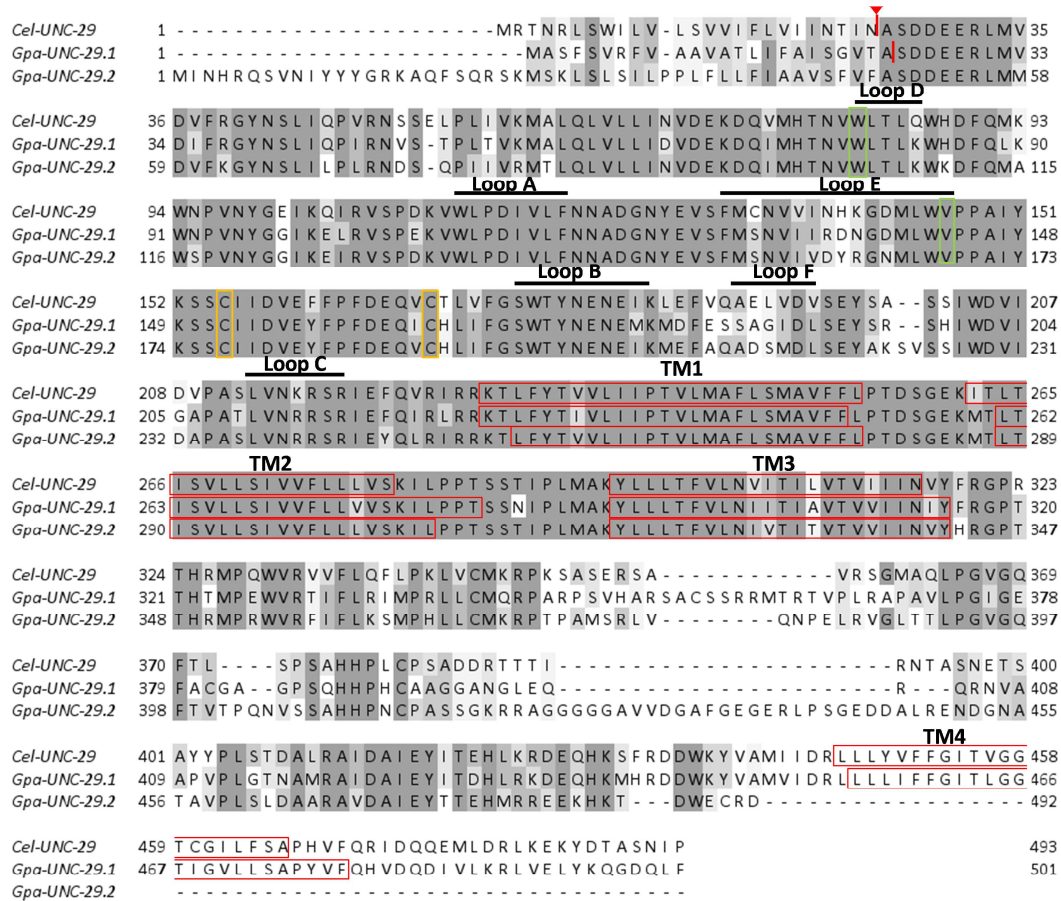


Figure 4-3: Alignment of Cel-UNC-29 with Gpa-UNC-29.1 and Gpa-UNC-29.2

Predicted signal peptide cleavage sites shown by a red arrow. Regions contributing to loops are labelled with a black bar above residues. Residues involved in providing the complementary face to agonist binding are highlighted with green boxes. Cysteines involved in forming the cys-loop are highlighted with yellow boxes. Transmembrane regions predicted by TMHMM are highlighted by red boxes.

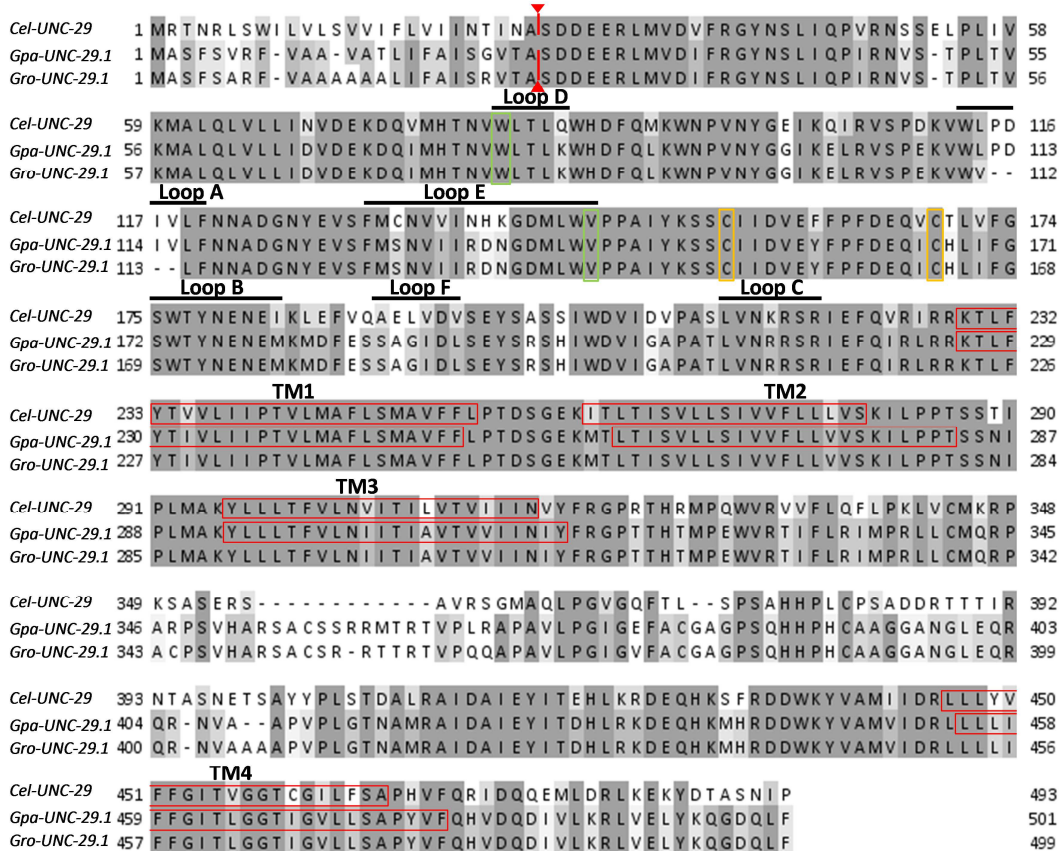
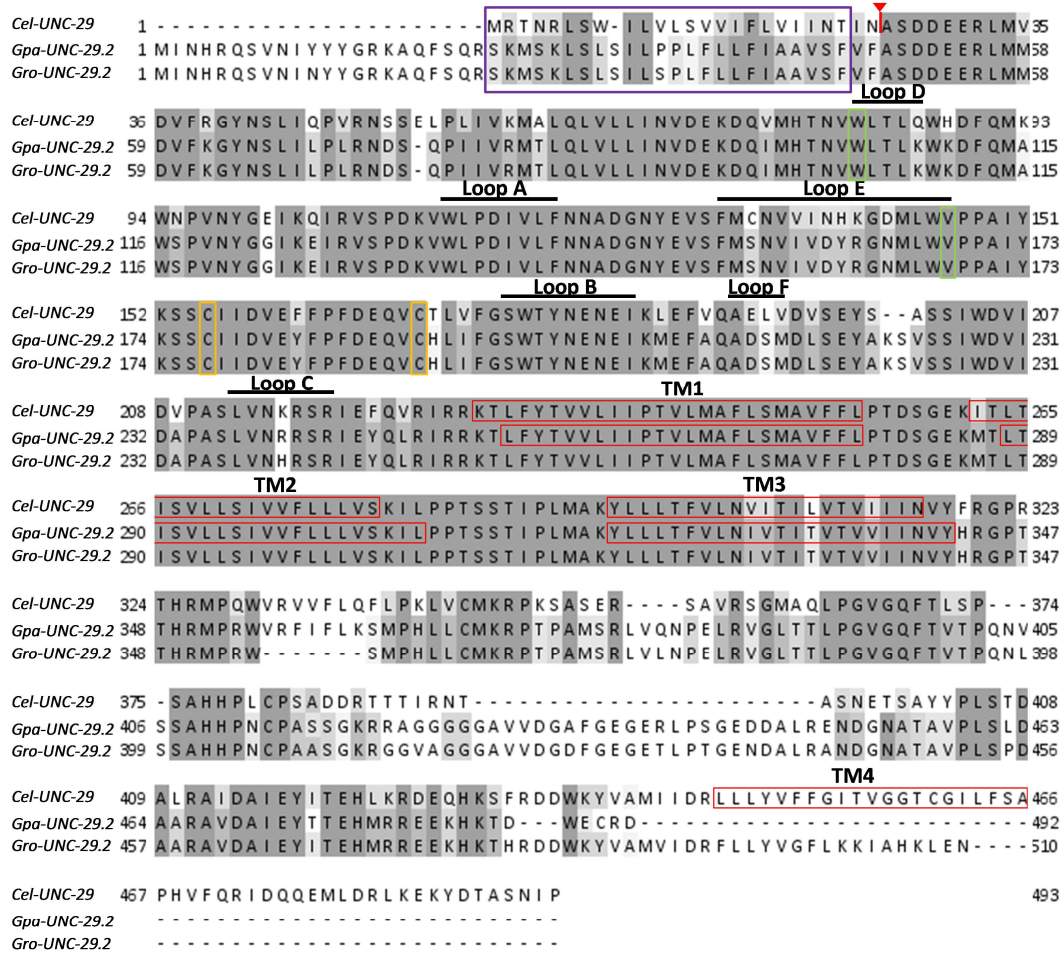


Figure 4-4: Alignment of Cel-UNC-29 with Gpa-UNC-29.1 and Gro-UNC-29.1

Red arrows indicate predicted signal peptide cleavage location. Regions contributing to loops are labelled with a black bar above residues. Residues involved in providing the complementary face to agonist binding are highlighted with green boxes. Cysteines involved in forming the cys-loop highlighted with yellow boxes. Transmembrane regions predicted by TMHMM are highlighted by red boxes and labelled.



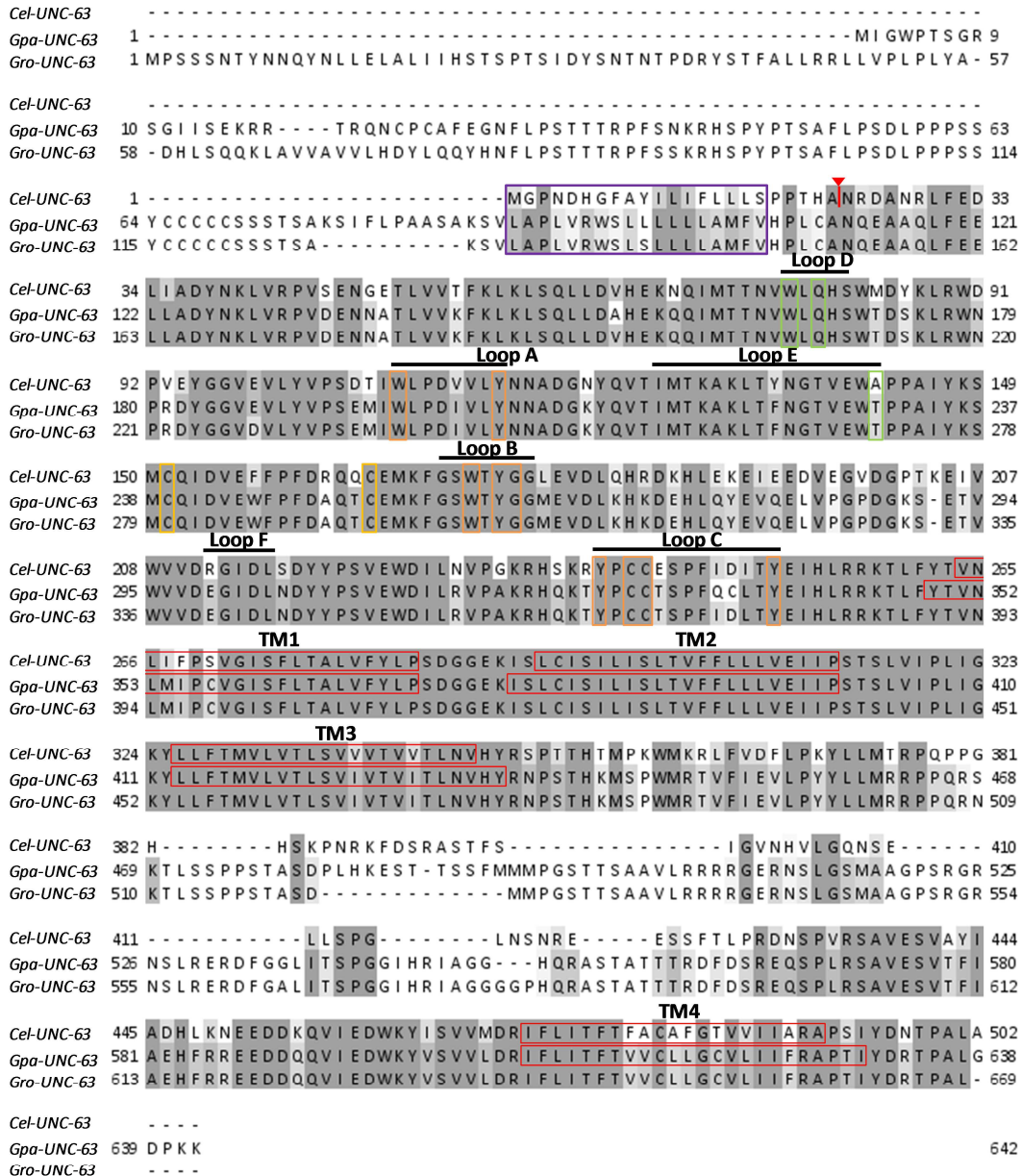


Figure 4-6: Alignment of Cel-UNC-63 with Gpa-UNC-63 and Gro-UNC-63

Red arrows indicate predicted signal peptide cleavage site. Purple box indicates possible residual signal peptide sequence in Gpa-UNC-63 and Gro-UNC-63. Regions contributing to loops are labelled with a black bar above residues. Residues involved in providing the principal face of agonist binding are highlighted in orange. Residues involved in providing the complementary face to agonist binding are highlighted with green boxes. Cysteines involved in forming the cys-loop are highlighted with yellow boxes. Transmembrane regions predicted by TMHMM are highlighted by red boxes and labelled.

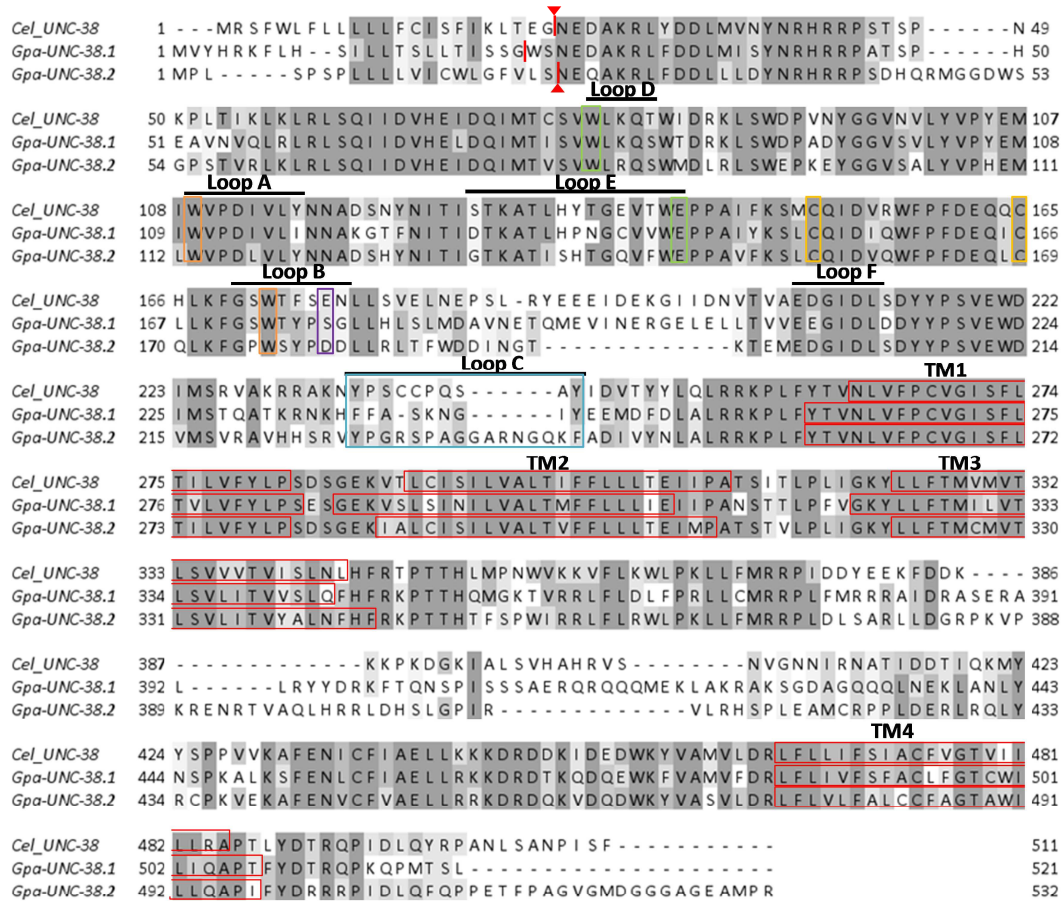


Figure 4-7: Alignment of Cel-UNC-38 with Gpa-UNC-38.1 and Gp-UNC-38.2

Red arrow indicates predicted signal peptide cleavage site. Regions contributing to loops are labelled with a black bar above residues. Residues involved in providing the principal face of agonist binding are highlighted in orange. Residues involved in providing the complementary face to agonist binding are highlighted with green boxes. Blue box highlights differences in the Loop C region in both *G. pallida* orthologues compared to the Ce-UNC-38. Purple box highlights residue changes in loop B which may affect levamisole sensitivity. Cysteines involved in forming the cys loop highlighted with yellow boxes. Transmembrane regions predicted by TMHMM are highlighted by red boxes and labelled.

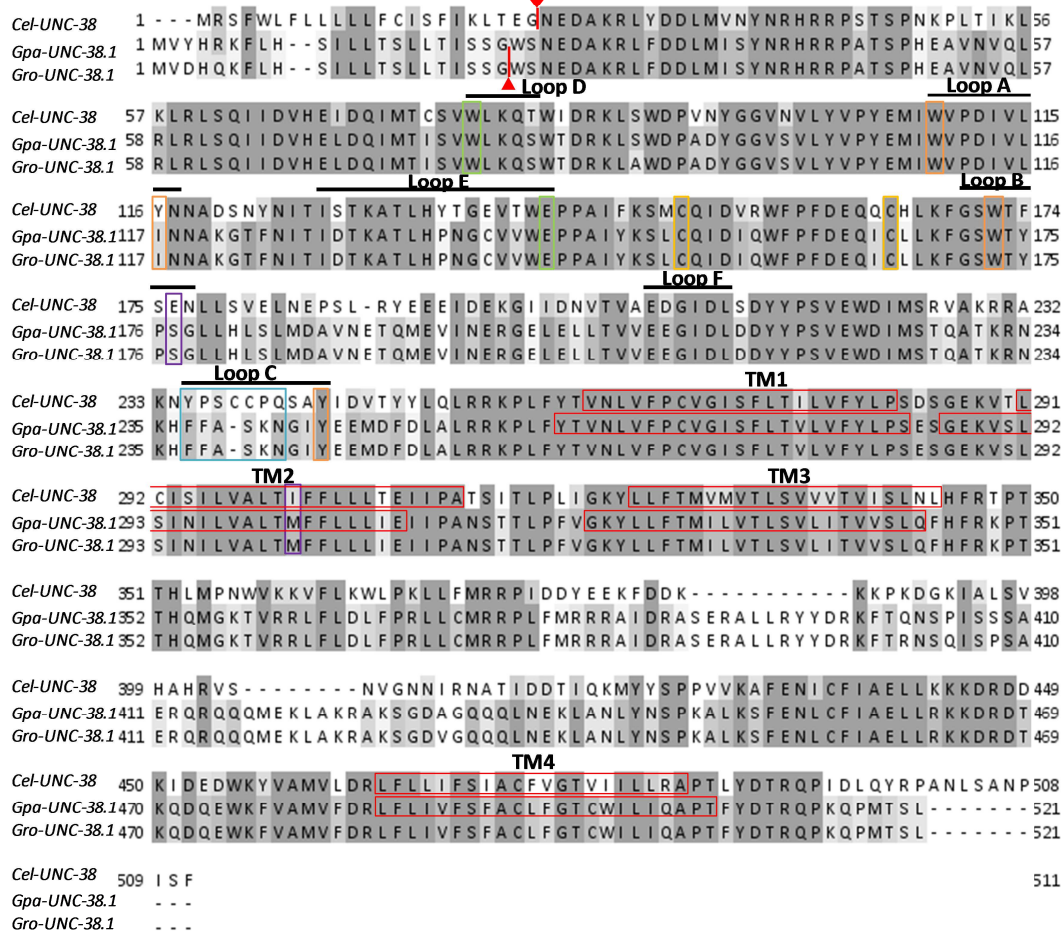


Figure 4-8: Alignments of Cel-UNC-38 with Gro-UNC-38.1 and Gro-UNC-38.1

Red arrow indicates predicted signal peptide cleavage site. Regions contributing to loops are labelled with a black bar above residues. Residues involved in providing the principal face of agonist binding are highlighted in orange. Residues involved in providing the complementary face to agonist binding are highlighted with green boxes. Blue box highlights differences in the Loop C region, where the YxxCC motif is absent. Purple box highlights residue changes which may affect levamisole sensitivity. Cysteines involved in forming the cys-loop highlighted with yellow boxes. Transmembrane regions predicted by TMHMM are highlighted by red boxes and labelled.

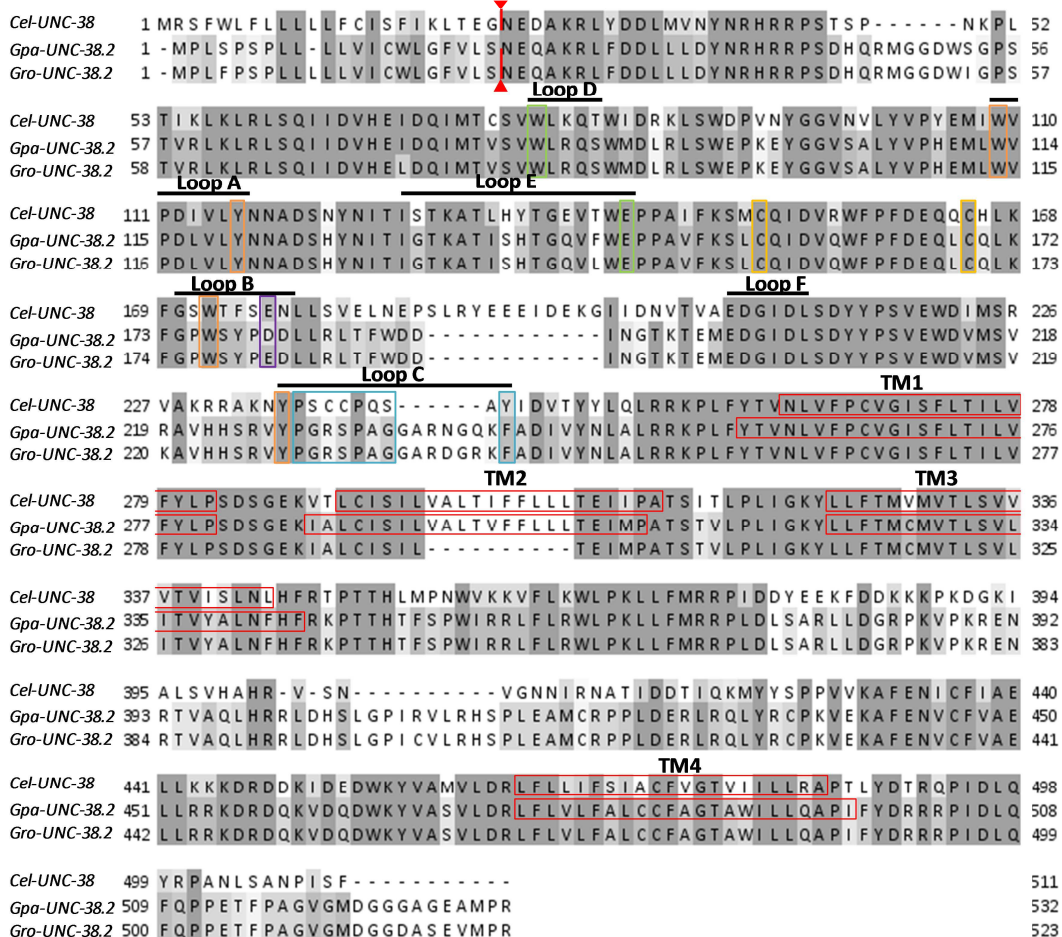


Figure 4-9: Alignments of Cel-UNC-38 with Gpa-UNC-38.2 and Gro-UNC-38.2

Some data is missing for Gro-UNC-38 sequence between residue 303 and 313. Red arrow indicates predicted signal peptide cleavage site. Regions contributing to loops are labelled with a black bar above residues. Residues involved in providing the principal face of agonist binding are highlighted in orange. Residues involved in providing the complementary face to the agonist binding are highlighted with green boxes. Blue box highlights differences in the Loop C region, where the YxxCC motif is absent. Purple box highlights residue changes which may affect levamisole sensitivity. Cysteines involved in forming the cys-loop are highlighted with yellow boxes. Transmembrane regions predicted by TMHMM are highlighted by red boxes and labelled.

a

```

MSLFGILLPFLAGILNGSNGVTFSTDGHPPSTVRSPLYANNEDEERLGIDLFRGY
NALIRPSPCQNSSVHVDFGMAMILLINVDEKNQIMQSNSVWLTLRWNDCRFAWSPA
DYGGLESLRVPVDPDVWVWDIVLFFNADGNYEVSYQSNVVVDHQGNVSWPPAIYKS
SCRIDVEYFPFDEQTCVLLFGSWTYGSDEVQLRWYNNRRFVELEDYSPSGIWDLMD
VPGRMSADRSRIAFYIVIRRKTLFYTVILIIPTVLMALSMALAFYLPAECSEKITL
AISILLALVVFLLGSKILPPTSDTIPLMAKYLLMTFVLNIVTIVSTVAVINVYFR
SAITHTMPGWRHLFLHLLPTLLAMKRPRQREMFRGTSVEEYQATANAEPAEPEGL
DTNLAMGPSTMAATMLPFLGQIGSVAHQKRQSWRQSRQRQKRRSDELDEAAEAD
DAAASPASSLRLSLSRSPSPLPQLMRRSWTGANLSMTGGGPRRGNRQICAQITGMM
DEQRMSKKLRLTIEAIAFIAEHIIKAEMSDKKVRRDDWRFISMVVDRVLLLLFFGITL
GGTIGILFSVPHAFELVDQQDILRRLSVRAQQLEGDG*KEMEFDRNLNSIFCFLSQ
LKPIFEVVPIRLGQKSATQF*RLQ*KYTNSVITSDVEERLIADLFRGYNHLIRPVL
NVSSTPLEIRFLSLALTLLINVDEKNQIMQTNVWPTMRWVDYQMWNPLEYGNIRTI
RVPPDKVWLFDIVLFNNADGNYEVSFYSNVVVEHNGEMLWVPPAIYKSSCIIDVEF
FPFDEQICAMIFGSWTFNKDEVVISYLNKRQAEELNDYSESGLIWDIMEVPGQLIHQ
KSKIAYQIRIRRKTLFYTVILIIPTVLMALSMLVFYLPAEADEKITLAI
SILLALVVFLLGSKILPPTSDTIPLIAKYLLMTFVMNIITILVTVIIINIYFRGP
TTHTMPREWVTEFLRYLPLFLMMNRPRRDSSEDPVGVAINRPGAHKSRLNAKAIKR
QNVGRNSISSFLGNTEDGIELGERARSQRQLRFMPGQFIEMSHSRREIRHHPRCSE
YAAATEAVQRRVDHLRRRRMSQPVITPARFPTHRDLGSDLSDMLTDQALQALDAVE
YITEHLRRDNLDKKIREQWKFVAMVIDRLLLYVFFGVTAGGTMGILFSAPNVFEYV
NQTAVIEELKRTAEAEMNL*

```

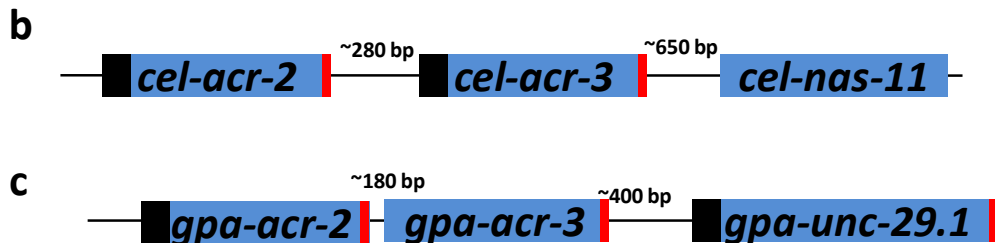


Figure 4-10: Schematics of the *acr-2 acr-3* operon in *C. elegans* and *G. pallida*

a) Translated sequence from cDNA of the *gpa-acr-2 gpa-acr-3* region from *G. pallida*. Dark blue shading highlights open reading frames. Light blue shading highlights region with sequence homology to *cel-acr-3*. Unhighlighted sequence contains stop codons indicated by *. b-c) Schematic order of genes from b) *C. elegans* and c) *G. pallida*. Black box indicates presence of signal peptide. Red box indicates stop codon. Distances between genes are genomic distances. Intron/exon boundaries are not represented. The gene structure is the same in *G. rostochiensis* as in *G. pallida*.

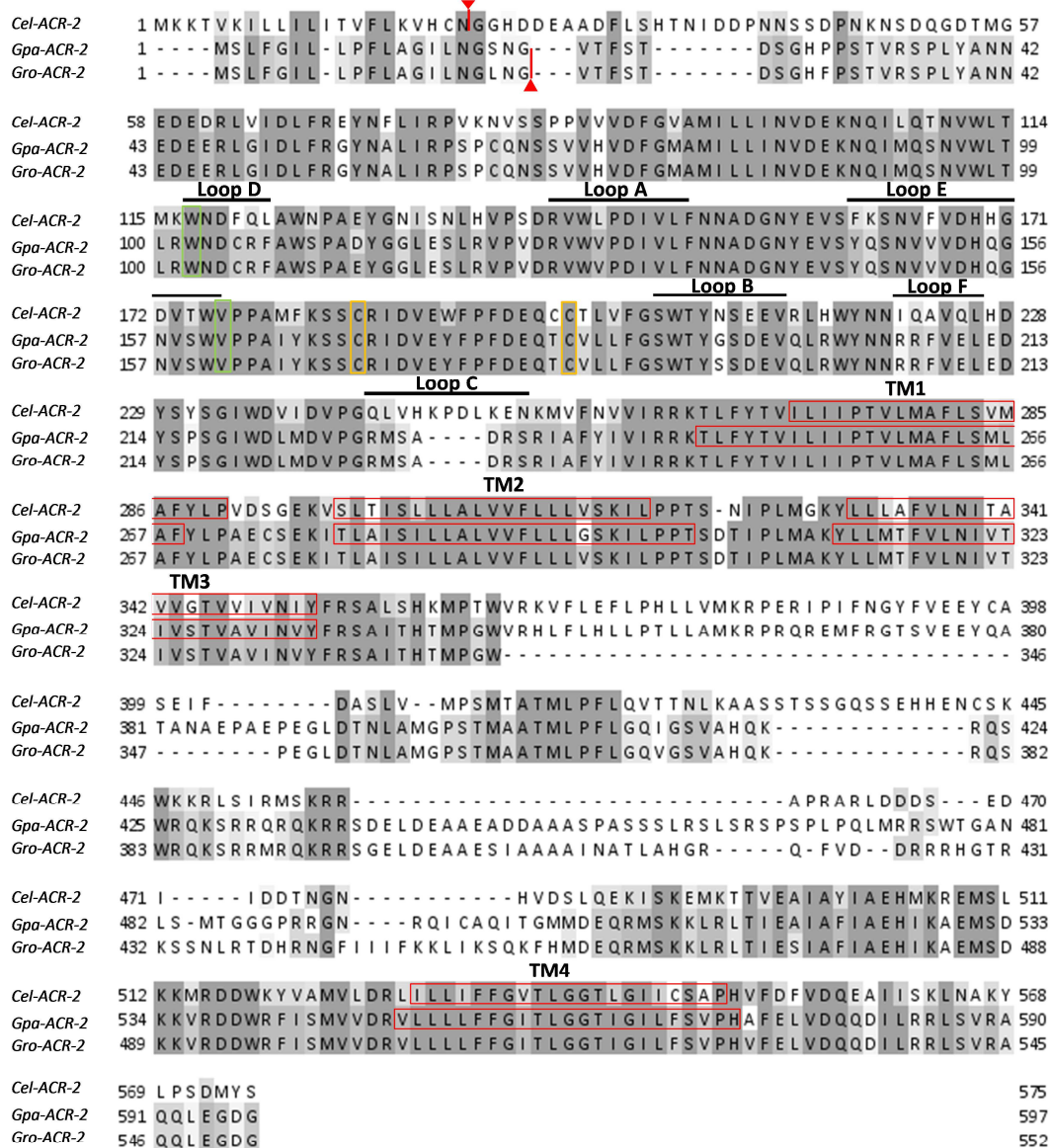


Figure 4-11: Alignment of Cel-ACR-2 with Gpa-ACR-2 and Gro-ACR-2

Red arrow indicates predicted signal peptide cleavage location. Regions contributing to loops are labelled with a black bar above residues. Residues involved in providing the complementary face to the agonist binding are highlighted with green boxes. Cysteines involved in forming the cys-loop are highlighted with yellow boxes. Transmembrane regions predicted by TMHMM are highlighted by red boxes and labelled.

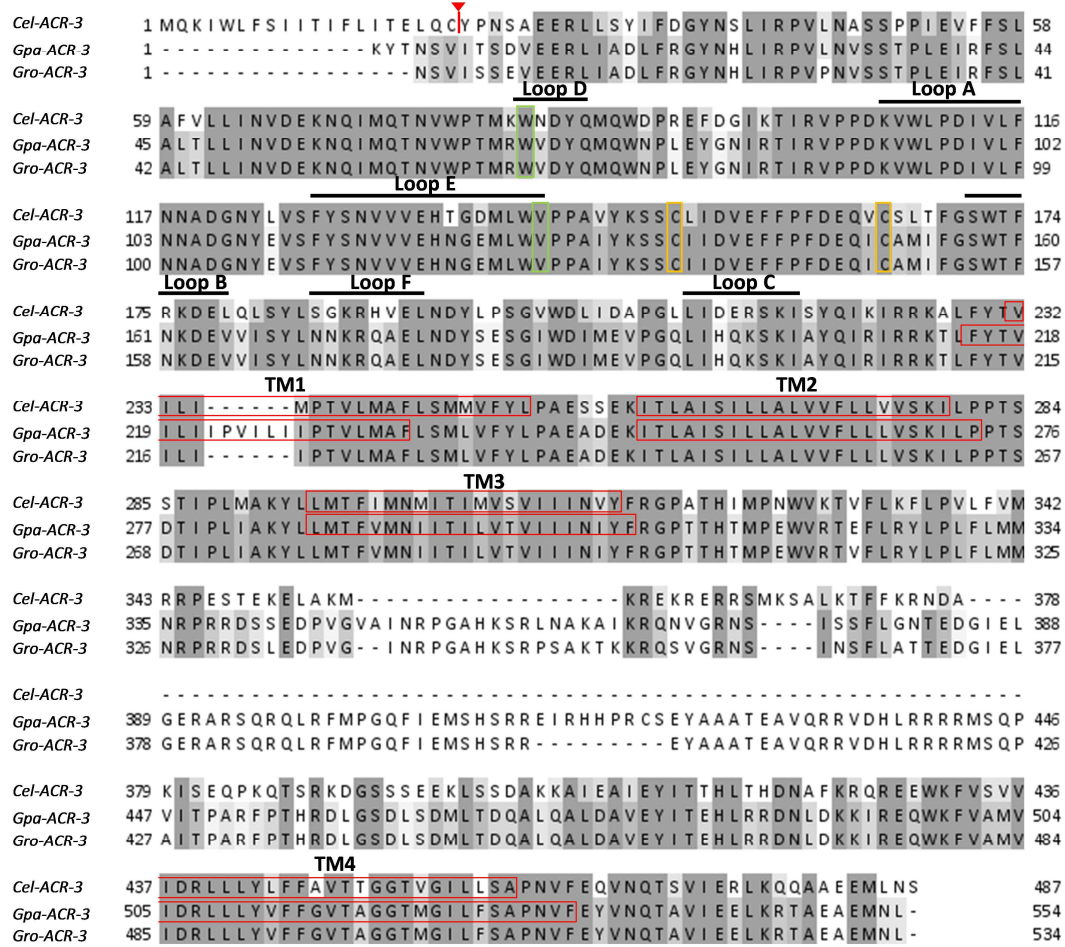


Figure 4-12: Alignment of Cel-ACR-3 with Gpa-ACR-3 and Gro-ACR-3

Red arrow indicates predicted signal peptide cleavage location. Signal peptide is missing for Gpa-ACR-3 and Gro-ACR-3. Regions contributing to loops are labelled with a black bar above residues. Residues involved in providing the complementary face to the agonist binding site are highlighted with green boxes. Cysteines involved in forming the cys-loop are highlighted with yellow boxes. Transmembrane regions predicted by TMHMM are highlighted by red boxes and labelled.

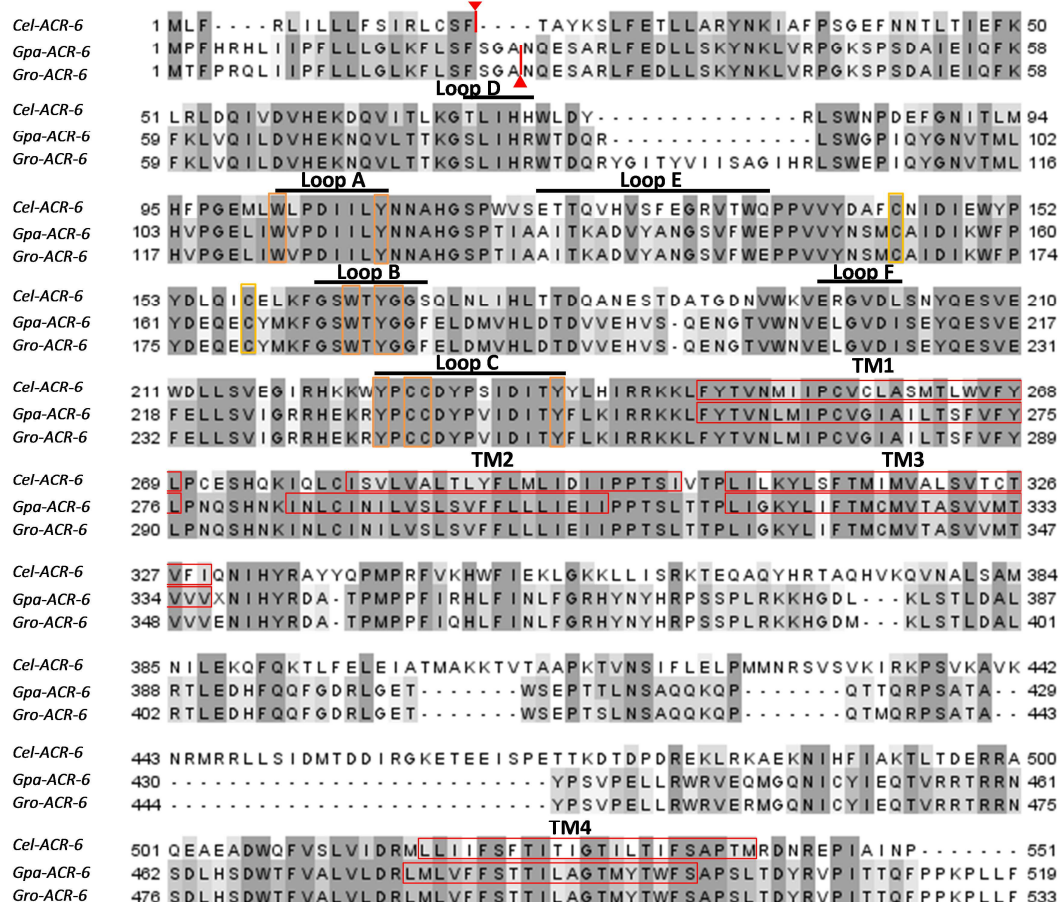


Figure 4-13: Alignment of Cel-ACR-6 with Gpa-ACR-6 and Gro-ACR-6

Red arrows indicate predicted signal peptide cleavage site. Regions contributing to loops are labelled with a black bar above residues. Residues involved in providing the principal face of the agonist binding site are highlighted in orange. Cysteines involved in forming the cys-loop are highlighted with yellow boxes. Transmembrane regions predicted by TMHMM are highlighted by red boxes and labelled.

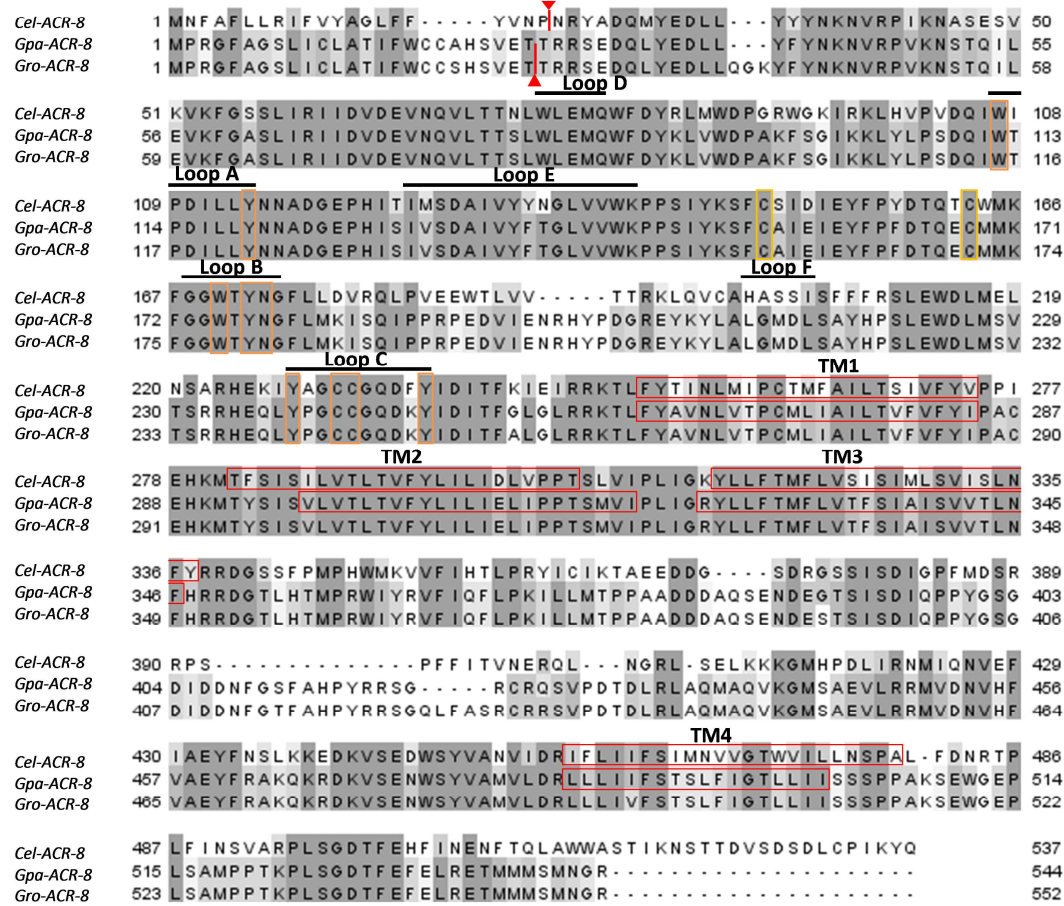


Figure 4-14: Alignment of Cel-ACR-8 with Gpa-ACR-8 and Gro-ACR-8

Red arrows indicate predicted signal peptide cleavage site. Regions contributing to loops are labelled with a black bar above residues. Residues involved in providing the principal face of the agonist binding site are highlighted in orange. Cysteines involved in forming the cys-loop are highlighted with yellow boxes. Transmembrane regions predicted by TMHMM are highlighted by red boxes and labelled.

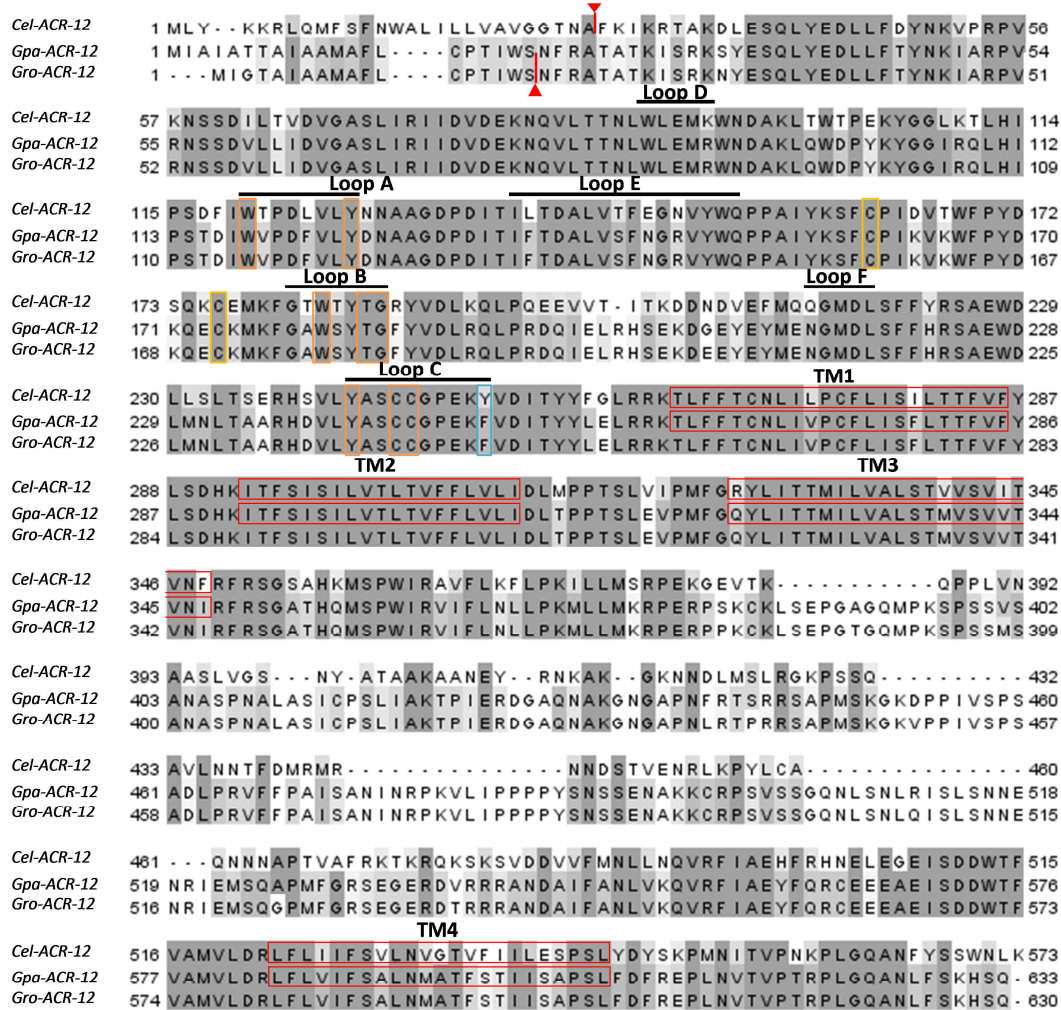


Figure 4-15: Alignments of Cel-ACR-12 with Gpa-ACR-12 and Gro-ACR-12

Red arrows indicate predicted signal peptide cleavage site. Regions contributing to loops are labelled with a black bar above residues. Residues involved in providing the principal face of agonist binding highlighted in orange. Residue highlighted in blue is a residue change that may affect acetylcholine binding. Cysteines involved in forming the cys-loop are highlighted with yellow boxes. Transmembrane regions predicted by TMHMM are highlighted by red boxes.

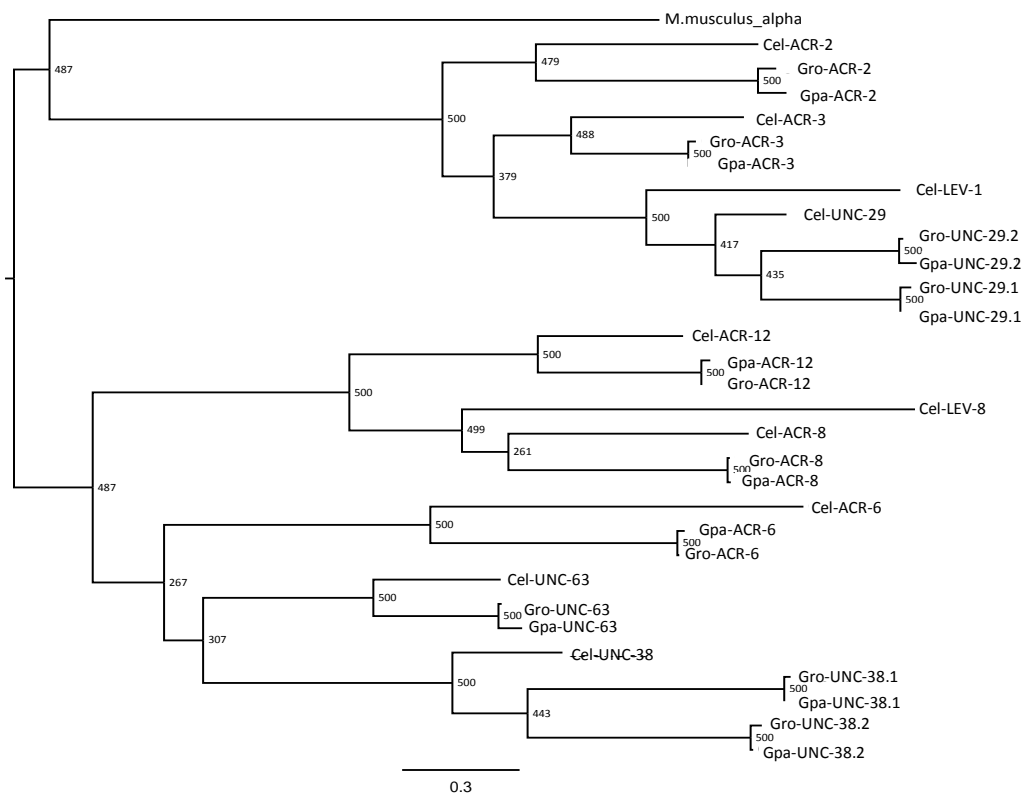


Figure 4-16: Phylogenetic tree of relationship between *C. elegans*, *G. pallida* and *G. rostochiensis* nAChR subunits of the UNC-38, UNC-29 and ACR-8 groups

Maximum likelihood phylogeny using predicted protein alignment of nicotinic acetylcholine receptor subunits. Bootstrap values for 500 iterations are labelled on nodes. Scale bar represents branch times. Subunits cluster by expected orthologues.

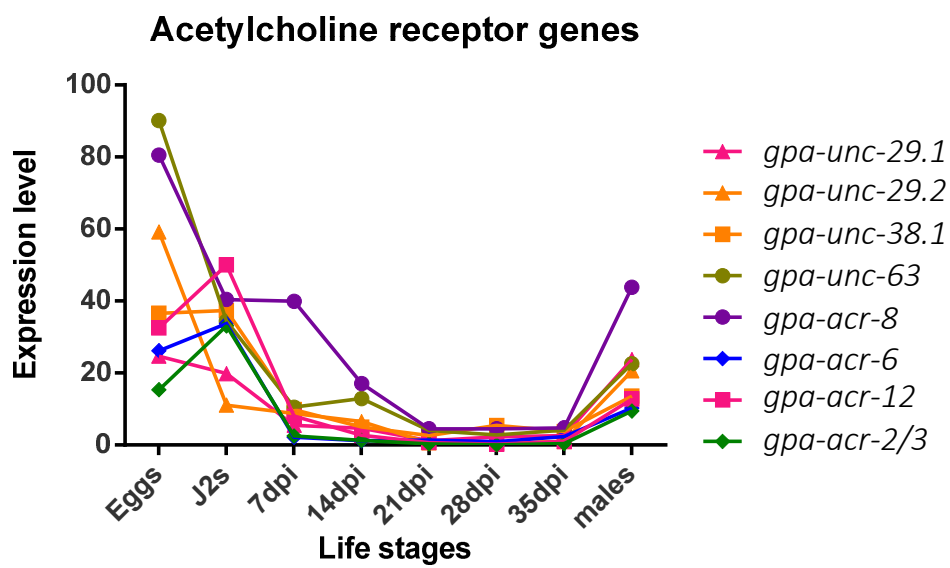


Figure 4-17: Expression levels of transcripts for identified orthologues of *C. elegans* genes from the UNC-38, UNC-29 and ACR-8 groups over the life-stages of *G. pallida*

Expression levels in the eggs, the motile stages (J2s and males) and sedentary stages (7-35 dpi females) for nicotinic acetylcholine receptor subunit genes in groups UNC-38, UNC-29 and ACR-8. Expression is generally higher in eggs, J2s and males.

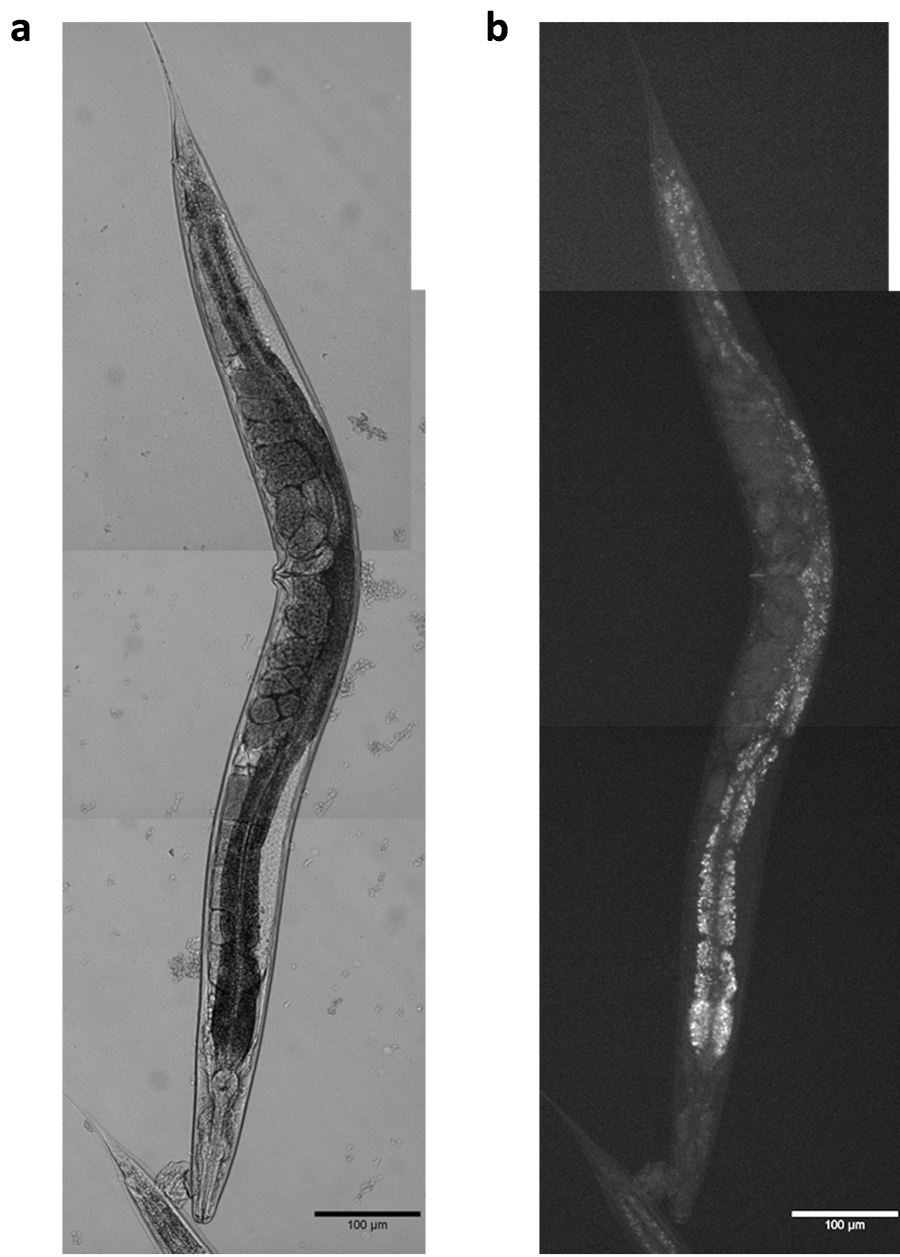


Figure 4-18: Auto-fluorescence of gut granules in N2 worms

Auto-fluorescence observed under GFP filters of the gut granules of an N2 worm. a) bright-field image of an adult hermaphrodite b) auto-fluorescence is typically brighter towards the anterior of the intestine and has a speckled appearance (Coburn and Gems 2013).

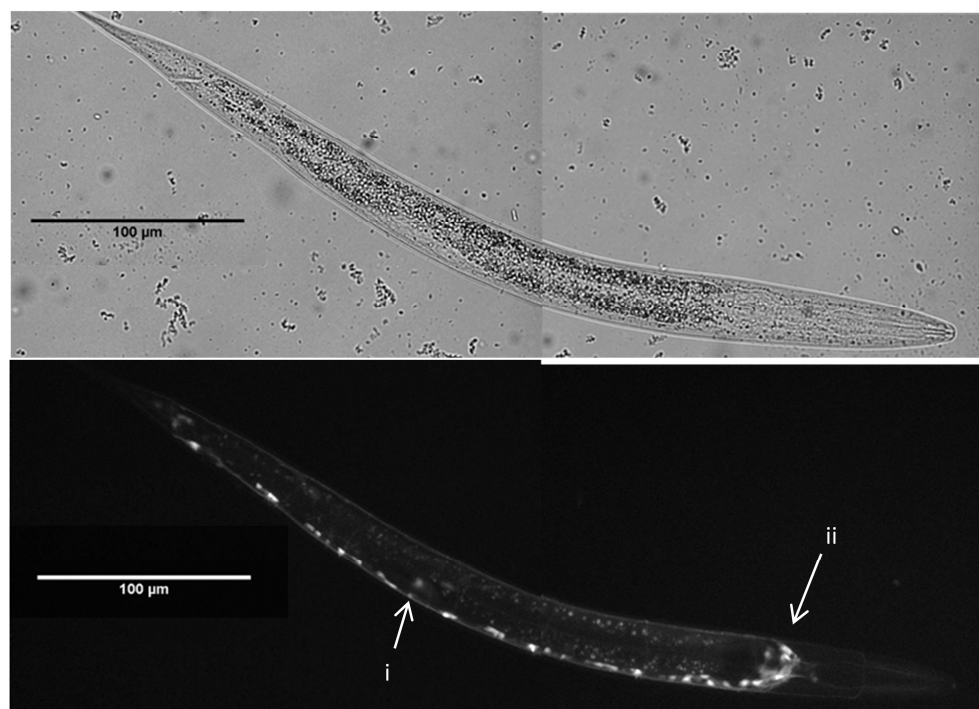
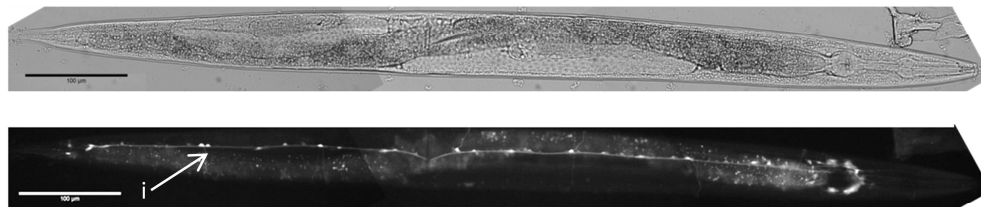
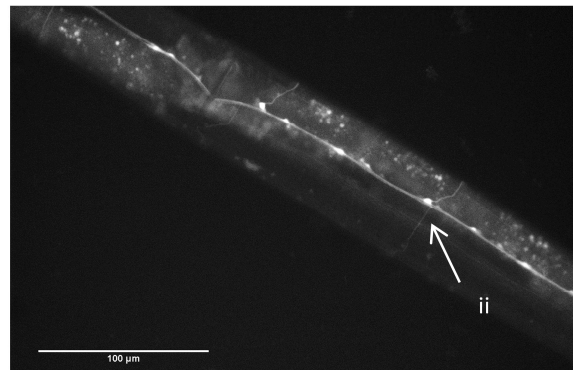
a**b****c**

Figure 4-19: GFP expression of *pgpa-acr-2* GFP reporter construct

a) GFP expression is seen in the ventral nerve cord (i) along the length of the nematode and in the nerve ring anterior to the pharyngeal bulb (ii) b) When the worm is orientated with the vulva facing upwards, GFP expression is observed along the whole length of the ventral nerve cord punctuated with clusters of brighter GFP expression (i). c) Very faint extensions from the ventral nerve cord to the dorsal cord can be seen which may represent the commissures (ii).

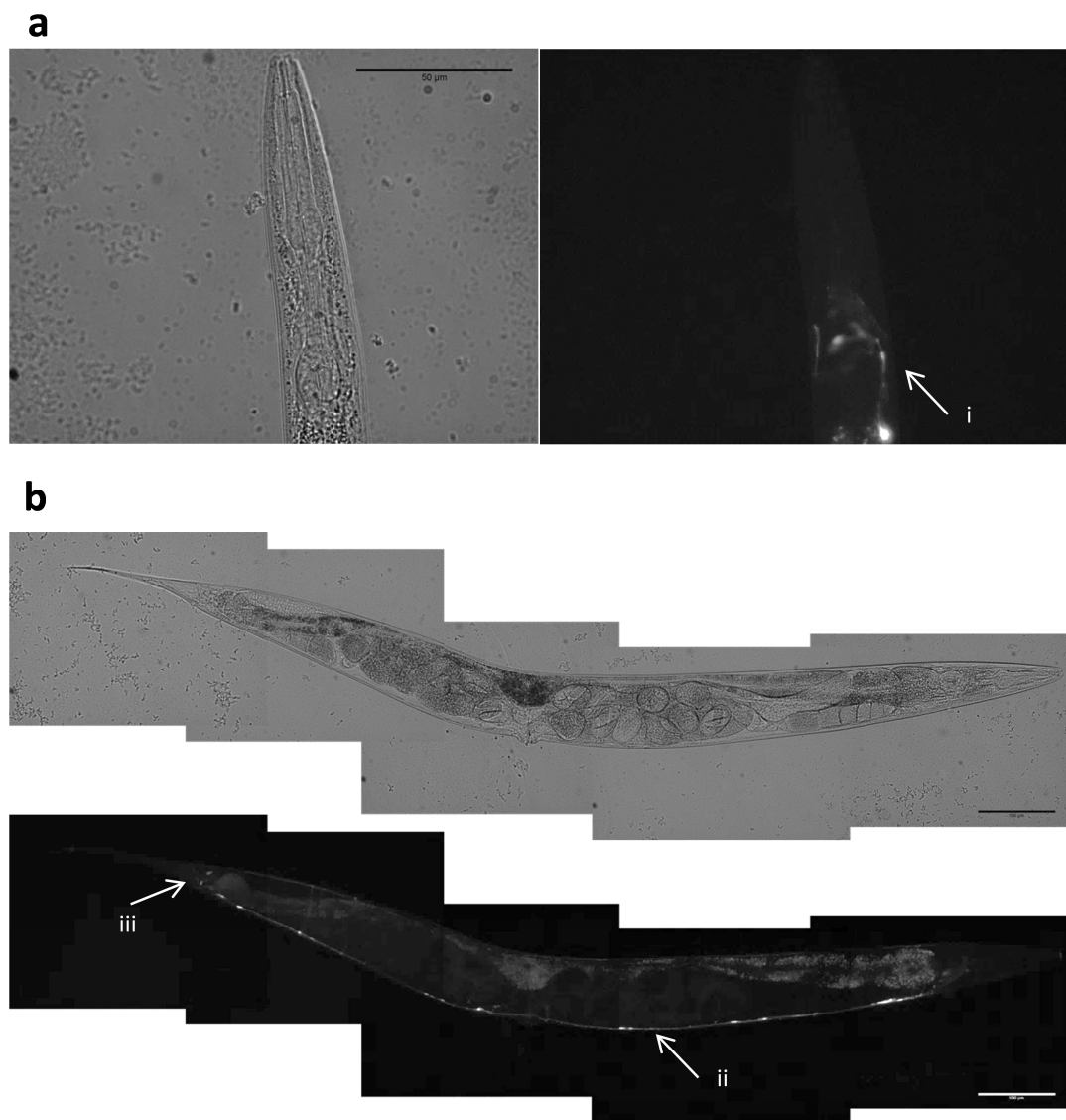


Figure 4-20: GFP expression of *pgpa-unc-63* GFP reporter construct

GFP expression directed by *pgpa-unc-63* was more variable between individual nematodes observed of the same line a) GFP expression was observed around the pharyngeal bulb in some individuals and possibly in the nerve ring (i). In other individuals, GFP expression was observed along the ventral side of the body but whether this represented expression in the ventral nerve cord or in the body wall muscle is not clear (ii). GFP expression was also observed at two paired locations in the tail region (iii).

4.4 Discussion

4.4.1 *G. pallida* and *G. rostochiensis* have fewer members of the ACR-16 group

Few orthologues were identified for *C. elegans* genes in the ACR-16 group of nicotinic acetylcholine receptors (Table 7). *Cel-acr-16* itself is present in body-wall muscle of *C. elegans* and is involved in locomotion (Touroutine *et al.* 2005; Towers *et al.* 2005). An orthologue of this gene is present in both *G. pallida* and *G. rostochiensis*. The roles of the other members of the ACR-16 group in *C. elegans* are not well characterised. *Cel-acr-7* is known to be expressed in the pharynx (Saur *et al.* 2013). *Cel-acr-15* is predicted to be expressed primarily in the neurons of *C. elegans* (Sellings *et al.* 2013) but an orthologue of this gene was not identified in *G. pallida* and *G. rostochiensis*. There is little published evidence of the expression pattern of the other group members. It may be postulated that this reduction in the *acr-16* group is due to a difference between a free-living life-style and a parasitic one, however the ruminant parasite *H. contortus* has a full complement of orthologues for members of the *acr-16* group (Laing *et al.* 2013). It may, however, be a feature of the more distantly related plant-parasitic nematodes and the difference in their life-style.

An orthologue of *cel-acr-23* is also absent in *G. pallida* and *G. rostochiensis*. This gene has been linked to monepantel sensitivity and is expressed in body wall muscle (Rufener *et al.* 2013), and its absence may have implications on the effect of monepantel on *G. pallida* and *G. rostochiensis* J2s.

4.4.2 The levamisole-sensitive nicotinic acetylcholine (L-nAChR) receptor of *G. pallida* and *G. rostochiensis* is likely to differ from that of *C. elegans*

Orthologues of *cel-lev-1* and *cel-lev-8* could not be identified in *G. pallida* or *G. rostochiensis* suggesting that this receptor type in body-wall muscle must be comprised differently in *Globodera*. The absence of these genes is supported by multiple lines of evidence from all available sequence resources. L-nAChRs are diverse in their arrangements in other parasitic nematodes, with differing stoichiometries of the receptor present in different organisms (Holden-Dye *et al.* 2013). The absence of *cel-lev-1* and *cel-lev-8* raises the question of which subunits replace them in *G. pallida*. Orthologues for *cel-lev-1* and *cel-lev-8* are also absent in the animal parasite *Ascaris suum* (Williamson *et al.* 2009) and although *H. contortus* contains an orthologue for *cel-lev-1*, it is lacking a signal peptide (Neveu *et al.* 2010). *Oesophagostomum dentatum*, a close relative of *A. suum*, also lacks *cel-lev-1* and *cel-lev-8* orthologues (Buxton *et al.* 2014).

4.4.2.1 Gpa-ACR-8 is a candidate to replace LEV-8 in the native *G. pallida* receptor

Cel-ACR-8 seems to be able to replace Cel-LEV-8 in the *C. elegans* receptor as channel activities elicited by acetylcholine and levamisole are lower in the double null mutant

of *cel-acr-8* and *cel-lev-8* than in either of the single null mutants (Hernando *et al.* 2012). Cel-ACR-8 also interacts with the other subunits of the L-nAChR and is expressed in body-wall muscle (Gottschalk *et al.* 2005). Hco-ACR-8 can also replace LEV-8 in the *H. contortus* receptor as expression of *hco-unc-29*, *hco-unc-38*, *hco-unc-63* and *hco-acr-8* in *Xenopus* oocytes generates a functional receptor. The resulting pentamer must comprise only those subunits, suggesting that LEV-1 is replaced by another subunit which is represented twice in the receptor (Boulin *et al.* 2011).

As such, Gpa-ACR-8 could be able to similarly replace LEV-8 in the *G. pallida* receptor. An orthologue of *cel-acr-8* was cloned from *G. pallida* and analysis of its sequence suggests it would be fully functional as an α -subunit (Figure 4-14). As Gpa-ACR-12 shows sequence homology with LEV-8, this sequence was also analysed for its potential role as an α -subunit. The *G. pallida* and *G. rostochiensis* equivalent of Y¹⁹⁸, one of the residues in loop C involved in acetylcholine binding, is a phenylalanine residue. In experiments on mammalian-type α -subunits (Figure 4-15), this Y198F mutation does not appear to affect the ability of acetylcholine to bind, but affects the binding of curariform drugs (Wang *et al.* 2003). However, a Y198F mutation in the mouse α -subunit did cause a decrease in channel activity elicited by acetylcholine (Tomaselli *et al.* 1991) making the result of this amino acid change unclear. In *C. elegans*, Cel-ACR-12 can associate with Cel-UNC-38 and Cel-UNC-63, but typically forms part of the neuronal nicotinic acetylcholine receptor (Jospin *et al.* 2009) and is only expressed in neurons (Gottschalk *et al.* 2005). The analysis of expression patterns of the orthologues identified in *G. pallida* would allow identification of genes that are expressed in the right location (body-wall muscle) and in the same place as each other, allowing the identification of candidates which may comprise the *G. pallida* L-nAChR.

4.4.2.2 Several candidates may replace LEV-1

The role of LEV-1 in *H. contortus* appears to be replaced by Hco-UNC-29, Hco-UNC-38, Hco-UNC-63 or Hco-ACR-8 (Boulin *et al.* 2011). The native receptors of *A. suum* may only consist of two subunits as expression of only Asu-UNC-29 and Asu-UNC-38 in *Xenopus* oocytes yields a functional receptor. However, no other combinations of subunits have been investigated and a functional receptor in *Xenopus* oocytes may not fully reflect the composition of the receptor in the nematode (Williamson *et al.* 2009). As UNC-29 is in the same group as LEV-1, it may be that Gpa-UNC-29.1 replaces LEV-1 in the *G. pallida* receptor and is represented multiple times. Gpa-UNC-29.2 is also a possible candidate, but may not be functional as it is predicted to lack a fourth transmembrane domain (Figure 4-5).

Gpa-ACR-2 and Gpa-ACR-3 are both non- α -subunits and may be able to take the place of LEV-1. Gpa-ACR-2 contains residues that would allow it to provide a complementary face for acetylcholine binding, and appears to be fully functional (Figure 4-11).

Gpa-ACR-3, however, does not appear to have a signal peptide and is possibly non-functional (Figure 4-12).

4.4.2.3 Gpa-UNC-63 may play an altered role

The amino acid sequences of Gpa-UNC-63 and Gro-UNC-63 are not predicted to contain signal peptides, required for the correct processing of the subunit and assembly in the ER, however there is sequence towards the N-terminal end of the protein that has some features of a vestigial signal peptide. Gpa-UNC-63 contains all important residues for providing the positive face of the acetylcholine binding pocket (Figure 4-6). It also contains residues that may contribute towards the complementary face of the binding pocket as some models of the *C. elegans* receptor suggest it may provide a complementary role (Hernando *et al.* 2012). The expression level of this gene suggests it is expressed at the same life-stages as the other nicotinic acetylcholine subunits (Figure 4-17), although how it is further processed is unknown. Rescue work using this gene to rescue *cel-unc-63* mutants of *C. elegans* or expression in *Xenopus* oocytes with other *C. elegans* receptors could be used to investigate whether or not Gpa-UNC-63 is functional.

4.4.2.4 Gpa-UNC-29.1 is a good orthologue of Cel-UNC-29, but Gpa-UNC-29.2 may not be functional

Gpa-UNC-29.1 contains all the features of a functional subunit, and residues that provide the complementary face of the interaction (Figure 4-4). It is likely to be a good functional orthologue of Cel-UNC-29.

Gpa-UNC-29.2 shares the key residues with Gpa-UNC-29.1, but appears to be truncated as it lacks a fourth transmembrane domain (Figure 4-5). This may prevent the subunit folding properly, and would disrupt the TM3-TM4 loop which is involved in receptor clustering (Kracun *et al.* 2008; Borges and Ferns 2001) and desensitisation (Lo *et al.* 2008). The presence of TM4 is essential for correct receptor assembly (Thompson, Lester and Lummis 2010). However, it would be worth confirming that the protein produced is non-functional by experimental methods as the results for transmembrane domain number are only a prediction. During initial cloning of this gene, the reverse primer was designed a further 177 bp downstream of the stop codon. However, all clones analysed contain a stop codon in this premature position truncating the protein before TM4. Further analysis of these regions by bioinformatics in the *G. rostochiensis* genome assembly also did not produce a protein which a fourth transmembrane domain.

Both Gpa-Unc-29.1 and Gpa-unc-29.2 are expressed at similar levels across the different life-stages of *G. pallida*, which does not exclude either from being a potential member of the L-nAChR.

Multiple paralogues of UNC-29 are also present in *H. contortus* (Hco-UNC-29.1-4) (Neveu *et al.* 2010). However, these share much closer homology to each other and to Cel-UNC-29 (~75%), than do the two orthologues of Cel-UNC-29 identified in *G. pallida* (~65%). A phylogenetic tree generated from amino acid sequences of UNC-29s identified in *G. pallida*, *H. contortus* and *C. elegans* suggests that all of the Hco-UNC-29 paralogues are more closely related to Cel-UNC-29 than either identified from *G. pallida* or *G. rostochiensis* (Figure 4-21).

4.4.2.5 Gpa-UNC-38.1 and Gpa-UNC-38.2 lack important determinants of an α -subunit

Cel-UNC-38 is an α -subunit. A pair of vicinal cysteines in loop C determine whether or not a subunit is α or non- α (Lukas *et al.* 1999). Neither orthologue of *cel-unc-38* identified in *G. pallida* and *G. rostochiensis* contains this characteristic vicinal cysteine, which may have implications for how the receptor functions (Figure 4-8).

Gpa-UNC-38.1 does not contain the equivalent of Y⁹³ residue in Loop A, which contributes to the acetylcholine binding pocket. The residue in this position is an isoleucine. There are no published reports of the effect of a Y93I mutation, but a Y93F mutation in a mouse α -subunit causes a 50-fold reduction in activity elicited by acetylcholine (Sine *et al.* 1994).

In Loop C, the equivalent residue of Y¹⁹⁰ is a phenylalanine in Gpa-UNC-38.1. The equivalent residue of the vicinal cysteines C¹⁹² and C¹⁹³ is a serine residue, as the loop C region is shorter overall. Although the equivalent residue of Y¹⁹⁸ is present in Gpa-UNC-38.1 the overall Loop C region is very different from that of Cel-UNC-38. These differing residues in Loop C could severely affect acetylcholine binding. The vicinal cysteines have been reported to be essential for acetylcholine binding (Kao *et al.* 1984). In studies conducted on an α -subunit from *Torpedo californica*, when either of the vicinal cysteines were mutated to a serine, and the mutant subunit expressed in *Xenopus* oocytes, no detectable current could be elicited by acetylcholine (Mishina *et al.* 1985). A Y190F mutation in the mouse α -subunit caused an over 50-fold reduction in channel activation by acetylcholine (Tomaselli *et al.* 1991).

In Loop B, the W¹⁴⁹ equivalent residue is present, but Y¹⁵² and G¹⁵³ are absent. These residues are also absent in Cel-UNC-38, which is reported to be an α -subunit in the L-nAChR and can assemble to form a functional receptor with non- α ACR-3 in *Xenopus* oocytes. The residues present in Loop B of Cel-UNC-38 are therefore sufficient to bind acetylcholine. However, Gpa-UNC-38.1 differs further. The equivalent residue of G¹⁵³ in Cel-UNC-38 is a glutamic acid residue. A G153E mutation in mammalian α -subunits has been demonstrated to increase channel opening currents in response to levamisole (Rayes *et al.* 2004) and has been linked to the increased sensitivity of nematode muscle to levamisole over mammalian muscle (Martin *et al.* 2012). The absence of this

glutamic acid residue in Gpa-UNC-38.1 may affect the ability of levamisole to bind to a receptor containing Gpa-UNC-38.1. A G153S mutation in a mouse α -subunit caused a reduction in channel activity elicited by acetylcholine binding (Sine *et al.* 1995). This suggests that these differences in Loop B of Gpa-UNC-38.1 may have effects on the ability of acetylcholine and levamisole to bind.

At position 278 in TM2 of the Cel-UNC-38, there is an isoleucine residue. The equivalent residue in Gpa-UNC-38 is a methionine. A mutation to a methionine at this position in Cel-ACR-2 has been shown to increase channel opening activity in response to acetylcholine receptor agonists (Jospin *et al.* 2009).

These changes in the three important loops that contribute to acetylcholine binding together with the change in TM2 which lines the channel pore raise important questions about the role of this subunit in the receptor. It may no longer be able to play the role of an α -subunit, and may be taking on different roles.

Gpa-UNC-38.2 shares many of the same features of Gpa-UNC-38.1, but differs in some regions (Figure 4-9). Y⁹³ of Loop A is present in Gpa-UNC-38.2. Loop B differs from Loop B of Cel-UNC-38 and also lacks E¹⁵³ associated with levamisole sensitivity; however this residue is predicted to be present in Gro-UNC-38.2. In Loop C, Y¹⁹⁰ is present but the vicinal cysteines C¹⁵² and C¹⁵³ are still absent. Y¹⁹⁸ is absent, and there is a phenylalanine in this position of Gpa-UNC-38.2. A Y198F mutation in the mouse α -subunit caused a decrease in channel activity elicited by acetylcholine, but not as much as the Y190F mutation (Tomaselli *et al.* 1991), however another study of this mutation showed acetylcholine binding was not affected (Wang *et al.* 2003).

Both Gpa-UNC-38.1 and Gpa-UNC-38.2 lack the determinants of an α -subunit which may affect acetylcholine binding and the binding of other agonists. Gpa-UNC-38.1 may be affected more strongly. If either of these subunits are part of the *G. pallida* receptor they may play an altered role.

4.4.2.6 UNC-38 orthologues in other plant-parasitic nematodes share the same features

Sequences of UNC-38 from other plant-parasitic nematode were identified from available bioinformatic data. The Y to I change at residue 93 and an absence of E¹⁵³ are shared with most plant-parasitic nematodes, except *Rotylenchulus reniformis*. The vicinal cysteines are also absent from all plant-parasitic nematodes sequences. The I to M change in TM2 is present in all plant-parasitic nematodes, apart from *R. reniformis* and *M. incognita* for which data is unavailable for this region. All members of the order Tylenchida also shared the absence of the YxxCC motif in the Loop C region. *Bursaphelenchus xylophilus*, although a plant-parasitic nematode, does contain a YxxCC motif in Bxy-UNC-38, but is a member of the Aphelenchida in clade 10 rather than the

Tylenchida of clade (Figure 4-22). Only one orthologue has been identified from *H. avenae*, *R. reniformis*, *H. schachtii*, *N. aberrans*, *M. hapla* and *M. incognita*. Due to the quality of the transcriptome databases used to obtain sequences for these orthologues, it is not yet possible to definitively determine if the presence of two orthologues of UNC-38 is restricted to *G. pallida* and *G. rostochiensis*.

This suggests that information learned from the study of the L-nAChR in *G. pallida*, may extend to other plant-parasitic nematodes as many features identified seem to be shared in the order Tylenchida.

4.4.3 The TM3-TM4 intracellular loop is generally larger in orthologues identified in plant-parasitic nematodes than in *C. elegans*

A general feature of all of the *Globodera* nAChRs identified in this chapter except Gpa-ACR-6 is that the intracellular region between TM3 and TM4 is longer than in the *C. elegans* orthologue. This same expansion was also seen in the glutamate-gated chloride channel class of cys-loop receptors in Chapter 3. As discussed in that chapter, this may have an effect on desensitisation or aggregation of the receptor (Lo *et al.* 2008; Kracun *et al.* 2008).

4.4.4 Work in other parasitic nematodes can provide insight for potential stoichiometries of the *G. pallida* receptor

Without complete data providing the expression patterns of genes encoding individual subunits, it is difficult to establish with certainty which subunits comprise the L-nAChR in body wall muscle.

Some inferences can be made from work conducted on this receptor type in other parasitic-nematodes. In *A. suum*, Asu-UNC-29 and Asu-UNC-38 were shown by immunofluorescent labelling to co-localise on *A. suum* muscle cell. Co-expression of cRNAs encoding these transcripts in *Xenopus* oocytes yielded functional channels and, by differing the ratio of subunit transcripts injected, the authors postulated two different arrangements of the receptor consisting of Asu-UNC-29 and Asu-UNC-38 can form (Figure 4-23a) (Williamson *et al.* 2009). Although an orthologue of *cel-unc-63* exists in *A. suum*, the potential role of this subunit was not investigated.

Functional receptors have also been expressed in *Xenopus* oocytes using *H. contortus* cRNAs for Hco-UNC-29, Hco-UNC-63 and Hco-UNC-38; and with Hco-UNC-29, Hco-UNC-63, Hco-UNC-38 and Hco-ACR-8. The relative current generated by acetylcholine was approximately ten times higher for the receptor that included Hco-ACR-8 and was more sensitive to levamisole (Boulin *et al.* 2011). Similar combinations of subunits have also been shown to produce functional receptors from *O. dentatum* (Buxton *et al.* 2014) (Figure 4-23b).

From these studies, a starting model of the *G. pallida* receptor is likely to comprise Gpa-UNC-29.1, Gpa-UNC-63, Gpa-ACR-8 and Gpa-UNC-38.1 or .2 and another subunit. Gpa-UNC-38.1 lacks the characteristic α -type residues, and may not contribute to the acetylcholine binding pocket. As Gpa-UNC-63 lacks a predicted signal peptide, the model may also comprise Gpa-UNC-38.1 or .2, Gpa-UNC-29.1 and Gpa-ACR-8 with two unknown subunits. Whether a subunit is represented multiple times or another subunit is involved which has not yet been shown to form a muscle-type receptor cannot be determined with this information (Figure 4-23c). Cel-ACR-2, Cel-ACR-3 and Cel-ACR-12 form part of the neuronal-type nicotinic acetylcholine receptor with Cel-UNC-29 and Cel-UNC-38 (Jospin *et al.* 2009), so a receptor involving ACR-2, ACR-3 or ACR-6 remains a possibility.

Subunit stoichiometry and identity has been demonstrated to have effects on channel opening. The two different functional stoichiometries of *H. contortus* subunits display different channel opening currents in response to levamisole, and are differentially activated by different drugs. The L-nAChR comprising Hco-UNC-29, Hco-UNC-38, Hco-UNC-63 and Hco-ACR-8 was most sensitive to levamisole, then acetylcholine > DMPP > pyrantel > nicotine. The L-nAChR comprising of Hco-UNC-29, Hco-UNC-38, Hco-UNC-63 was most sensitive to pyrantel, then DMPP > acetylcholine > nicotine > levamisole (Boulin *et al.* 2011). Injecting different ratios of *A. suum* subunits into *Xenopus* oocytes (3xUNC-29: 2xUNC-38 or 3xUNC-38:2xUNC-29) produced two different functional receptor types; one more sensitive to levamisole than nicotine, the other more sensitive to nicotine than levamisole (Williamson *et al.* 2009). The different combinations of receptor subunits in *O. dentatum* yielded a range of potential receptors some with a higher sensitivity to levamisole (Ode-UNC-29, Ode-UNC-63, Ode-UNC-38, Ode-ACR-8); some with a higher sensitivity to acetylcholine (Ode-UNC-29, Ode-UNC-63, Ode-UNC-38). The calcium permeability of the receptor also varied depending on the stoichiometry of the receptor (Buxton *et al.* 2014).

It therefore seems likely that the native *G. pallida* receptor, with its different stoichiometry, will have different pharmacological properties from the *C. elegans* receptor. Furthermore, due to differences in the key loops of Gpa-UNC-38 these pharmacological properties may be different from those of animal-parasitic nematodes. As these differences appear to be shared by other plant-parasitic nematodes, it may be that the structure of the native *G. pallida* receptor is shared across plant-parasitic nematodes and may provide a specific target for control.

4.4.5 The *cel-acr-2 cel-acr-3* operon found in *C. elegans* appears to be conserved in *G. pallida*, but may include *gpa-unc-29.1*

The *cel-acr-2 cel-acr-3* (Baylis *et al.* 1997) operon of *C. elegans* links the two genes together. In *G. pallida* this operon is conserved, although the translated sequence of *gpa-acr-3* lacks a signal peptide. The region between the end of *gpa-acr-2* and

beginning of *gpa-acr-3* was cloned from cDNA further substantiating the operonic status of the two genes, but no evidence of a signal peptide was found (Figure 4-10a). The distance between *gpa-acr-2* and *gpa-acr-3* was also shorter than between *cel-acr-2* and *cel-acr-3* suggesting there may have been some loss of sequence. Amplification of the intervening region between *gpa-acr-2* and *gpa-acr-3* from cDNA may also be beneficial, but may prove difficult if it is rapidly processed. *Gpa-unc-29.1* is also located 400 bp downstream of the end of *gpa-acr-3* (Figure 4-10c), while in *C. elegans* an unrelated gene, *nas-11*, is downstream of *acr-3* (Figure 4-10b). This *gro-acr-2 gro-acr-3 gro-unc-29.1* structure is conserved in *G. rostochiensis*. It is possible that *gpa-unc-29.1* is linked to *acr-2* and *acr-3* as part of the operon. However, if this were the case it may be expected that the expression levels of *gpa-acr-2 gpa-acr-3* and *gpa-unc-29.1* would be closely related to each other (Figure 4-17), although post-transcriptional regulation could affect expression levels. The analysis of whether *gpa-unc-29.1* retains sufficient upstream sequence for a promoter region and regulatory elements could determine if these genes are linked.

4.4.6 Phylogenetic relations of subunits show that orthologues are the best identified, despite differences in sequence

A phylogenetic tree generated to represent the relationship between the nAChR orthologues identified in *G. pallida* and *G. rostochiensis* shows that they cluster with their predicted groups. The tree predicts any gene duplications that have arisen from a common ancestor related to the *C. elegans* gene, and not from a common ancestor prior to the *C. elegans* gene. In other words, the duplication is likely to have occurred after Clade 9 and Clades 10-12 diverged from each other. This is the case for the two orthologues of Cel-UNC-38 and Cel-UNC-29 identified in *G. pallida* and *G. rostochiensis* (Figure 4-16). Such duplication and subsequent independent evolution of genes may have led to the large diversity of nicotinic acetylcholine receptors in nematodes.

4.4.7 *C. elegans* as a heterologous system for analysis of *G. pallida* promoter activity using GFP transcriptional fusions

Preliminary work showed that the promoter regions of *G. pallida* are sufficient to drive GFP expression in *C. elegans* despite their evolutionary distance. Although similar work has been conducted using promoter regions of other genes to drive GFP expression in *C. elegans* (Qin *et al.* 1998; Costa *et al.* 2009), this is the first example of using promoter regions of nAChRs from a plant-parasitic nematode to drive GFP expression in *C. elegans*.

For *pgpa-acr-2* the observed pattern of expression is similar to that observed using the promoter region of *cel-acr-2* of *C. elegans*. In *C. elegans* expression is reported in the ventral nerve cord, the nerve ring, the vulval muscles and the DA, VB and VA neurons (Qi *et al.* 2013). This pattern of expression is also seen in the *G. pallida pgpa-acr-2* lines

(Figure 4-19), with expression in the ventral nerve cord, and at distinct clusters (likely the DA, VB and VA neurons) and in the nerve ring. However, expression in the vulval muscles was not observed as J2s lack this structure.

For *pgpa-unc-63* expression was less consistent between individuals, but in similar locations to that for *cel-unc-63*. In *C. elegans*, *cel-unc-63* is expressed in the body wall muscles, the ventral nerve cord, head neurons and in muscles of the sphincter (Culetto *et al.* 2004). Although GFP expression from *pgpa-unc-63* is observed in the head region (Figure 4-20a) and along the ventral side of the body (Figure 4-20b), it is not clear if this expression is in the body wall muscles. GFP expression in the tail region may also indicate association with the sphincter muscles.

Although GFP expression directed in *C. elegans* by *G. pallida* promoter regions was successful, it was hard to determine if the specific pattern was in agreement with that which has been observed for *C. elegans*. To circumvent this problem, lines expressing both the promoter region of *C. elegans* and the promoter region of *G. pallida* driving two different reporter genes could be generated to determine if the two marker genes co-localise. This would be particularly beneficial for determining if expression is seen in the ventral nerve cord or in the body wall muscle.

This work only used transcriptional fusions, using the promoter region directly upstream of the coding region for GFP. There is evidence in *C. elegans* that some transcriptional elements are present in the first intronic region of genes in addition to the promoter region and may affect expression (Choi and Newman 2006). As the first intron was not included in these constructs, some regulatory elements may be absent and the expression pattern incomplete. Nevertheless, further analysis of the expression patterns for all nAChRs identified in *G. pallida* will be beneficial to determine their potential roles.

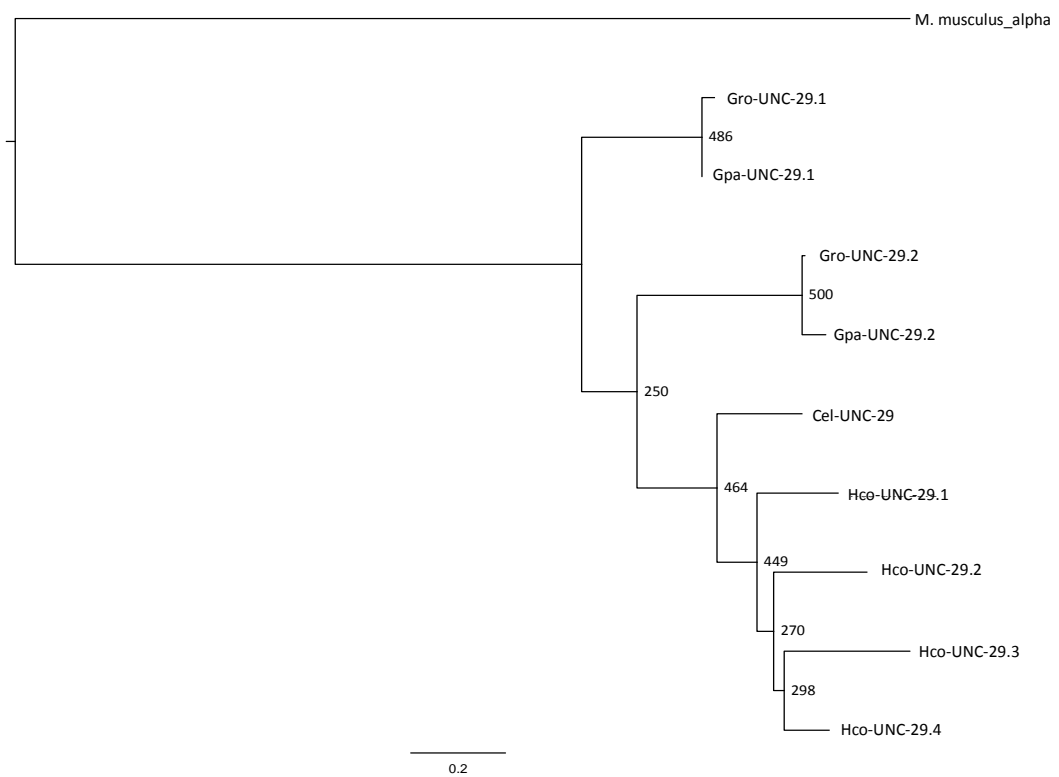


Figure 4-21: Phylogenetic tree of relationship between paralogues of UNC-29 identified in *G. pallida*, *G. rostochiensis*, *H. contortus* and *C. elegans*

Maximum likelihood phylogeny (Bootstrap 500) using predicted protein alignments of paralogues of UNC-29 identified in *G. pallida*, *G. rostochiensis*, *H. contortus* and *C. elegans*. Scale bar represents branch times. Hco-UNC-29 cluster together, and are more distantly related to Gpa- or Gro- UNC-29s than Cel-UNC-29.

	Loop A	Loop B	Loop C	TM2
	86	93 147	154 189	198 245
<i>M. musculus alpha</i>	WRP D V V L Y	GTWTYDGS	F Y S S CCP-----TTPY	LSI S V L L S LTVFLLVIVELIPS
<i>C. elegans</i>	WVP D I V L Y	G S WT T FS E N	Y P S S CCP-----QS-AY	LCI S I L VALT I FF L LLTEIIIPA
<i>A. suum</i>	WVP D I V L Y	G S WT Y SE D	Y P S S CCP-----QSDAY	LCI S I L VALT V FF L LLTEIIIPA
<i>H. contortus</i>	WVP D I V L Y	G S WT Y SEN	Y P S S CCP-----QS-AY	LCI S I L VALT I FF L LLTEIIIPA
<i>B. xylophilus</i>	WVP D I V L Y	G S WSFPKR	Y I G C CP-----ESGDF	LV I S I L V S A F Y FLILTEVMPA
<i>G. pallida</i> .1	WVP D I V L I	G S WT Y PS G	FFAS-----KNGIY	LS I N I L V ALT M FF F LLL I EIIIPA
<i>G. pallida</i> .2	WVP D L V L Y	GPWSYP D	YPGRSPAGGARN---GQKF	LCI S I L VALTVFF L LLTEIMPA
<i>G. rostochiensis</i> .1	WVP D I V L I	G S WT Y PS G	FFAS-----KNGIY	LS I N I L V ALT M FF F LLL I EIIIPA
<i>G. rostochiensis</i> .1	WVP D L V L Y	- - - - -	YPGRSPAGGARD---GRKF	LCI S I L VAL-----TTEIMPA
<i>R. reniformis</i>	WVP D L V L Y	G S WSYSED	FMGS-----KNGDY	LCI S I L VALTVFF L LAEIMPA
<i>M. incognita</i>	- P D I V L I	ASWSFP T N	FMGS-----KNGDY	LS I N I L V ALT-----
<i>M. hapla</i>	WVP D I V L I	ASWSFP T N	FMGS-----KNGDY	LS I N I L V ALT M FF F LLL I EIIIPA
<i>N. aberrans</i>	WVP D I V L I	G S WSYP A N	F Y GS-----KNGDY	LS I N I L V ALT M FF F LLL I EIIIPA
<i>H. schachtii</i>	WVP D I V L I	G S WT Y PS G	FFGS-----KNGIY	LS I N I L V ALT M FF F LLL I EIIIPA
<i>H. avenae</i>	WVP D L V L Y	G S WSYPAD	YPRRSSAGGPNNVQHKKKF	LCI S I L VT L TVFF L LLTEIMPT

Figure 4-22: Loops A-C and transmembrane domain 2 of UNC-38 in plant-parasitic nematodes compared to *C. elegans*, animal-parasitic nematodes and the mouse α -subunit

In Loop A, Y⁹³ is an isoleucine in most plant-parasitic nematodes. In Loop B, G¹⁵³ is an E in *C. elegans* and animal-parasitic nematodes, but this residue is highly variable in plant-parasitic nematodes. In Loop C, the YxxCC motif is absent from all plant-parasitic nematodes. In TM2, most plant-parasitic nematodes have a methionine linked to increased levamisole sensitivity at position 255. Plant-parasitic nematodes are indicated by a green background. Residue numbering is given for the α -subunit from *Mus musculus* (mouse)

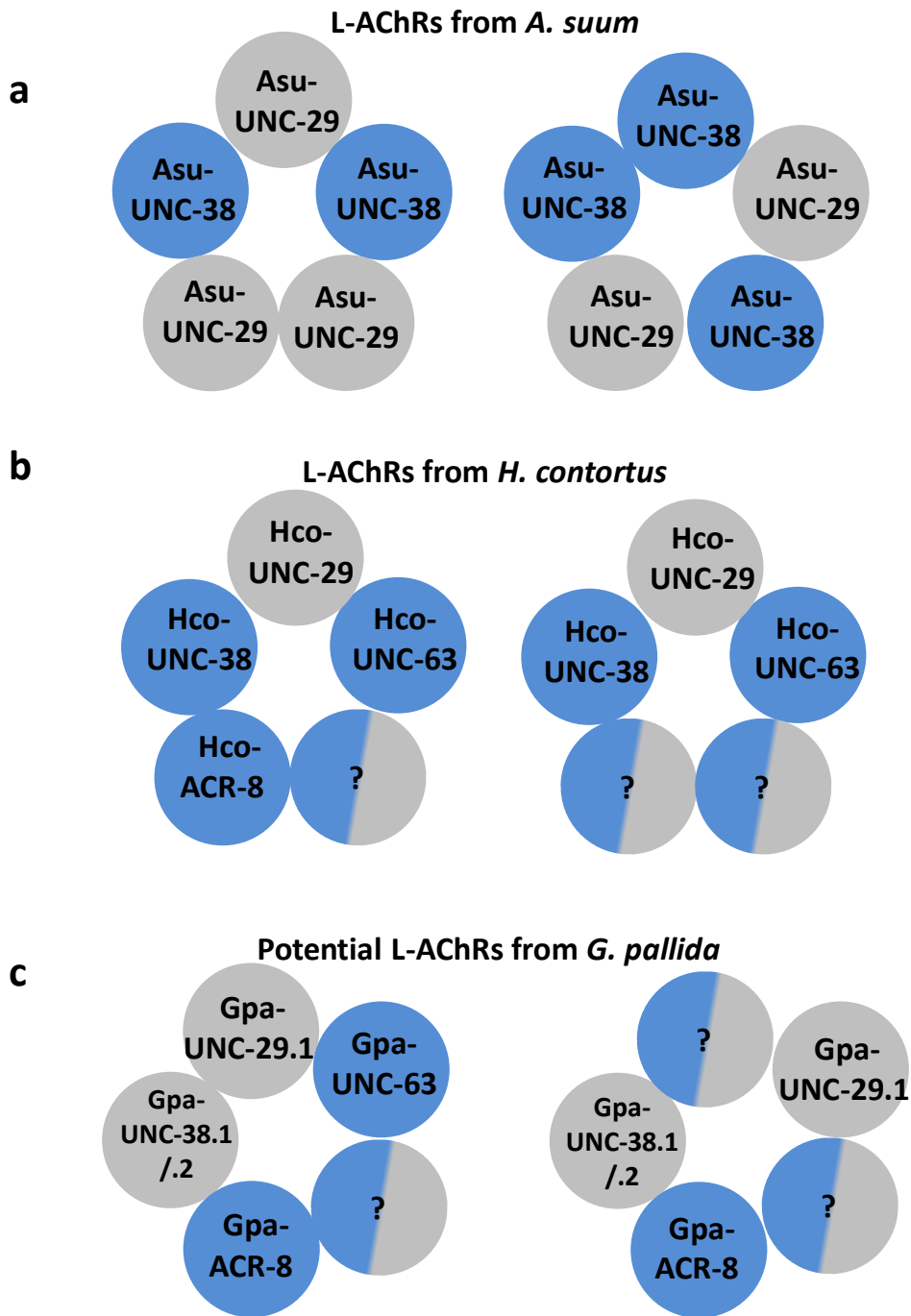


Figure 4-23: Stoichiometries of L-nAChRs in animal-parasitic nematodes deduced by expression in *Xenopus* oocytes and a starting model for the native *G. pallida* receptor

a) Two functional arrangements of the receptor from *A. suum* b) Two possible arrangements of the receptor from *H. contortus* and *O. dentatum* c) Potential arrangements of the *G. pallida* receptor. Blue circles are α-subunits, grey circles are non-α. Unknown subunits are bi-coloured.

Summary

- There is a reduction in the number of nAChRs in *G. pallida* and *G. rostochiensis* compared to *C. elegans*
- Fewer members of the ACR-16 group are present in *G. pallida* and *G. rostochiensis*
- The composition of the levamisole-sensitive nicotinic acetylcholine receptor of *G. pallida* and *G. rostochiensis* differs from that of *C. elegans*
- Amino acid sequences of Gpa-UNC-38.1 and Gpa-UNC-38.2 differ in positions which may affect function and pharmacology
- Use of *G. pallida* nAChR promoter regions can direct GFP expression in *C. elegans* which allows spatial expression to be analysed

5. Characterisation of the effect of levamisole in *Globodera pallida* and *Globodera rostochiensis*

5.1 Introduction

5.1.1 Determining the effect of levamisole on *G. pallida* and *G. rostochiensis* J2s

Levamisole is used as a veterinary anthelmintic for livestock (Coles, East and Jenkins 1975). It is a nAChR agonist that belongs to a class of imidazothiazole derivatives. The structure of the molecule is shown in Figure 5-1. The mode of action and target of levamisole was initially deduced in *C. elegans* although it had been used as an anthelmintic for many years previously and its effect on animal parasitic nematodes such as *A. suum* and *O. dentatum* had been observed (Harrow and Gration 1985). Levamisole elicits spastic paralysis in the target organism by opening L-type nAChRs in body wall muscle. Calcium then enters the sarcomere and causes uncoordinated muscle contraction leading to paralysis. In *C. elegans* the EC₅₀ of paralysis is 9 µM after 1 hour levamisole exposure (Qian *et al.* 2008). Levamisole additionally stimulates egg-laying behaviours of adult hermaphrodites (Trent, Tsung and Horvitz 1983). Treatment of adult hermaphrodites with levamisole also causes rapid shrinkage of *C. elegans* to about 90% of the initial body length, due to contraction of body wall muscle. This shrinkage occurs within 30 seconds in response to 100 µM levamisole (Mulcahy, Holden-Dye and O'Connor 2013), and can be observed in response to as little as 10 µM levamisole (Lewis *et al.* 1980). As J2s of plant-parasitic nematodes do not lay eggs, egg-laying behaviour cannot be used to determine levamisole sensitivity. However, the effect of levamisole on paralysis and shrinkage can be assessed.

5.1.2 Use of transgenic *C. elegans* to investigate endogenous genes of *G. pallida*

The ability of orthologous genes identified in a non-model organism to functionally rescue mutants of *C. elegans* allows the function of the gene to be more clearly understood. The CGC provides a bank of thousands of mutant lines for individual genes which allow such complementation experiments. Most heterologous rescue experiments to date have used *H. contortus* genes to rescue *C. elegans* mutants. For example, *C. elegans daf-21 (hsp-90)* null mutants can be partially rescued by *hsp-90* from *H. contortus* (Gillan *et al.* 2009). The ability of a previously uncharacterised glutamate-gated chloride channel subunit (*hco-glc-6*) to restore ivermectin sensitivity to the insensitive *C. elegans* triple-mutant, contrasting with the lack of rescue by *hco-glc-2*, provided information about the likely roles of these subunits in *H. contortus* (Glendinning *et al.* 2011).

Mutant strains of *C. elegans* are available with mutations in different genes encoding L-nAChR subunits from the CGC. The *unc-38* mutant lacks a functional L-nAChR

receptor in body wall muscle and has reduced thrashing activity in liquid, and increased resistance to levamisole (Lewis *et al.* 1987; Fleming *et al.* 1997).

5.1.3 *Xenopus* oocytes as a heterologous expression system for investigation of ion channels and receptors

The eggs of the South African Tree Frog have been a valuable tool in scientific research since the late 1950s. The oocytes are large (1-1.2 mm) and remain viable for long periods of time outside of the frog. In the 1970s it was demonstrated that injection of haemoglobin mRNA into the oocyte would lead to translation and synthesis of the protein (Gurdon 1971). Later work showed that receptors could be expressed on the oocyte surface by injection of mRNA-encoding the receptors of interest (Gundersen, Miledi and Parker 1983; Miledi, Parker and Sumikawa 1982). Since then, the expression of receptors in *Xenopus* oocytes combined with electrophysiology has been used to investigate receptor biology from pharmacology to assembly and stoichiometry. Stage V or VI oocytes are used in electrophysiological studies. The oocyte has two distinct halves, a dark pigmented animal pole and the non-pigmented vegetal pole. It is surrounded by a vitelline membrane, which does not contain channels that may interfere with electrophysiological recordings. An outer follicular layer with blood vessels and ion channels must be removed prior to working with the oocytes. Commonly, cRNAs encoding a receptor or a mix of cRNAs encoding subunits of a receptor are injected into the oocyte and are incubated for 2-5 days (depending on the type of receptor to be expressed). After incubation, the ion channel or receptor is expressed on the oocyte surface and the properties of the channel can be investigated by electrophysiology (Bianchi and Driscoll 2006).

Electrophysiological recordings are carried out by the two-electrode clamp method. One electrode (voltage-sensing) penetrates the membrane and measures the membrane potential. This is compared to the command voltage (set by user). A second electrode (bath-electrode) penetrates the membrane and injects current to bring the difference between membrane potential and command voltage to 0. As the oocyte is exposed to different receptor agonists, the receptors open causing the membrane potential to change. The voltage-sensing electrode detects this change, and the bath-electrode records the amount of current required to bring the membrane potential back to the command voltage. Larger concentrations of agonists will cause larger receptor opening currents and require more current to be injected by the bath electrode. The amount the bath-electrode has to inject at each agonist concentration to maintain the membrane potential is recorded to produce a dose-response curve (Bianchi and Driscoll 2006).

Expression of receptors in oocytes, and the effect of exposure to various agonists and antagonists have allowed the pharmacology of different receptors to be investigated. This has been particularly useful for characterising the pharmacology of novel

receptors (Dufour *et al.* 2013; Yassin *et al.* 2001) or to investigate the effect of aberrant mutant phenotypes that may lead to anthelmintic resistance (Boulin *et al.* 2011). It has also allowed the native conformation of multimeric receptors to be deduced, based on the ability of subunits to assemble and express in *Xenopus* oocytes. The likely native conformation of the *C. elegans* L-nAChR in body wall muscle (Boulin *et al.* 2008), and of the orthologous receptors in *H. contortus* (Boulin *et al.* 2011), *O. dentatum* (Buxton *et al.* 2014) and *A. suum* (Williamson *et al.* 2009) have been deduced by this methodology. It has also proved useful for establishing that a single subunit is sufficient for robust functional expression of homomeric receptors, (Raymond, Mongan and Sattelle 2000).

In some cases, robust expression in this heterologous system requires addition of ancillary factors that assist in assembly of receptors. Three ancillary factors are required for robust expression of the *C. elegans* L-nAChR in *Xenopus* oocytes. RIC-3 is a chaperone protein, present in the endoplasmic reticulum (ER) and involved in the folding and processing of the L-nAChR subunits (Millar 2008). UNC-74 is a thioredoxin, another ER protein believed to assist in correct protein folding (Haugstetter, Blicher and Ellgaard 2005). UNC-50 is present in the Golgi apparatus and appears to be essential for trafficking of L-nAChR subunits to the correct location (Eimer *et al.* 2007). However, all of these ancillary factors are not required for all nAChRs as expression of ACR-16 is robust with only the addition of RIC-3. The absence of the correct ancillary factors may prevent the proper expression of a heterologously expressed receptor, or may affect the properties and pharmacology of the expressed receptor as RIC-3 has been shown to affect subunit ratios (Ben-Ami *et al.* 2005).

There are some species for which heterologous expression of acetylcholine receptors in *Xenopus* oocytes has been troublesome. The study of the nAChRs of insects has been hindered by the difficulty expressing insect nAChRs in *Xenopus* oocytes. To investigate the pharmacology of these, α -nAChR subunits from insects are co-expressed with β -nAChR subunits from vertebrates to create hybrid receptors (Thany *et al.* 2007).

In this chapter, the effect of levamisole on *G. pallida* and *G. rostochiensis* J2s has been investigated. In chapter 2, key residues involved in levamisole sensitivity and that define Cel-UNC-38 as an α -subunit have been identified as absent in Gpa-UNC-38.1 and Gpa-UNC-38.2. In this chapter, the role of Gpa-UNC-38.1 and its ability to replace Cel-UNC-38 has been investigated by the use of thrashing assays on a strain of *C. elegans* expressing Gpa-UNC-38.1. Gpa-UNC-38.1 has also been expressed in *Xenopus* oocytes replacing Cel-UNC-38 in the native *C. elegans* receptor in order to characterise these differences.

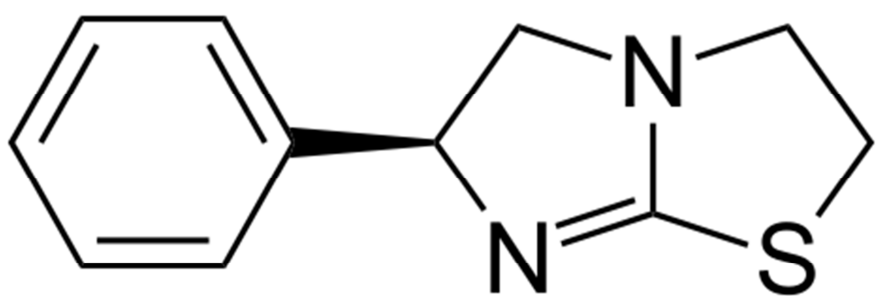


Figure 5-1: Chemical structure of levamisole

The chemical structure of levamisole.

Aims

- Assess effect of levamisole on *G. pallida* and *G. rostochiensis* J2s
- Investigate effect of altered L-nAChR subunits

5.2 Materials and methods

5.2.1 Assessment of effect of levamisole on *G. pallida* and *G. rostochiensis* J2s

5.2.1.1 Production of levamisole treatment plates

9 cm plates containing 10 ml of agar (0.25% Tween-20, 10 mM Hepes and 1% high-strength agar at pH 7.2) were produced. Appropriate concentrations of levamisole or water control were added to the molten agar before pouring. Plates were dried for one hour upside-down on the bench to evaporate excess moisture, and then left overnight at room-temperature before use.

5.2.1.2 Assessment of average speed

50-100 J2s were placed onto a solid agar plate and left to orientate in the dark for 2 hours. Two minute video clips of the plates were taken at 0.73x magnification on a M165FC Leica microscope at 4 frames per second (fps). These were repeated several times per plate in order to sample all worms on the plate and across multiple plates. These images were then loaded into ImageJ (Abramoff 2004). Image type was converted from RGB to 8-bit. The “subtract background” tool was used to smooth out the background of the image (settings: rolling ball radius: 50 pixels; light background, sliding paraboloid, disable smoothing). The threshold tool (threshold setting: maxentropy) was used to allow only J2s to be selected. The wrMTrck plugin (Pedersen 2010) was then run to determine maximum speed of worms. An ImageJ macro was written to provide the same settings each time this was run:

```
run("Set Scale...", "distance=0.1 known=1 pixel=1 unit=um");
//setTool("hand");
run("wrMTrck ", "minsize=50 maxsize=10000 maxvelocity=100 maxareachange=50 mintracklength=50
bendthreshold=1 binsize=0 showpathlengths showlabels showpositions showsummary smoothing
rawdata=0 benddetect=3 fps=4 backsub=1 threshmode=Otsu fontsize=16");
```

An example of image processing can be seen in Figure 5-2.

A minimum of 180 worms per levamisole concentration were sampled, over 3 separate repeats for *G. pallida* J2s. For *G. rostochiensis* J2s a minimum of 20 worms per concentration were sampled over 2 separate repeats.

5.2.1.3 Assessment of shrinkage at 2 hours over a range of levamisole concentrations

The WrMTrck plugin also collects perimeter information for detected objects. The perimeter output was divided by two to provide approximated length estimation for the range of levamisole concentrations after 2 hours.

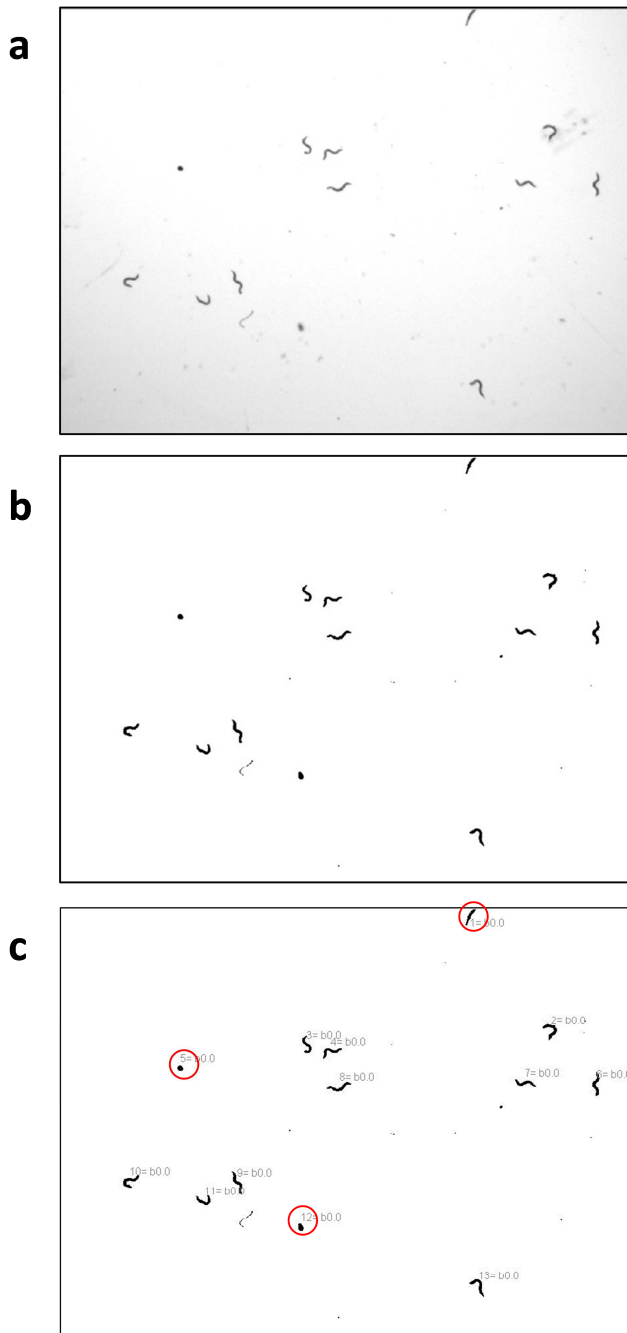


Figure 5-2: Image processing steps to determine average speed of *G. pallida* and *G. rostochiensis* J2s

a) Snapshot of single frame from raw image collection. The background lighting is uneven and contrast between worm objects and background is unclear b) Image after the background has been removed (“subtract background”) and image has been processed to highlight objects (“threshold”). c) Image after wrMTrck plugin has been run. Individual objects are assigned numbers. Data are output to a separate spreadsheet. Red circles indicate numbered objects which must be manually removed from the data set as they are non-worm objects, or are not fully in the field-of-view.

5.2.1.4 Assessment of shrinkage over 20 minutes in response to a high dose of levamisole

To analyse shrinkage, a single J2 was added in 1 µl of water to an agar plate (made as in 5.2.1.1) containing either 200 mM levamisole or water. In total, 21 J2s were analysed for the control condition and 42 J2s for the levamisole condition. As soon as the liquid had absorbed into the plate and the J2 had come into contact with the test medium, a reference image was taken ($t=0$). A further image was taken every minute for 20 minutes. Length of the J2 was measured at each time point using the measure tool in ImageJ. Length was presented as a percentage of the reference image and linear regression was used to determine if the slopes differed significantly. A Leica M165FC microscope along with a Qimaging Fast1394 QiCAM camera and Qcapture Pro 7 software was used to capture images.

5.2.1.5 Assessment of shrinkage over 24 hours in response to a low dose of levamisole

A single J2 in 1 µl of water was placed on a 5 cm agar plate (made to the same recipe as in 5.2.1.1) containing 100 µM levamisole or water. An image was taken immediately at $t= 0$. Plates were covered in foil and left at 20 °C for 24 hours. The J2 was then photographed again. Length of J2s at $t = 0$ and $t = 24$ were measured using ImageJ.

5.2.2 Heterologous expression of *Gpa-unc-38.1* in *C. elegans*

5.2.2.1 Production of the *Gpa-unc-38* and *Cel-unc-38* line

Gpa-unc-38.1 and *Cel-unc-38* lines were generated by microinjection in Southampton. The constructs were generated as described in 6.2.2. Anna Crisford carried out the microinjections and selection of the positive lines. The *unc-38(x20)* line was used as the background line for mutant-rescue and was obtained from the CGC. Transgenic *C. elegans* Lines were made by the same methodology as in 6.2.5.

5.2.3 Selection of *C. elegans* worms for use in thrashing assays

Due to the nature of transformation by microinjection, which introduces transgenes by formation of extrachromosomal arrays that segregate in a non-Mendelian fashion, not all individuals in the line carry the injected transgene. Co-injection of the GFP marker gene is necessary for selection. For transgenic lines, 24 hours prior to assay, L4-stage hermaphrodites that expressed the GFP marker in the pharynx as visualised using a Leica M165FC microscope with Lumen 200 fluorescence illumination system, were transferred onto a fresh NGM-lite plate. For control non-transgenic lines the L4-stages were selected and transferred onto fresh NGM-lite plates.

5.2.3.1 Thrashing assays

Assays were conducted in 12 well plates. Each well contained 900 µl M9 buffer (+0.01% BSA). Six L4+1 worms from each line to be analysed were transferred into individual wells. The worms were allowed to rest for 10 mins to allow dissipation of changes in behaviour due to handling. The basal thrashing rate of each worm was calculated by counting the number of thrashes in a minute. A thrash was counted as the bend of the worm from one side of its body to the other and back (Figure 5-3). After this 100 µl of the appropriate levamisole solution (10x stock solution in M9 buffer) was added to make a total volume of 1 ml liquid in each well. Further thrashing counts (thrashes / min) were carried out at t = 10 min and t = 30 min. Six worms could be analysed in each iteration of the assay. Assays were conducted at room temperature, and under 30x magnification. Each day, six individuals of each line were analysed to reduce day-to-day variation within the data. The wild-type line (N2), background line (*unc-30(x20)*) and two transgenic lines expressing *cel-unc-38* or *gpa-unc-38.1* were analysed. Assays were conducted at 0, 10, 50 and 100 µM concentrations of levamisole. A minimum of 18 worms were assessed for each line at each concentration.

5.2.4 Expression of *gpa-unc-38.1* to replace *cel-unc-38* in the *C. elegans* receptor in *Xenopus* oocytes

Data in this section were collected with the kind help of Claude Charvet, at the INRA Loire Valley Centre.

5.2.4.1 Subcloning of *gpa-unc-38.1* into the oocyte expression vector pTB207

The pTB207 vector was obtained from Claude Charvet, INRA. The *Gpa-unc-38.1* cDNA sequence was excised from pCR™8 by restriction digest with EcoRI and the DNA fragment isolated following gel electrophoresis. pTB207 was cut with EcoRI and treated with shrimp alkaline phosphatase (NEB) to prevent religation of the vector. In a 20 µl reaction, 1 µl of ligase, 2 µl of 10 x ligation buffers and insert to vector DNA in a 3:1 ratio was added. Ligation of *gpa-unc-38.1* into pTB207 was conducted overnight at 4 °C using T4 ligase (NEB). After transformation into competent cells, positive colonies with inserts in the correct orientation were selected by colony PCR using the T7F primer and the *gpa-unc-38.1* R primer. A map of the vector used is shown in Figure 5-4.

5.2.4.2 Preparation of vector for cRNA transcription

The pTB207:*Gpa-unc-38.1* vector was linearised in preparation for cRNA transcription. Six µg of vector was digested with NheI for 2 hours at 37 °C. The digested DNA was cleaned used the NucleoSpin® Gel and PCR clean-up kit according to the manufacturer's instructions. Briefly, 5x volume of buffer NTB was added to digested DNA. The DNA was added to the spin column and briefly centrifuged to bind DNA to

the column. The membrane was washed by adding 700 µl NT3 followed by brief centrifugation. A second wash was performed and the column dried by an additional minute of centrifugation. DNA was eluted by adding 30 µl NE buffer to the membrane, following by centrifugation. A second elution was taken from the column in order to check linearisation by gel electrophoresis.

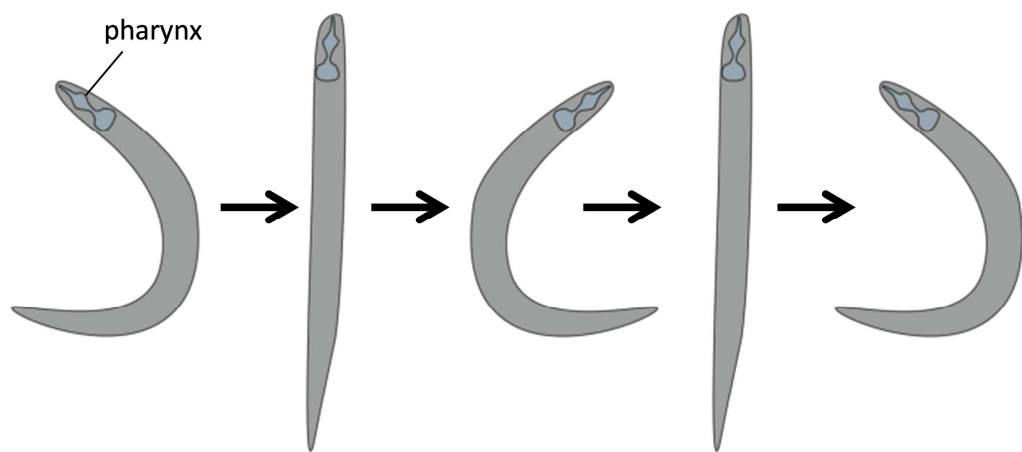


Figure 5-3: Schematic of a single *C. elegans* thrash in liquid

A single thrash is counted as the full curl from one side of the body, to the other and back again.

5.2.4.3 Preparation of cRNAs for injection into *Xenopus* oocytes

The mMessage mMachine T7 kit (Ambion) was used to produce cRNAs according to the manufacturer's instructions. Briefly, 1 µl of linearised pTB207:*gpa-unc-38.1* was used in a 20 µl reaction with 10 µl 2X NTP/CAP, 2 µl 10x reaction buffer, 2 µl enzyme mix and nuclease-free water. This reaction was incubated at 37 °C for 2 hours. 30 µl of LiCl precipitation solution was added to the reaction to precipitate cRNA. The mixture was chilled at -20 °C overnight, and then centrifuged for 15 mins at 4°C and maximum speed. The supernatant was removed, and the pellet washed twice with 500 µl 70% ethanol. The tube was centrifuged briefly, and the ethanol removed. Pellets were left until dry, and then cRNA was resuspended in 65 µl nuclease-free water. Integrity of RNA was checked by gel electrophoresis and quantified using a Nanodrop spectrophotometer.

5.2.4.4 Preparation of injection mixes

Two injection mixes were produced. 10 µl of mix contained *cel-unc-63*, *cel-lev-1*, *cel-lev-8*, *hco-ric-3*, *hco-unc-50*, *hco-unc-74* (cRNAs provided by Claude Charvet) and either *gpa-unc-38.1* (for analysis of the chimeric receptor) or *cel-unc-38* (for the native receptor) at a final concentration of 50 ng/µl. The ancillary factors (RIC-3, UNC-50, UNC-74), required for robust expression of L-nAChRs in *Xenopus* oocytes, from *H. contortus* were used as they had been demonstrated to be effective previously in the laboratory where this experiment was conducted.

5.2.4.5 Storage and preparation of *Xenopus* oocytes prior to injection

Excised *Xenopus* ovaries obtained from (NASCO Fort Atkinson, Wisconsin, USA) were stored in incubation buffer (100 mM NaCl, 2 mM KCl, 1 mM CaCl₂, 1 mM MgCl₂, 5 mM HEPES, 100 mM Na pyruvate, 10 ml penicillin (10,000 units/ml), 10 ml streptomycin (10,000 µg / ml)) at 4°C. This solution was changed every two days during storage. Prior to injection, oocytes were incubated for 1 hour at room temperature in 2 mg/ml collagenase. The oocytes were then washed 3x in incubation buffer. After this, the follicular membrane that surrounds the oocytes was removed carefully with fine-tipped tweezers.

5.2.4.6 Injection of *Xenopus* oocytes with cRNA injection mixture

Oocytes were microinjected with approximately 72 nl of injection mixture. The needle was controlled using a micromanipulator and injection pressure was generated by the Nanoject II™. After injection, the oocytes were transferred to individual U-shaped wells in a 96-well plate with 200 µl incubation buffer. The injected oocytes were incubated at 19 °C for 4-5 days. Incubation buffer was changed every 2 days.

5.2.4.7 Voltage-clamp recordings from injected oocytes

Oocytes were incubated in 200 µl of 100 µM BAPTA-AM (Sigma), a chelating agent, for 2 hours minimum in order to remove calcium and endogenous Ca²⁺ dependent chloride currents. Oocytes were voltage clamped at -60 mV using an oocyte clamp (OC-725C) and amplified with a Digidata 1322A amplifier. Clampex 10.2 was used to acquire data on a desktop computer. During recording, the oocyte was continuously perfused in a gravity-fed system with recording buffer (100 mM NaCl, 2.5 mM KCl, 1 mM CaCl₂, 5 mM HEPES, pH 7.3). Currents elicited by 1, 3, 10, 30, 100, 300 and 1000 µM acetylcholine and 1, 3, 10, 30, 100 and 300 µM levamisole were recorded. Dilutions of all agonists were made on the day. Agonist was perfused across the oocyte for 10 seconds. Agonists were perfused starting with the lowest concentration, and the membrane potential was allowed to recover to baseline before the next agonist was perfused. Clampfit was used to analyse the acquired data. Further characterisation of receptor response to other nicotinic acetylcholine receptor agonists was conducted by Claude Charvet. This included pyrantel, nicotine and DMPP (dimethylphenylpiperazinium).

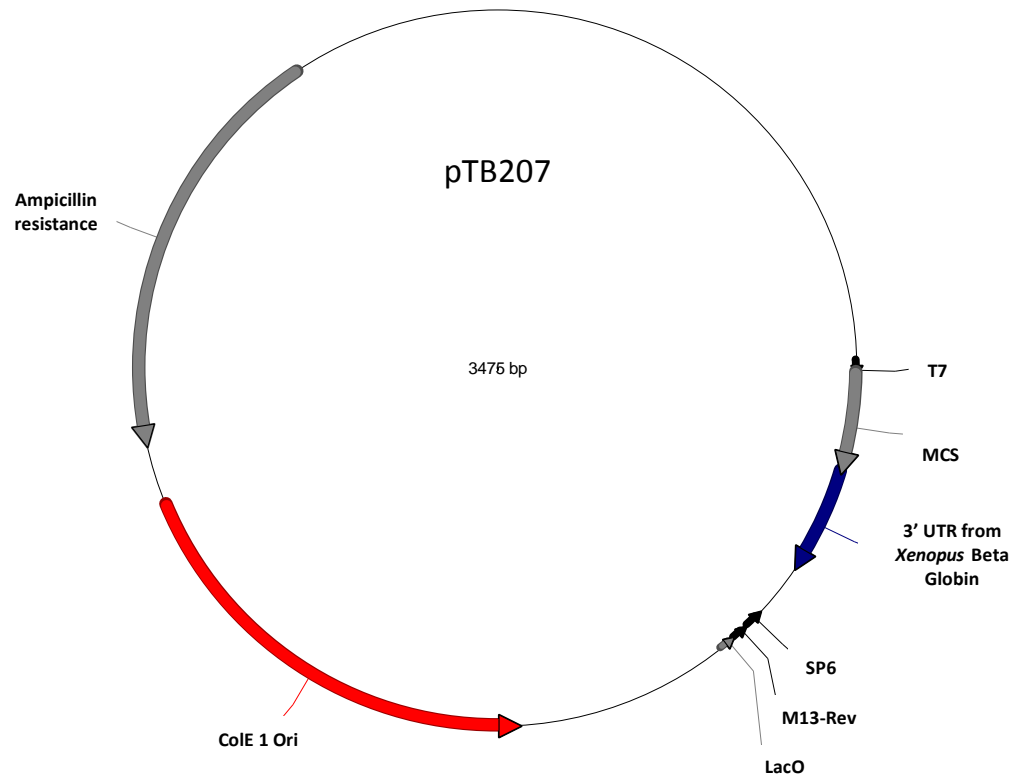


Figure 5-4: Vector map of pTB207

pTB207 was used to produce cRNAs for injection into *Xenopus* oocytes. The plasmid contains ampicillin resistance and a multiple cloning site facilitates cloning into the vector. 3' UTR from *Xenopus* β -globin gene aids transcript stabilisation.

5.3 Results

5.3.1 *G. pallida* J2s have higher resistance to levamisole than *C. elegans*

The EC₅₀ – the concentration at which 50 % of individuals displayed paralysis – of levamisole in *C. elegans* is 9 µM (Qian *et al.* 2008). *Globodera pallida* was found to be more resistant to levamisole than *C. elegans* with a calculated EC₅₀ of 19.7 mM – approximately 2000 fold higher than for *C. elegans* (Figure 5-5a). *G. pallida* exposed to low levamisole (\leq 5 mM) concentrations largely remained unaffected and maintained speed similar to that of unexposed J2s after 2 hours. At 2.5 mM levamisole exposure *G. pallida* J2s were observed to increase in speed after 2 hours (Figure 5-5b)

5.3.2 *G. rostochiensis* J2s are less resistant to levamisole than *G. pallida*, but are more resistant than *C. elegans*

The EC₅₀ of *G. rostochiensis* J2s was calculated to be 5.6 mM. Although this is less than that of the *G. pallida* J2s, it is still far higher than that of *C. elegans* (~500 fold higher). As for *G. pallida*, exposure to a low dose of levamisole, 0.625 mM, increased the speed of *G. rostochiensis* J2s, although this increase was not statistically significant (Figure 5-6).

5.3.3 Levamisole induces shrinkage of *G. pallida* J2s

Levamisole induces rapid shrinkage of *C. elegans*, mediated by contraction of the body wall muscle. The maximal shrinkage rate is ~10% of untreated body length (Mulcahy, Holden-Dye and O'Connor 2013). Levamisole also induced contraction of body wall muscle and shrinkage in *G. pallida*, and the maximal shrinkage rate was approximately 10% of the untreated body length after 2 hr exposure to levamisole. The concentration of the drug required to achieve this maximal shrinkage rate was 40 mM, higher than that for *C. elegans* (Figure 5-7a)

5.3.4 Levamisole induces shrinkage of *G. rostochiensis* J2s

G. rostochiensis J2s also shrank in response to levamisole. Maximal shrinkage for *G. rostochiensis* J2s occurred at 10 mM, and the maximal shrinkage rate was approximately 20% of untreated body length after 2 hour exposure to levamisole (Figure 5-7b).

5.3.5 Treatment of *G. pallida* J2s with high concentration of levamisole induces shrinkage within a short time period

To investigate if levamisole entry into *G. pallida* J2s was responsible for the apparent increase in resistance, the shrinkage rate was investigated. Shrinkage is rapid for *C. elegans* and maximal shrinkage occurs within 30 seconds in response to 100 µM levamisole (Mulcahy, Holden-Dye and O'Connor 2013), approximately 10x the EC₅₀.

Globodera pallida J2s were exposed to 200 mM levamisole, approximately 10x the calculated EC₅₀ for this species, or a control plate and individual worms were imaged every minute for 20 minutes. J2s exposed to levamisole shrank steadily over 20 minutes reaching a minimal size of 92% of original length (Figure 5-8a). Shrinkage began rapidly as at the first measurement, in the delay between putting the J2 on the plate and taking the measurement, at 0 minutes, levamisole exposed J2s were already shorter than control J2s (Figure 5-8b).

5.3.6 Treatment of *G. pallida* J2s with low concentration of levamisole does not induce shrinkage over 24 hours

It was reasoned that if levamisole could diffuse slowly across the cuticle over time, a low dose of levamisole may be sufficient to induce shrinkage if enough time were allowed. To investigate this, J2s were exposed to 100 µM levamisole for 24 hours. There was no significant difference in length between control J2s and levamisole-treated J2s at either 0 or 24 hours. Similarly, there was no significant difference between the 0 and 24 hour time points for either treatment (Figure 5-9). 100 µM levamisole induces shrinkage rapidly in *C. elegans*, but here it has been demonstrated that this concentration does not have a paralytic effect even after 24 hour exposure.

5.3.7 Gpa-UNC-38.1 is able to rescue the basal thrashing rate of *C. elegans unc-38(x20)* mutants, but not full sensitivity to levamisole

The *unc-38(x20)* mutant strain of *C. elegans* is functionally null for UNC-38 (Fleming *et al.* 1997). These null mutants display reduced thrashing rate in liquid compared to wild-type (N2) and following levamisole exposure, the thrashing rate of the null mutants does not decrease to the same level as the wild-type. The ability of Gpa-UNC-38.1 to rescue these phenotypes was investigated by microinjection of *gpa-unc-38.1* cDNA under the control of the *myo-3* promoter which directs expression in body wall muscle (line created by Anna Crisford, Southampton).

Gpa-unc-38.1 was able to rescue thrashing rate in the absence of levamisole as no significant difference was observed between wild-type (N2) thrashing rate and that of *unc-38(x20)* mutants rescued with *gpa-unc-38.1* in the absence of levamisole. On exposure to 10 µM levamisole, the thrashing rate of wild-type (N2) worms reduced by approximately 20 %. The thrashing rate of *Cel-unc-38*-rescued mutant worms also reduced by approximately 20 % in response to levamisole. In contrast, the thrashing rate of *gpa-unc-38.1* rescued worms was not reduced in response to 10 µM levamisole after 30 minutes (Figure 5-10).

On exposure to 50 µM levamisole, the thrashing rate of the *gpa-unc-38.1* line did not reduce to the level seen in the wild-type. Thrashing rate of the *gpa-unc-38.1*-rescued

worms was significantly higher than that of the wild-type worms after 10 minutes and 30 minutes exposure. In contrast, *unc-38(x20)* mutants rescued with *cel-unc-38* regained full sensitivity to levamisole as no significant difference in thrashing rate was observed from wild-type under 50 µM levamisole exposure (Figure 5-11). On exposure to 100 µM levamisole, thrashing rate of the *gpa-unc-38.1*-rescued lines did not reduce to the levels of the wild-type or *cel-unc-38*-rescued lines (Figure 5-12).

Examination of the thrashing rates at t = 30 mins, over the full range of levamisole concentrations tested showed that the response of the wild-type and *cel-unc-38* rescued line were not significantly different from each other (linear regression, p> 0.1). The response of the *gpa-unc-38*-rescued line was significantly different from the wild-type, *cel-unc-38*-rescued line and *unc-38(x20)* (Figure 5-12).

Gpa-UNC-38.1 is able to rescue the uncoordinated phenotype, and seemingly replace *Cel-UNC-38* in the receptor, although it appears to alter the sensitivity of the receptor to levamisole.

5.3.8 Expression of *gpa-unc-38.1* with *C. elegans* subunits to produce a chimeric receptor does not alter response to levamisole compared to the native *C. elegans* receptor.

cRNA encoding *gpa-unc-38.1* was injected into *Xenopus* oocytes along with cRNAs encoding the remaining *C. elegans* subunits, *cel-unc-29*, *cel-unc-63*, *cel-lev-8*, *cel-lev-1* and the ancillary factors required for robust expression, *hco-ric-3*, *hco-unc-50* and *hco-unc-74*. This mixture produced a functional receptor in *Xenopus* oocytes presumably consisting of the five injected subunits. Oocytes were also injected with cRNAs encoding the complete native *C. elegans* receptor (i.e. using *cel-unc-38*) to compare recordings in response to levamisole and acetylcholine.

Currents recorded for the chimeric receptor were within the nA (nanoamp) range on the first set of oocyte injections, and in the µA range on the second set. A dose-response curve was produced in response to acetylcholine and levamisole for both the chimeric receptor and the native receptor. The EC₅₀ of acetylcholine was 18.4 µM for the chimeric receptor, and 19.3 µM for the native receptor. For levamisole, the EC₅₀ was 6.6µM for the chimeric receptor and 5.7µM for the native receptor (Figure 5-14). A representative example of the response of a single oocyte to the full range of acetylcholine and levamisole concentrations for both the native and chimeric receptors is shown in (Figure 5-15).

5.3.9 Expression of *gpa-unc-38.1* with *C. elegans* subunits demonstrates the same pharmacology as the native *C. elegans* receptor

A panel of agonists of nicotinic acetylcholine receptors was used to determine any differential pharmacology of the native and chimeric receptors. In addition to

acetylcholine and levamisole, pyrantel (another anthelmintic and agonist of L-type nAChRs); nicotine (agonist of N-type nAChRs) and DMPP were used. The native *C. elegans* receptor was activated preferentially by acetylcholine > levamisole > DMPP > pyrantel with little response to the addition of nicotine. The chimeric receptor produced the same pharmacological response (Figure 5-16).

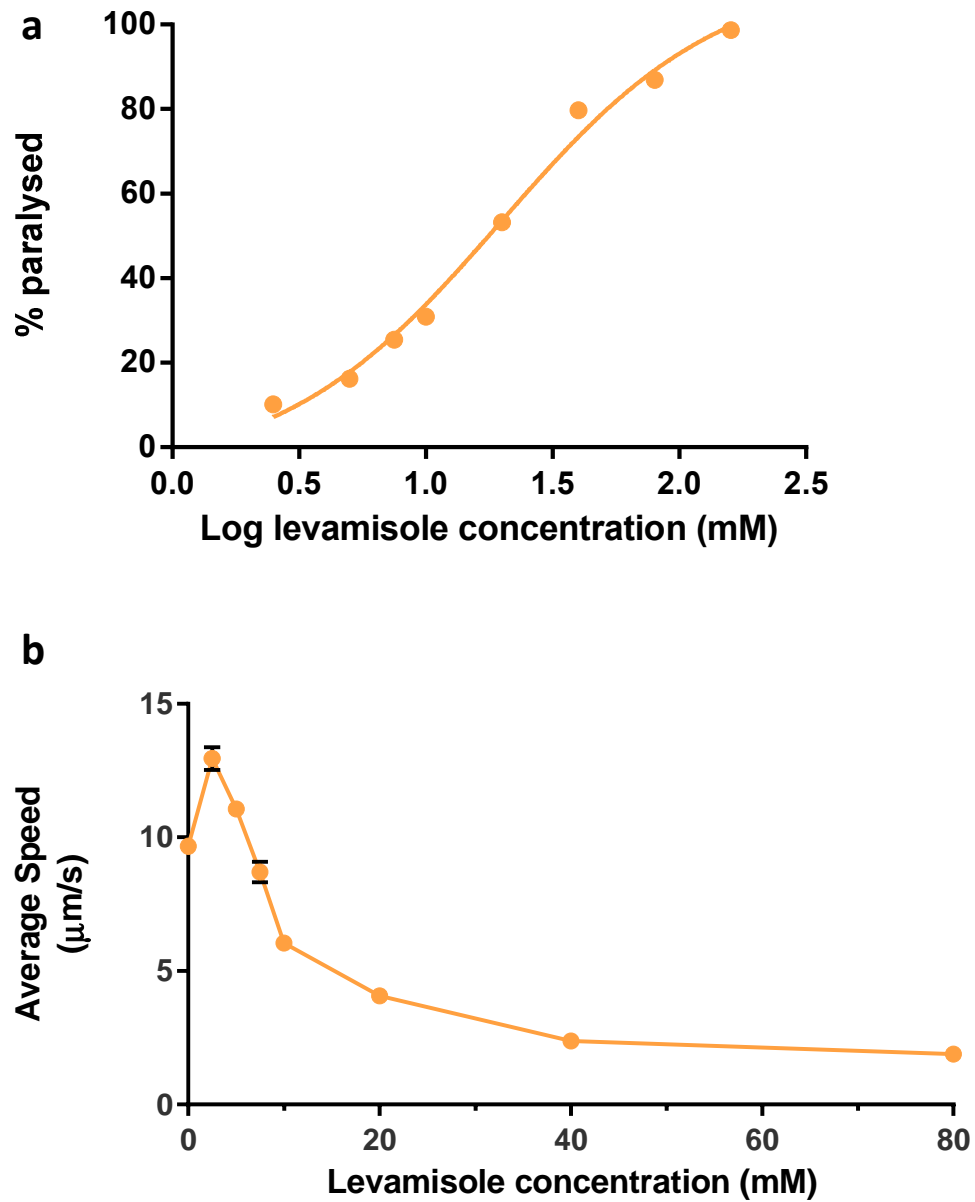


Figure 5-5: Effect of levamisole on *Globodera pallida* J2s

Effect of levamisole on *G. pallida* J2s at a range of levamisole concentrations. a) Percentage of J2s paralysed at each concentration was calculated. The EC₅₀ was determined to be 19.74 mM by log(agonist) vs response (three parameters) calculations. b) Effect of levamisole concentration on average speed of *G. pallida* J2s. One-way ANOVA (Tukey's multiple comparison) showed significance ($p<0.01$) for all comparisons, apart from 7.5 mM vs 0, 20 mM vs 40 mM and 40 mM vs 80 mM. n-values: 0 (1018), 2.5 mM (416), 5 mM (833), 7.5 mM (339), 10 mM (597), 20 mM (206), 40 mM (188), 80 mM (185). Error bars represent SEM.

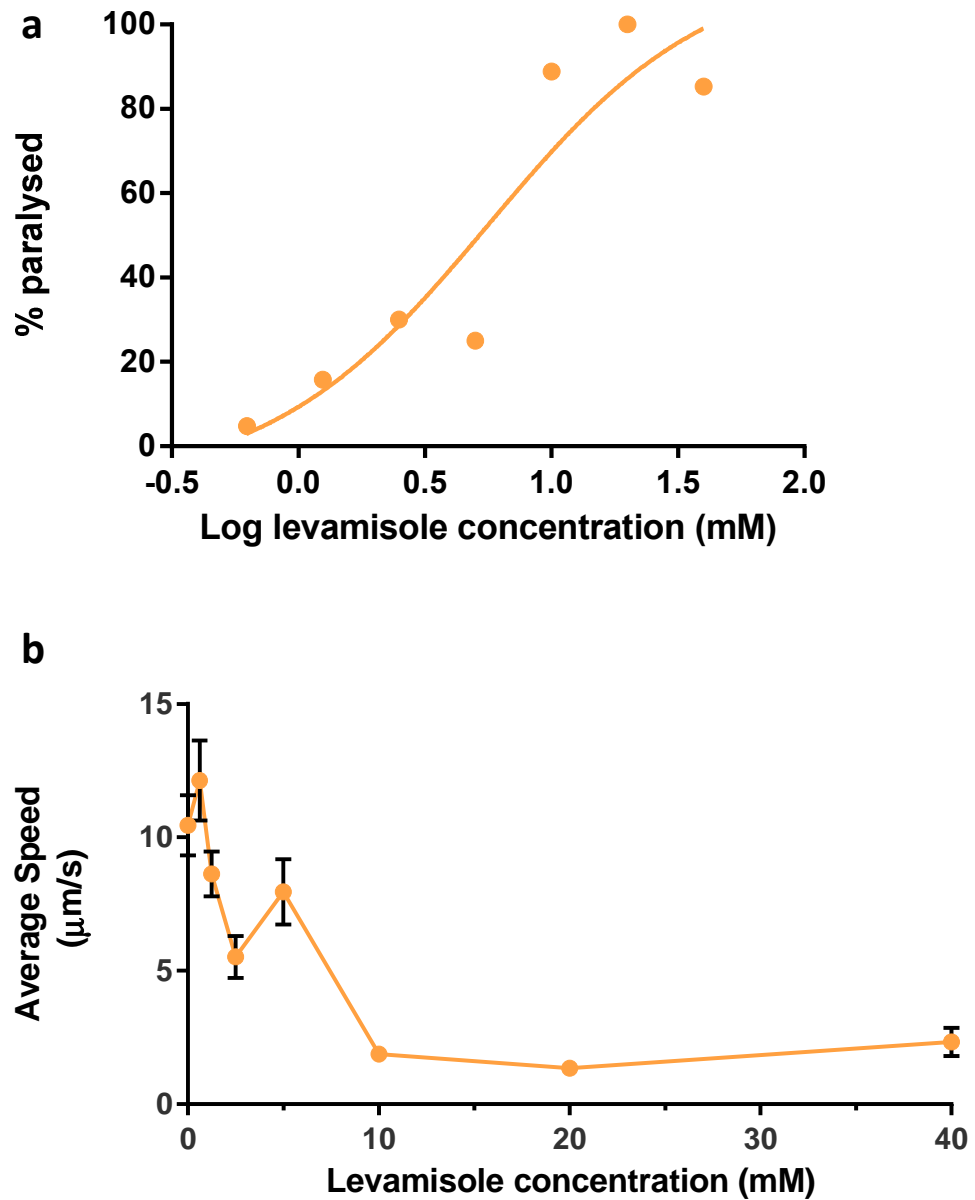


Figure 5-6: Effect of levamisole on *Globodera rostochiensis* J2s

Effect of levamisole on *G. rostochiensis* J2s at a range of levamisole concentrations. a) The percentage of J2s paralysed at each concentration was calculated. The EC₅₀ was determined to be 5.6 mM by log(agonist) vs response (three parameters) calculations. b) Effect of levamisole concentration on average speed of *G. rostochiensis* J2s (One-way ANOVA (Tukey's multiple comparison) showed significance ($p<0.01$) for comparisons: 0 vs 2.5 mM and 0 vs 10, 20, 40 mM. b) The percentage of J2s paralysed at each concentration was calculated. The EC₅₀ was determined to be 5.6 mM by log(agonist) vs response (three parameters) calculations. n-values: 0 (28), 0.625 mM (22), 1.25 mM (39), 2.5 mM (21), 5 mM (29), 10 mM (28), 20 mM (20), 80 mM (35). Error bars represent SEM.

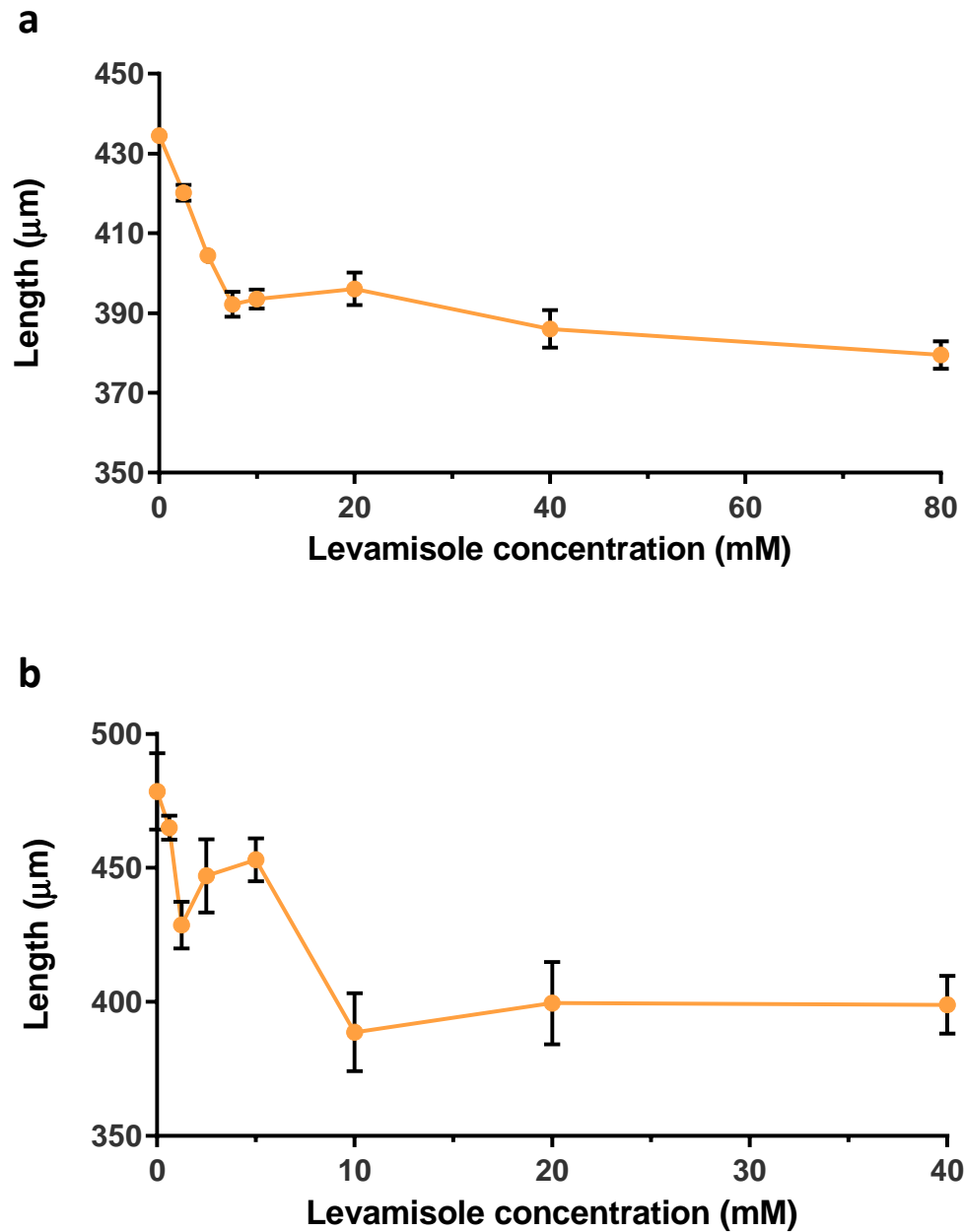


Figure 5-7: Effect of a range of levamisole concentrations on J2 length after 2 hours exposure

a) Length of *G. pallida* J2s after 2 hours exposure to a range of levamisole concentrations. Decrease in length of J2s is significant (One-way ANOVA (Tukey's multiple comparison), $p<0.01$), between 0 mM levamisole and all levamisole concentrations and between 2.5 mM levamisole and all other levamisole concentrations. b) Decrease in length of *G. rostochiensis* J2s (One-way ANOVA (Tukey's multiple comparison, $p<0.05$). Significant decrease in length between 0 mM and 1.25 mM, 10 mM, 20 mM and 40 mM. N-values as described in Figure 5-5 and Figure 5-6. Error bars represent SEM.

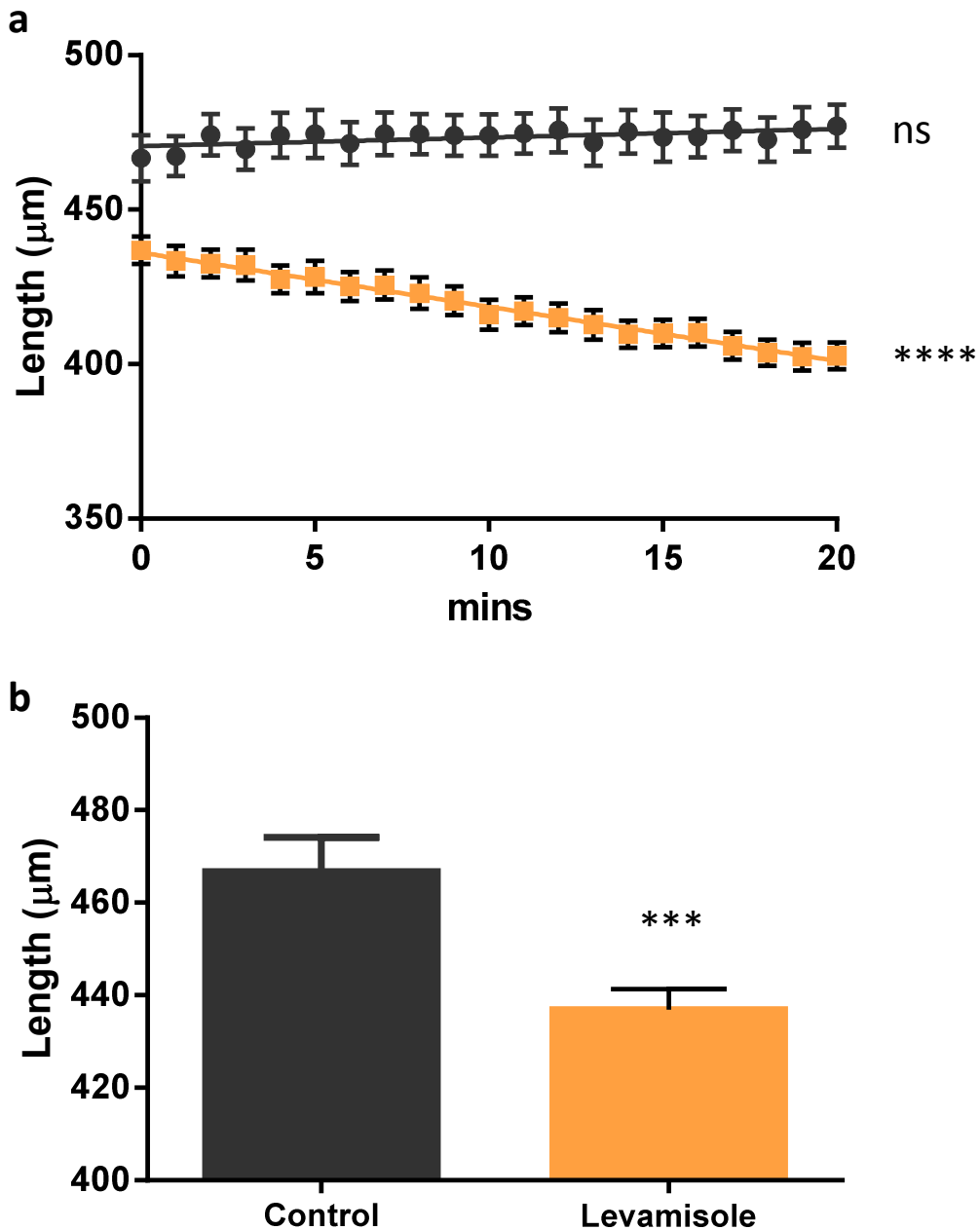


Figure 5-8: Effect of high doses of levamisole on *G. pallida* J2s

a) The effect of 200 mM levamisole on the length of *G. pallida* J2s over 20 minutes. Control worms ($n=21$) did not change in length over 20 minutes (linear regression, $p=0.26$). Levamisole-treated worms decreased in length over 20 minutes (linear regression, $p=<0.0001$). b) The immediate effect of a high dose (200 mM) of levamisole was also investigated as experimental technique resulted in a delay between first exposure of J2 to levamisole and first image capture. Levamisole treated worms ($n=42$) at the first measurement were shorter than control worms (unpaired t-test, $p=<0.001$), indicating an immediate contraction.

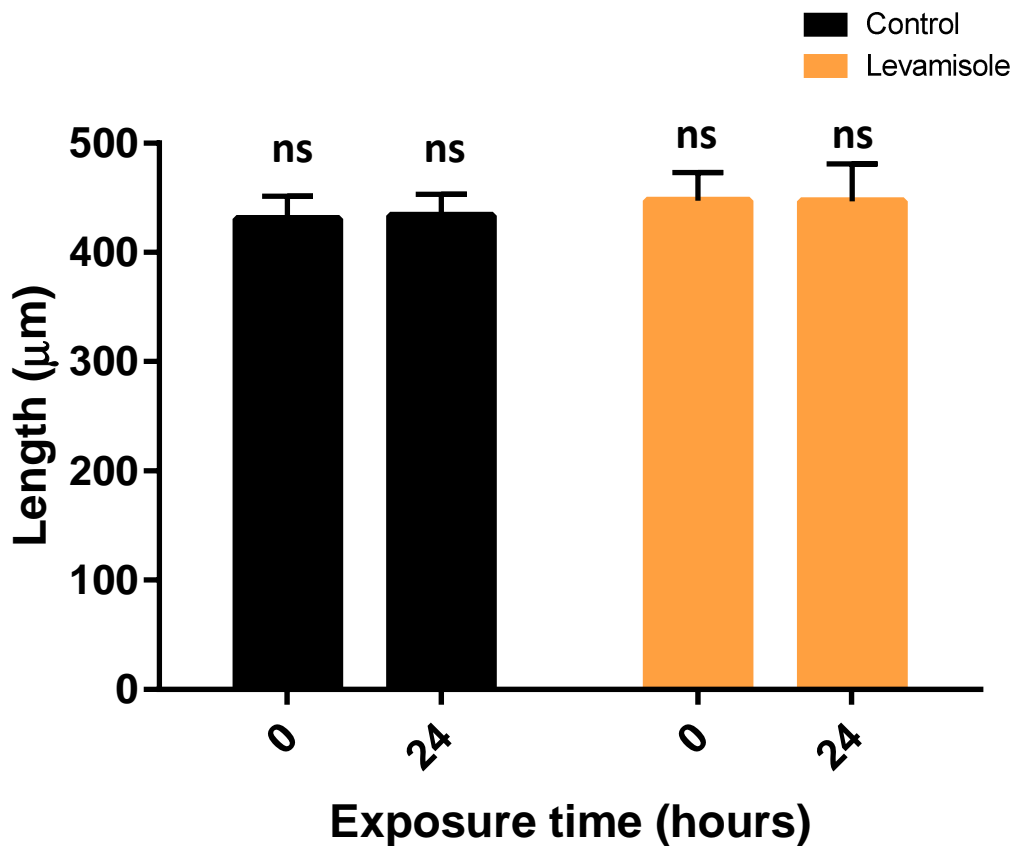


Figure 5-9: Effect of a low dose of levamisole after 24 hour exposure

The effect of a low dose (100 μM levamisole) on *G. pallida* J2s for 24 hours. No significant difference was detected between control worms ($n=19$) between 0 and 24 hours, or between levamisole-treated ($n=20$) worms between 0 and 24 hours. There was also no significant difference between control and levamisole-treated worms at 0 hr, or at 24 hr (2-way ANOVA, Sidak's multiple comparison). Error bars represent SEM.

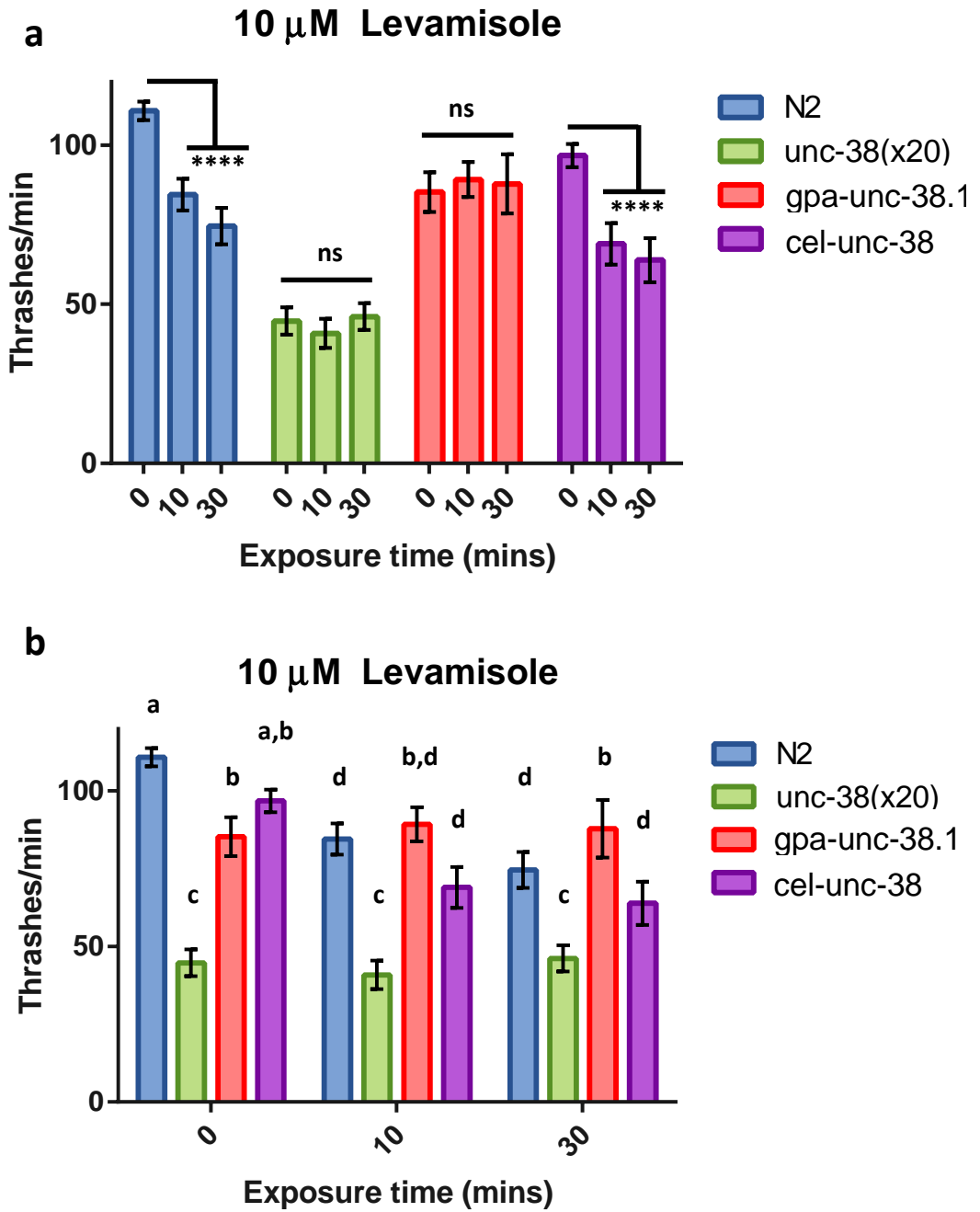


Figure 5-10: Effect of 10 μ M levamisole on thrashing rate of *C. elegans*

a) Thrashing rate of wild-type (N2) worms decreased by approximately 20 % in response to 10 μ M levamisole. *Unc-38(x20)* worms did not change in thrashing rate. Thrashing rate of *Gpa-unc-38.1*-rescued worms did not change. Thrashing rate of *Cel-unc-38*-rescued worms decreased by 20% (Two-way ANOVA, Tukey's multiple comparison test). b) Comparison of thrashing rates of the lines at each time point at 10 μ M. Lowercase letters indicate statistically homogenous subsets (Two-way ANOVA, Tukey's multiple comparison test). Error bars represent SEM.

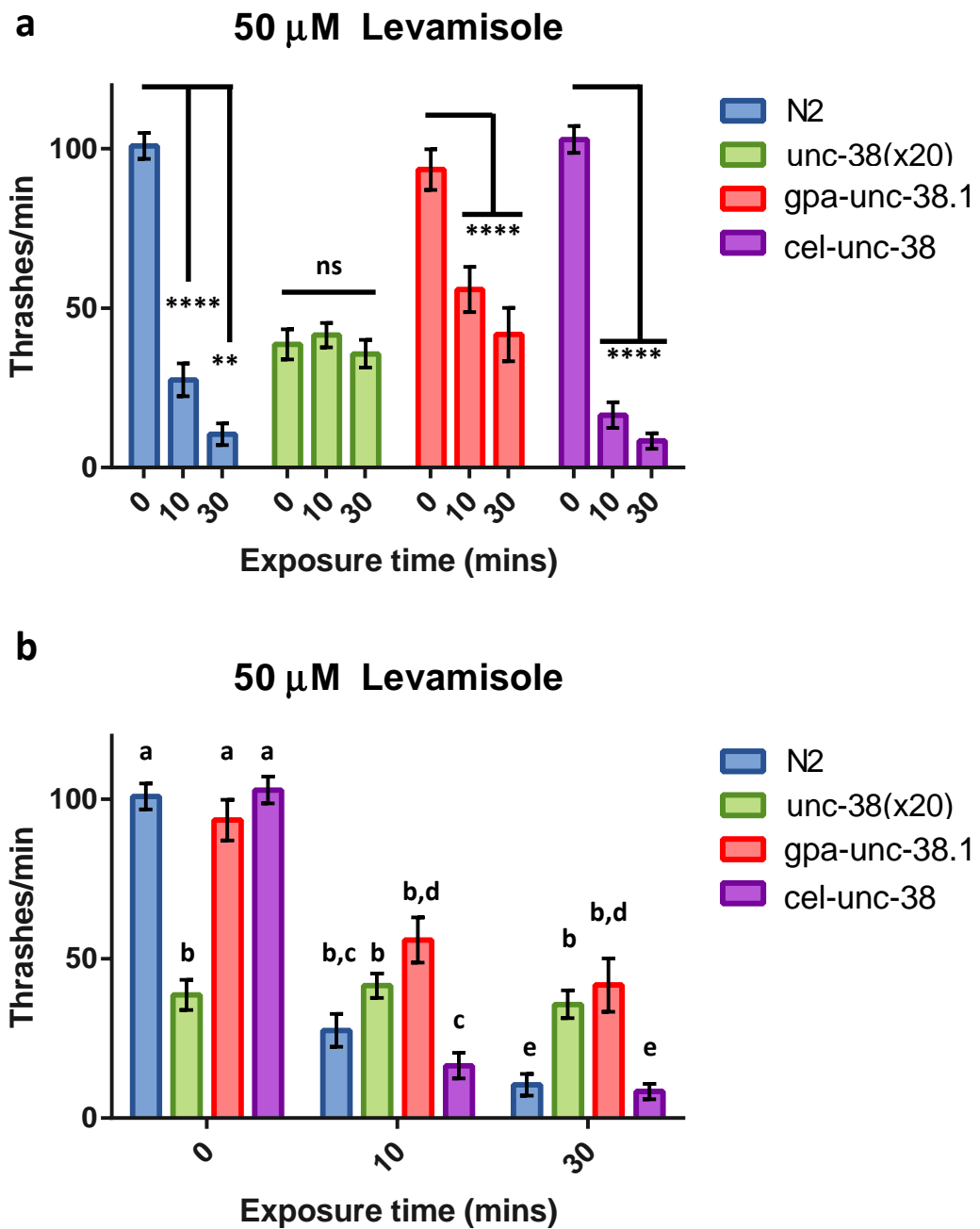


Figure 5-11: Effect of 50 μ M levamisole on thrashing rate of *C. elegans*

a) Thrashing rate of wild-type (N2) worms decreased by around 90% by end of assay. Thrashing rate of *Unc-38(x20)* remained constant throughout assay. Thrashing rate of *Gpa-unc-38.1*-rescued worms reduced by approximately 50% and *Cel-unc-38*-rescued by around 90%. b) Comparison of thrashing rates of the lines at each time point at 50 μ M. Lowercase letters indicate statistically homogenous subsets (Two-way ANOVA, Tukey's multiple comparison test). Error bars represent SEM.

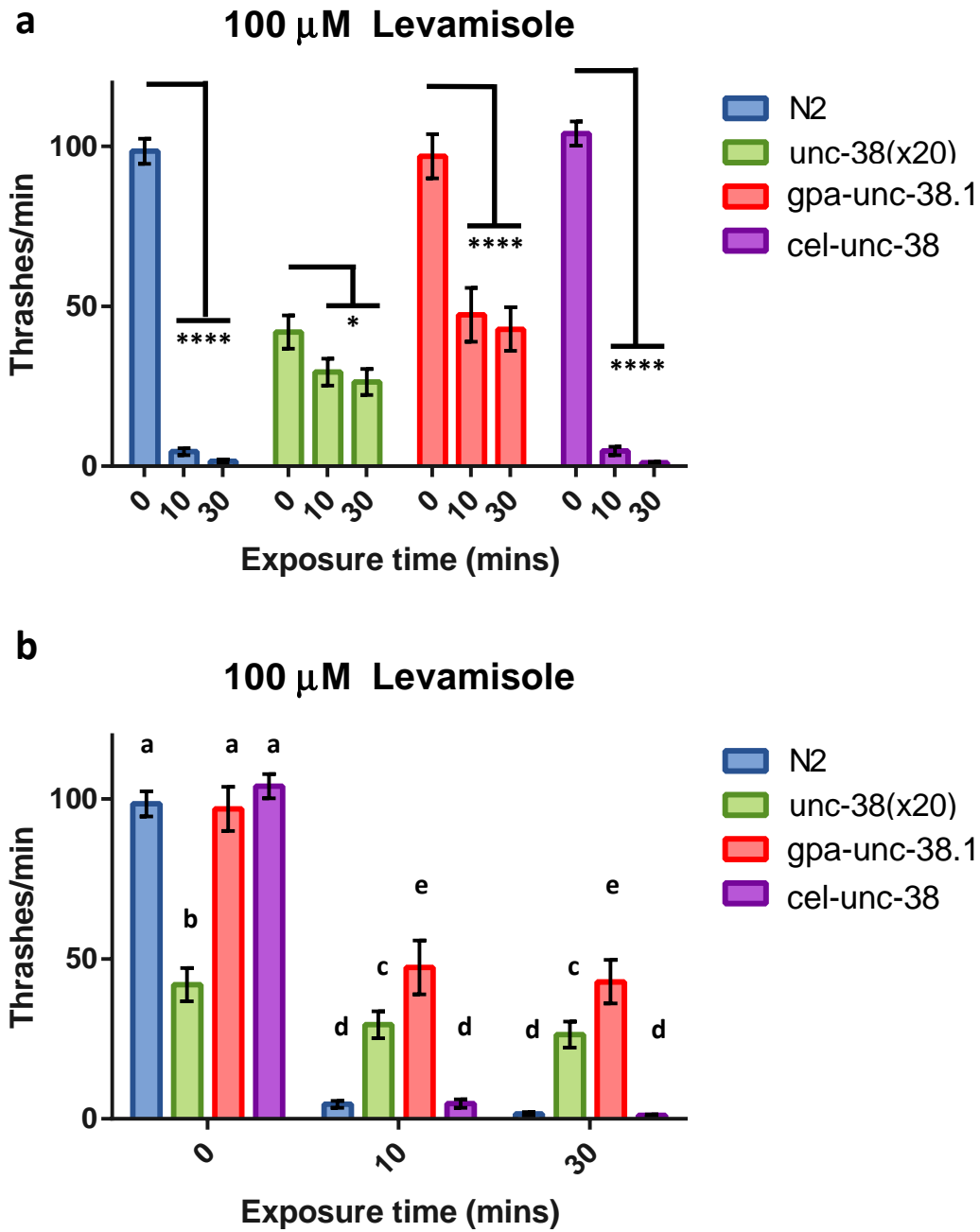


Figure 5-12: Effect of 100 μ M levamisole on thrashing rate of *C. elegans*

a) Thrashing rate of N2 and *cel-unc-38* reduced by approximately 95% by end of assay. At this concentration, *unc-38(x20)* worms reduced their thrashing rate slightly. *Gpa-unc-38.1* worms reduced their thrashing rate by approximately 50%. b) Comparison of thrashing rates of the lines at each time point at 100 μ M. Lowercase letters indicate statistically homogenous subsets (Two-way ANOVA, Tukey's multiple comparison test). Error bars represent SEM.

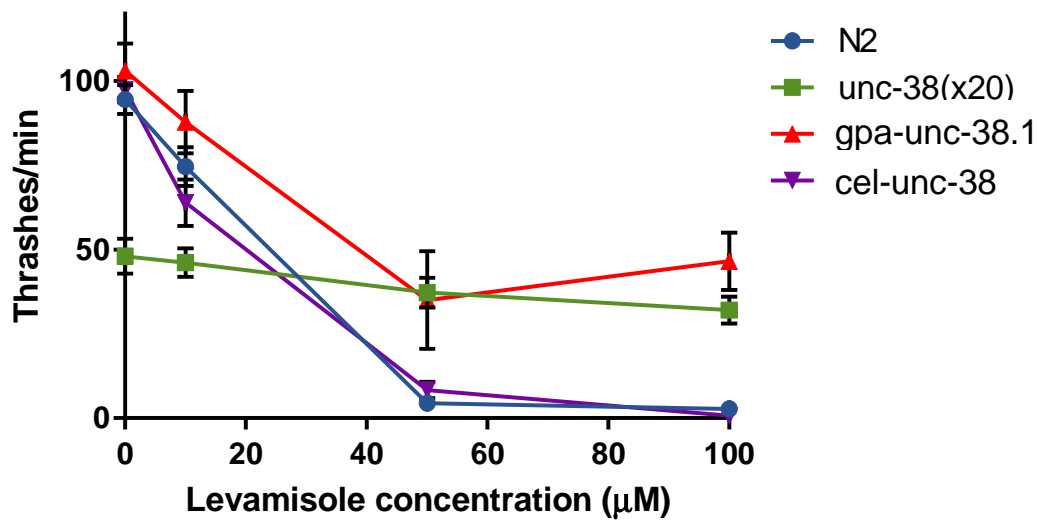


Figure 5-13: Comparison between the lines of thrashing rate after 30 mins exposure to the range of levamisole concentrations

The N2 and *cel-unc-38* thrashing rates decreased by the same amounts in response to increase in levamisole concentration. The slopes of these lines were not significantly different from each other. *Gpa-unc-38.1* had a significantly different slope from N2 and *cel-unc-38*, indicating it is more resistant to levamisole (linear regression). Error bars represent SEM.

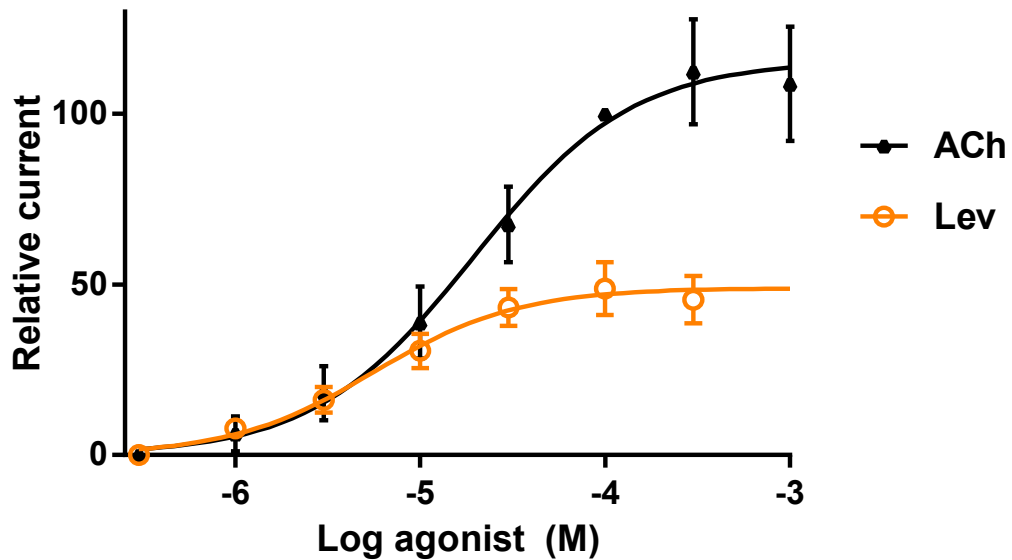
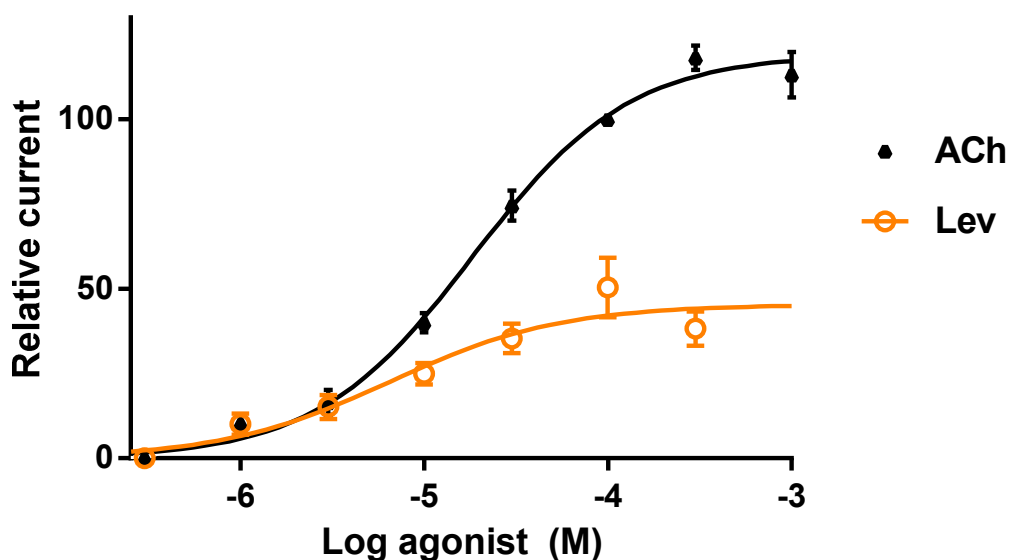
a**b**

Figure 5-14: Dose-response curve for acetylcholine and levamisole on the native and chimeric L-type nAChR receptors

a) Dose response curve for the native *C. elegans* L-type nAChR receptor expressed in *Xenopus* oocytes for acetylcholine (n=9) and levamisole (n=7). The EC₅₀ of acetylcholine is 19.3 µM ± 1.1 and of levamisole is 5.7 µM ± 1.2. b) Dose-response for the chimeric-type nAChR receptor for acetylcholine (n=7) and levamisole (n=7). The EC₅₀ of acetylcholine is 18.4 µM ± 1.1 and of levamisole is 6.6 µM ± 1.5. Current is expressed as relative current, normalised to the current elicited by 100 µM acetylcholine. Error bars represent SEM.

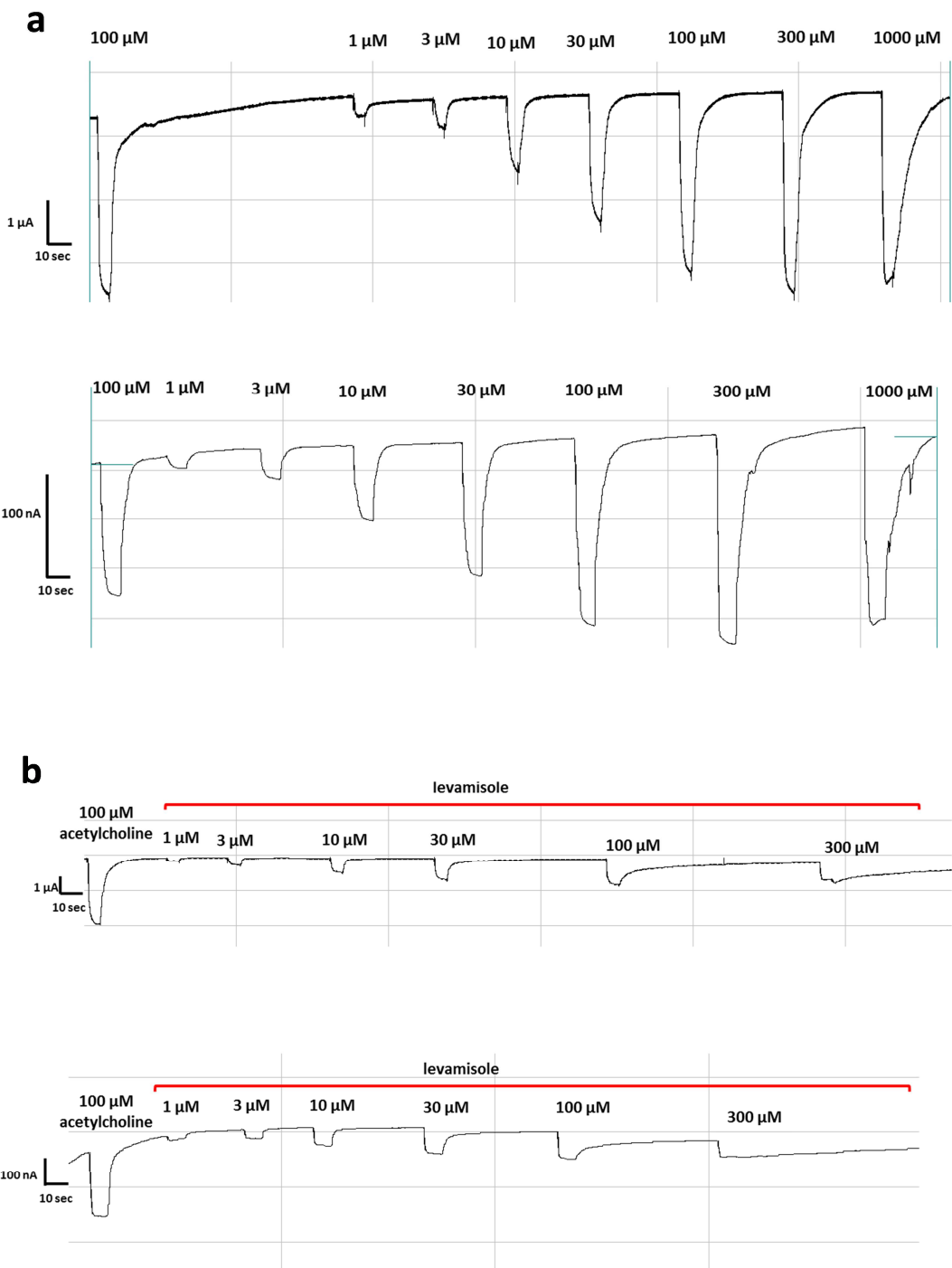
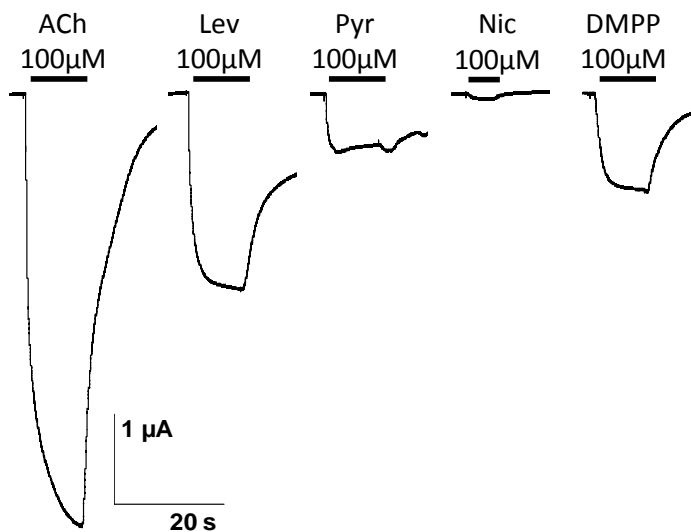


Figure 5-15: Examples of current recordings for the full range of concentrations of acetylcholine and levamisole for the native and chimeric L-type nAChR expressed in *Xenopus* oocytes

Representative recordings of the current in response to a) acetylcholine for the native (top) and chimeric (bottom) receptor and b) levamisole for the native (top) and chimeric (bottom) receptor.

a Native *C. elegans* receptor



Chimeric receptor

b

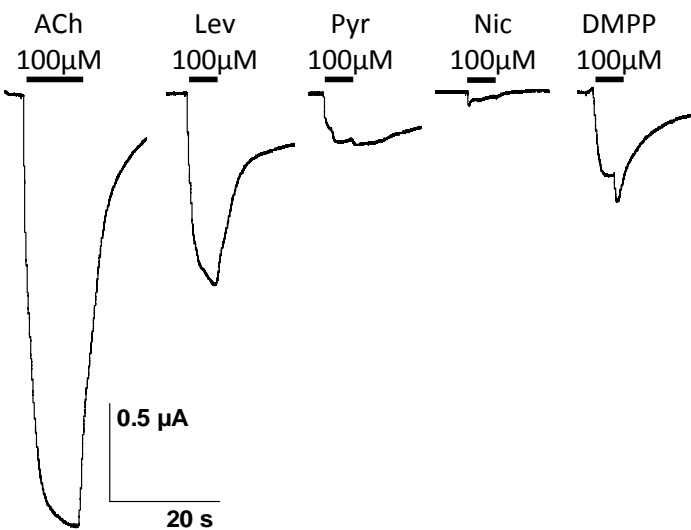


Figure 5-16: Response of the native and chimeric L-type nAChR in response to a panel of nicotinic acetylcholine receptor agonists

Response of a) the native *C. elegans* and b) chimeric L-type nAChR receptor to a panel of nicotinic acetylcholine receptor agonists; acetylcholine, levamisole, pyrantel, nicotine and DMPP. Both are most strongly activated by acetylcholine, then levamisole, then DMPP and then pyrantel. Neither is activated by nicotine.

5.4 Discussion

5.4.1 *G. pallida* and *G. rostochiensis* J2s are more resistant to levamisole than *C. elegans*.

G. pallida and *G. rostochiensis* J2s were observed to be more resistant than *C. elegans* to levamisole. As J2s of plant-parasitic nematodes typically move more slowly than *C. elegans*, a video-capture method was used to assess average speed after 2 hours of exposure to a range of levamisole concentrations. This allowed the speed of the worm to be calculated over a 2 min time period, and allowed high throughput sampling of the speed of many worms as 20-30 worms could be captured per video. This demonstrated that *G. pallida* and *G. rostochiensis* J2s retain their speed at relatively high doses of levamisole compared to *C. elegans*. There is even some evidence that suggests a mild stimulatory action of levamisole as, compared to the control, there is an increase in the average speed of *G. pallida* J2s (at 2.5 mM levamisole exposure) and *G. rostochiensis* J2s (0.625 mM levamisole exposure). The EC₅₀ of paralysis in response to levamisole (19.74 mM for *G. pallida* and 5.6 mM for *G. rostochiensis*) was calculated to be higher than that of *C. elegans* (9 µM (Qian *et al.* 2008)).

It was reasoned that this increased resistance to levamisole may be due to physical barriers of levamisole entering the worm, molecular differences of the levamisole receptors of *G. pallida* and *G. rostochiensis* or a combination of factors. In *C. elegans*, the cuticle is known to partially impede the entry of levamisole as cut nematodes are more sensitive to levamisole than intact nematodes (Lewis *et al.* 1980). Shrinkage experiments of *G. pallida* J2s in response to high doses of levamisole indicated that the cuticle is likely to be permeable to levamisole as the J2s shrink in response. However, the receptor itself is not activated by low doses as exposure for 24 hours to 100 µM levamisole does not induce any change in length. As *C. elegans* shrinks rapidly (within 30 secs) in response to a levamisole concentration approximately 10x the EC₅₀ (100 µM) (Mulcahy, Holden-Dye and O'Connor 2013), it was reasoned that *G. pallida* J2s would also shrink rapidly in response to exposure to a concentration of levamisole 10x the EC₅₀ (200 mM) if their cuticle was also permeable. *G. pallida* J2s did shrink rapidly in response to a high dose of levamisole, although the length of the worm steadily decreased during the 20 minute duration of the assay. To identify whether low exposures of levamisole would diffuse across the cuticle slowly, and be able to induce shrinkage after a long period of exposure, J2s were exposed to low doses of levamisole for 24 hours. After this time, no significant change was found between levamisole treated worms and control treated worms, indicating that the nAChR that is the target of levamisole is likely to provide the main mechanism of increased resistance in *G. pallida* and *G. rostochiensis*.

5.4.2 Analysis of *gpa-unc-38.1*-rescued *C. elegans* line suggests *gpa-unc-38.1* is likely to play a role in this increased resistance

Previous analysis of the amino acid sequence of *gpa-unc-38.1* had highlighted key amino acid differences between the *G. pallida* orthologue and the *C. elegans* sequence. In particular, the YxxCC motif present in Loop C involved in acetylcholine binding (Kao *et al.* 1984) and a glutamate residue linked to levamisole sensitivity (Rayes *et al.* 2004) were absent in the *G. pallida* sequence. Additionally, a residue in transmembrane domain 2 was identified as having potential involvement in affecting channel opening properties and levamisole sensitivity (Jospin *et al.* 2009).

Unc-38(x20) worms lack a functional *unc-38* gene due to the absence of the third exon caused by a mutation in the splice acceptor site (Fleming *et al.* 1997). Absence of the UNC-38 subunit prevents assembly of the receptor, leading to the absence of the L-type nAChR receptor in the body-wall muscle (Boulin *et al.* 2008). In thrashing assays, the phenotype of this can be observed as a reduction of roughly 50% in the thrashing rate in liquid compared to wild-type and increased resistance to levamisole. N-type nAChR receptors in the body wall muscle (Touroutine *et al.* 2005; Richmond and Jorgensen 1999) that are unaffected by the absence of *unc-38* account for the residual movement of the *unc-38(x20)* worms.

It was demonstrated by analysis of the transgenic lines, that *gpa-unc-38.1* is able to rescue basal thrashing, but not levamisole sensitivity of *C. elegans unc-38(x20)* mutants. As both basal thrashing and levamisole sensitivity were fully restored in *cel-unc-38*-rescued lines, this difference in levamisole sensitivity observed in the *gpa-unc-38.1*-rescued lines is unlikely to be a side effect of the microinjection technique used to produce the lines. Although data for one line of *gpa-unc-38.1* is shown in this chapter, two lines were also created and analysed for *gpa-unc-38.1*, which both demonstrated the same behaviour. As the basal thrashing rate of *unc-38(x20)* worms is rescued by transformation with *gpa-unc-38.1*, it can be assumed that *gpa-unc-38.1* is able to assemble with the four remaining L-nAChR *C. elegans* subunits and produce a functional receptor which is able to bind acetylcholine.

There are two possible hypotheses for why *gpa-unc-38.1* is able to rescue the binding of acetylcholine, despite lacking the vicinal cysteines that define *cel-unc-38* as an α -subunit. Firstly, *gpa-unc-38.1* may bind acetylcholine directly. As discussed in previous chapters, this goes against several lines of evidence regarding the role of the vicinal cysteines in α -type subunits. Mutagenesis of the vicinal cysteines has demonstrated that they are essential, and other residues in Loop C are also involved in binding acetylcholine (Mishina *et al.* 1985; Tomaselli *et al.* 1991). As these important residues are absent in *gpa-unc-38.1* it is surprising that this subunit is able to rescue the basal thrashing rate of *unc-38(x20)* mutants. However, an explanation may be sought from the contribution of the other subunits in the receptor to acetylcholine

binding. As discussed in Chapter 4, there are two proposed conformations of the L-type nAChR (Figure 5-17). In one, there are two postulated acetylcholine binding sites situated between the positive face of UNC-63 and the negative face of UNC-29, and another between the positive face of UNC-38 and the negative face of LEV-1. Two non-consecutive binding sites for acetylcholine are sufficient for efficient opening of the channel, while a single binding site only provides transient opening currents (Rayes *et al.* 2009). As this conformation of the L-type nAChR has only two binding sites, one of which would be disturbed by the substitution of *gpa-unc-38.1*, this is unlikely to be the conformation of the receptor. In the second possible conformation of the receptor, there are three postulated acetylcholine binding sites, one between the positive face of LEV-8 and UNC-29, one between the positive face of UNC-38 and the negative face of UNC-63 and one between the positive face of UNC-63 and LEV-1. Substitution of *gpa-unc-38.1* would disrupt the agonist binding site between UNC-38 and UNC-63, but the others should remain intact providing a sufficient number of non-consecutive binding sites between subunits. This model of native conformation of the *C. elegans* receptor, and the effect of substituting Gpa-UNC-38.1 may explain the ability of Gpa-UNC-38.1 to rescue the thrashing activity, and thus acetylcholine binding activity of the *unc-38(x20)* mutants despite lacking the key motifs involved in acetylcholine binding. This could also still account for the observation that levamisole sensitivity is not fully restored to the *gpa-unc-38.1* rescued *unc-38(x20)* mutants as Gpa-UNC-38.1 has assembled with the receptor, but does not contain the glutamate at position 153 associated with levamisole sensitivity (Rayes *et al.* 2004).

5.4.3 Expression of *gpa-unc-38.1* to replace *cel-unc-38* in *Xenopus* oocytes does not support a difference in levamisole binding for *gpa-unc-38.1*

The expression of chimeric receptors to examine properties of particular subunits is done routinely in the studies on insect nicotinic acetylcholine receptors. The nAChRs of insects, for reasons that are not well understood, have been difficult to express in *Xenopus* oocytes. Chimeric genes based on vertebrate subunits in which loops from insect nAChRs have been substituted have been used to investigate neonicotinoid sensitivity (Shimomura *et al.* 2005). Commonly, α -subunits from insects required the expression of β -vertebrate subunits alongside them in order to yield functional receptors (Ballivet *et al.* 1996; Huang *et al.* 1999; Bertrand *et al.* 1994). In this work, a similar chimeric approach has been taken to investigate the Gpa-UNC-38.1 subunit.

The expression of *gpa-unc-38.1* with the remaining *C. elegans* subunits (*unc-29*, *unc-63*, *lev-1* and *lev-8*) and the required ancillary factors (*ric-3*, *unc-50* and *unc-74* from *H. contortus*) was able to yield a functional receptor in *Xenopus* oocytes. However, the dose-response curve for both acetylcholine and levamisole was determined to be very similar between the chimeric receptor (with *gpa-unc-38.1*) and the native receptor (with *cel-unc-38*). Both the chimeric and native receptors also

shared a similar pharmacological response to a panel of nicotinic acetylcholine receptor agonists. This evidence suggests that there is no difference in the acetylcholine binding activity of the chimeric channel compared to the native channel. This is in agreement with the data obtained from the rescue lines, where *gpa-unc-38.1* is able to rescue *unc-38(x20)* mutant perhaps due to the location of the other agonist binding sites on the receptor, which are unaffected by the presence of *gpa-unc-38.1* or *cel-unc-38*.

However, the observation that the EC₅₀ for levamisole does not change between the native and chimeric receptor is more surprising, and appears to be contradictory to the results obtained from the rescue lines. In theory, the chimeric receptor expressed in *Xenopus* oocytes should be a reconstitution of the receptor in the *gpa-unc-38.1* rescued line and should behave in the same manner. Other factors such as a side-effect of the *unc-38(x20)* background of the mutant worm can be discounted, as *cel-unc-38* was able to rescue the levamisole sensitivity of the *unc-38(x20)* worms. Additionally, the effects of varying copy number of the heterologously expressed gene has been diminished as two separate lines for both *cel-unc-38* and *gpa-unc-38.1*-rescued lines were created, which yielded consistent results (Anna Crisford, personal communication). It is also contrary to previous studies which identify *cel-unc-38* and the glutamate at position 153 in loop B as involved in levamisole sensitivity (Rayes *et al.* 2004; Martin and Robertson 2007). It is difficult to reconcile the mismatch between the levamisole sensitivity of the rescued lines and the reported levamisole sensitivity from the *Xenopus* oocyte work.

One explanation may be that Gpa-UNC-38.1 was unable to assemble with the remaining *C. elegans* subunits, and that the recordings obtained for the chimeric receptor were actually the recordings for a receptor comprising only of the four subunits, *cel-unc-29*, *cel-unc-63*, *cel-lev-1* and *cel-lev-8*. Several lines of evidence argue against this as a possibility. In Boulin *et al.* (2008), 8 genes (five subunits and 3 ancillary factors) were required for robust expression of the L-type nAChR in *Xenopus* oocytes. Omission of any of the five subunits resulted in channel recordings that were 97% lower than that of the complete receptor. A similar reduction in channel opening is observed when *hco-unc-38* is omitted from the injected cRNAs to produce functional L-type nAChRs of *H. contortus* (Boulin *et al.* 2011). Functional receptors have been produced with only *unc-29*, *lev-1*, and *unc-38*, however the currents obtained for these in response to levamisole and acetylcholine are very low (~5nA) (Fleming *et al.* 1997). Additionally, the pharmacology of the chimeric and native receptor are very similar to each other (acetylcholine > Lev > DMPP, Pyr > Nic). The pharmacology of the three-subunit receptor produced by Fleming *et al.* (1997) is very different from this (Lev > acetylcholine > DMPP), and it might be expected, if only a four subunit-type receptor were produced in the chimeric receptor experiment, the pharmacology of that receptor would be different.

The role of the ancillary factors used in this experiment may be of consideration. RIC-3, UNC-50 and UNC-74 have been identified as essential for robust expression of both the *C. elegans* L-type nAChR (Boulin *et al.* 2008) and the *H. contortus* L-type nAChR (Boulin *et al.* 2011). RIC-3 has been shown to affect the arrangement and stoichiometry of some receptors. For example, for the DEG-2/DEG-3 type receptor, the presence of RIC-3 increases the number of DEG-3 subunits in the receptor (Ben-Ami *et al.* 2005). It is possible, that use of the ancillary factors from *H. contortus* rather than from *C. elegans* affects receptor stoichiometry due to the different affinities RIC-3 from both species may have. This may lead to a different arrangement of subunits being expressed in the *gpa-unc-38.1*-rescued *unc-38(x20)* lines compared to the arrangement in the heterologous expressed chimeric receptor, which may have an impact on how and where levamisole binds. However, this hypothesis does not account for the reported importance of the glutamate at position 153 in Loop B of Cel-UNC-38.

Contrary to expectations, a difference in the EC₅₀ values obtained for levamisole between the native *C. elegans* receptor and the chimeric receptor that contains *gpa-unc-38.1* was not identified. However, the ability of *gpa-unc-38.1* to rescue the thrashing rate of the *unc-38(x20)* worms despite lacking key motifs involved in acetylcholine binding, but not levamisole sensitivity is consistent in different transgenic lines. These contradictory results from two different experiments cannot yet be reconciled. Although acetylcholine-binding rescue may be a matter of *gpa-unc-38.1* filling a purely structural role, its role in levamisole resistance in *G. pallida* J2s is still unclear.

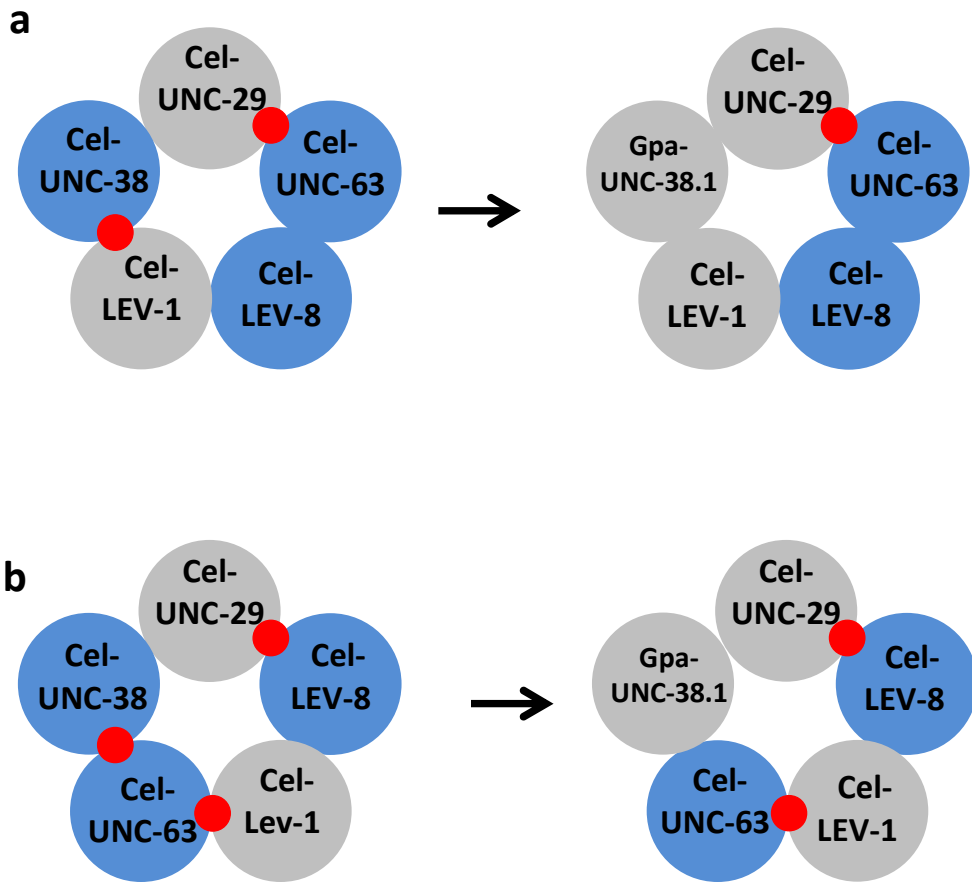


Figure 5-17: Potential changes caused in acetylcholine binding sites on the L-type nAChR caused by substituting Gpa-UNC-38.1 on different conformations of the native *C. elegans* receptor

a) Schematics of one possible conformation of the native L-type nAChR and the possible effect on acetylcholine binding sites of substitution of Gpa-UNC-38.1. In the original conformation, only two canonical acetylcholine binding sites are present. This is reduced to one if Gpa-UNC-38.1 is substituted in place of Cel-UNC-38. b) Another possible conformation of native L-type nAChR. Three acetylcholine binding sites are present in this conformation. On substitution of Gpa-UNC-38.1, two are present. Potential agonist binding sites are represented with a red circle, α -subunits are coloured in blue and non- α are coloured in grey.

Summary

- *G. pallida* and *G. rostochiensis* are less sensitive to levamisole than *C. elegans*
- This resistance may be due to the differences in the composition of the L-nAChR and key differences in the amino acid sequence of Gpa-UNC-38.1
- Rescue of *unc-38(x20)* mutants with *gpa-unc-38.1* restores basal thrashing activity but not full sensitivity to levamisole
- *Gpa-unc-38.1* can be used to replace *cel-unc-38* to produce a functional receptor in *Xenopus* oocytes, but no difference in current induced by levamisole was observed

6. Investigation into the significance of key amino acid motif differences between Cel-UNC-38 and Gpa-UNC-38.1

6.1 Introduction

The use of chimeric genes can facilitate the understanding about which key amino acid motifs affect aspects of protein function. As discussed in the Introduction, transformation techniques have not been developed for plant-parasitic nematodes and *C. elegans* has been used as a heterologous expression system to characterise the role of genes from parasitic nematodes.

6.1.1 Transformation of *C. elegans* by microinjection

Transformation by microinjection is a well-established technique in *C. elegans* and may be used to investigate the role of genes by mutant rescue, the down-regulation of genes by RNAi, gene expression patterns via promoter-reporter constructs and sub-cellular localisation of GFP-tagged proteins.

DNA is injected into the gonads of young adult hermaphrodites. The two gonads of *C. elegans* are U-shaped structures, connected in the centre at the vulva. Oocytes within the gonad follow a continuum of development. Nuclei are individually enveloped by plasma membrane, and line up along the proximal arm of the gonad. Each oocyte enters the spermatheca, located near the vulva, and is fertilised. Developed mature eggs are situated at the vulva ready for egg-laying and mitotic cells are present towards the distal ends of the gonad. DNA is injected into the cytoplasmic core of the distal germ line where developing germ nuclei arrested in meiosis I are abundant. As *C. elegans* is transparent, the needle can be inserted into the correct position and the injection of liquid into the gonad can be easily observed by a visible swelling of the organ. Injection in this location allows many nuclei to be bathed in the injection mixture (Stinchcomb *et al.* 1985).

6.1.2 Fate of DNA introduced by microinjection

The fate of DNA introduced into the gonad of *C. elegans* is not well characterised. The injected DNA is expressed in the F1 generation following microinjection (generally 20-50 transgenic individuals are obtained), but mosaic expression is typically observed. In some members of the F1 generation, the injected DNA becomes the target of recombination reactions which assemble it into large extra chromosomal arrays. Most transformants obtained at the F1 generation will not transmit the transgene to the F2 generation (Mello and Fire 1995). The concentration of DNA injected influences the likelihood of large, stable extrachromosomal arrays forming. Total concentrations lower than 50 ng/ μ l are less likely to form stable arrays. Arrays that assemble to a size

of over 700 kb become heritable (Mello *et al.* 1991). It has been estimated that a transformed cell contains between 70-300 plasmid copies comprising multiple copies of both marker plasmid and transgene plasmid (Stinchcomb *et al.* 1985). The structure of the extrachromosomal arrays is found to be very different between independently transformed lines, even if obtained from the same microinjected adult. This leads to considerable variation in the copy number of the introduced transgene between independent lines. However, within the same transformed line the structure of the arrays appears to be stable (Stinchcomb *et al.* 1985). For this reason, it is preferable to generate multiple independently transformed lines in order to determine any effect due to variation in copy number. Even in stably transformed lines, the inheritance of the extrachromosomal arrays is non-Mendelian. A transformed adult does not pass the extrachromosomal array to 100% of its progeny. The percentage of transmission may vary from 10 to 90% of the progeny that inherit the extrachromosomal array.

Extrachromosomal arrays very rarely integrate into the genome, although integration can be induced by mutagenesis. Techniques use a mutagenic agent (EMS, X-ray, gamma-ray) to induce chromosomal breaks. Subsequent screening for transformed lines with 100% transmission rate of the transgenic marker selects for integration of the extrachromosomal array into the genome (Mello and Fire 1995).

As a transgene is often introduced under the control of a promoter on the introduced vector, it is possible that this promoter does not fully mimic the endogenous expression of the gene. This, along with the copy number issue, must also be considered when drawing conclusions from a microinjection experiment.

6.1.3 Choice of marker gene

The marker gene allows selection of transformants. It should enable easy identification of transformants, but not interfere with any further experimental work.

The *rol-6* gene encodes a collagen gene. *Rol-6* is a popular marker due to its easy identification under 5x magnification. In L2-stage worms and later, this marker is observed as a right-handed rolling phenotype. *Unc-22* antisense DNA is a marker which interferes with normal expression of *UNC-22* (a muscle filament protein). Transformed worms have low mobility and a twitching phenotype. *Pha-1(+)* encodes a bZip-like transcription factor. This marker requires the injection of *pha-1* (*e2123ts*) mutant animals which are embryonic lethal at 25°C. The *Pha-1(+)* marker rescues this phenotype allowing transformants to be selected by survival of progeny at 25 °C. Readily visible expression of GFP under the control of a different promoter is also commonly used as a transformation marker. Currently available constructs include *unc-119::GFP* (expressed in neurones), *g/r-1::GFP* (expressed in interneurons) (Hope 1999) and *pmyo-2::GFP* (expressed in pharyngeal muscle) (Gonzalez-Serricchio and Sternberg 2006).

The appropriate marker gene depends on experimental design. Any experiment which requires analysis of locomotion in transformants would not favour a marker gene that affects normal locomotion behaviour (e.g. *rol-6* and *unc-22* antisense DNA). Mutant rescue experiments which require a particular mutant background line to be injected would also not favour a marker gene which requires a particular host strain (e.g. *pha-1*). The use of a GFP reporter construct as a selection marker requires a fluorescence microscope for selection of initial transformants and maintenance of the transformed line.

6.1.4 The use of *C. elegans* to analyse *cel-unc-38* and *gpa-unc-38.1* chimeric genes

In order to investigate the significance of the key amino acid differences between Cel-UNC-38 and Gpa-UNC-38.1, chimeric genes were generated in which these residues were swapped. The rationale behind the selection of these changes is discussed in 4.4.2.5. The chimeric genes were transformed into *C. elegans* (background: *unc-38(x20)*) and the effect of the key amino acid swaps on the ability to restore levamisole sensitivity and the ability to restore basal thrashing was analysed. In this experiment, *pmyo-2::GFP* has been selected as the marker gene as it does not interfere with locomotion and is only expressed in pharyngeal muscle limiting interaction with body-wall muscle.

Aims

- Explore key amino acid residues that may account for difference in levamisole sensitivity between Cel-UNC-38 and Gpa-UNC-38.1
- Investigate the effect of the absence of the YxxCC motif in Gpa-UNC-38.1

6.2 Materials and methods

6.2.1 Production of chimeric *unc-38* coding sequences by Spliced Overlap Extension

Chimeric genes were produced incorporating sequences from *cel-unc-38* and *gpa-unc-38.1* (Figure 6-1). A two-step process was used to produce chimeric coding regions of *unc-38* with altered sequences. Each coding region was first amplified in two halves by primers designed to introduce the desired sequence change and provide an overhang complementary to the other half of the gene. Products were amplified from *G. pallida unc-38.1* cDNA clone in the pCR™8/GW/TOPO® vector or *C. elegans unc-38* cDNA clone in the pCR™8/GW/TOPO® vector, using Platinum Taq High Fidelity (Invitrogen, UK). The thermocycling program was conducted on a Biorad T100 thermocycler and comprised an initial denaturing step at 94°C for 2 min, 30 steps of denaturing at 94°C for 30 secs, 55°C annealing for 30 secs and an extension at 68°C for 1.5 min (1 min/kb of amplified product). The two products were then isolated by gel extraction and 5 µl of each amplified fragment was mixed. A second reaction amplified the complete coding region with the altered sequence as the overlapping products allowed extension across the whole gene. A schematic of this process can be seen in Figure 6-2. Primers used can be found in Table 8. An example of the products of this process as seen on an agarose gel is shown in Figure 6-3. Each full-length chimeric coding region was cloned into the pCR™8/GW/TOPO® vector to form an entry clone as in 3.2.14. Clones were sequenced to ensure that the desired changes had been made, and that no errors had been introduced elsewhere in the sequence.

The constructs produced will be referred to by the following nomenclature for the rest of the chapter:

Gpa-unc-38.1-H236_I234delinsNYPSCCPGSA

Cel-unc-38-N234_I242delinsHFFASKNGI

Gpa-unc-38.1-Y175_G178delinsFSEN

Cel-unc-38-F174_N177delinsYPSG

Gpa-unc-38.1-M302I

Cel-unc-38-I301M

6.2.2 Generation and transformation of constructs

Gateway® cloning was used to transfer each chimeric gene produced in 6.2.1 to the pDEST-myo3 destination vector (obtained from Anna Crisford, University of Southampton). The vector contains the promoter region for the *myo-3* gene and drives expression in body wall muscle (Okkema et al. 1993). Recombination sites downstream of the promoter region (attR1 and attL1) allow genes from compatible Entry Clones to

be inserted into the vector (Figure 1.5). The destination vector itself was propagated by selection on ampicillin/chloramphenicol plates in One Shot® ccdB Survival™ 2 T1R Competent cells (Invitrogen, UK). After recombination with an Entry Clone to produce an Expression vector, the ccdB gene is excised and the Expression vector may be propagated in standard competent cells.

100 ng of the Entry clone was added to 150 ng of pDEST-myo3 and TE buffer (pH 8) to a final volume of 8 µl. 2 µl of thawed LR Clonase™ (Invitrogen, UK) was added to the mixture. The reaction was incubated at 25 °C for 1 hr. 1 µl of Proteinase K was added to terminate the reaction and incubated at 37 °C for 10 minutes.

6.2.3 Preparation of other materials for microinjection

Needles for microinjection were made from aluminosilicate glass tubes (1.0 OD x .5 ID) (Sutter, USA). Needles were pulled to a fine point using a needle puller (Sutter instruments, P-2000). Agarose pads for mounting worms during microinjection were prepared on glass microscope slides. Molten 2% agarose was dropped onto the centre of the glass slide. Another glass slide was placed at a 90° angle to the bottom slide and was used to press the drop of agarose into a thin and smooth surface.

6.2.4 Production of injection mixture

An injection mixture was produced comprising 30 ng/µl of an Expression vector and 50 ng/µl pPD118.33. pPD118.33 was used as a marker gene for the transformation process, and contains the *myo-2* promoter and the coding sequence for GFP. The *myo-2* promoter drives expression in the pharyngeal muscles of *C. elegans* (Okkema *et al.* 1993) providing a clear marker for transformation (Figure 6-4). To remove contaminants and allow smooth unhindered flow of injection mixture, the mixture was centrifuged at 14,500 rpm three times. Each time, the top half of the injection mixture was transferred to a fresh tube and the bottom half discarded. This was carried out early on each day of microinjection. Needles were loaded with injection mixture by capillary action.

6.2.5 Transformation of *C. elegans* by microinjection

Hermaphrodite *C. elegans* (Strain, *unc-38(x20)*) were transformed by microinjection. 24 hours prior to microinjection, L4 hermaphrodites (identified by a white-patch near the centre of the body) were transferred onto a fresh NGM-lite plate to ensure that young adult worms would be injected the following day. Individual hermaphrodites were mounted onto 2% agarose pads into a drop of halocarbon oil to immobilise them for microinjection. Microinjection was carried out using an inverted microscope. Needle manipulations were carried out using an Injectman NI 2 micromanipulator. Injection pressure was generated by FemtoJet. DNA was injected into the distal arm of either one or both gonads until the organs appeared swollen (Figure 6-4a).

Microinjected worms were transferred to individual plates in a drop of M9 buffer and stored at 20 °C for 3-4 days. Transformants were selected from the progeny of injected hermaphrodites by selecting GFP expressing worms, which will additionally contain the transgene of interest as well (Figure 6-4b). Individual transformed animals from this F1 generation were transferred onto fresh plates (1 per plate) and the progeny of these examined for GFP expression. Any lines still displaying the GFP marker in the F2 generation were characterised as stable transformed lines.

6.2.6 Maintenance of transformed stable lines

Independent lines resulting from transformation events were maintained separately on NGM-lite plates seeded with OP50. Every 3-4 days, 15 GFP-expressing individuals per line were transferred to new plates in order to maintain healthy populations.

6.2.7 Analysis of mutant lines rescued by chimeric genes

Preliminary analysis of thrashing rate over the full range of levamisole concentrations (0, 1, 10, 50, 100 µM) was carried out as described in 5.2.3.1. Undergraduate students assisted in collecting preliminary data, allowing a large number of worms to be analysed. This data was used subsequently used to select concentrations of levamisole at which to conduct more thorough analysis. Each day, per assay, the wild-type (N2), the mutant background (*unc-38(x20)*), the line transformed with *cel-unc-38* or the line transformed with *gpa-unc-38.1* and two independent mutant lines transgenic for one the chimeric genes were analysed. The control line used was determined by the backbone of the mutant line that was analysed. A minimum of 24 worms per line per levamisole concentration were analysed. Each assay was repeated twice. Analysis of the *Cel-unc-38-F174_N177delinsYPSG* line is an exception, due to technical difficulties. The effect of the marker gene was tested by analysing the thrashing rate of *unc-38(x20)* worms transformed with *pmyo-2::GFP* alone. There was no significant difference in thrashing rate between *unc-38(x20)* and mutant worms transformed with *pmyo-2::GFP*.

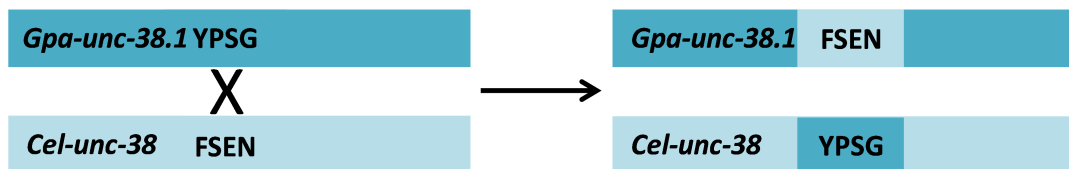
a



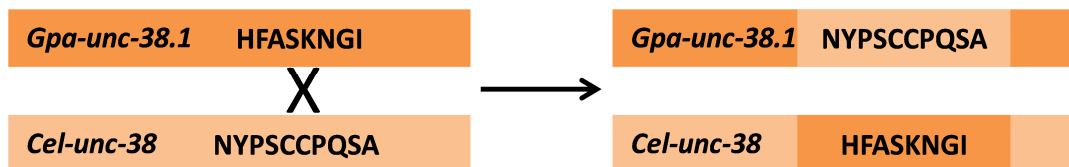
TM2



b



c



d

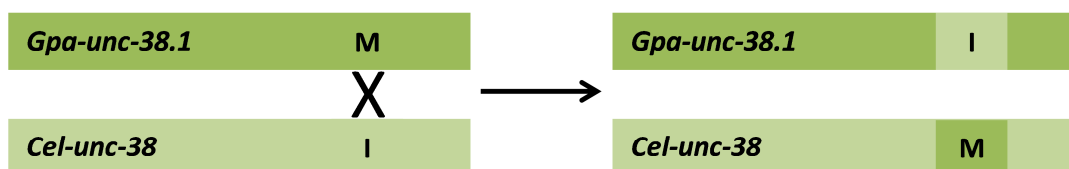


Figure 6-1: Schematic of chimeric genes produced by Spliced Overlap Extension

- a) Alignments between *Cel-unc-38* (top) and *Gpa-unc-38.1* (bottom) showing key amino acid differences in loop B, loop C and transmembrane domain 2. b-d) Schematic of chimeric genes produced by spliced overlap extension

Chimeric gene	Process	Template	Forward Primer	Reverse Primer
<i>G. pallida</i> - NYPSCCPQSA sequence swap	PCR1 rxn 1	<i>G. pallida unc-38</i> in pCR™8/GW/TOPO®	GGTATATGCAAAACATATGCTTT	ctgtggacaacaacttggatagtCTTGTTCGTTGGTCGCCTG
	PCR1 rxn 2		ccaagtttgtccacagagtgcTACGAAGAGATGGATTTGACTTGGC	GGTATATGCAAAACATATGCTTT
	PCR2	Mixed products of PCR1	CTGATGGTCTATCACCGGAA	GGTATATGCAAAACATATGCTTT
<i>C. elegans</i> - HFASKNGI sequence swap	PCR1 rxn 1	<i>C. elegans unc-38</i> in pCR™8/GW/TOPO®	ATGCGCTTTTGGTTATTCC	accatttttgatgcaaaaaatgCTTGCTCTTGGCAACTC
	PCR1 rxn 2		tttttgcataaaaatggatcTATATTGATGTTACTTATTACCTCC	CTCAGAAACTAATTGGATTAGCAG
	PCR2	Mixed products of PCR1	CTGATGGTCTATCACCGGAA	CTCAGAAACTAATTGGATTAGCAG
<i>G. pallida</i> – single I > M change	PCR1 rxn 1	<i>G. pallida unc-38</i> in pCR™8/GW/TOPO®	CTGATGGTCTATCACCGGAA	GCAACAAAAAGAAGATTGTGAGAGCAG
	PCR1 rxn 2		CACAATCTCTTTGGCTTATCGAG	GGTATATGCAAAACATATGCTTT
	PCR2	Mixed products of PCR1	CTGATGGTCTATCACCGGAA	GGTATATGCAAAACATATGCTTT
<i>C. elegans</i> – single M > I change	PCR1 rxn 1	<i>C. elegans unc-38</i> in pCR™8/GW/TOPO®	ATGCGCTTTTGGTTATTCC	GTGAGCAGCAAGAACATAGTCAGGC
	PCR1 rxn 2		CCTTGACTATGTTCTTCTGCTGCTCACT	CTCAGAAACTAATTGGATTAGCAG
	PCR2	Mixed products of PCR1	ATGCGCTTTTGGTTATTCC	CTCAGAAACTAATTGGATTAGCAG
<i>G. pallida</i> – FSEN > YPSG change	PCR1 rxn 1	<i>G. pallida unc-38</i> in pCR™8/GW/TOPO®	CTGATGGTCTATCACCGGAA	ttcagaaaAAGTCCAGGATCAAATTGAGAAG
	PCR1 rxn 2		GGACttttctgaaatCTGCTTCATC	GGTATATGCAAAACATATGCTTT
	PCR2	Mixed products of PCR1	CTGATGGTCTATCACCGGAA	GGTATATGCAAAACATATGCTTT
<i>C. elegans</i> – YPSG > FSEN change	PCR1 rxn 1	<i>C. elegans unc-38</i> in pCR™8/GW/TOPO®	ATGCGCTTTTGGTTATTCC	tccagacggtaTGTCCAGGAGCCGAAC
	PCR1 rxn 2		tacccgctggaCTGCTCTCCGTGGAATTGAACGAACCA	CTCAGAAACTAATTGGATTAGCAG
	PCR2	Mixed products of PCR1	ATGCGCTTTTGGTTATTCC	CTCAGAAACTAATTGGATTAGCAG

Table 8: Primers used for Spliced Overlap Extension PCRs

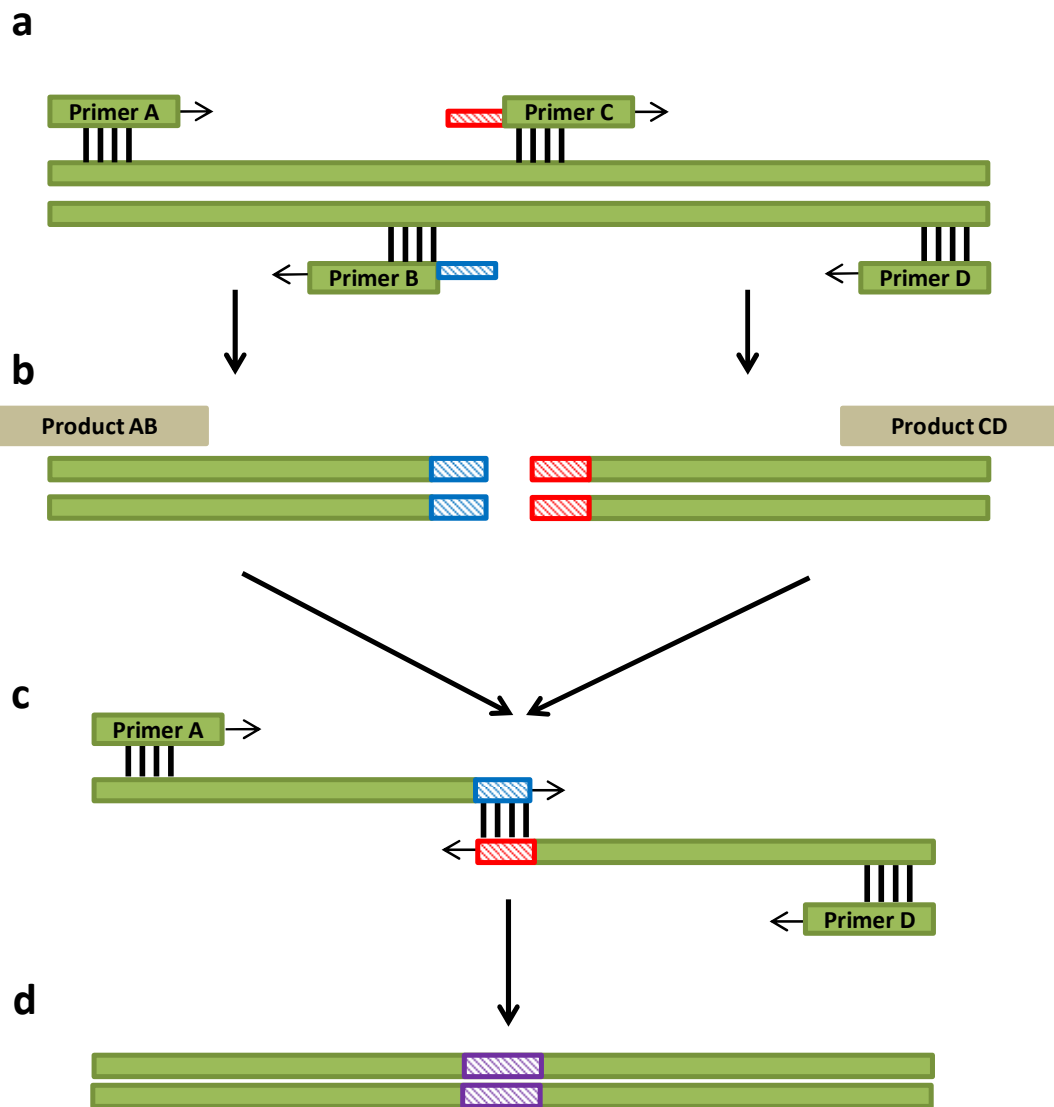


Figure 6-2: Schematic of Spliced Overlap Extension PCRs

a) The gene is amplified in two halves in separate PCRs using Primers A and B or Primers C and D. Primers B and C are designed to introduce the desired mutation (coloured blue and red). b) Products AB and CD are produced, which now incorporate the desired mutation. c) A second PCR is conducted using primers A and D to amplify the full gene. The overlap introduced between the two halves allows them to anneal, and the complete coding region to be amplified. d) The full-length product is produced with the desired mutation.

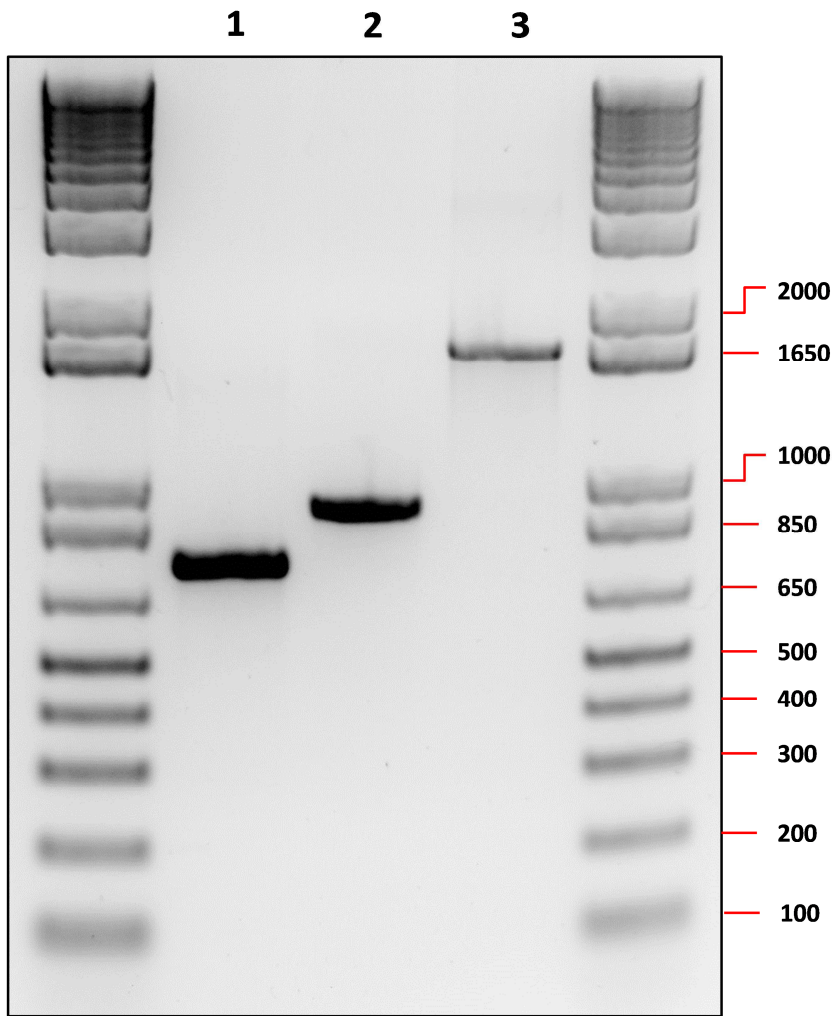


Figure 6-3: Products of Spliced Overlap Extension visualised by agarose gel electrophoresis

Lane 1 and 2 contain products AB and CD respectively after the first round of amplification. Lane 3 contains the full length chimeric gene amplified after the second PCR. Invitrogen 1Kb+ ladder was used and values are indicated in bp.

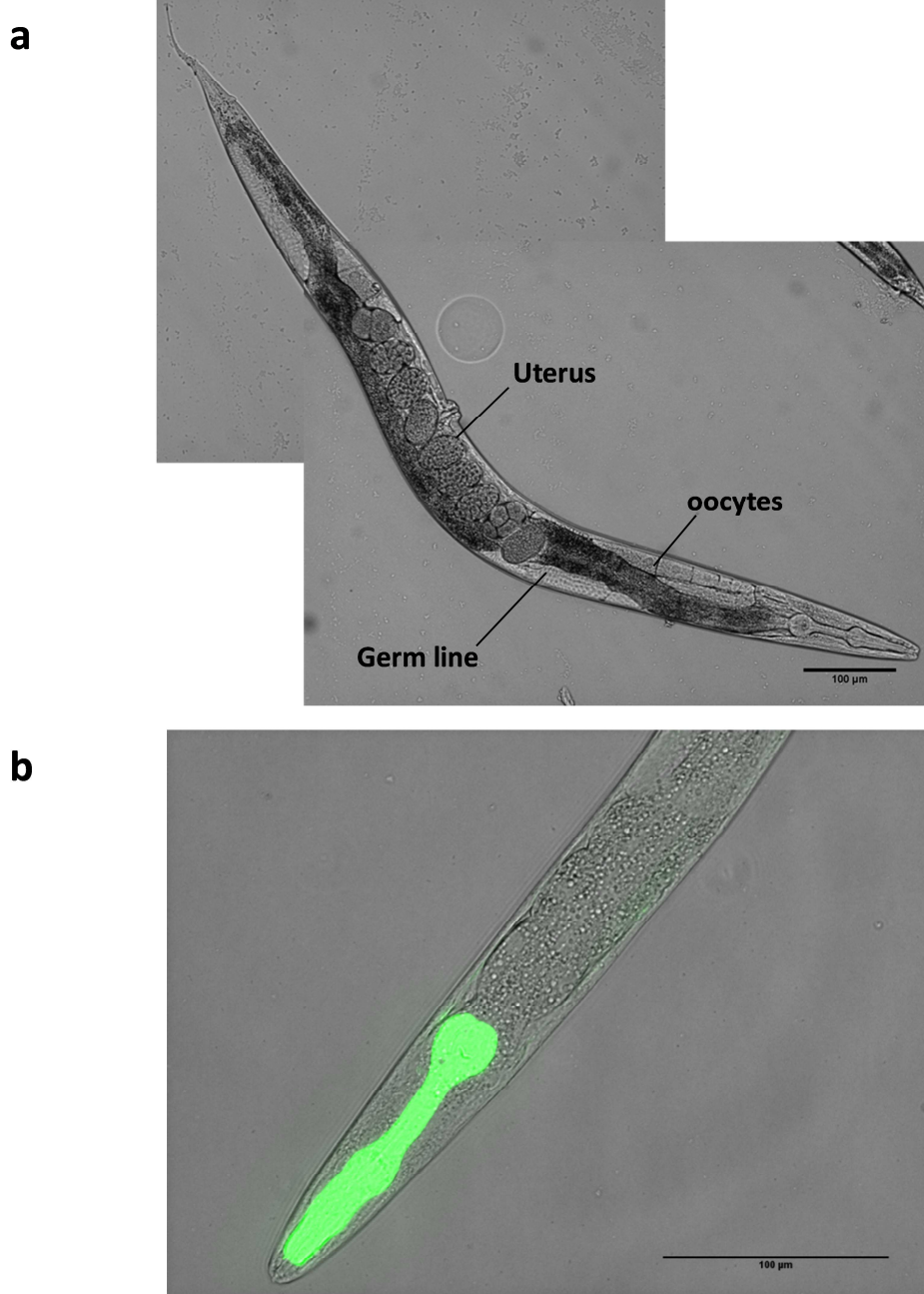


Figure 6-4: Example of suitable hermaphrodite for microinjection and marker gene for selection of transformants

- a) A young-adult hermaphrodite. In the uterus, a row of developed mature eggs can be seen. Towards the distal end of the gonad, individual development oocytes are shown. At the distal end, the germ line filled with developing nuclei can be seen. Injection in this location floods many developing nuclei with the transforming DNA. Image taken under 10x magnification b) The *pmyo-2::GFP* marker gene was used to select positive transformants. This drives GFP expression in the pharynx and allows for simple selection. Image taken under 20x magnification.

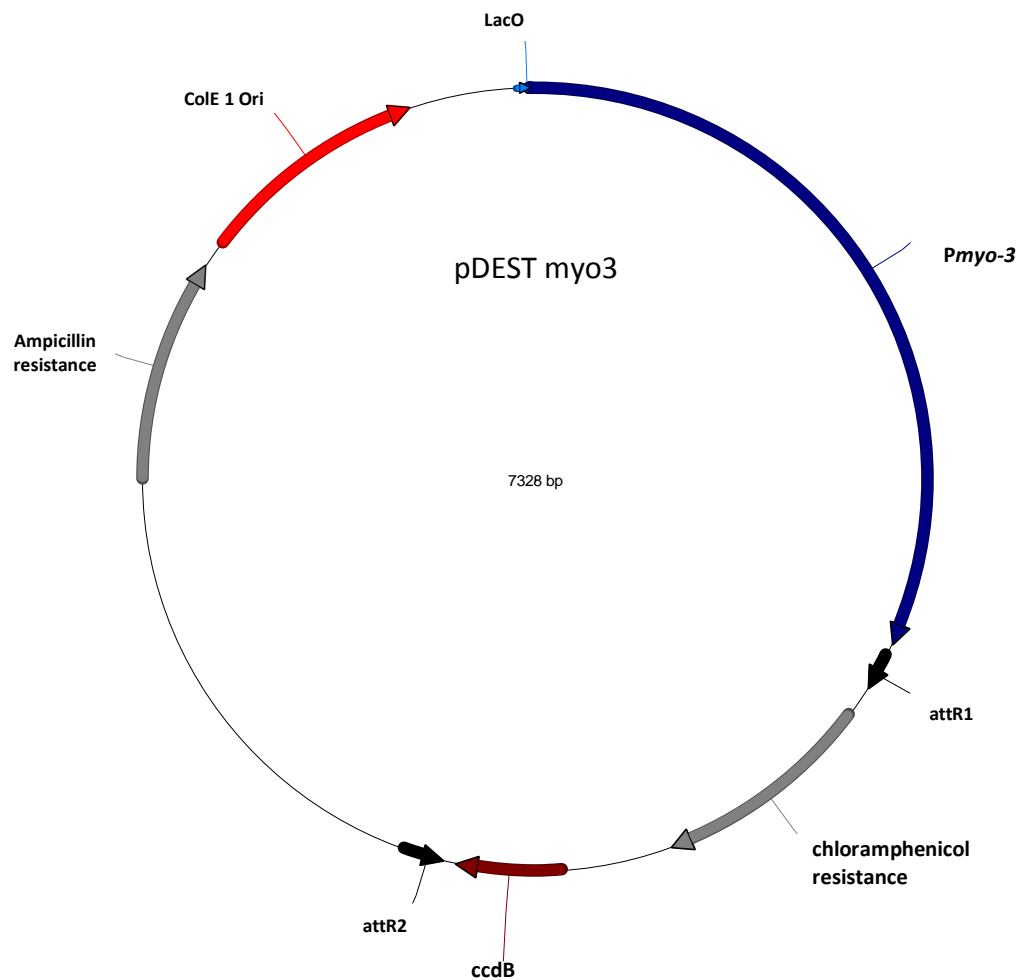


Figure 6-5: Vector map of pDEST-myo3

pDEST-myo3 was used as a destination vector. Chimeric genes produced by spliced overlap extension were cloned into pDEST-myo3 by GATEWAY® cloning. The insertion sites are downstream of the *myo-3* promoter which drives expression in body-wall muscle of *C. elegans*

6.3 Results

The chimeric transgene lines were analysed by thrashing assays. Both the ability of the chimeric gene to rescue basal thrashing, and its effect on levamisole sensitivity were investigated. Each assay analysed the wild-type strain (N2); the mutant strain *unc-38(x20)*; the transgenic line rescued with *cel-unc-38* (if the chimeric gene was based on *cel-unc-38*) or *gpa-unc-38.1* (if the chimeric gene was based on *gpa-unc-38.1*) to allow comparison to the native gene and two independent transgenic lines for one of the chimeric genes. Throughout these assays, the thrashing rate of the *unc-38(x20)* does not change significantly unless stated otherwise.

6.3.1 The YxxCC motif involved in acetylcholine binding

The effect of addition of the YxxCC motif to *Gpa-unc-38.1* and the removal of the YxxCC motif from *Cel-unc-38* was investigated.

6.3.1.1 Addition of the YxxCC motif to *Gpa-unc-38.1* does not affect ability of chimeric genes to rescue basal thrashing or levamisole sensitivity

Preliminary data collected at a range of levamisole concentrations for wild-type (N2) and *unc-38(x20)* compared to the two independent transformations with *Gpa-unc-38.1-H236_I234delinsNYPSCCPGSA* indicates that this chimeric gene does not affect rescue of basal thrashing rate compared to the wild-type of *gpa-unc-38.1* and that levamisole sensitivity is not affected. To confirm this, further assays were conducted at 50 µM levamisole and 100 µM levamisole (Figure 6-6).

In the assay conducted for 50 µM levamisole, basal thrashing was fully rescued in the *Gpa-unc-38.1* line and the two lines transgenic for *Gpa-unc-38.1-H236_I234delinsNYPSCCPGSA* (L1 and L2) as the thrashing rates for these lines at t= 0 mins were not significantly different from N2. After addition of levamisole, at t= 10 mins, the thrashing rates of *gpa-unc-38.1* and the two chimeric transgene lines were significantly higher than the N2 strain but were not significantly different from each other. At t= 30 mins, the thrashing rate of the N2 strain was further reduced. The thrashing rates of the *gpa-unc-38.1* transgenic line and two chimeric transgene lines were not significantly lower than at t= 10 mins and were not significantly different from each other (Figure 6-7).

In the assay conducted for 100 µM levamisole, basal thrashing rate was again fully rescued by *Gpa-unc-38.1* and one of the two chimeric transgene lines (L1). However, whilst the rate of the L2 chimeric transgene line was not significantly different from either L1 or *gpa-unc-38.1*, and it was increased significantly compared to *unc-38(x20)*, it was not fully restored to the wild-type. After addition of levamisole, at t= 10 mins, the thrashing rates of all lines declined and were not significantly different from each other. However, after 30 minutes the N2 thrashing rate had decreased further and was

significantly lower than all other lines. The thrashing rates of the *gpa-unc-38.1* line and two chimeric transgene lines did not decrease after t= 10 mins, and were not significantly different from each other at t= 30 mins (Figure 6-8).

6.3.1.2 Removal of the YxxCC motif from *cel-unc-38* does not affect ability of chimeric genes to rescue basal thrashing, or affect sensitivity to levamisole

Preliminary data were collected at a range of levamisole concentrations for the 30 minute time point for the wild-type (N2), *unc-38(x20)* and the two independent transformations of *Cel-unc-38-N234_I242delinsHFFASKNGI*. The thrashing rate of the two chimeric transgene lines reduce in response to levamisole exposure similarly to wild-type (N2). Further assays were conducted at 50 µM and 100 µM (Figure 6-9).

In the assay conducted for 50 µM levamisole, basal thrashing at t=0 mins for *cel-unc-38*, and the two chimeric transgene lines are rescued fully compared to wild-type (N2). On addition of levamisole at t= 10 mins, the thrashing rate of all lines (except *unc-38(x20)*) was found to be not significantly different from each other. At t= 30 mins, the thrashing rate of all lines (except *unc-38(x20)*) had reduced further and are not significantly different from each other (Figure 6-10).

At t= 0 mins, for the assay conducted for 100 µM levamisole, basal thrashing rate for the *cel-unc-38* and two chimeric transgene lines are fully rescued to wild-type. At t= 10 mins the thrashing rate of all lines (except *unc-38(x20)*) were significantly reduced and were not significantly different from each other. At t= 30 mins, the thrashing rate of all lines (except *unc-38(x20)*) reduced further but remained non-significantly different from each other. In this experiment, the thrashing rate of the *unc-38(x20)* line reduced significantly throughout the duration of the experiment to 63% of initial thrashing rate (Figure 6-11).

6.3.2 Investigation into the effect of a glutamate residue in loop B, which may be involved in levamisole sensitivity

The effect of introducing a glutamate into loop B of *gpa-unc-38.1* and the removal of glutamate from loop B of *cel-unc-38* was investigated. This residue had been identified as being involved in levamisole sensitivity (Rayes *et al.* 2004).

6.3.2.1 Introduction of a glutamate residue in loop B of *gpa-unc-38.1* does not affect ability of chimeric genes to rescue basal thrashing and does not affect levamisole sensitivity

Preliminary data collected at the 30 minute time point at a range of levamisole concentrations for the chimeric lines *Gpa-unc-38.1-Y175_G178delinsFSEN* suggested that these chimeric genes were not more sensitive to levamisole, as they retained more resistance to levamisole than the wild-type (N2) worms. Preliminary data also

suggested that there may be an effect on basal thrashing. Further experiments were conducted at 50 µM and 100 µM (Figure 6-12).

In the 50 µM levamisole assay, basal thrashing is rescued to wild-type levels for *gpa-unc-38.1* and both chimeric gene lines at t= 0 mins. At t= 10 mins, the thrashing rate of the *gpa-unc-38.1* and N2 strain was reduced and are not significantly different from each other. The thrashing rates of both chimeric transgene lines are significantly higher than the N2 and *gpa-unc-38.1* lines. At t= 30 mins, the thrashing rate of the N2 strain has reduced further, but the thrashing rate of the *gpa-unc-38.1* line is significantly higher than that of the N2 strain. The thrashing rate of the two chimeric transgene lines is reduced from t= 10 mins, and are not significantly different from *gpa-unc-38.1* (Figure 6-13).

In the 100 µM levamisole assay, basal thrashing is rescued to wild-type (N2) levels for *gpa-unc-38.1* and one of the chimeric transgene lines (L1) at t= 0 mins. Although, L2 is not rescued to wild-type (N2) levels in this experiment, the basal thrashing rate of the L2 line has been seen to be at wild-type levels in previous assays, and is also significantly higher than that of the *unc-38(x20)* line indicating that thrashing rate is rescued from the *unc-38(x20)* background. At t= 10 mins, the thrashing rate of the N2 strain is significantly lower than all other lines. The thrashing rate of the *gpa-unc-38.1* line is not significantly different from transgenic chimeric line L2. The thrashing rate of the chimeric lines L1 and L2 are not significantly different from each other. At t = 30 mins, the thrashing rate of the N2 strain is significantly lower than at t = 10 mins, and lower than all other lines. The thrashing rates of the *gpa-unc-38.1* line and L1 and L2 are significantly higher (Figure 6-14).

6.3.2.2 Removal of a glutamate residue from loop B of *cel-unc-38* does not affect ability of chimeric genes to rescue basal thrashing and does not affect levamisole sensitivity

Only preliminary data is available for the chimeric gene *Cel-unc-38-F174_N177delinsYPSG*, as only one independently transformed line was successfully generated for this chimeric gene. The line obtained had a low percentage of transformants per generation, and was therefore difficult to obtain enough transgenic individuals to analyse each assay. The transformants also were slow-growing. The line was difficult to maintain and died out before a full analysis could be made.

The preliminary results for this line at a range of levamisole concentrations after 30 minutes indicated that the response to levamisole is likely to be similar to that of the wild-type N2 line (Figure 6-15).

In the 50 µM assay, at t= 0 mins, the thrashing rate of the chimeric transgene lines line was rescued to wild-type levels and was not found to be significantly different to wild-type (N2). At t= 10 mins, the thrashing rate of both the transgenic chimeric line and the wild-type line was significantly lower and were not significantly different to each other. At t= 30 mins, the thrashing rate of the wild-type (N2) line and the transgenic chimeric line reduced further, and were not significantly different from each other (Figure 6-16).

In the 100 µM assay, basal thrashing of the chimeric transgene lines were not found to be fully rescued to wild-type levels. At t= 10 mins, the thrashing rate of both the chimeric transgene lines line and the wild-type (N2) strain reduced to the same extend and were not found to be significantly different from each other. At t= 30 mins, the thrashing rate of the wild-type (N2) line and the transgenic chimeric line did not reduce significantly further (Figure 6-17).

6.3.3 Investigation into a single amino acid residue change in transmembrane domain 2 which may affect channel opening properties and levamisole sensitivity

The effect of a single amino acid change in the second transmembrane domain of *cel-unc-38* and *gpa-unc-38.1* was investigated. A valine to methionine substitution in the neuronal subunit *acr-2* has previously been shown to affect channel opening properties and cause a hyperactive response to acetylcholine (Jospin *et al.* 2009).

6.3.3.1 A methionine to isoleucine change in the TM2 domain of *gpa-unc-38.1* affects the ability of the chimeric gene to rescue basal thrashing, but not levamisole sensitivity

Preliminary results gathered for the 30 minute time point at a range of levamisole concentrations for thrashing rates of the line *Gpa-unc-38.1-M302I* indicated that basal thrashing rate may be impaired for this line. Levamisole sensitivity did not appear to be affected. Further assays were conducted at 50 µM and 100 µM levamisole (Figure 6-18).

In the assay conducted for 50 µM, basal thrashing at t= 0 mins was not rescued to wild-type levels for the chimeric transgene lines L1 and L2. The thrashing rate of *Gpa-unc-38.1* was fully rescued to wild-type (N2) levels, and was not significantly different to the wild-type strain. The thrashing rate of the chimeric transgene lines L1 and L2 are significantly higher than the *unc-38(x20)* line, indicating that the lines were successfully rescued from the mutant background to some extent. At t= 10 mins, thrashing rate of the L1 and L2 lines did not decrease from the rate at t= 0 mins. Wild-type (N2) thrashing rate decreased and no significant differences in thrashing rates were found between any of the lines at this time point. At t= 30 mins, the

thrashing rates of the chimeric transgene lines had decreased significantly from t= 10 mins, but were not significantly different to the *gpa-unc-38.1* line or the *unc-38(x20)* line. The wild-type (N2) line decreased significantly from t= 10 mins, and were significantly different from all other lines (Figure 6-19).

In the 100 µM levamisole assay, basal thrashing rate at t= 0 mins was not rescued to wild-type (N2) levels for the chimeric transgene lines. Although L1 was found to be not significantly different to the *unc-38(x20)* line in this instance, it was also found to be not significantly different to the L2 line. The basal thrashing rate of the *gpa-unc-38.1* line was rescued to wild-type levels. At t= 10 mins, thrashing rates of the chimeric transgene lines were significantly reduced, although they were not significantly different to each other or the *gpa-unc-38.1* line. The thrashing rate of the wild-type (N2) line was significantly lower than all other lines. At t= 30 mins, the thrashing rate of the wild-type (N2) line is significantly reduced but the thrashing rate of the chimeric transgene lines were not significantly reduced from t= 10 mins, and were not significantly different from each other (Figure 6-20).

6.3.3.2 An isoleucine to methionine change in *cel-unc-38* increases basal thrashing rate and increases levamisole sensitivity

Preliminary data for the 30 minute time point at a range of levamisole concentrations for the transgenic chimeric line *Cel-unc-38-I301M* indicated rescue of basal thrashing to wild-type (N2) levels, but showed an increase in sensitivity to levamisole for the two chimeric transgene lines. 10 µM and 50 µM levamisole was selected for further assays (Figure 6-21).

In the 10 µM levamisole assay, the basal thrashing rates at t= 0 mins of the chimeric transgene lines were found to be significantly higher than that of the wild-type (N2) strain indicating that the worms are thrashing faster. On addition of levamisole, at t= 10 mins, the thrashing rate of the wild-type (N2) worms reduced by 10% of initial thrashing rate, and this reduction is not significantly different to that of the *cel-unc-38* line. In contrast, the thrashing rate of both chimeric transgene lines was reduced by over 50% and was significantly different from wild-type (N2) and *cel-unc-38* thrashing rates. At t= 30 mins, thrashing rates of the N2 and *cel-unc-38* lines did not reduce significantly from thrashing rates in t= 10 mins. However the thrashing rates of both the chimeric transgene lines were further reduced to a total of 10% of initial thrashing rate and were not significantly different from each other (Figure 6-22).

In the assay conducted for 50 µM, the basal thrashing rate at t= 0 mins of the chimeric transgene lines was also found to be significantly higher than that of the N2 strain and *cel-unc-38* lines. At t= 10 mins, thrashing rates of the N2 strain and *cel-unc-38* line reduced to the same extent, but the thrashing rate of the two chimeric transgene lines

was significantly lower. At t= 30 mins, all lines (except *unc-38(x20)*) were found to be not significantly different to each other (Figure 6-23).

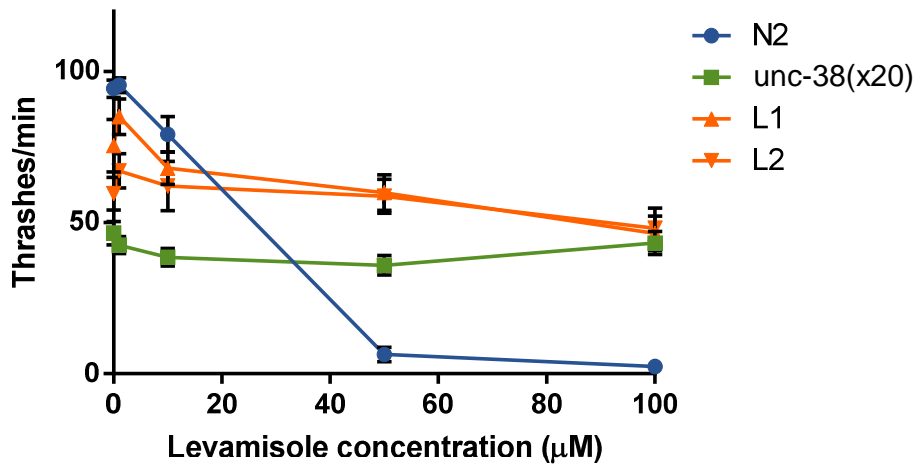


Figure 6-6: Thrashing rate after 30 mins exposure to a range of levamisole concentrations for *Gpa-unc-38.1-H236_I234delinsNYPSCCPGSA*

Preliminary data for *Gpa-unc-38.1-H236_I234delinsNYPSCCPGSA* L1 and L2 indicated that these lines had higher levamisole resistance than the wild-type N2. N = 30 for each levamisole concentration per line. Error bars represent SEM.

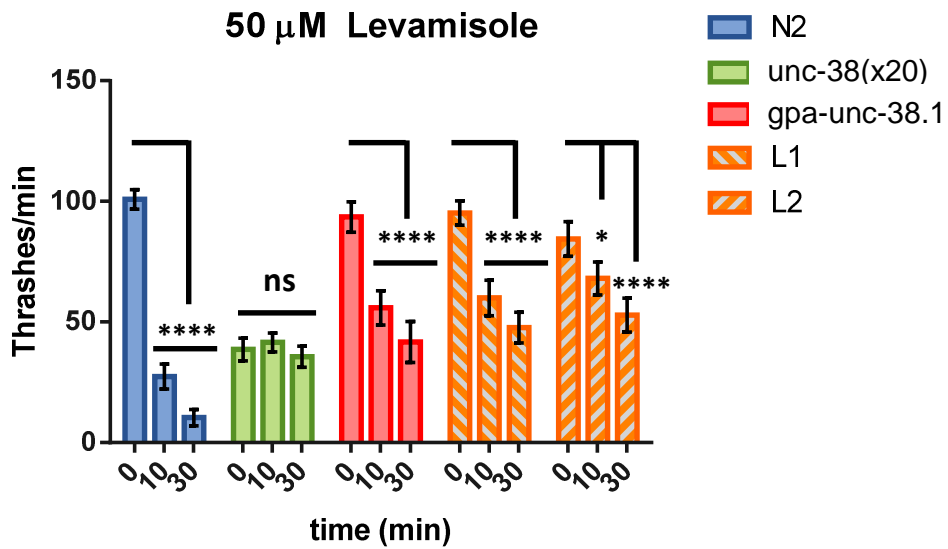
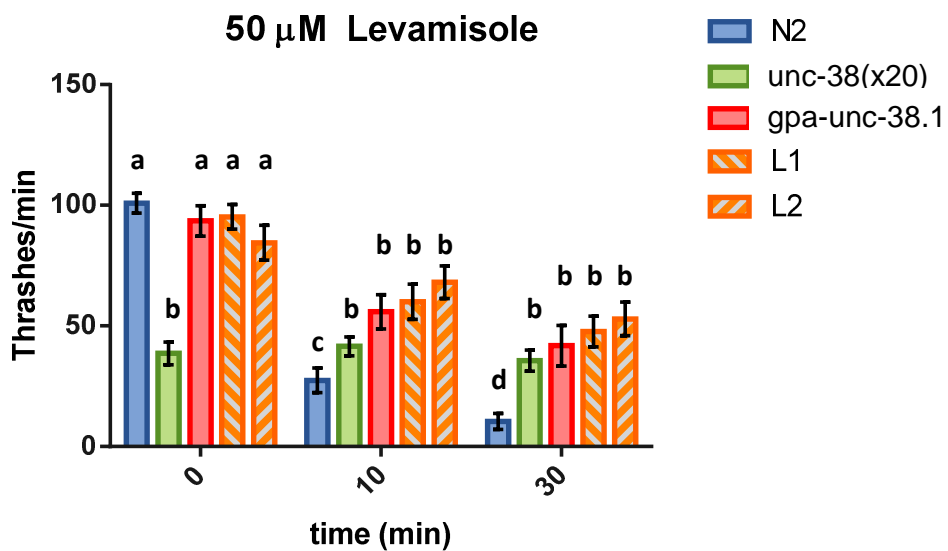
a**b**

Figure 6-7: Effect of 50 μ M levamisole on thrashing rate of *Gpa-unc-38.1-H236_I234delinsNYPSCCPGSA*

N2, *unc-38(x20)* and *gpa-unc-38.1* were used as controls. Same data is presented organised by line and by time point a) Thrashing rate of N2 lines is reduced by approximately 90% after 30 minute exposure to levamisole. Thrashing rate of the two transgenic lines L1 and L2 was reduced by approximately 60% by end of assay. Stars indicate significance of change in thrashing from $t = 0$ mins ($p = \leq 0.5$ (*); $p = \leq .0001$ (***)). (Two-way ANOVA, Tukey's multiple comparison). b) Comparison of thrashing rates of all lines at each time point. Letters shared between bars indicate statistically homogeneous subsets (Two-way ANOVA, Tukey's multiple comparison). N = 24 for each line. Error bars represent SEM.

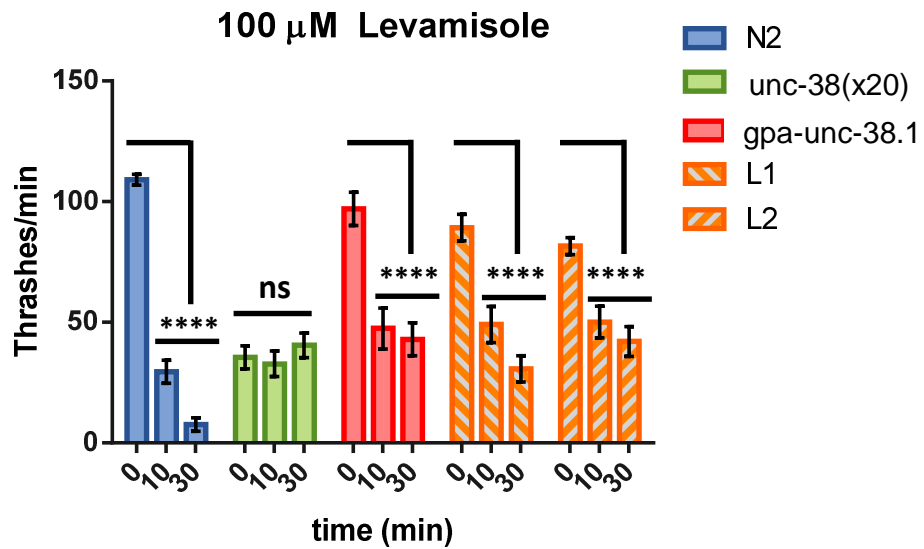
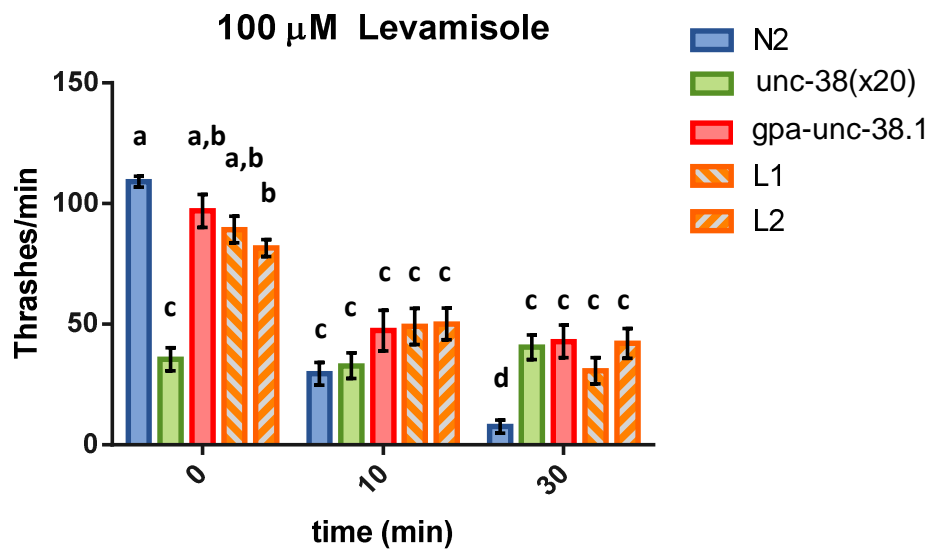
a**b**

Figure 6-8: Effect of 100 μ M levamisole on thrashing rate of *Gpa-unc-38.1-H236_I234delinsNYPSCPGSA*

N2, *unc-38(x20)* and *gpa-unc-38.1* were used as controls. Same data is presented organised by line and by time point. a) Thrashing rate of N2 strain reduced by approximately 95% after 30 minute exposure to levamisole. The thrashing rate of the two transgenic lines L1 and L2 reduced by approximately 50% by end of assay. Stars indicate significance of change in thrashing from t = 0 mins ($p = \leq 0.0001$ (****)). (Two-way ANOVA, Tukey's multiple comparison). b) Comparison of thrashing rates of all lines at each time point. Letters shared between bars indicate statistically homogeneous subsets (Two-way ANOVA, Tukey's multiple comparison). N = 24 for each line. Error bars represent SEM.

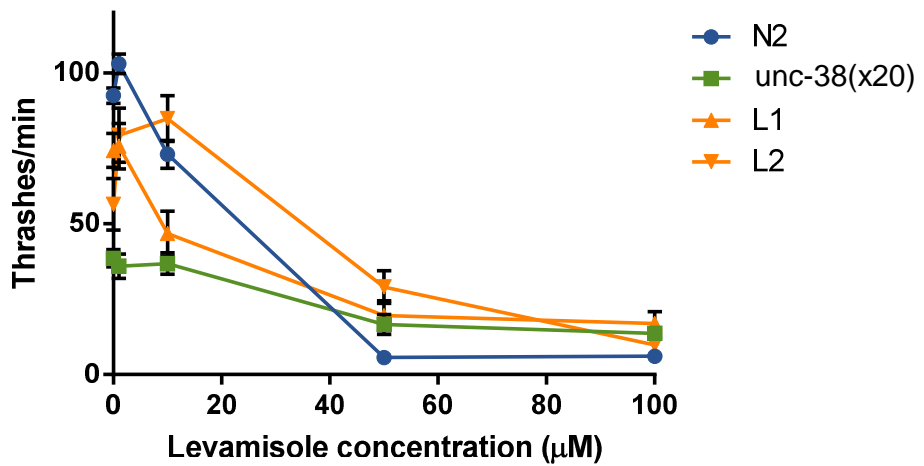


Figure 6-9: Thrashing rate after 30 mins exposure to a range of levamisole concentrations for *Cel-unc-38-N234_I242delinsHFFASKNGI*

Preliminary data for *Cel-unc-38-N234_I242delinsHFFASKNGI* transgenic lines L1 and L2 indicated that the levamisole responsiveness of this chimeric gene was similar to that of the wild-type N2. N = 30 for each levamisole concentration per line. Error bars represent SEM.

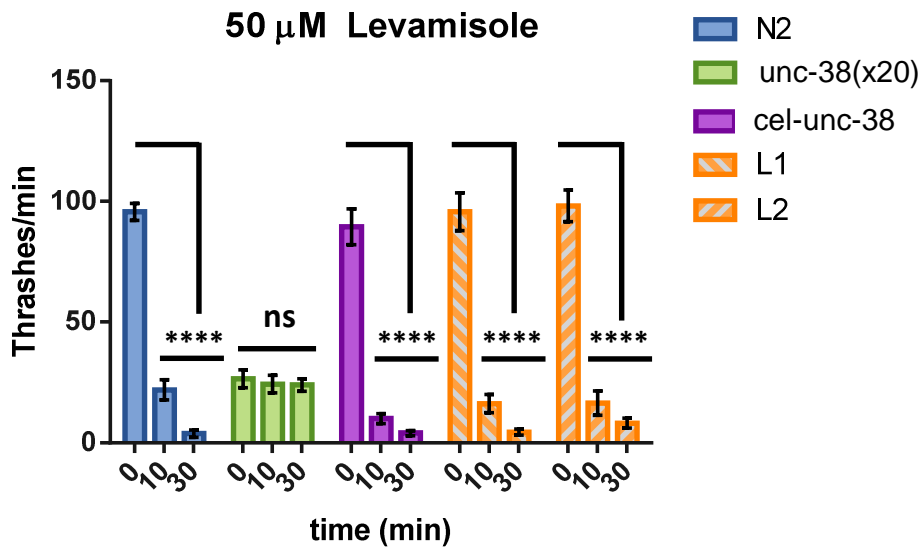
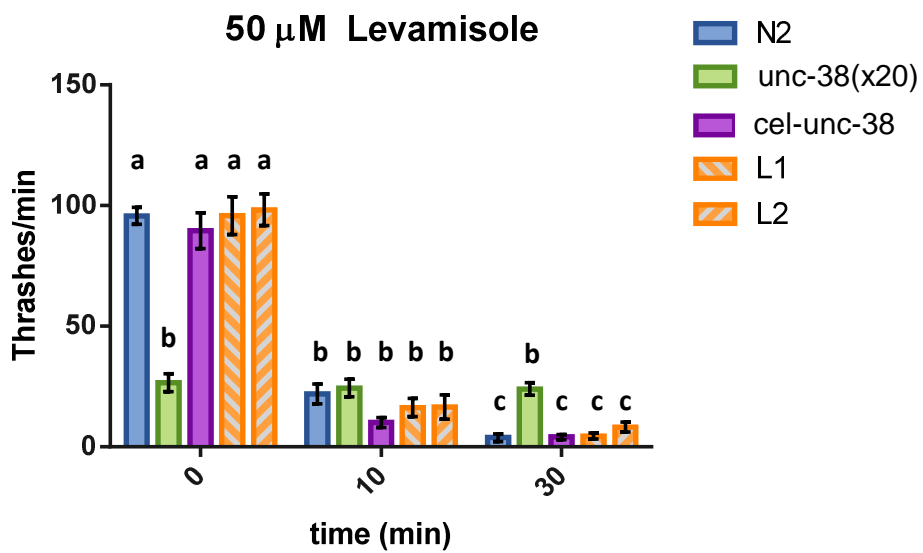
a**b**

Figure 6-10: Effect of 50 μ M levamisole on thrashing rate of *Cel-unc-38-N234_I242delinsHFFASKNGI*

N2, *unc-38(x20)* and *cel-unc-38* were used as controls. Same data is presented organised by line and by time point. a) Thrashing rates of all lines (except *unc-38(x20)*) reduced by approximately 95% after 30 minutes exposure to levamisole. Stars indicate significance of change in thrashing from $t = 0$ mins ($p = \leq 0.0001$ (****)). (Two-way ANOVA, Tukey's multiple comparison). b) Comparison of thrashing rates of all lines at each time point. Letters shared between bars indicate statistically homogeneous subsets (Two-way ANOVA, Tukey's multiple comparison). N = 24 for each line. Error bars represent SEM.

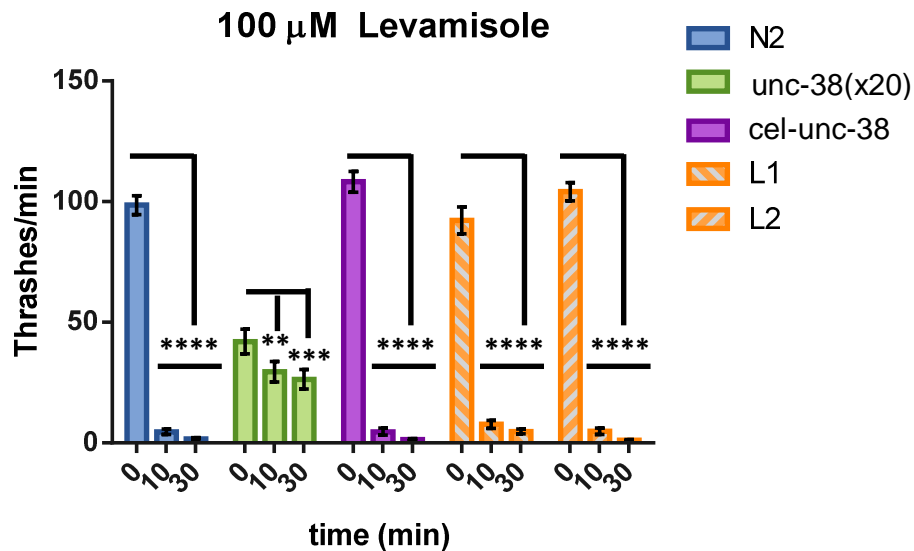
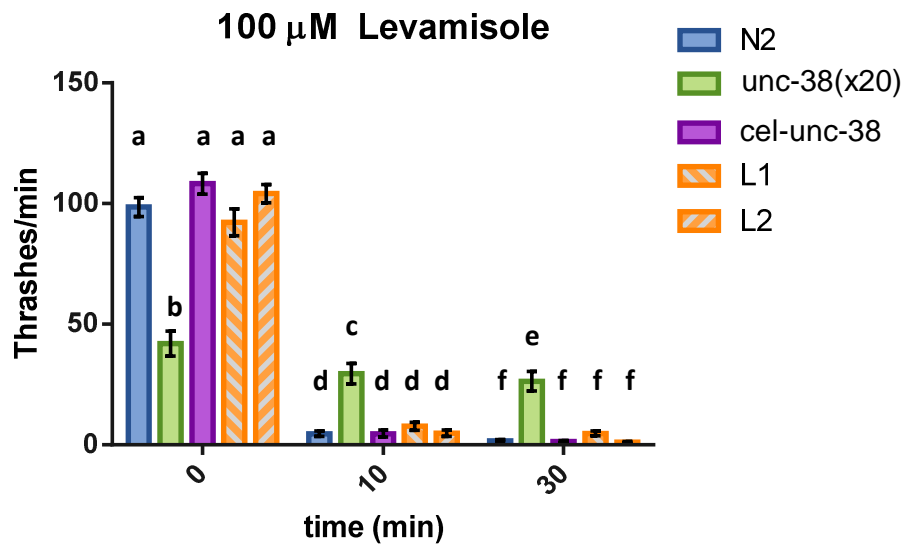
a**b**

Figure 6-11: Effect of 100 μ M levamisole on thrashing rate of *Cel-unc-38-N234_I242delinsHFFASKNGI*

N2, *unc-38(x20)* and *cel-unc-38* were used as controls. Same data is presented organised by line and by time point. a) Thrashing rates of all lines (except *unc-38(x20)*) were reduced by over 95% after 30 minutes exposure to levamisole. Stars indicate significance of change in thrashing from t = 0 mins ($p = \leq .0001$ (****)). (Two-way ANOVA, Tukey's multiple comparison). b) Comparison of thrashing rates of all lines at each time point. Letters shared between bars indicate statistically homogeneous subsets (Two-way ANOVA, Tukey's multiple comparison). N = 24 for each line. Error bars represent SEM.

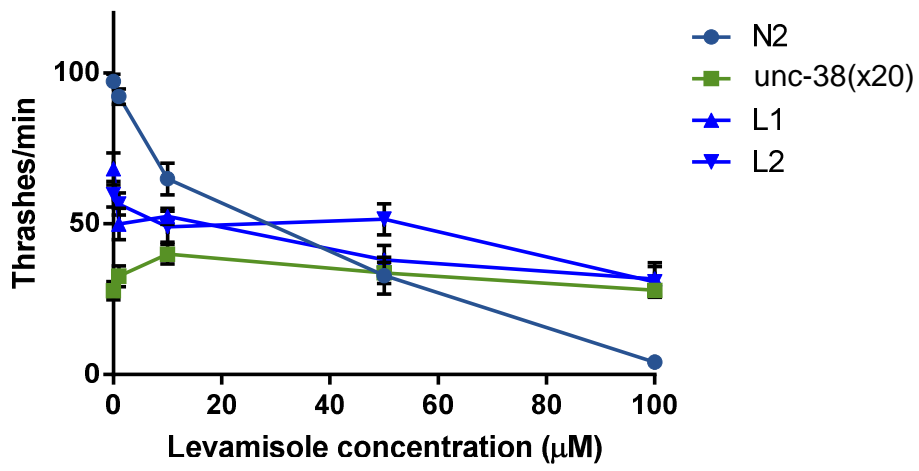


Figure 6-12: Thrashing rate after 30 mins exposure to a range of levamisole concentrations for *Gpa-unc-38.1-Y175_G178delinsFSEN*

Preliminary data for *Gpa-unc-38.1-Y175_G178delinsFSEN* transgenic lines L1 and L2 indicated that resistance to levamisole remained high in the chimeric lines compared to wild-type (N2). N = 30 for each levamisole concentration per line. Error bars represent SEM.

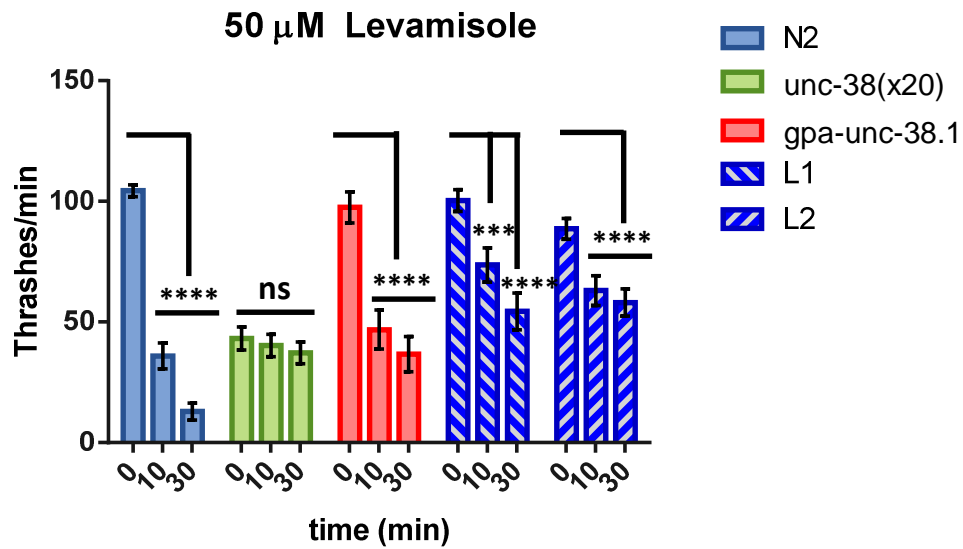
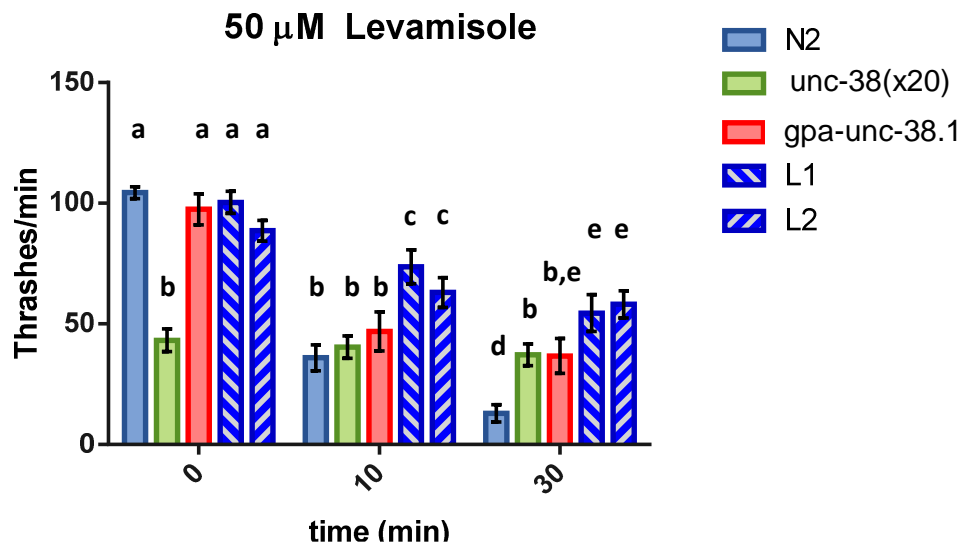
a**b**

Figure 6-13: Effect of 50 μ M levamisole on thrashing rate of *Gpa-unc-38.1-Y175_G178delinsFSEN*

N2, *unc-38(x20)* and *gpa-unc-38.1* were used as controls. Same data is presented organised by line and by time point. a) After 30 minutes exposure to levamisole thrashing rate of all lines (except *unc-38(x20)*) had fallen. Thrashing rate of the N2 strain reduced by approximately 95%. The thrashing rate of the *gpa-unc-38.1*, L1 and L2 lines reduced by approximately 40%. Stars indicate significance of change in thrashing from $t = 0$ mins ($p = \leq .001$ (**); $p = \leq .0001$ (****)). (Two-way ANOVA, Tukey's multiple comparison). b) Comparison of thrashing rates of all lines at each time point. Letters shared between bars indicate statistically homogeneous subsets (Two-way ANOVA, Tukey's multiple comparison). N = 24 for each line. Error bars represent SEM.

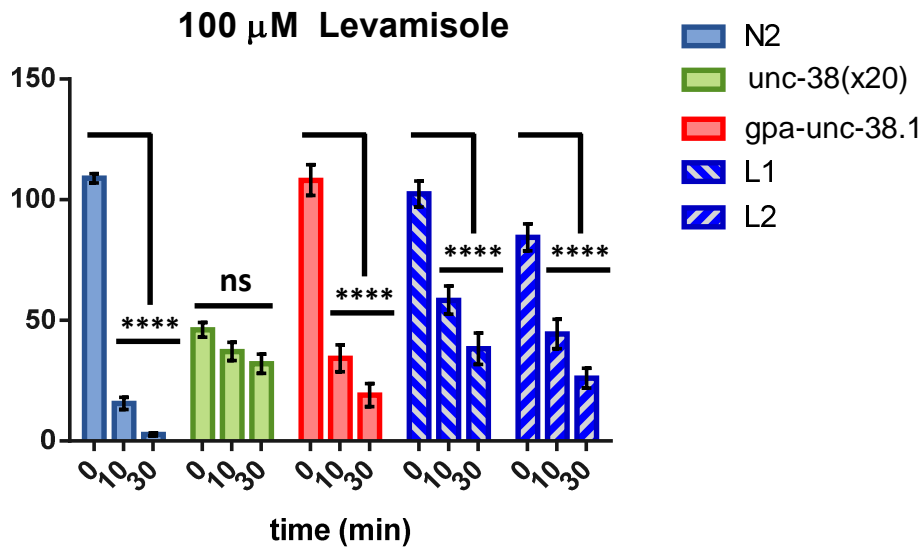
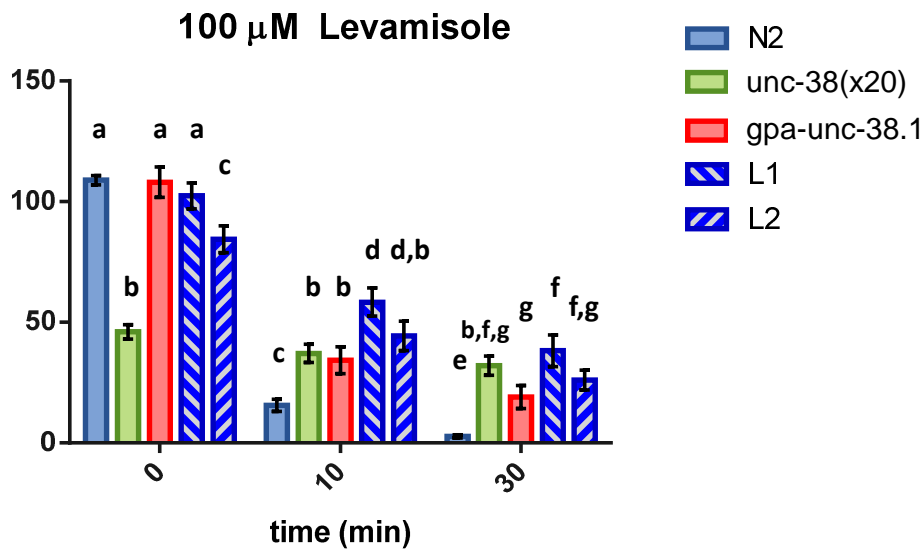
a**b**

Figure 6-14: Effect of 100 μ M levamisole on thrashing rate of *Gpa-unc-38.- Y175_G178delinsFSEN*

N2, *unc-38(x20)* and *gpa-unc-38.1* were used as controls. Same data is presented organised by line and by time point. a) After 30 minutes exposure to levamisole, the thrashing rate of the wild-type (*N2*) strain reduced by over 97%. The thrashing rate of the *gpa-unc-38.1*, L1 and L2 lines were significantly higher than wild-type. Stars indicate significance of change in thrashing from $t = 0$ mins ($p = \leq .0001$ (****)). (Two-way ANOVA, Tukey's multiple comparison). b) Comparison of thrashing rates of all lines at each time point. Letters shared between bars indicate statistically homogeneous subsets (Two-way ANOVA, Tukey's multiple comparison). $N = 24$ for each line. Error bars represent SEM.

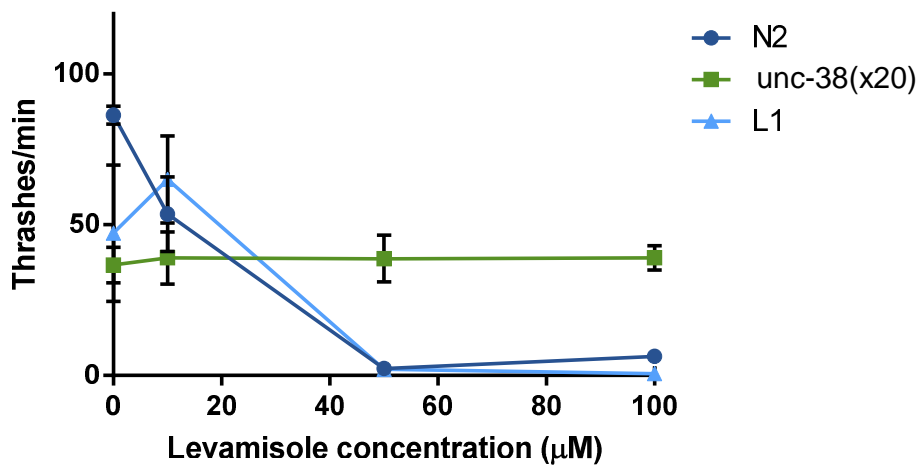


Figure 6-15: Thrashing rate after 30 mins exposure over a range of levamisole concentrations for *Cel-unc-38-F174_N177delinsYPSG*

Preliminary data for *Cel-unc-38-F174_N177delinsYPSG* indicated that it has a similar response as the wild-type (N2) strain to levamisole. N = 6 for each levamisole concentration per line. Error bars represent SEM.

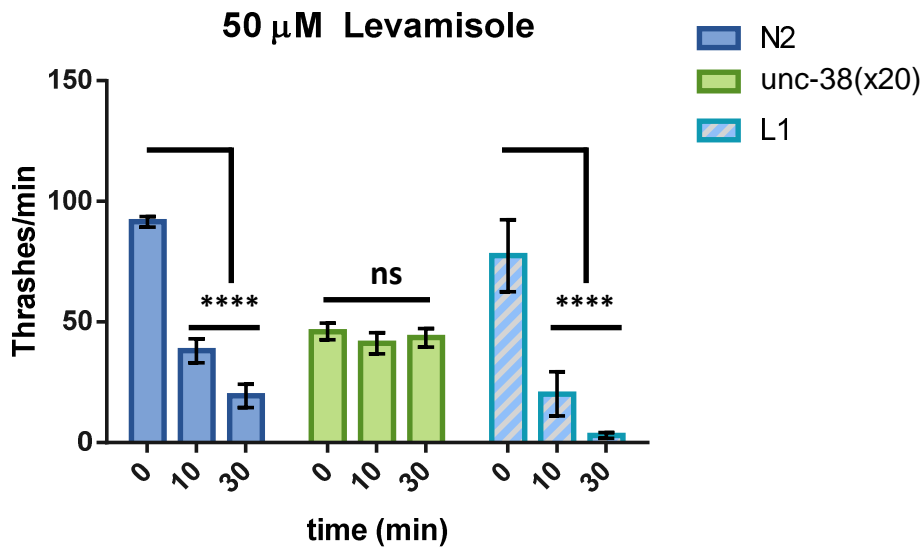
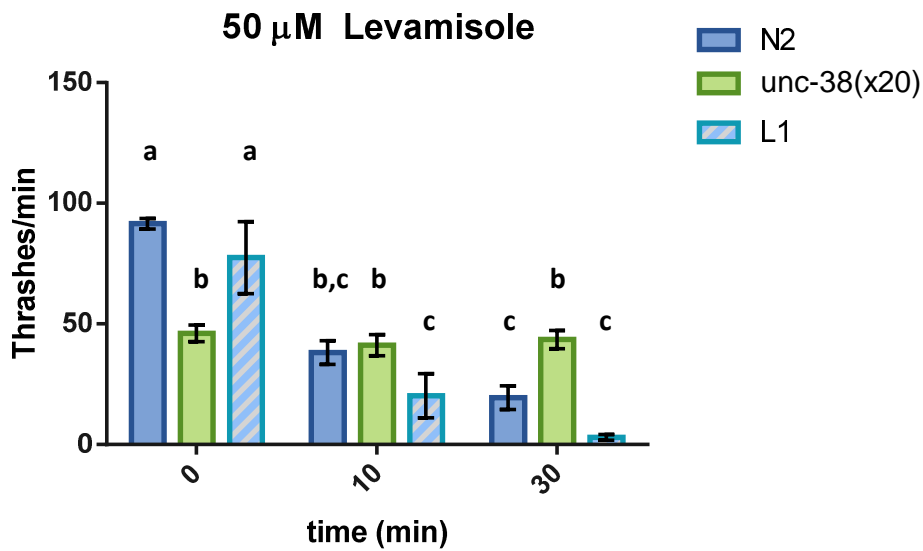
a**b**

Figure 6-16: Effect of 50 μ M levamisole on thrashing rate of *Cel-unc-38-F174_N177delinsYPSG*

Graphs shown from preliminary data set as only one transformed line was produced for this construct, which was difficult to work with technically. N2 and *unc-38(x20)* were used as controls. Same data is presented organised by line and by time point. a) Thrashing rate of L1 reduced in response to levamisole to the same extent as the wild-type N2 strain. Stars indicate significance of change in thrashing from $t = 0$ mins ($p = \leq .0001$ (****)). (Two-way ANOVA, Tukey's multiple comparison). b) Comparison of thrashing rates of all lines at each time point. Letters shared between bars indicate statistically homogeneous subsets (Two-way ANOVA, Tukey's multiple comparison). N = 6 for each line. Error bars represent SEM.

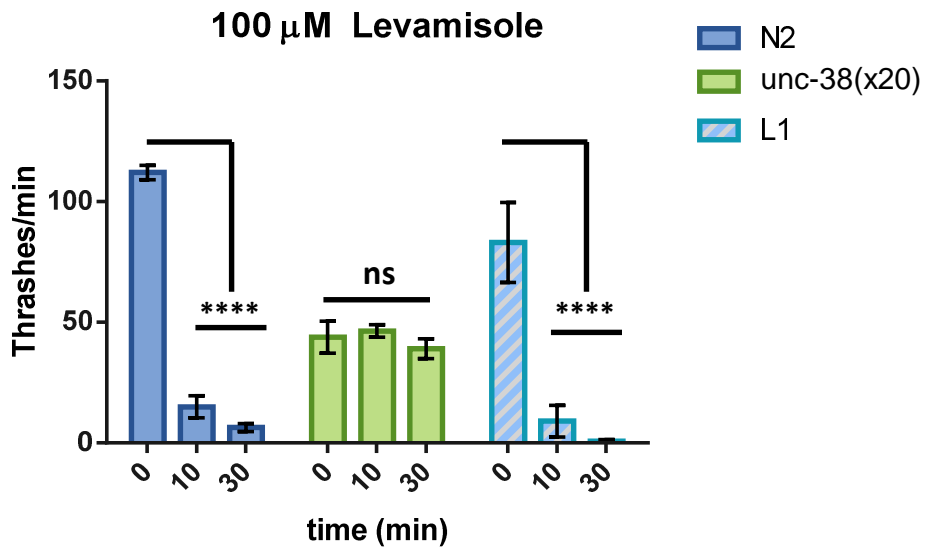
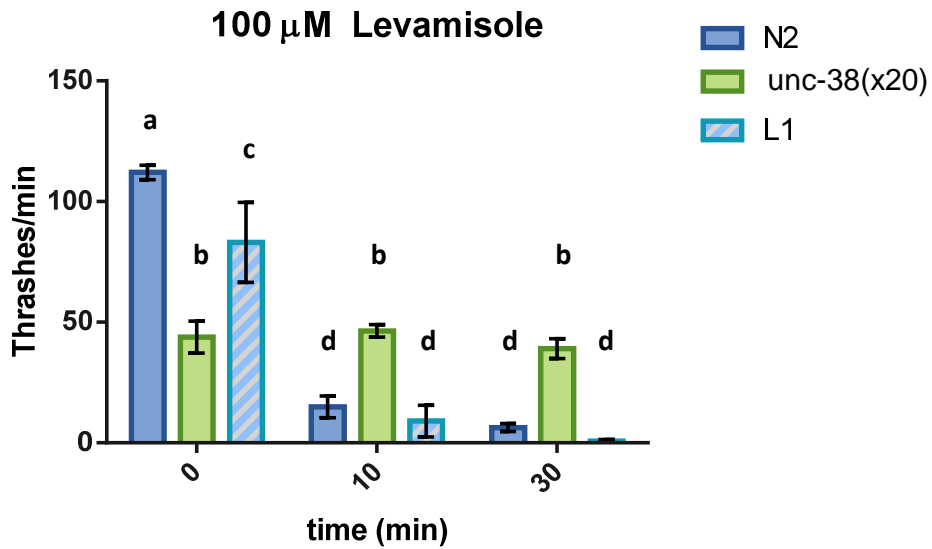
a**b**

Figure 6-17: Effect of 100 μ M levamisole on thrashing rate of *Cel-unc-38-F174_N177delinsYPSG*

Graphs shown from preliminary data set as only one transformed line was produced for this construct, which was difficult to work with technically. N2 and *unc-38(x20)* were used as controls. Same data is presented organised by line and by time point. a) Thrashing rate of L1 in response to levamisole was equal to that of the wild-type (N2) strain. Stars indicate significance of change in thrashing from t = 0 mins ($p = \leq .0001$ (****)). (Two-way ANOVA, Tukey's multiple comparison). b) Comparison of thrashing rates of all lines at each time point. Letters shared between bars indicate statistically homogeneous subsets (Two-way ANOVA, Tukey's multiple comparison). N = 6 for each line. Error bars represent SEM.

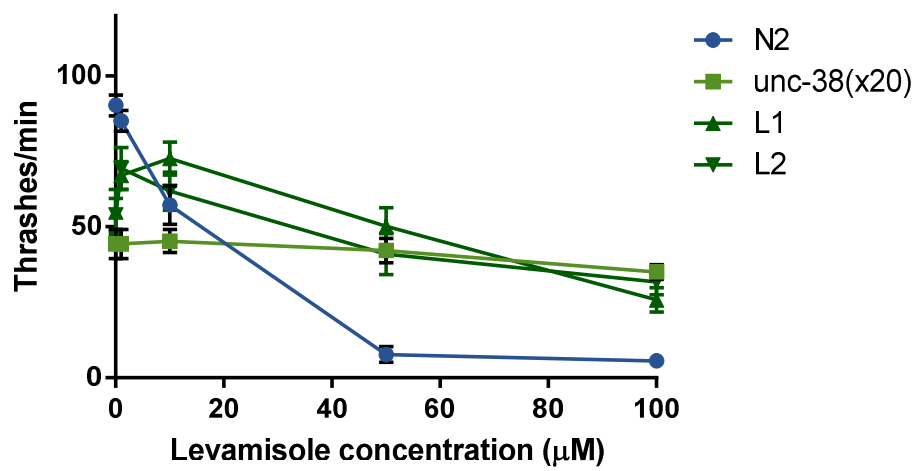


Figure 6-18: Thrashing rate after 30 mins exposure over a range of levamisole concentrations for *Gpa-unc-38.1-M302I*

Preliminary data for the *Gpa-unc-38.1-M302I* transgenic lines indicated resistance to levamisole remained high, but the rescue of basal thrashing may be affected. $N = 30$ for each levamisole concentration for each line. Error bars represent SEM.

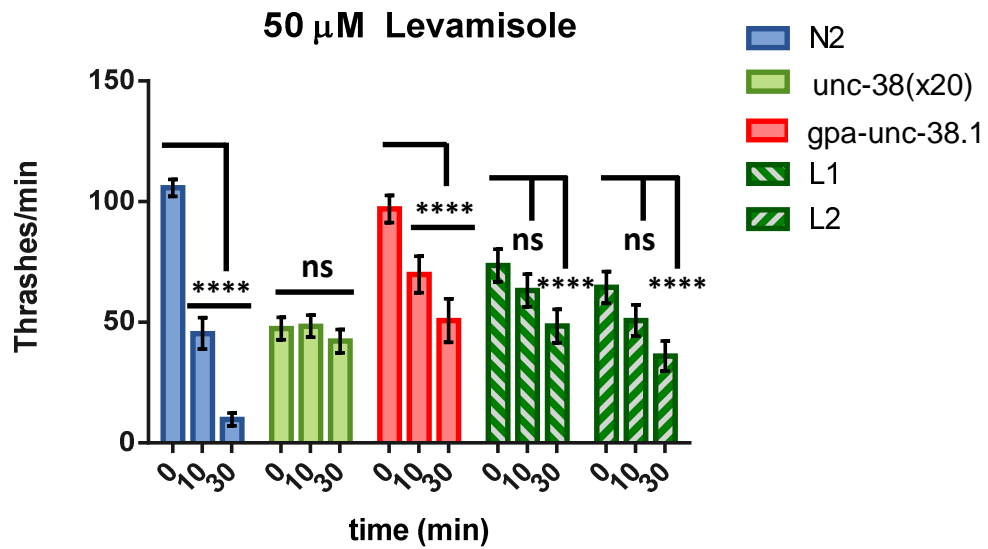
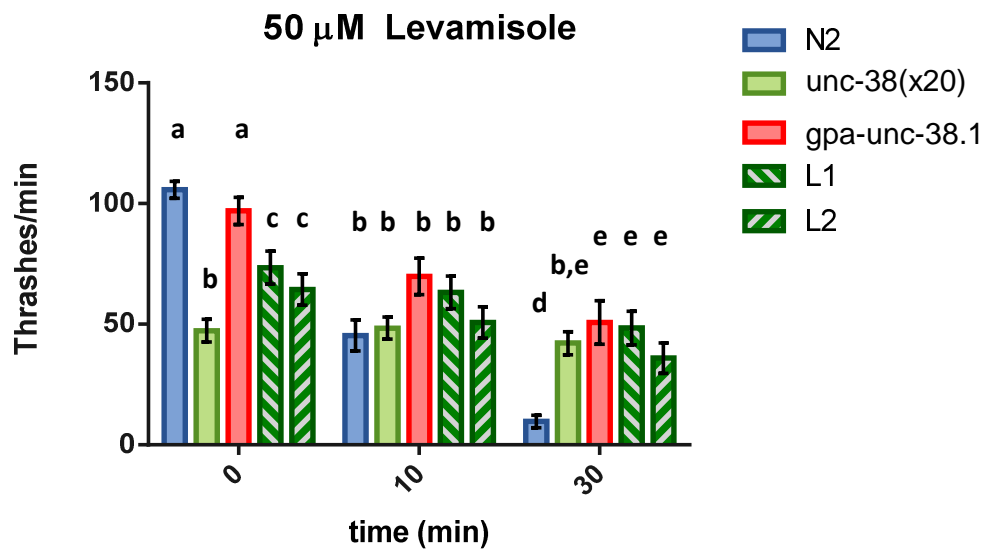
a**b**

Figure 6-19: Effect of 50 μ M levamisole on thrashing rate of *Gpa-unc-38.1-M3021*

N2, *unc-38(x20)* and *gpa-unc-38.1* were used as controls. Same data is presented organised by line and by time point. a) The thrashing rate of the L1 and L2 lines was not reduced in response to levamisole to the same extent as the wild-type (N2) strain. Stars indicate significance of change in thrashing from $t = 0$ mins ($p = \leq .0001$ (****)). (Two-way ANOVA, Tukey's multiple comparison). b) Comparison of thrashing rates of all lines at each time point. Letters shared between bars indicate statistically homogeneous subsets (Two-way ANOVA, Tukey's multiple comparison). $N = 24$ for each line. Error bars represent SEM.

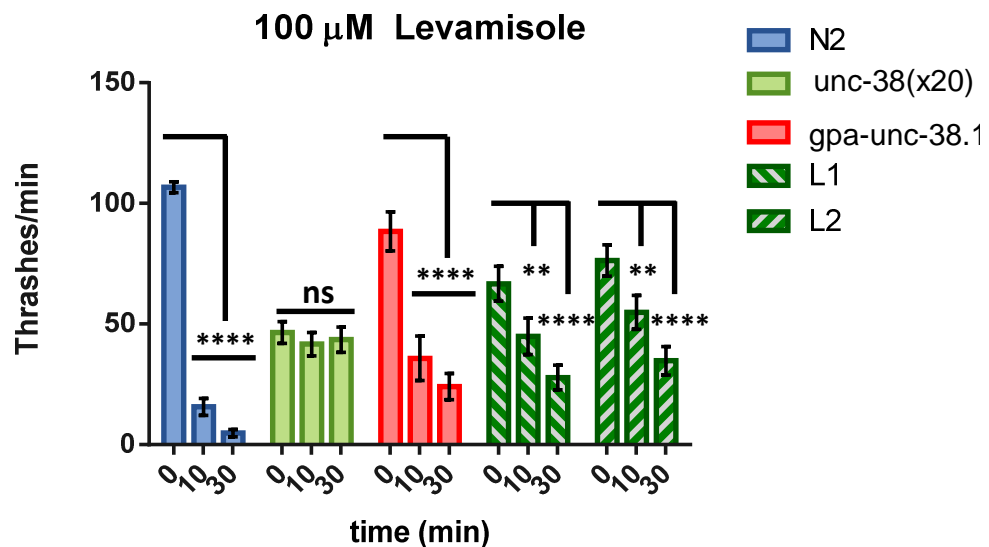
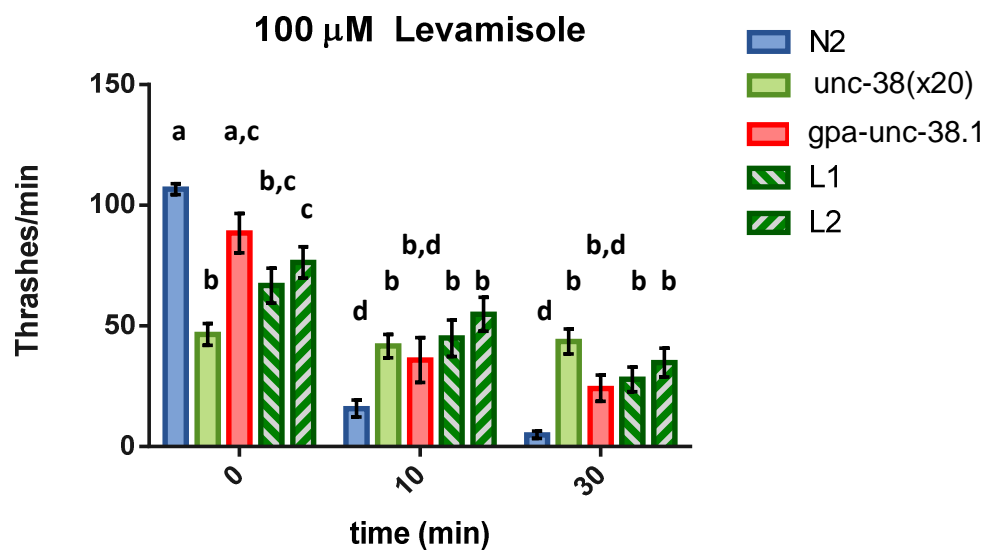
a**b**

Figure 6-20: Effect of 100 μ M levamisole on thrashing rate of *Gpa-unc-38.1-M302I*

N2, *unc-38(x20)* and *gpa-unc-38.1* were used as controls. Same data is presented organised by line and by time point. a) The thrashing rate of the L1, L2 and *gpa-unc-38.1* lines were less affected by levamisole than the wild-type (N2) strain. Stars indicate significance of change in thrashing from $t = 0$ mins ($p = \leq .01$ (**); $p = \leq .0001$ (****)). (Two-way ANOVA, Tukey's multiple comparison). b) Comparison of thrashing rates of all lines at each time point. Letters shared between bars indicate statistically homogeneous subsets (Two-way ANOVA, Tukey's multiple comparison). N = 24 for each line. Error bars represent SEM.

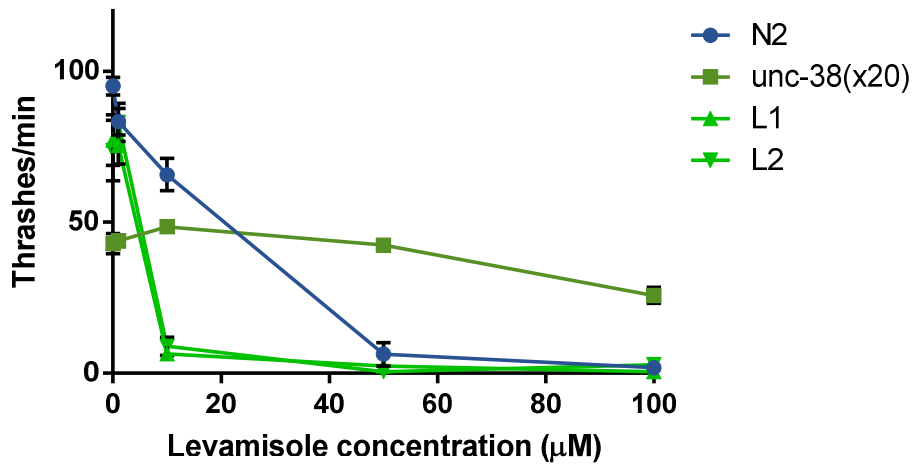


Figure 6-21: Thrashing rate at 30 mins over a range of levamisole concentrations for *Cel-unc-38-I301M*

Preliminary data for the *Cel-unc-38-I301M* transgenic lines indicated that these lines are much more sensitive to levamisole than the wild-type (N2) strain. This difference was particularly evident at 10 μM and 50 μM concentrations of levamisole. $N = 30$ for each levamisole concentration for each line. Error bars represent SEM.

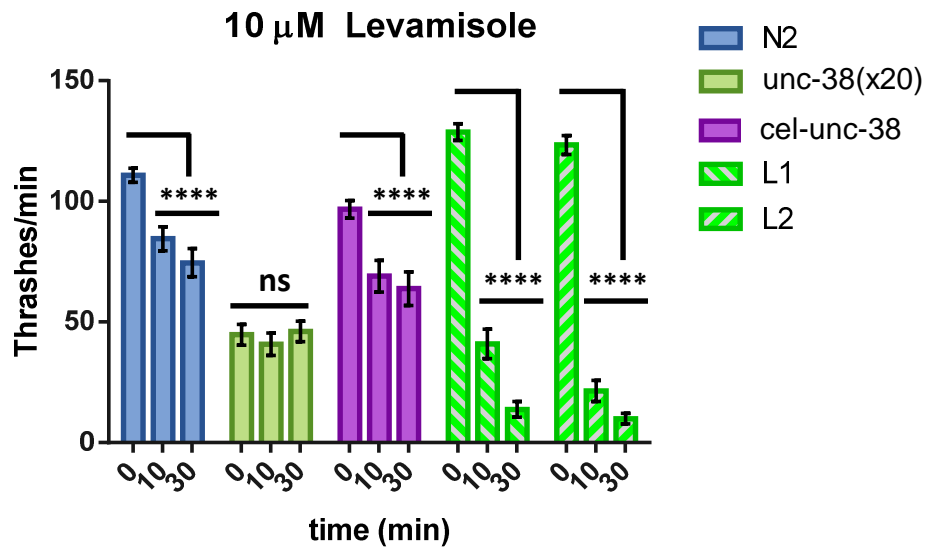
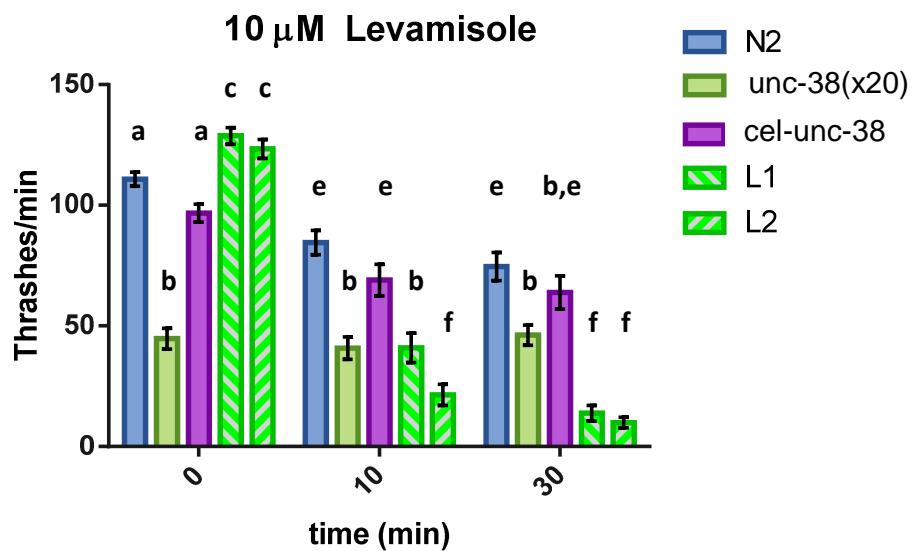
a**b**

Figure 6-22: Effect of 10 μ M levamisole on thrashing rate of *Cel-unc-38-I301M*

N2, *unc-38(x20)* and *cel-unc-38* were used as controls. Same data is presented organised by line and by time point. a) At 10 μ M, the thrashing rate of the L1 and L2 lines reduced more than the wild-type (N2) strain after 30 minutes levamisole exposure. For the wild-type line, thrashing rate fell by approximately 20%, and for L1 and L2 the thrashing rate fell by 90%. Stars indicate significance of change in thrashing from t = 0 mins ($p = \leq 0.0001$ (****)). (Two-way ANOVA, Tukey's multiple comparison). b) Comparison of thrashing rates of all lines at each time point. Letters shared between bars indicate statistically homogeneous subsets (Two-way ANOVA, Tukey's multiple comparison). N = 24 for each line. Error bars represent SEM.

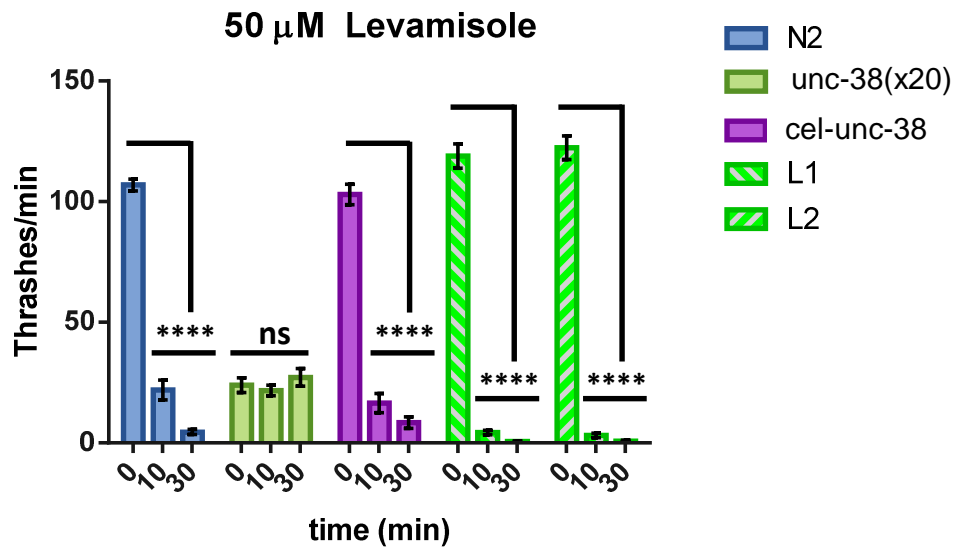
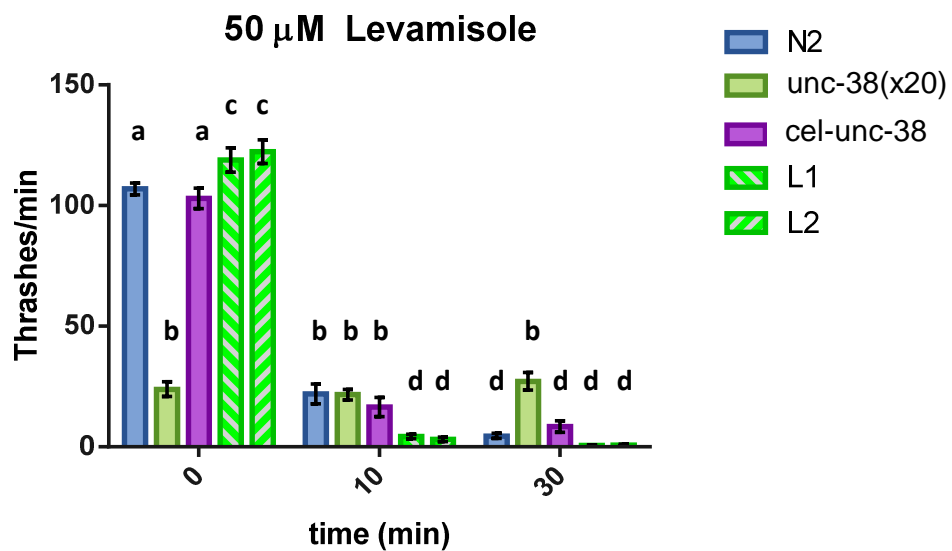
a**b**

Figure 6-23: Effect of 50 μ M levamisole on thrashing rate of *Cel-unc-38-I301M*

N2, *unc-38(x20)* and *cel-unc-38* were used as controls. Same data is presented organised by line and by time point. a) At 50 μ M levamisole, the thrashing rate of the wild-type (N2), *cel-unc-38* and L1 and L2 chimeric lines was reduced. Stars indicate significance of change in thrashing from t = 0 mins ($p = \leq 0.0001$ (****)). b) Comparison of thrashing rates of all lines at each time point. Letters shared between bars indicate statistically homogeneous subsets (Two-way ANOVA, Tukey's multiple comparison). N = 24 for each line. Error bars represent SEM.

6.4 Discussion

C. elegans has been used as a heterologous system to investigate anthelmintic resistance in parasitic nematodes in previous studies. Resistance of *H. contortus* to benzimidazoles is linked to a single phenylalanine to tyrosine amino acid change at position 200 in an allele of *tub-1* found in resistant *H. contortus* populations. *C. elegans* was used as a heterologous system to demonstrate that *H. contortus tub-1* containing Phe200 was able to rescue the sensitivity of *C. elegans ben-1* mutants to thiabendazole. In contrast, the Tyr200-containing allele of *H. contortus tub-1* was unable to rescue the benzimidazole sensitivity, so confirming its role in the observed resistance (Kwa *et al.* 1995).

Here, a similar approach has been used to investigate key amino acid residues within Gpa-UNC-38.1 which may be linked to differing functions of the gene such as its role as an α -subunit and the differences in levamisole sensitivity identified in Chapter 5. Although two orthologues of *Cel-unc-38* were identified, both Gpa-UNC-38.1 and Gpa-UNC-38.2 share similar key amino acid differences. For this reason, investigation of only *gpa-unc-38.1* was undertaken.

6.4.1 Considerations involved in working with transgenic lines of *C. elegans*

Transformation of *C. elegans* by microinjection does not produce a transgenic line in which the transgene perfectly mimics an endogenous gene. The extrachromosomal arrays produced by microinjection contain multiple copies of the introduced transgene and marker gene and copy number cannot be controlled. Expression level of the introduced transgene is therefore unpredictable. For these reasons multiple independent lines should be analysed to account for differences due to transgene copy number. Here, two independently transformed lines were obtained for each chimeric gene (apart from *Cel-unc-38-F174_N177delinsYPSG*). Additionally, each chimeric gene transgenic line was analysed alongside the line rescued with the non-chimeric gene, as a control for effects of the transformation technique.

Off-target effects of the marker gene must also be considered. The *myo-2::GFP* should not interfere with locomotion or thrashing rate, however the growth and development of transgenic worms was impaired for some lines (personal observation). This may be linked to toxic effects of overexpression of GFP in the pharyngeal muscles of *C. elegans*, which leads to the impairment of feeding ability (Anna Crisford, personal communications (Fleenor *et al.*)). Where possible, such lines were not used. Additionally, some lines exhibited low transmission rates of the extrachromosomal arrays to the progeny (e.g. <10%), which made it difficult to select sufficient transgenic worms for assays at the correct life-stage.

The transgene was expressed under control of the *myo-3* promoter which drives expression in the body-wall muscle. *Cel-unc-38* is expressed both in body-wall muscle and in neurones throughout the body (Gottschalk *et al.* 2005). Cel-UNC-38 has been shown to form part of a neuronal nAChR present in motor neurones that innervate the ventral and dorsal muscles. This neuronal nAChR forms a functional receptor consisting of Cel-UNC-38, Cel-ACR-2, Cel-ACR-3, Cel-UNC-63 and Cel-ACR-12 that is activated by acetylcholine, but not levamisole (Jospin *et al.* 2009). As *cel-unc-38* was able to fully rescue basal thrashing and levamisole sensitivity under the control of the *myo-3* promoter, and the neuronal receptor is not sensitive to levamisole, the role of this receptor was not investigated in this work. It is currently also unknown which subunits comprise the neuronal receptor in *G. pallida*.

6.4.2 Limitations of thrashing assay analysis

Thrashing assays are time-consuming to conduct, particularly if multiple lines are to be assessed on the same day to control for environmental variables. Preliminary data were therefore collected for each chimeric transgene line at all levamisole concentrations at a single time point to highlight any differences between these and the control lines and to identify which levamisole concentrations were of particular interest. Due to the fast thrashing rate of wild-type (N2) worms in liquid, thrashing assays are also subject to experimental error and fatigue. Software is available for the automated measurements of thrashing (Buckingham and Sattelle 2009). Attempts to create and optimise a similar approach with the equipment and software available in this laboratory were not successful.

Other factors such as temperature and age of worms also impact the thrashing rate of *C. elegans* (Mulcahy, Holden-Dye and O'Connor 2013). As ambient temperature of the laboratory could not be precisely controlled, this effect was mitigated by analysis of all lines for each levamisole concentration on the same day, and on two separate occasions. Life-stage was controlled by selection of L4-stage worms on the previous day, to ensure all worms analysed were at the same life-stage.

6.4.3 The YxxCC motif is non-essential in both *Gpa-UNC-38.1* and *Cel-UNC-38* to basal thrashing function of the reconstituted receptor

Work in Chapter 5 indicated that *gpa-unc-38.1* is able to rescue the basal thrashing rate of *C. elegans unc-38(x20)* mutants to wild-type levels, despite lacking the YxxCC motif involved in formation of the acetylcholine binding site. One possible explanation for this result is that *gpa-unc-38.1* is only required to perform a structural role in assembly of the receptor and does not directly take part in acetylcholine binding.

To test if removal of an agonist binding site could still lead to full rescue of basal thrashing a construct was made which removed the YxxCC motif from Cel-UNC-38

(*Cel-unc-38-N234_I242delinsHFFASKNGI*). This allowed the function of a receptor with only two non-consecutive agonist binding sites to be investigated. A reciprocal construct reintroduced the YxxCC motif from the *C. elegans* gene into Gpa-UNC-38.1 (*Gpa-unc-38.1-H236_I234delinsNYPSCCPGSA*) to produce a receptor with three agonist binding sites (Figure 6-24a).

Cel-unc-38-N234_I242delinsHFFASKNGI rescued basal thrashing to the same level as the wild-type strain and the line rescued with *cel-unc-38*. This supports the hypothesis that only two non-consecutive agonist binding sites are required for receptor function. The observed rescue of basal thrashing was therefore likely due to a structural requirement for an UNC-38-like subunit to reform the pentameric receptor structure, although acetylcholine binding occurs at agonist binding sites between other subunits. This seems to be analogous to the mechanism by which *Gpa-unc-38.1* rescues basal thrashing.

Similarly, no difference in basal thrashing was observed between lines rescued with *Gpa-unc-38.1-H236_I234delinsNYPSCCPGSA* and the native *Gpa-unc-38.1*. Here, three agonist binding sites are theoretically formed as the YxxCC motif has been introduced into the sequence of Gpa-UNC-38.1. However it is not known if this new agonist binding site is actually binding acetylcholine or if only two agonist binding sites are being used (Figure 6-24b). If the former is the case, then clearly the presence of an extra site is not affecting this aspect of receptor function.

No change in levamisole sensitivity compared with lines rescued by the unaltered counterparts was conferred by either *Cel-unc-38-N234_I242delinsHFFASKNGI* or *Gpa-unc-38.1-H236_I234delinsNYPSCCPGSA*. However the YxxCC motif is not predicted to be involved in levamisole binding.

6.4.4 The glutamate residue in loop B of Cel-UNC-38 may not be involved in levamisole sensitivity

Cel-UNC-38 has a glutamate residue in loop B of the extracellular domain. In a study conducted by Rayes *et al.* (2004), replacement of a glycine residue with a glutamate residue in a similar position in loop B of mouse α -subunits increased channel opening by levamisole. Mutation of other residues in loop B did not affect levamisole sensitivity. It was reasoned that the absence of a glutamate residue in this position in Gpa-UNC-38.1 may be responsible for its inability to fully restore levamisole sensitivity in the rescue experiments described in 5.3.7. Thus chimeric genes were created to test this hypothesis. The glutamate residue was removed from Loop B of Cel-UNC-38 by swapping in the Gpa-UNC-38.1 Loop B sequence creating the chimeric gene *Cel-unc-38-F174_N177delinsYPSG*. Accordingly the glutamate residue was introduced into Loop B of Gpa-UNC-38.1 creating *Gpa-unc-38.1-Y175_G178delinsFSEN*.

The construct *Gpa-unc-38.1-Y175_G178delinsFSEN* rescued basal thrashing activity of the *unc-38(x20)* mutant, indicating that it assembled normally to form the L-nAChR in *C. elegans*. However, no increase in levamisole sensitivity was observed and the thrashing rates of the two chimeric transgene lines remained higher than that of the N2 worms in response to 50 and 100 µM levamisole. This indicates that the absence of the glutamate residue in loop B of Gpa-UNC-38.1 does not account for the reduced levamisole sensitivity. In loop B of other α-subunits a tyrosine and glycine residue are also involved in forming the acetylcholine binding pocket. Both Cel-UNC-38 and Gpa-UNC-38.1 lack these residues. The change effected in loop B of *Gpa-unc-38.1-Y175_G178delinsFSEN* also does not seem to affect acetylcholine binding as basal thrashing is unaffected.

Unfortunately, due to technical issues a full analysis of *Cel-unc-38-F174_N177delinsYPSG* could not be undertaken as only a single transgenic line was generated for this construct. The slow-growth of the lines can most likely be attributed to the toxic nature of the *pmyo-2::GFP* marker gene at high concentrations rather than expression of the chimeric gene (Fleenor *et al.*). Transmission of the marker gene to the next generation was low, but within the parameters expected for microinjection.

Some cautious conclusions can nevertheless be drawn from the preliminary data generated for *Cel-unc-38-F174_N177delinsYPSG* 50 µM and 100 µM levamisole. The data suggest that the basal thrashing rate of this line is fully rescued and that levamisole sensitivity is the same in the chimeric transgene line and wild-type worms. If the presence of a glutamate residue in loop B was responsible for levamisole sensitivity in nematode muscle, it would be expected that its removal would increase levamisole resistance.

Although Rayes *et al.* (2004) addresses the mutation of a mammalian α-subunit to include a glutamate in loop B and the subsequent increase in opening of the receptor in response to levamisole, the reciprocal mutation of removing the glutamate from loop B of Cel-UNC-38 and analysing channel opening response was not undertaken.

Here, the removal of the glutamate residue from loop B of Cel-UNC-38 did not increase levamisole resistance and nor did addition of a glutamate residue into loop B of Gpa-UNC-38.1. The glutamate in loop B may not play such an important role in levamisole sensitivity as previously stated however fundamental differences in the experiments carried out should be considered. Rayes *et al.* (2004) expressed the mutagenised mammalian α-subunits in HEK293 cells (along with β, δ, and ε subunits that comprise a mammalian-type receptor) and receptor opening currents in response to perfusion with agonists were measured using patch clamp techniques. This does not report on the effect of increased channel opening on the muscle and whether or not this increase would be physiologically relevant. Equally, the experiments described

here do not report on the changes in channel opening properties of the receptor caused by these chimeric genes. It may be that channel opening properties have changed, but are not translated to a phenotype which can be assessed by thrashing assays. Expression of the chimeric subunits in *Xenopus* oocytes and measurement of changes in channel opening rates in response to levamisole and acetylcholine would be beneficial to confirm these observations.

6.4.5 Amino acid changes in transmembrane domain 2 affect channel opening properties in response to agonist binding

The second transmembrane domain of each subunit of cys-loop ligand-gated ion channels contributes towards forming the lining of the central channel pore (Figure 6-25a). A combination of pore diameter and the characteristics of the amino acids orientated towards the lining of the channel pore affect what can pass through. Typically negatively charged amino acids are present at the intracellular mouth of cation selective channels (Keramidas *et al.* 2004).

Mutations at position 13 in transmembrane domain 2 of nAChRs of *C. elegans* (Treinin and Chalfie 1995; Jospin *et al.* 2009) produce receptors with irregular functions. Mutations in this position in human-type nAChRs have also been linked to the disease myasthenia gravis. In Gpa-UNC-38.1, a methionine is present at position 13 on transmembrane domain 2 whereas the equivalent residue in Cel-UNC-38 is an isoleucine. A mutation from a valine to a methionine residue in this position in Cel-ACR-2 produced a gain-of-function mutant termed *acr-2(n2420gf)* (Figure 6-25b). These worms convulse, are uncoordinated and are more sensitive to aldicarb and levamisole in paralysis assays (Jospin *et al.* 2009 (Fig 2C)). Gpa-UNC-38.1 does not have an increased sensitivity phenotype compared to Cel-UNC-38 and therefore chimeric genes were created to test the importance of this residue in receptor function.

The chimeric gene *Gpa-unc-38.1-M302I* was unable to rescue basal thrashing, although thrashing rate was significantly higher than the *unc-38(x20)* background indicating that some rescue of basal thrashing had occurred, although not to wild-type levels. Resistance to levamisole also remained higher than wild-type in these lines. In contrast, the chimeric gene *Cel-unc-38-I301M* conferred both increased sensitivity to levamisole and increased basal thrashing rate. This increased levamisole sensitivity was particularly pronounced at 10 µM levamisole. This observation is similar to that observed by Jospin *et al.* (2009), with a valine to methionine change at this position in transmembrane domain 2 in the *acr-2(n2420gf)*. When Cel-ACR-2(V13'M)R was expressed in *Xenopus* oocytes with the remaining subunits of the *C. elegans* neuronal receptor, sensitivity to DMPP was increased greatly and sensitivity to levamisole and choline increased slightly compared to the wild-type receptor (Jospin *et al.* 2009 (Fig 7 A and B)). The phenotype of this line was hypothesised to be due to increased excitability of the neurons expressing *acr-2(n2420gf)* and increased calcium influx.

However, unlike *acr-2(n2420gf)*, no convulsive phenotype was observed for *Cel-unc-38-I301M*. As *acr-2* is expressed in the VA, VB, DB and DA neurons (Figure 1-4), which are involved in regulating the balance between the excitation and inhibition that drives locomotion in *C. elegans*, the increase in activity caused by *acr-2(n2420gf)* may disrupt this balance (Jospin *et al.* 2009). *Cel-unc-38-I301M*, under the *myo-3* promoter, would only be expressed in the body wall muscle and not the interconnecting neurons and thus would not play a role in balancing excitation and relaxation. The faster rate of basal thrashing may be due to increased activation of the L-nAChR expressed in the body wall, leading to increased calcium influx and increased muscle contraction. As the worms of this line thrash normally, albeit faster, it is not known how the balance of relaxation is maintained. The increased thrashing rate of *Cel-unc-38-I301M* is likely due to a hyperactive response to acetylcholine, as observed for the *acr-2(n242gf)* mutant (Jospin *et al.* 2009 (Fig 5a)).

The increased sensitivity of *Cel-unc-38-I301M* may be due to similar mechanisms. Although binding of levamisole to the receptor is likely to remain unchanged, the channel could remain open for longer leading to increased calcium influx and increased muscle contraction. It follows that levamisole affects paralysis by the same mechanism (unbalanced activation of L-nAChR in the body-wall muscle), but as the receptor is more highly excitable, paralysis occurs at a lower dose. It is unclear why a methionine residue in this position affects conductance. Both a valine to methionine change (as in *acr-2(n2420gf)*) and an isoleucine to methionine change (as in *Cel-unc-38-I301M*) are substitutions of one hydrophobic amino acid for another hydrophobic amino acid. However, it seems clear that the presence of a methionine in this position alters the pore domain in a way which increases receptor activity.

It has been demonstrated that a methionine in this position in *acr-2* (Jospin *et al.* 2009) and in *Cel-unc-38-I301M* increases the sensitivity of the *C. elegans* mutant to levamisole probably due to increased excitability of the receptor. It follows that Gpa-UNC-38.1 should also show some evidence of increased receptor excitability due to the methionine in TM2. Removal of a methionine from Gpa-Unc-38.1 impairs the ability of *Gpa-unc-38.1-M302I* to rescue basal thrashing, which suggests it has a more fundamental role in this subunit.

6.4.6 The basis of levamisole resistance for Gpa-UNC-38.1 has not been established

Gpa-UNC-38.1-transformed *unc-38(x20)*-worms have higher levamisole resistance than wild-type *C. elegans*. As *unc-38(x20)* transformed with Cel-UNC-38 displayed wild-type levamisole sensitivity, it is unlikely that this increased resistance is a side-effect of the microinjection technique. In this chapter, the molecular basis of the increased resistance was explored by focusing on candidate amino acid residues identified from the literature (Jospin *et al.* 2009; Rayes *et al.* 2004). The consequence of Gpa-UNC-38.1 lacking the characteristics of an α -subunit was also investigated.

None of the changes made to Gpa-UNC-38.1 restored levamisole sensitivity to this subunit, and no changes increased the resistance to levamisole of Cel-UNC-38. One of the analysed chimeric constructs (*Cel-unc-38-I301M*) conferred increased sensitivity, which has raised more questions about the levamisole resistance of Gpa-UNC-38.1.

There is currently an apparent discrepancy between the data obtained for expression of Gpa-UNC-38.1 in *Xenopus* oocytes (which does not seem to indicate an increase in levamisole resistance associated with this subunit) and the result obtained by thrashing analysis of transgenic mutant lines carrying Gpa-UNC-38.1 and the chimeric transgene Gpa-UNC-38.1 constructs (which consistently show increased levamisole resistance). Further work is required to rationalise this data from two different experimental techniques, which may be due to the difference between expression in a heterologous and endogenous system. The expression of the chimeric transgenes in described in this chapter in *Xenopus* oocytes may be beneficial in this regard.

6.4.6.1 Cel-UNC-38 has been defined as an α -subunit, but may not be directly involved in agonist binding

Cel-UNC-38 is defined as an α -subunit due to the presence of the vicinal cysteines in loop C of the extracellular domain. Loop B however lacks some residues associated with acetylcholine binding, although it is unclear how stringently required these residues are for formation of the acetylcholine binding pocket.

An interesting result from this work is that removal of the YxxCC motif from Cel-UNC-38 does not have an overall effect on the ability of the receptor to bind acetylcholine as basal thrashing is rescued to wild-type levels. This has two possible explanations: Multiple agonist binding sites, including one formed by Cel-UNC-38, may be present on the receptor and removal of one still leaves sufficient agonist binding sites for acetylcholine binding and receptor function. Alternatively, Cel-UNC-38 may not normally form a functional agonist binding site at all (due to differences in residues of Loop B) and therefore the removal of the YxxCC motif does not affect basal thrashing as it never formed a binding site.

Although recordings from receptors were generated by expression of only *cel-lev-1*, *cel-unc-29* and *cel-unc-38* in *Xenopus* oocytes (Fleming *et al.* 1997), the currents elicited by acetylcholine were very low. However, as *cel-unc-38* is the only α -type subunit in that mix, it must be able to contribute towards the binding of acetylcholine to some extent, albeit inefficiently. Equally, the low currents generated with this combination of subunits in *Xenopus* oocytes may also be due to the fact that several required subunits (*lev-8* and *unc-63*) were absent (Boulin *et al.* 2008). If this were the case, Cel-UNC-38 may also be fulfilling a merely structural role in the receptor rather than having a direct role in acetylcholine binding. It may also explain the loss of the YxxCC motifs from the plant-parasitic nematode UNC-38s. If Cel-UNC-38 does not

provide an acetylcholine binding site, and nor does the UNC-38 of the common ancestor between *C. elegans* and plant-parasitic nematodes, the selection pressure to keep the residues may be removed.

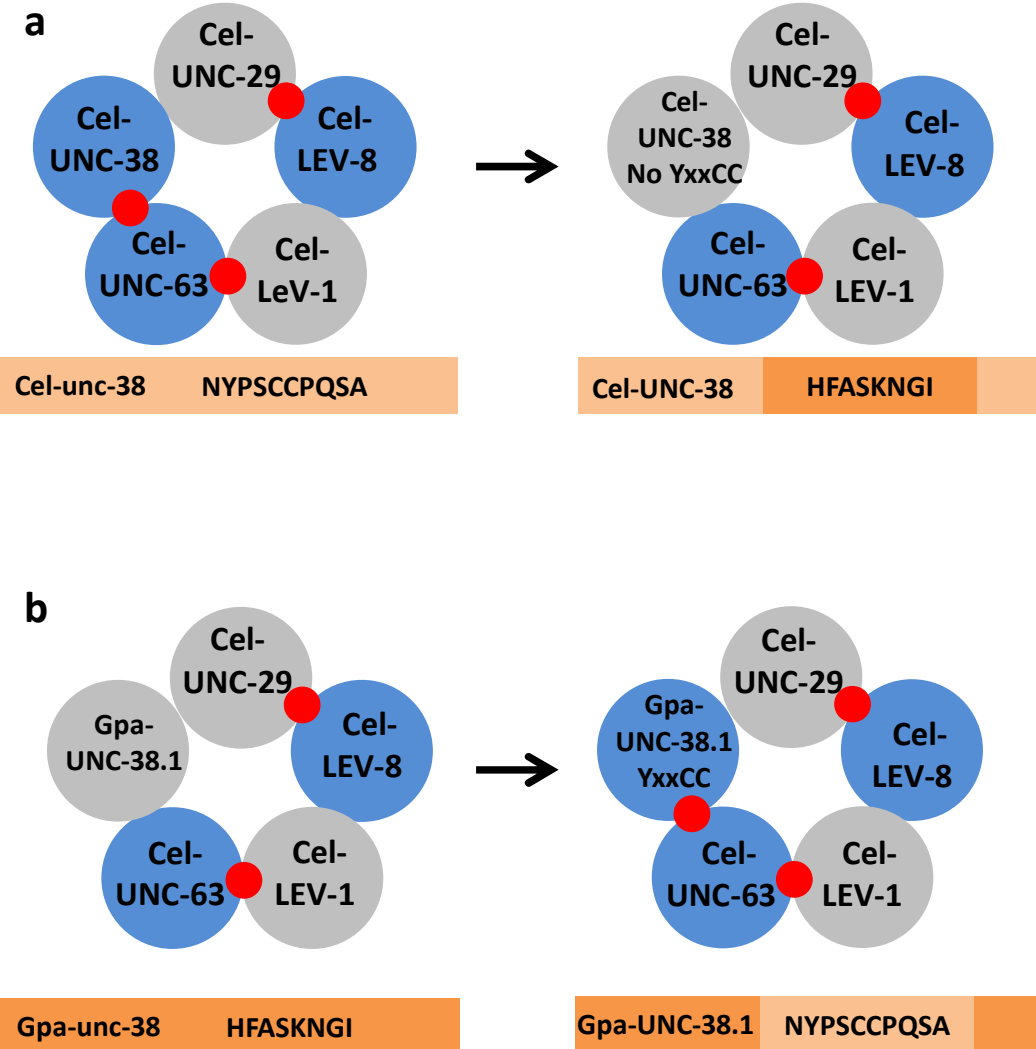


Figure 6-24: Schematic of potential effects of addition or removal of the YxxCC motif from *gpa-unc-38.1* or *cel-unc-38*

a) Removal of the YxxCC motif from Cel-UNC-38 should remove an agonist binding site, leaving only two in the receptor containing chimeric Cel-UNC-38. b) Addition of a YxxCC motif to Gpa-UNC-38.1 could possibly form a third agonist binding site in the receptor containing the chimeric gene. Potential agonist binding sites are represented by the red circles, α -subunits are coloured in blue and non- α subunits are coloured in grey.

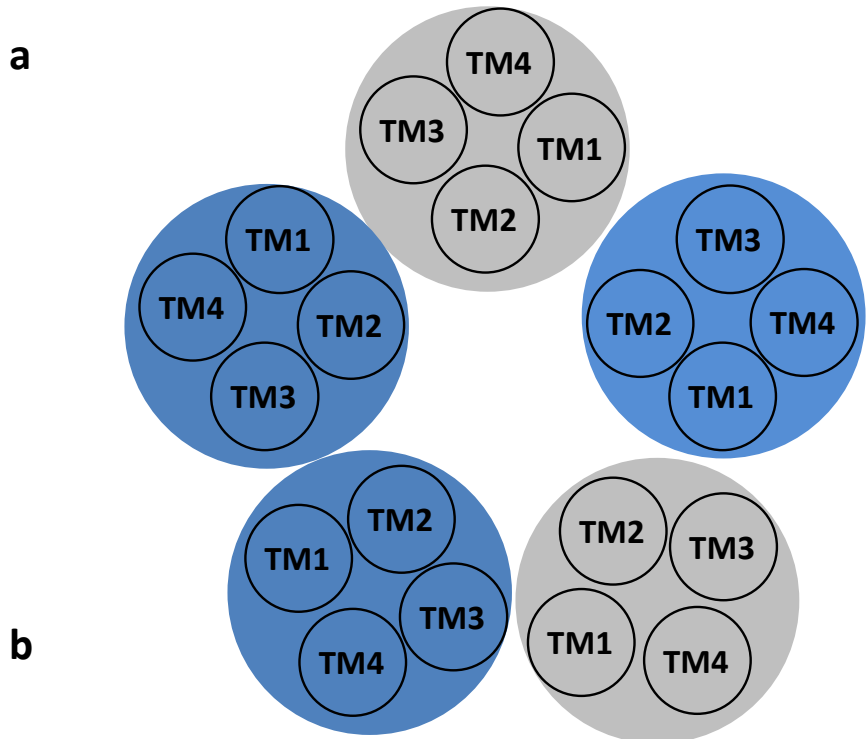


Figure 6-25: Schematics of the transmembrane 2 (TM2) region of nAChR subunits

a) Orientation of TM2 towards the inside of the pore in the pentameric receptor. b) Adapted from Jospin *et al.* (2009). Alignment of TM2 region of Gpa-UNC-38, Cel-UNC-38 and Cel-ACR-2. Residues coloured in red are orientated towards the pore. If position 13 is mutated to a methionine residue in Cel-ACR-2 or Cel-UNC-38 locomotion and levamisole sensitivity phenotypes are observed.

Summary

- Gpa-UNC-38.1 rescues basal thrashing by structural reformation of the receptor rather than direct binding of acetylcholine
- Glutamate residue in Loop B has no impact on levamisole sensitivity
- Alterations in transmembrane domain 2 affect levamisole sensitivity of Cel-UNC-38
- Basis of levamisole resistance of Gpa-UNC-38.1 not identified

7. GENERAL DISCUSSION

7.1 Host-seeking is a common and essential behaviour for plant-parasitic nematodes

All plant-parasitic nematodes must be able to locate and move towards their host in the soil. Host invasion also requires co-ordinated movement and migration through host-root tissue to reach a suitable position in which to induce a feeding site. Disruption of these processes has been demonstrated to impair the ability of the nematode to infect their host. Expression *in planta* of a synthetic peptide which disrupts chemoreception has been demonstrated to reduce the ability of *G. pallida* to infect by 50% (Liu *et al.* 2005). This technology has been successfully used to generate transgenic plantain with a level of resistance in the field against *Radopholus similis* and *Helicotylenchus multicinctus* (Tripathi *et al.* 2015). Other methods used to disrupt chemosensation and locomotion include the targeting of *fhp*-genes. Downregulation of *fhp-18* induced by RNAi reduced the ability of *M. incognita* to infect tomato roots by reducing the number of J2s which reached the root (Dong *et al.* 2013).

J2s, once hatched from the egg, are reliant on reaching host roots in order to complete the life cycle. As J2s do not feed during the infective stage, locomotion and host-invasion rely on limited, stored lipid reserves. The utilisation of this lipid reserve is slow - an estimated 50% of total lipids is used 36 days after hatching (Storey 1984) - but hatched J2s are more vulnerable to other abiotic effects such as desiccation. The induction of paralysis or disruption of chemoreception therefore affects J2s by increasing the use of lipid reserves and the time spent in the soil where they are vulnerable to abiotic factors.

The neuromuscular system is essential for coordinated movement and drugs targeting this system can induce paralysis and inhibit invasion behaviours. Targeting of this system would also affect males of amphimictic species, such as cyst nematodes. In these species the male must be able to locate the female on the root in order for fertilisation to occur (Riga *et al.* 1996).

7.2 Differences in complement of cys-loop receptors indicate that *G. pallida* and *G. rostochiensis* may have distinct pharmacological neuromuscular targets

The key aspects of neurotransmission, such as the neurotransmitters used, are likely to be the same in *C. elegans*, *G. pallida* and *G. rostochiensis*. This is supported by the identification of genes involved in neurotransmitter synthesis in *G. pallida* and *G. rostochiensis* as well as previous published work exploring the response of J2s to exogenously applied neurotransmitters (see 3.4.2).

Differences in the complement of cys-loop receptors present in *G. pallida* and *G. rostochiensis* were identified for the glutamate-gated chloride channel family and the nicotinic acetylcholine receptor subunit family. The differing composition of receptors due to the different complement of cys-loop receptor subunits may affect their pharmacology, and sensitivity to the anthelmintics that are known to target these receptors. In *C. elegans*, *cel-glc-1*, *cel-avr-14* and *cel-avr-15* have been linked to ivermectin sensitivity (Dent *et al.* 2000). In *G. pallida* and *G. rostochiensis*, orthologues for *cel-glc-1* and *cel-avr-15* have not been identified. Two orthologues of *cel-avr-14* were identified, although it is not known whether or not both confer sensitivity to ivermectin in the plant-parasitic nematodes. The gene *hco-glc-5* has been shown to be involved in the ivermectin sensitivity of *H. contortus* (Glendinning *et al.* 2011), demonstrating that glutamate-gated chloride channel subunits not present in *C. elegans* may also be involved in ivermectin sensitivity.

For nAChR subunits, *G. pallida* and *G. rostochiensis* have fewer members than *C. elegans* with 20 nAChRs identified in the plant-parasitic nematodes and 28 in *C. elegans*. In addition to these 28 genes in *C. elegans*, there are three more predicted nAChRs the function of which has not yet been analysed (Rand 2006). In particular, the ACR-16 group of *G. pallida* and *G. rostochiensis* is smaller than that of *C. elegans* with orthologues identified for only four out of the ten members. Although orthologues of most members of the UNC-38, UNC-29 and ACR-8 groups were identified in *G. pallida* and *G. rostochiensis*, orthologues of all genes known to comprise the levamisole-sensitive nicotinic acetylcholine receptor of *C. elegans* were not found. This receptor comprises Cel-UNC-38, Cel-UNC-63, Cel-UNC-29, Cel-LEV-1 and Cel-LEV-8 (Boulin *et al.* 2008; Lewis *et al.* 1980) in *C. elegans*, but orthologues for *cel-lev-1* and *cel-lev-8* were not identified in *G. pallida* and *G. rostochiensis*. Two orthologues were also identified for *cel-unc-38* and *cel-unc-29* in both plant-parasitic nematode species. In other parasitic nematode species where the levamisole-sensitive nicotinic acetylcholine receptor has been investigated, similar losses and duplications have taken place. *H. contortus* lacks an orthologue of *cel-lev-8*, and although an orthologue of *cel-lev-1* can be found it lacks a signal peptide. Four orthologues of *cel-unc-29* have also been found in *H. contortus*. *A. suum* lacks orthologues for both *cel-lev-1* and *cel-lev-8* and a single orthologue has been identified for each of *cel-unc-38*, *cel-unc-29* and *cel-unc-63* (Williamson *et al.* 2009). Receptors comprising differing complements of these subunits, were found to have different pharmacological properties, affecting sensitivity to levamisole amongst other receptor agonists (Boulin *et al.* 2011; Williamson *et al.* 2009; Buxton *et al.* 2014). In the *H. contortus* receptor, Hco-ACR-8 was found to play an essential role in levamisole sensitivity (Boulin *et al.* 2011).

7.3 Bioassays and functional experimentation supported a difference in resistance to levamisole and linked it to *Gpa-unc-38.1*

Both *G. pallida* and *G. rostochiensis* were found to be more resistant to levamisole than *C. elegans*. A comparison of EC₅₀ values suggested that the two plant-parasitic nematode species were 500-2000 fold more resistant than *C. elegans* (Qian *et al.* 2008). As the L-nAChR of *G. pallida* and *G. rostochiensis* must differ from that of *C. elegans*, and as the composition of the receptor had been shown to affect sensitivity to agonists in the literature, it was hypothesised that this increased resistance to levamisole found in *G. pallida* was due to differences in the composition of the native receptor.

As the loop B region of *cel-unc-38* had been identified as particularly important in the levamisole sensitivity of *C. elegans* (Rayes *et al.* 2004), the amino acid sequences of *Gpa-unc-38.1* and *gpa-unc-38.2* were investigated. The glutamate residue linked to levamisole sensitivity (Rayes *et al.* 2004) was found to be absent in loop B of both *gpa-unc-38.1* and *gpa-unc-38.2*. Additionally, the absence of residues in loop C essential for acetylcholine binding, particularly the lack of the vicinal cysteines (Kao *et al.* 1984), was also found in both genes. This was predicted to affect function of the subunit. *Gpa-unc-38.1* was tested for its ability to rescue the phenotype of *unc-38(x20)* mutants, which are uncoordinated and levamisole resistant (Lewis *et al.* 1987; Fleming *et al.* 1997). *Gpa-unc-38.1* was able to rescue basal thrashing activity of the receptor, suggesting reconstitution of the L-nAChR by replacing *cel-unc-38*, but not levamisole sensitivity. However, when *Gpa-unc-38.1* was expressed alongside *cel-unc-29*, *cel-unc-63*, *cel-lev-1* and *cel-lev-8* in *Xenopus* oocytes, the sensitivity to levamisole was not found to differ from the native *C. elegans* receptor.

7.4 Motif swaps between *Cel-unc-38* and *Gpa-unc-38.1* did not elucidate the basis of levamisole resistance of *G. pallida*

Gpa-unc-38.1 was able to rescue thrashing rate of *unc-38(x20)* mutants, but not full levamisole sensitivity. Chimeric genes have been used to investigate insect-nicotinic acetylcholine receptors, where regions hypothesised to be responsible for imidacloprid sensitivity were substituted into the chicken $\alpha 4$ -subunit to investigate if imidacloprid sensitivity could be conferred (Shimomura *et al.* 2005). A similar approach was used to investigate key motifs of *Gpa-unc-38.1*. Addition of the YxxCC motif to *gpa-unc-38.1* and removal of the motif from *cel-unc-38* did not affect the rescue of basal thrashing, indicating that acetylcholine was binding between different subunits on the reconstituted receptor. This suggested that *gpa-unc-38.1* played a structural role in rescuing basal thrashing and receptor function. Addition of the Loop B glutamate reported to be involved in levamisole sensitivity (Rayes *et al.* 2004) to *gpa-unc-38.1* did not increase levamisole sensitivity, and the removal of the Loop B glutamate from *cel-unc-38* did not increase levamisole resistance. This suggested that the role of the

loop B glutamate may not be critical to levamisole resistance. Levamisole sensitivity was increased by substitution of a methionine into transmembrane domain 2 of *cel-unc-38*. A similar hyperactivity of the receptor has been observed by a valine to methionine change in the same position of transmembrane domain 2 in *cel-acr-2* (Jospin *et al.* 2009). Removal of the methionine residue for an isoleucine residue in *gpa-unc-38.1* did not affect levamisole sensitivity, but affected the ability of the construct to rescue basal thrashing. This highlighted the importance of transmembrane domain 2 in its ability to affect sensitivity of the receptor, as this region lines the channel pore and affects channel opening properties (Keramidas *et al.* 2004).

7.5 The levamisole resistance of *G. pallida*

The molecular basis for the increased levamisole resistance found in *Gpa-unc-38.1*-rescued lines was not identified by the experiments conducted. This may be due to other residues within the Gpa-UNC-38.1 sequence which were not explored in this work, or the increased resistance may be due to changes in conformation of the other four subunits which led to levamisole binding less efficiently. Although it has been observed consistently that transgenic lines carrying *gpa-unc-38.1* or any of the chimeric variations increased levamisole resistance compared to wild-type and *cel-unc-38*-rescued lines, the data obtained when *gpa-unc-38.1* was expressed in *Xenopus* oocytes with the remaining *C. elegans* subunits did not identify a significant difference between channel activities elicited by levamisole compared to the native *C. elegans* receptors.

7.5.1 The whole native *G. pallida* receptor must be considered

The reconstitution of the whole native *G. pallida* receptor in *Xenopus* oocytes will allow the basis of levamisole resistance to be resolved as it would allow the pharmacology of the whole receptor to be characterised. However, many nAChR subunits (at least 20) are present in *G. pallida* and identifying which of these are likely to make up the native *G. pallida* L-nAChR requires consideration. This work may be guided by evidence provided from work on other parasitic nematodes such as *H. contortus* (Boulin *et al.* 2011), *A. suum* (Williamson *et al.* 2009) and *O. dentatum* (Buxton *et al.* 2014). However, these nematodes are more closely related to *C. elegans* and there may have been more divergence in the composition of this receptor over the evolutionary distance between *C. elegans* and plant-parasitic nematodes.

Due to the possibility that the roles of nAChR subunits may be very different in plant-parasitic nematodes, a cautious approach may include the use of *G. pallida* promoter sequences to drive GFP expression to identify where these candidate genes are expressed. As no transformation technique exists for *G. pallida*, *C. elegans* would have to be used as a heterologous system for this work. Some success for using

G. pallida promoter regions of nAChRs to drive GFP expression has already been achieved indicating that this may be a good approach. However, differences in the promoter regions between the species and how they interact with transcription factors may lead to differences in the patterns of expression.

The simple expression of candidate subunits in *Xenopus* oocytes without establishing whether or not they are likely to be expressed in the same place may be problematic as some subunits can be represented in multiple pentameric receptors. For example, Cel-UNC-38 in *C. elegans* is part of the L-nAChR and the neuronal nAChR (Jospin *et al.* 2009) and Cel-ACR-12 is part of the neuronal receptor, but has also been identified as a member of a separate receptor present in GABAergic neurons (Pettrash *et al.* 2013).

The possibility that a range of receptors consisting of different combinations and ratios of nAChR subunits may be present in the body-wall muscle of *G. pallida*, as is found in *O. dentatum* (Robertson, Bjorn and Martin 1999) cannot be excluded.

7.5.2 Other genes that are not nAChRs have also been associated with levamisole resistance

Other genes have been associated with levamisole resistance in *C. elegans*, but have not been considered in this work. Some proteins modulate levamisole sensitivity by affecting the efficiency of receptor assembly, or by affecting downstream signalling events.

UNC-50, RIC-3 and UNC-74 are accessory proteins, involved in the correct assembly of the receptor. These are also the ancillary factors that are essential for expression of the receptor in *Xenopus* oocytes (Boulin *et al.* 2008). RIC-3 is a chaperone protein, located in the endoplasmic reticulum and is involved in folding and processing (Millar 2008). UNC-74 is a thioredoxin and assists in the correct folding of proteins by promoting disulphide bond formation. UNC-50 is present in the Golgi apparatus, and is required for correct trafficking of nAChR subunits. The absence of any of these affects levamisole sensitivity by altering the number of functional L-nAChRs that are expressed. NRA-2 and NRA-4 are present in the endoplasmic reticulum and affect subunit composition (Almedom *et al.* 2009).

Other proteins that have been shown to interact with the L-nAChR are TAX-6, a calcineurin, which negatively regulates receptor function; NRA-1, a copine, which controls expression levels of synaptic levamisole receptors and SOC-1, an adaptor protein, which is also involved in receptor expression (Gottschalk *et al.* 2005). The OIG-4, LEV-9 and LEV-10 proteins function as a complex and its presence facilitates clustering of L-nAChRs at the neuromuscular junction (Rapti, Richmond and Bessereau 2011; Gally *et al.* 2004). MOLO-1, a single-pass transmembrane protein associates with L-NAChRs and acts as an auxiliary protein (Boulin *et al.* 2012). TPA-1 is predicted to be

involved in phosphorylation and the adaptation response of the receptor (Waggoner *et al.* 2000).

UNC-68, UNC-22 and UNC-11 are involved in the contraction of the body wall muscle. UNC-68 is a ryanodine receptor, which amplifies the calcium signal caused by opening of the L-nAChR by releasing stored calcium ions to generate sufficient levels of calcium for muscle contraction (Maryon, Coronado and Anderson 1996). UNC-22 and LEV-11 encode muscle proteins which are essential for muscle contraction. Mutations of these confer levamisole resistance by reducing response to the drug (Martin *et al.* 2012; Williams and Waterston 1994; Moerman *et al.* 1988).

A search for orthologues of these genes in the genome sequence of *G. rostochiensis* shows that orthologues for all of these genes with the exception of SOC-1 are present. As most of these genes are associated with the clustering of nAChRs or the mediation of muscle contraction downstream of the receptor, it may be expected that impaired locomotion would be observed if they were involved in levamisole resistance. However, as the J2s of most species move in a coordinated manner, these genes are likely to function normally.

7.5.3 Mechanisms of levamisole resistance in animal-parasitic nematodes

Resistance to levamisole in animal-infecting nematodes has attracted particular attention in the literature (Kaplan 2004). The molecular mechanisms behind the levamisole resistance of some parasitic nematodes have been identified, and to date all are linked to subunits of the L-nAChR.

In *O. dentatum*, levamisole resistance has been linked to the loss of a specific receptor in body wall muscle (Robertson, Bjorn and Martin 1999), which has been shown to correlate to a receptor consisting of the subunits Ode-UNC-29, Ode-UNC-63, Ode-UNC-38 and Ode-ACR-8 (Buxton *et al.* 2014). Comparison between transcriptomes of resistant and sensitive isolates of *O. dentatum* identified the downregulation of *Ode-unc-63* and the upregulation of *Ode-acr-21* and *Ode-acr-25* in the resistant isolates. This suggested that loss of one acetylcholine receptor type could be compensated for by upregulation of another to allow continued activation of the body wall muscle (Romine, Martin and Beetham 2014).

The expression of truncated transcripts of nAChR subunits, often produced by alternate splicing, has also been associated with levamisole resistance. Truncated transcripts of *Hco-acr-8b*, generated by a splice variant of the gene, have been linked to levamisole resistance in *H. contortus* (Fauvin *et al.* 2010). Reduced transcription of *Hco-unc-63a* and *Hco-unc-29* has also been linked to levamisole resistance of *H. contortus* (Sarai *et al.* 2013). Truncated transcripts of *unc-63* were also found in

levamisole resistant isolates of *H. contortus*, *T. circumcincta* and *T. colubriformis* (Neveu *et al.* 2010; Boulin *et al.* 2011).

These observations highlight that changes to the L-nAChR subunit composition is sufficient to alter levamisole sensitivity.

7.6 Cys-loop receptors are a diverse class and are the target of many anthelmintics and antiparasitics

Cys-loop receptors are the targets of many drugs used to control nematodes of both veterinary and human importance, as well as the target of drugs used to control insect pests. Different drugs target different classes of cys-loop receptors. The three widely used antiparasitics ivermectin, levamisole and fipronil target glutamate-gated chloride channels, nicotinic acetylcholine receptors and GABA-gated chloride channels respectively.

Recent use of genomics has revealed that different species have different complements of cys-loop receptors. The glutamate-gated chloride channels are unique to invertebrates making these a potential target for drugs that do not affect vertebrate hosts. However, among invertebrates differences in the complement of cys-loop receptors also exist, leading to different compounds having a greater effect on some species than others. A list of drugs that target cys-loop receptors is provided in Table 9.

The nAChRs in particular have been used as a target for drugs designed against nematode infection, as well as other pests. The diversity of nAChR subunits present between different species has made them a useful target. In mammals, 16 genes encode nicotinic acetylcholine receptors (Millar and Gotti 2009), in insects 10-12 nAChR genes have been found (Jones and Sattelle 2010) and in nematodes the range seems to be particularly variable with only 8 nAChR-encoding genes having been identified in *T. spiralis* so far (Williamson, Walsh and Wolstenholme 2007) and over 30 identified in *C. elegans* (Jones *et al.* 2007). For example, levamisole and imidacloprid both target nAChRs, but levamisole is typically used to treat nematode infections while imidacloprid is used to treat biting insects such as fleas (Raymond and Sattelle 2002).

As *G. pallida* and *G. rostochiensis* have been shown to have a distinct complement of cys-loop receptors, even in comparison to other nematodes, it may be that novel drug targets can be identified to control plant-parasitic nematode infection. Further work on the nAChRs and glutamate-gated chloride channels would be beneficial, as well as examination of other plant-parasitic nematodes in the order Tylenchida in order to identify targets unique to this order.

7.7 Alternate splicing and RNA editing further increase diversity of nAChRs

Although fewer genes encoding nAChRs have been found in insects than in nematodes, the diversity of subunits is increased by alteration of the transcripts from the genomic sequence.

7.7.1 RNA editing

RNA editing is the modification of adenosine residues to inosine (A to I editing) in pre-mRNA transcripts by adenosine deaminases (Seeburg 2002). The presence of an inosine residue is read as a guanosine residue, and thus RNA editing can change which amino acid residue is present in the translated protein.

RNA editing has been observed to occur in one nAChR gene of the honey bee *Apis mellifera* (Jones *et al.* 2006) and in five nAChR genes of the fruit fly *Drosophila melanogaster* (Jones and Sattelle 2010). Some of these sites of RNA editing are conserved across the different insect species, while in some species these same sites lacked RNA editing, but were genetically encoded as guanosine residues. Examples are also found of RNA editing events which are species-specific (Jin *et al.* 2007). Some of these RNA editing sites occur in places which are strongly related to receptor function, such as around Loop E of the acetylcholine binding site (Grauso *et al.* 2002).

While RNA editing is known to occur in *C. elegans* and its presence is essential for normal behaviour (Tonkin *et al.* 2002), no sites associated with RNA editing have been found for any of the nAChR genes of *C. elegans* or any other nematode. As RNA editing events may increase the amount of diversity of nAChRs within and between nematode species, exploration of RNA editing events may be interesting. The actions of RNA editing may be pertinent for nAChR genes identified from genomic sequences as this may not reflect the amino acid sequence of the mature protein.

7.7.2 Alternate splicing

Alternate splicing is the differential inclusion or exclusion of exons from the same gene leading to different mRNA and different mature proteins (isoforms). Different isoforms can alter properties of the mature protein. *Cel-avr-14*, which encodes a glutamate-gated chloride channel, is differentially spliced to give rise to two isoforms: Cel-avr-14A and Cel-avr-14B. There is evidence to suggest that Cel-avr-14B binds ivermectin more effectively than Cel-avr-14A (Dent *et al.* 2000).

There are limited confirmed examples of nAChR genes of *C. elegans* which are alternately spliced, although *cel-acr-19*, *cel-acr-24*, *cel-lev-1*, *cel-acr-17*, *cel-acr-20* and *cel-des-2* have predicted splice variants on Wormbase. In insect nAChRs, examples of alternate splicing are widespread. The *Drosophila* nAChR subunits (D α 4 and D α 6) are

alternately spliced to produce five splice variants for both D α 4 (Lansdell and Millar 2000) and D α 6 (Grauso *et al.* 2002). Similar splice variants have also been found in the orthologues of these genes in other insect species (Jin *et al.* 2007). Some of these splice variants had severe impacts on the receptor function and assembly. A splice variant of D α 4 in which exon 2 is missing seemed to impair the ability of the receptor to assemble (Lansdell and Millar 2000), and some splice variants of D α 6 result in proteins with differing amino acids for the Loop D and second transmembrane region (Jin *et al.* 2007).

This level of alternate splicing in nAChRs has not been observed in nematodes. However, there are examples of alternate splicing events which introduce premature stop codons and lead to truncated proteins. In *H. contortus* alternative splicing has been identified in *hco-unc-63* (Neveu *et al.* 2010) and *hco-acr-8* (Fauvin *et al.* 2010) leading to truncated versions of these proteins and is associated with levamisole resistant populations.

The possibility that nAChRs identified from *G. pallida* and *G. rostochiensis* can be altered by either RNA editing or alternate splicing has not been investigated by this work. If these events took place, it would expand the diversity of the subunits found in these species and may allow more novel targets to be identified.

7.8 Specificity is key in drug design

The diversity observed in the nAChRs makes them a prospective target for new drug design which is specific to their target organisms. The current controversy regarding the use of neonicotinoids demonstrates that off-target effects must be considered carefully as they can become damaging to the ecosystem (Whitehorn *et al.* 2012; Godfray *et al.* 2014).

Studies into the nAChR family, and other cys-loop receptors, of nematodes have revealed that different species of nematodes have different complements of nAChR subunits, which may allow for targeting of specific nematode families such as the plant-parasitic nematodes of the order Tylenchida and avoid targeting the beneficial nematodes of the soil environment.

The use of *Xenopus* oocytes as a heterologous expression system would be useful to determine sensitivity of receptors to different drugs. Potential novel targets could be expressed in this system, and the responsiveness of the channel probed and compared to those from off-target organisms. Although this system has proved problematic for the expression of nAChRs from insects, which require the expression of vertebrate β -subunits alongside the insect subunit to investigate the pharmacology (Thany *et al.* 2007; Bertrand *et al.* 1994), *Xenopus* oocytes have been used successfully to express receptors from a range of different nematodes (Boulin *et al.* 2011; Boulin *et al.* 2008;

Williamson *et al.* 2009; Buxton *et al.* 2014). Furthermore, the expression of *Cel-acr-23* in *Xenopus* oocytes has been used to demonstrate that this subunit, novel to nematodes, is the target of the novel anthelmintic monepantel (Rufener *et al.* 2013).

3D modelling of drug interactions may also be of use to predict drug sensitivity. Homology modelling of subunits based on templates produced from X-ray crystal structures can generate predictions for how various drugs will interact with the receptor by running simulations *in silico*.

7.9 *C. elegans* as a model for plant-parasitic nematodes

C. elegans has been used as a model for many nematode parasites, including veterinary parasites. As discussed in the introduction, there are many reasons why *C. elegans* is used as a model organism.

Results obtained in this work indicate that, despite the evolutionary distance between *C. elegans* and plant-parasitic nematodes of the order Tylenchida, it is useful as a heterologous system to investigate plant-parasitic nematode genes. It has been shown that the promoter regions of nAChR genes from *G. pallida* can function to drive GFP expression in *C. elegans*. It was also shown that *Gpa-unc-38.1* can partially functionally complement the *unc-38(x20)* strain of *C. elegans*.

However, in some respects relying too much on *C. elegans* can be problematic. Some cys-loop receptors seem to have a different composition in *C. elegans* than in parasitic nematodes. For example, functional orthologues of *cel-lev-1* and *cel-lev-8* are not found in most parasitic nematode species. As these comprise the L-nAChR of *C. elegans*, receptors of a different composition are clearly present in parasitic nematodes. However, due to the resources available for *C. elegans* and the ease with which it can be genetically manipulated, it still remains a beneficial model organism.

7.10 Duplications and deletions of cys-loop receptor subunits is common throughout the phylum Nematoda, and leads to the diversity of subunits found

A phylogenetic tree is shown in Figure 7-1, incorporating subunits associated with anthelmintic sensitivity (ivermectin, levamisole and monepantel), and other members of their groups, from *C. elegans* and from the parasitic nematode species *H. contortus*, *O. dentatum*, *A. suum*, *B. malayi* and *G. pallida*. This information is also summarised in Table 10.

The positioning of orthologues in relation to each other reflects the evolutionary distance between species. According to the clades described by van Megen *et al.* (2009), *C. elegans*, *H. contortus* and *O. dentatum* are within clade 9, with *C. elegans* in the order Rhabditida and *H. contortus* and *O. dentatum* both in the order Strongylida.

A. suum and *B. malayi* are in clade 8, the former in the order Ascaridida and the latter in the order Spirurida, while *G. pallida* is in Clade 12 in the order Tylenchida. In the phylogenetic tree (Figure 7-1), the orthologues of *H. contortus* and *O. dentatum* are typically clustered together, with the *C. elegans* orthologues as the next closest related. The orthologues from *B. malayi* and *A. suum* are likewise closely related to each other, but are in sister groups to the orthologues of *C. elegans*, *H. contortus* and *A. suum* and share a common ancestor. The *G. pallida* orthologue is predicted to have split from a common ancestor basal to all other orthologues identified here, as a result of the position of *G. pallida* in Clade 12. This description is particularly well represented by the GLC-2 orthologues. The orthologues cluster together within their orthologous groups and further cluster within their groups (e.g. Orthologues of members of the UNC-38 group, ACR-6, UNC-38 and UNC-63).

Some deletion and duplication events are highlighted, as well as the identification of novel subunits. For LEV-8, a full-length sequence has only been identified in *C. elegans*. It is absent in *H. contortus* (Laing *et al.* 2013), but a partial sequence related to LEV-8 was identified in *O. dentatum* (Romine, Martin and Beetham 2013). The authors of this paper postulated that the identification of a partial sequence for LEV-8 in *O. dentatum* may be evidence that the loss of this gene is a recent deletion. The duplications of UNC-29 in *G. pallida* (where two orthologues are found) and in *H. contortus* (four paralogues) seem to be entirely separate events. Both Gpa-UNC-29.1 and Gpa-UNC-29.2 are predicted to have arisen from an ancestor basal to all of the Hco-UNC-29 paralogues and these paralogues arisen from a common ancestor related to Cel-UNC-29. For UNC-38 this duplication only takes place in *G. pallida* (and, as discussed in 4.4.2.6, *G. rostochiensis*), but it is not clear whether or not this duplication extends into other plant-parasitic nematodes due to lack of complete genome data.

Two novel genes were identified in *H. contortus* belonging to the glutamate-gated chloride channel family, which were named *Hco-glc-5* and *Hco-glc-6* (Laing *et al.* 2013). The orthologue identified from NCBI and listed in Romine, Martin and Beetham (2013) for AVR-15 for *O. dentatum* clusters with *Hco-glc-6* leading to the conclusion that the orthologue identified as *Od-avr-15* is in fact likely to be *Od-glc-6*. Similarly, the orthologue obtained from NCBI for AVR-14 for *O. dentatum* (*Od-AVR-14*) associates with *Hco-GLC-5*, suggesting misidentification of this orthologue. This may also have implications for the two orthologues of Cel-AVR-14 identified for *G. pallida*, as Gpa-AVR-14.1 associates with Cel-AVR-14 isoform a, but Gpa-AVR-14.2 is predicted to share a common ancestor with *Hco-GLC-5* and *Od-AVR-14* which may indicate that Gpa-AVR-14.2 is a novel gene similar to *Hco-GLC-5*.

Other absences from this phylogenetic tree are harder to draw conclusions from, as absence of identification from bioinformatic data does not necessarily mean absence

from the genome. As a case in point, in Laing *et al.* (2013), a phylogenetic tree is shown which includes Hco-ACR-3 and Hco-ACR-12. Sequences for these were not included in this phylogenetic tree as they could not be identified in the *H. contortus* database available on NCBI. For this reason, it cannot be stated with certainty that the absences of orthologues for particular genes (e.g. absence of Bma-GLC-3 and absence of Bma-GLC-4 and AsuGLC-4) are representative of a true deletion, or a by-product of data availability of genome assembly. While absences of orthologues in *G. pallida* can be presumed with more confidence due to factors such as full access to genome and transcriptome data, and the availability of a closely related species *G. rostochiensis* as a comparison, the same is not true for the other parasitic nematodes. There are also gaps in data due to lack of research focus. Much attention has been given to the subunits known to be involved in sensitivity to anthelmintic drugs, but other members of some groups are less well characterised (e.g. the ACR-16 group and the other members of the DEG-3 group) and were not included for this reason.

It does seem to be clear, however, that duplications of subunits are common in the phylum Nematoda and probably deletions as well. The issue of when a duplication results in evolution of a new gene, and when to assign a new name rather than numbering, is harder to determine.

7.11 Further directions

7.11.1 Further work on nAChRs

The role of nAChRs of *G. pallida* and other plant-parasitic nematodes will be the subject of much future work. Although orthologues of all members of the UNC-38, ACR-8 and UNC-29 group have been investigated, and if present, cloned from *G. pallida*, functional studies have only been conducted on one gene (*gpa-unc-38.1*). Functional studies on the remaining members are yet to be conducted.

Furthermore, although members of the DEG-3 and ACR-16 groups have been identified in *G. pallida* and *G. rostochiensis*, no members of these groups have been cloned. The number of members of the ACR-16 group is particularly reduced compared to *C. elegans*. As all members of this group have been found in other parasitic nematodes (e.g. *H. contortus* (Laing *et al.* 2013)), this reduction in the ACR-16 group in both *G. pallida* and *G. rostochiensis* may be common to all plant-parasitic nematodes and may be worth exploring further. Characterisation of *gpa-acr-16*, for which the *C. elegans* orthologue forms a homomeric pentameric receptor in body-wall muscle, may be of particular interest. Further rescue studies using mutant *C. elegans* could be beneficial in this respect, to see if the *G. pallida* orthologue is able to rescue the mutant phenotype. If suitable *C. elegans* mutants are available for other subunits (i.e. with a visible phenotype), a mutant-rescue strategy can be applied to many of these

genes. Some examples of mutant strains which could be used are *unc-63(b404)* and *unc-29 (e193)* (both uncoordinated and levamisole resistant).

The use of *Xenopus* oocytes as a heterologous expression system, will allow the identification of those subunits which may associate to form receptors, and their pharmacology to be determined. Unlike mutant-rescue experiments, this would not rely on the presence of suitable *C. elegans* mutants to work with. This system could be used to investigate the likely composition of receptors using those which have been identified in *C. elegans* as a template. This not only includes the identification of the composition of the *G. pallida* L-nAChR present in body wall muscle, but could also be used to investigate the orthologues of components of the neuronal receptor (*cel-acr-2*, *cel-acr-3*, *cel-unc-38*, *cel-acr-12* and *cel-unc-63* (Jospin *et al.* 2009) the *cel-deg-2* *cel-deg-3* receptor (Treinin *et al.* 1998) and the homomeric receptor comprised of *cel-acr-16* (Touroutine *et al.* 2005).

Further work investigating the expression patterns of *G. pallida* nAChRs by use of their promoter regions to drive GFP expression in *C. elegans* would also be beneficial as it would allow their location to be identified. This would allow confirmation that subunits which can associate in a heterologous system (*Xenopus* oocytes) could also associate *in vivo*.

7.11.2 Further work on other cys-loop receptor members and neurotransmitter synthesis genes

Other members of the cys-loop receptor family have been identified, which could also be investigated in similar experiments. Two orthologues of *cel-avr-14* were identified in both *G. pallida* and *G. rostochiensis*, and their role in binding ivermectin could be investigated by use in mutant-rescue experiments. As *G. pallida* and *G. rostochiensis* lack orthologues for the other two genes associated with ivermectin sensitivity (*cel-avr-15* and *cel-glc-1*), it could be that these two orthologues of *cel-avr-14* are the sole determinant of ivermectin sensitivity in *G. pallida*. A highly ivermectin resistant strain of *C. elegans* could be used (e.g. DA1316) to determine if rescue with either orthologue (*gpa-avr-14.1* or *gpa-avr-14.2*) is sufficient to restore ivermectin sensitivity. A similar approach was used to highlight the role of *hco-glc-6* in ivermectin sensitivity of *H. contortus* (Glendinning *et al.* 2011).

Some work with other orthologues identified in Chapter 3 is already being conducted by collaborating labs. These include the investigation of genes encoding the serotonin receptor *gpa-ser-7*, the tryptophan hydroxylase *gpa-tph-1* (serotonin biosynthesis) and the glutamate transporter *gpa-eat-4*. Functional characterisation of these has been conducted by mutant-rescue experiments and the functional study of behaviours. In a similar way, the other components identified could be investigated such as *gpa-unc-25* (involved in GABA biosynthesis) and *gpa-cha-1* (acetylcholine synthesis). Both of these

genes have mutant phenotypes for which mutant rescue could be quantified such as aldicarb and levamisole hypersensitivity for *cel-unc-25* (Vashlishan *et al.* 2008).

7.11.3 Further aspects of gene regulation to be considered

The cys-loop receptor genes identified may also be regulated and organised in different ways, such as by alternate splicing, RNA editing and gene organisation. Further exploration of operon conservation between the species would be useful, particularly for the *acr-2 acr-3* operon discussed in 4.4.54.3.3.1. The majority of operons in *C. elegans* are SL2-type, formed by trans-splicing using a SL2 small nuclear ribonucleoprotein particle which joins 3' end to 5' end of a downstream mRNA. The presence of SL2 elements in the *C. elegans* genome has been linked to genes that are likely to be part of an operon (Blumenthal *et al.* 2002). Such an approach could be used to identify operons in *G. pallida*, by identifying genes that produce SL2-containing mRNAs and then checking the gene structure to identify if they are likely to be within operons (i.e. in close proximity to an upstream gene).

This approach may identify potential new operons formed in *G. pallida* or *G. rostochiensis*, such as that described in 4.4.5 which may consist of *gpa-acr-2 gpa-acr-3 gpa-unc-29.1*. The rate of operon formation in nematodes is 3.3 times greater than that of operon loss, suggested that new operons may be found (Qian and Zhang 2008). The role of alternate splicing and RNA editing in *G. pallida* gene regulation has not yet been explored. This may have implications for the diversity of cys-loop receptors identified.

7.12 The cys-loop ligand-gated ion channel gene family is a source of potential targets for anthelmintic design

The diversity of cys-loop receptors between species provides a wealth of potential targets for drug design. Although cys-loop receptors are common all animals, species-specific variations allow the targeted control of particular pests without damaging off-target species. Anthelmintics commonly target cys-loop receptors, and it has been shown that the presence or absence of particular subunits or the composition of receptors can affect the pharmacology of the receptor and thus the efficacy of the anthelmintic.

This provides a mechanism to target all plant-parasitic nematodes of the order Tylenchida, and a novel method of control for the most damaging plant-parasitic nematodes of essential crops.

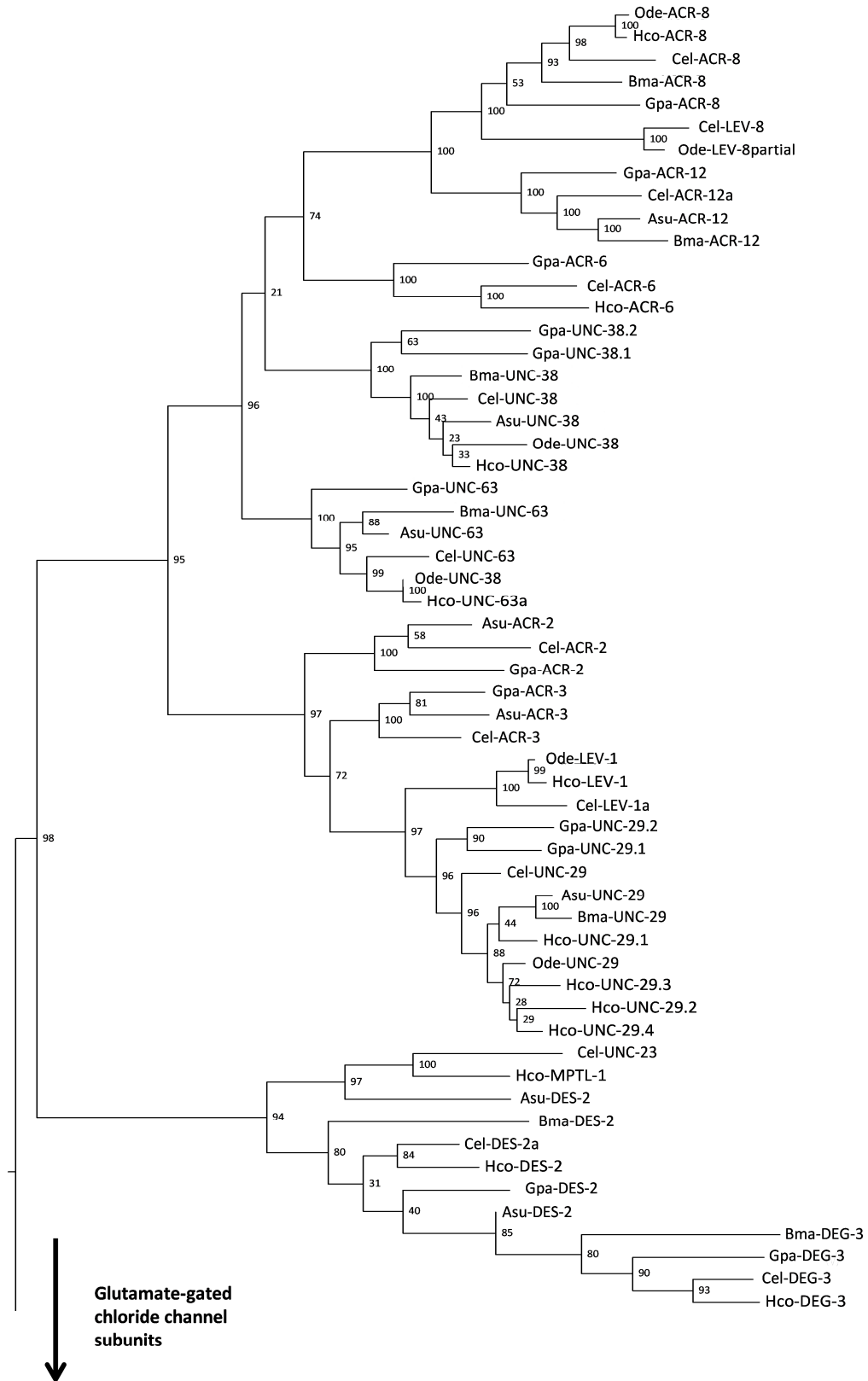
Drug	Target	Main use	References
Macrocyclic lactones e.g. ivermectin	Glutamate-gated chloride channels	Human and veterinary applications	(Geary 2005)
Piperazine derivatives e.g. diethylcarbamazine	GABA receptor agonist	Human	(Bockarie and Deb 2010)
Tetrahydropyrimidine derivatives e.g. pyrantel and oxantel	nAChRs	Human and veterinary applications	(Kopp <i>et al.</i> 2008)
Amino-acetonitrile derivatives e.g. Monepantel	nAChRs	Veterinary applications	(Sager <i>et al.</i> 2009)
Tribendimidine	L-nAChRs	Human applications	(Hu, Xiao and Aroian 2009)
Spiroindoles e.g. Derquental	nAChRs	Veterinary applications	(Little <i>et al.</i> 2011)

Table 9: Examples of drugs targeting cys-loop receptors

<i>C. elegans</i>	<i>G. pallida</i>	<i>H. contortus</i>	<i>A. suum</i>	<i>B. malayi</i>	<i>O. dentatum</i>
<i>Cel-lev-1</i>	-	Y (no SP)	-	-	Y
<i>Cel-lev-8</i>	-	-	-	-	Y (partial)
<i>Cel-unc-29</i>	2 x	4 x	Y	Y	Y
<i>Cel-unc-38</i>	2 x	Y	Y	Y	Y
<i>Cel-unc-63</i>	Y (no SP)	Y	Y	Y	Y
<i>Cel-acr-8</i>	Y	Y	-	Y	Y
<i>Cel-acr-23</i>	-	-	-	-	-
	-	<i>Hco-mptl-1</i>	-	-	-
<i>Cel-deg-3</i>	Y	Y	Y	Y	-
<i>Cel-des-2</i>	y	Y	Y	Y	-
<i>Cel-glc-1</i>	-	-	-	-	-
<i>Cel-glc-2</i>	Y	Y	Y	y	Y
<i>Cel-glc-3</i>	Y	Y	-	-	Y
<i>Cel-glc-4</i>	Y	y	-	-	Y
	-	<i>Hco-glc-5</i>	-	-	Y
	-	<i>Hco-glc-6</i>	-	-	-
<i>Cel-avr-14</i>	2 x	Y	Y	Y	Y
<i>Cel-avr-15</i>	-	Y	-	-	Y

Table 10: Complement of genes encoding members of nAChR subunits and glutamate-gated chloride channel subunits in different nematode species

Data collated from NCBI databases, (Williamson, Walsh and Wolstenholme 2007; Romine, Martin and Beetham 2013). Y indicates an orthologue is present, no SP indicates that a signal peptide is not predicted. – indicates that an orthologue is not present. Numbers x indicates the number of orthologues for the *C. elegans* gene found in that species. Novel genes in species are also listed.



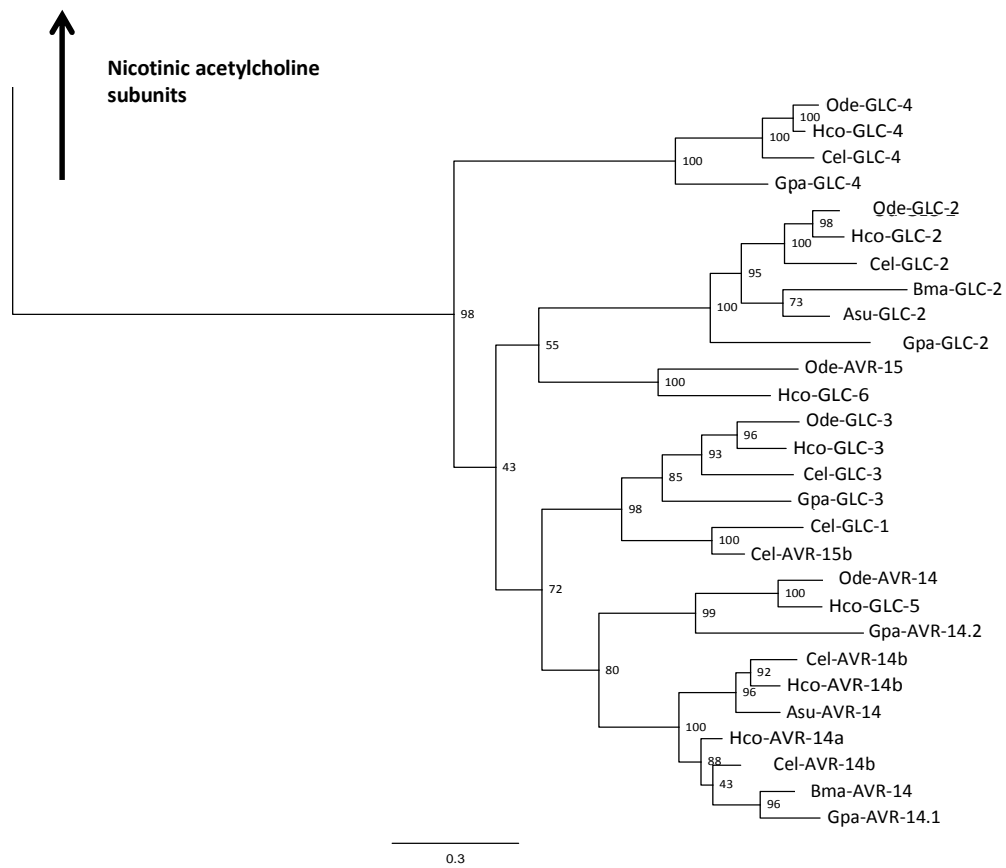


Figure 7-1: Maximum Likelihood tree of nAChRs and Glutamate-gated chloride channels associated with anthelmintic sensitivity from *C. elegans*, *H. contortus*, *O. dentatum*, *A. suum*, *B. malayi* and *G. pallida*.

The phylogenetic tree using predicted protein alignments (generated by Clustal Omega (Sievers *et al.* 2011)). Sequences were obtained from NCBI and Wormbase, with reference to published data (Laing *et al.* 2013; Williamson, Walsh and Wolstenholme 2007; Romine, Martin and Beetham 2013). Bootstrap values for 100 iterations are labelled on nodes. Scale bar represents average number of substitutions per site. MEGA6 was used to compute the ML tree (Tamura *et al.* 2013). Orthologues cluster first by orthologous group, and then in relation to the evolutionary distance between species.

8. References

- ABAD, P., J. GOUZY, J.-M. AURY, P. CASTAGNONE-SERENO, E. G. J. DANCHIN, E. DELEURY, L. PERFUS-BARBECH, V. ANTHOUPARD, F. ARTIGUENAVE, V. C. BLOK, M.-C. CAILLAUD, P. M. COUTINHO, C. DASILVA, F. DE LUCA, F. DEAU, M. ESQUIBET, T. FLUTRE, J. V. GOLDSTONE, N. HAMAMOUCH, T. HEWEZI, O. JAILLON, C. JUBIN, P. LEONETTI, M. MAGLIANO, T. R. MAIER, G. V. MARKOV, P. MCVEIGH, G. PESOLE, J. POULAIN, M. ROBINSON-RECHAVI, E. SALLET, B. SEGURENS, D. STEINBACH, T. TYTGAT, E. UGARTE, C. VAN GHELDER, P. VERONICO, T. J. BAUM, M. BLAXTER, T. BLEVE-ZACHEO, E. L. DAVIS, J. J. EWBACK, B. FAVERY, E. GRENIER, B. HENRISSAT, J. T. JONES, V. LAUDET, A. G. MAULE, H. QUESNEVILLE, M.-N. ROSSO, T. SCHIEX, G. SMANT, J. WEISSENBACH and P. WINCKER. 2008. Genome sequence of the metazoan plant-parasitic nematode *Meloidogyne incognita*. *Nature Biotechnology*, **26**(8), pp.909-915.
- ABOOBAKER, A. A. and M. L. BLAXTER. 2003. Use of RNA interference to investigate gene function in the human filarial nematode parasite *Brugia malayi*. *Molecular and Biochemical Parasitology*, **129**(1), pp.41-51.
- ABRAMOFF, M. D., MAGALHAES, P.J., RAM, S.J. 2004. Image Processing with ImageJ. *Biophotonics International*, **11** (issue 7), pp.36-42.
- ALFONSO, A., K. GRUNDAHL, J. S. DUERR, H. P. HAN and J. B. RAND. 1993. The *Caenorhabditis elegans* unc-17 gene - a putative vesicular acetylcholine transporter. *Science*, **261**(5121), pp.617-619.
- ALFONSO, A., K. GRUNDAHL, J. R. MCMANUS and J. B. RAND. 1994. Cloning and characterization of the choline acetyltransferase structural gene (cha-1) from *C. elegans*. *J Neurosci*, **14**(4), pp.2290-300.
- ALKEMA, M. J., M. HUNTER-ENSOR, N. RINGSTAD and H. R. HORVITZ. 2005. Tyramine functions independently of octopamine in the *Caenorhabditis elegans* nervous system. *Neuron*, **46**(2), pp.247-260.
- ALMEDOM, R. B., J. F. LIEWALD, G. HERNANDO, C. SCHULTHEIS, D. RAYES, J. PAN, T. SCHEDLETZKY, H. HUTTER, C. BOUZAT and A. GOTTSCHALK. 2009. An ER-resident membrane protein complex regulates nicotinic acetylcholine receptor subunit composition at the synapse. *The EMBO journal*, **28**(17), pp.2636-2649.
- ALTUN, Z. and D. HALL. 2005. Hermaphrodite anatomy. *WormAtlas*"(ZF Altun and DH Hall, Eds.) <http://www.wormatlas.org/handbook/excretory.htm>.
- ARAVIND, L. 2001. DOMON: an ancient extracellular domain in dopamine β -monooxygenase and other proteins. *Trends in Biochemical Sciences*, **26**(9), pp.524-526.
- ARIAS, H. R. 2000. Localization of agonist and competitive antagonist binding sites on nicotinic acetylcholine receptors. *Neurochemistry International*, **36**(7), pp.595-645.
- AWAN, F. and W. HOMINICK. 1982. Observations on tanning of the potato cyst-nematode, *Globodera rostochiensis*. *Parasitology*, **85**(01), pp.61-71.
- BAKKER, E., U. ACHENBACH, J. BAKKER, J. VAN VLIET, J. PELEMAN, B. SEGERS, S. VAN DER HEIJDEN, P. VAN DER LINDE, R. GRAVELAND and R. HUTTEN. 2004. A high-resolution map of the H1 locus harbouring resistance to the potato cyst nematode *Globodera rostochiensis*. *Theoretical and applied genetics*, **109**(1), pp.146-152.

- BALIŃSKI, A., Y. SUN and J. DZIK. 2013. Traces of marine nematodes from 470 million years old Early Ordovician rocks in China. *Nematology*, **15**(5), pp.567-574.
- BALLIVET, M., C. ALLIOD, S. BERTRAND and D. BERTRAND. 1996. Nicotinic Acetylcholine Receptors in the Nematode *Caenorhabditis elegans*. *Journal of Molecular Biology*, **258**(2), pp.261-269.
- BARGMANN, C. I. 2006. Chemosensation in *C. elegans*. WormBook: The Online Review of *C. elegans* Biology
- BARTOS, M., K. L. PRICE, S. C. R. LUMMIS and C. BOUZAT. 2009. Glutamine 57 at the Complementary Binding Site Face Is a Key Determinant of Morantel Selectivity for $\alpha 7$ Nicotinic Receptors. *Journal of Biological Chemistry*, **284**(32), pp.21478-21487.
- BAYLIS, H. A., K. MATSUDA, M. D. SQUIRE, J. T. FLEMING, R. J. HARVEY, M. G. DARLISON, E. A. BARNARD and D. B. SATTELLE. 1997. ACR-3, a *Caenorhabditis elegans* nicotinic acetylcholine receptor subunit. Molecular cloning and functional expression. *Receptors Channels*, **5**(3-4), pp.149-58.
- BEN-AMI, H. C., L. YASSIN, H. FARAH, A. MICHAELI, M. ESHEL and M. TREININ. 2005. RIC-3 affects properties and quantity of nicotinic acetylcholine receptors via a mechanism that does not require the coiled-coil domains. *Journal of Biological Chemistry*, **280**(30), pp.28053-28060.
- BENDEZU, I. F., K. EVANS, P. R. BURROWS, D. DE POMERAI and M. CANTO-SAENZ. 1998. Inter and intra-specific genomic variability of the potato cyst nematodes *Globodera pallida* and *G. rostochiensis* from Europe and South America using RAPD-PCR. *Nematologica*, **44**(1), pp.49-61.
- BERTRAND, D., M. BALLIVET, M. GOMEZ, S. BERTRAND, B. PHANNAVONG and E. GUNDELINGER. 1994. Physiological properties of neuronal nicotinic receptors reconstituted from the vertebrate $\beta 2$ subunit and *Drosophila* α subunits. *European Journal of Neuroscience*, **6**(5), pp.869-875.
- BIANCHI, L. and M. DRISCOLL. 2006. Heterologous expression of *C. elegans* ion channels in *Xenopus* oocytes.
- BLAXTER, M. 2011. Nematodes: The Worm and Its Relatives. *Plos Biology*, **9**(4).
- BLAXTER, M. L., P. DE LEY, J. R. GAREY, L. X. LIU, P. SCHELDEMAN, A. VIERSTRAETE, J. R. VANFLETEREN, L. Y. MACKEY, M. DORRIS, L. M. FRISSE, J. T. VIDA and W. K. THOMAS. 1998. A molecular evolutionary framework for the phylum Nematoda. *Nature*, **392**(6671), pp.71-75.
- BLUMENTHAL, T., D. EVANS, C. D. LINK, A. GUFFANTI, D. LAWSON, J. THIERRY-MIEG, D. THIERRY-MIEG, W. L. CHIU, K. DUKE and M. KIRALY. 2002. A global analysis of *Caenorhabditis elegans* operons. *Nature*, **417**(6891), pp.851-854.
- BOCKARIE, M. J. and R. M. DEB. 2010. Elimination of lymphatic filariasis: do we have the drugs to complete the job? *Curr Opin Infect Dis*, **23**(6), pp.617-20.
- BORGES, L. S. and M. FERNS. 2001. Agrin-induced phosphorylation of the acetylcholine receptor regulates cytoskeletal anchoring and clustering. *The Journal of cell biology*, **153**(1), pp.1-12.

- BOULIN, T., A. FAUVIN, C. L. CHARVET, J. CORRET, J. CABARET, J. L. BESSEREAU and C. NEVEU. 2011. Functional reconstitution of *Haemonchus contortus* acetylcholine receptors in *Xenopus* oocytes provides mechanistic insights into levamisole resistance. *British Journal of Pharmacology*, **164**(5), pp.1421-1432.
- BOULIN, T., M. GIELEN, J. E. RICHMOND, D. C. WILLIAMS, P. PAOLETTI and J.-L. BESSEREAU. 2008. Eight genes are required for functional reconstitution of the *Caenorhabditis elegans* levamisole-sensitive acetylcholine receptor. *Proceedings of the National Academy of Sciences of the United States of America*, **105**(47), pp.18590-18595.
- BOULIN, T., G. RAPTI, L. BRISEÑO-ROA, C. STIGLOHER, J. E. RICHMOND, P. PAOLETTI and J.-L. BESSEREAU. 2012. Positive modulation of a Cys-loop acetylcholine receptor by an auxiliary transmembrane subunit. *Nature neuroscience*, **15**(10), pp.1374-1381.
- BREJC, K., W. J. VAN DIJK, R. V. KLAASSEN, M. SCHUURMANS, J. VAN DER OOST, A. B. SMIT and T. K. SIXMA. 2001. Crystal structure of an ACh-binding protein reveals the ligand-binding domain of nicotinic receptors. *Nature*, **411**(6835), pp.269-76.
- BRENNER, S. 1974. The genetics of *Caenorhabditis elegans*. *Genetics*, **77**(1), pp.71-94.
- BRITTON, C. and L. MURRAY. 2002. A cathepsin L protease essential for *Caenorhabditis elegans* embryogenesis is functionally conserved in parasitic nematodes. *Molecular and Biochemical Parasitology*, **122**(1), pp.21-33.
- BROCKIE, P. J. and A. V. MARICQ. 2002. Ionotropic glutamate receptors in *Caenorhabditis elegans*. *Neuro-Signals*, **12**(3), pp.108-125.
- BUCKINGHAM, S. D. and D. B. SATTELLE. 2009. Fast, automated measurement of nematode swimming (thrashing) without morphometry. *Bmc Neuroscience*, **10**(1), p84.
- BUXTON, S. K., C. L. CHARVET, C. NEVEU, J. CABARET, J. CORRET, N. PEINEAU, M. ABONGWA, E. COURTOT, A. P. ROBERTSON and R. J. MARTIN. 2014. Investigation of Acetylcholine Receptor Diversity in a Nematode Parasite Leads to Characterization of Tribendimidine- and Derquantel-Sensitive nAChRs. *PLoS Pathog*, **10**(1), pe1003870.
- CASSADA, R. C. and R. L. RUSSELL. 1975. The dauerlarva, a post-embryonic developmental variant of the nematode *Caenorhabditis elegans*. *Developmental biology*, **46**(2), pp.326-342.
- CASTAGNONE-SERENO, P. 2002. Genetic variability of nematodes: a threat to the durability of plant resistance genes? *Euphytica*, **124**(2), pp.193-199.
- CASTAGNONE-SERENO, P. 2006. Genetic variability and adaptive evolution in parthenogenetic root-knot nematodes. *Heredity*, **96**(4), pp.282-289.
- CHASE, D. L., J. S. PEPPER and M. R. KOELLE. 2004. Mechanism of extrasynaptic dopamine signaling in *Caenorhabditis elegans*. *Nature neuroscience*, **7**(10), pp.1096-1103.
- CHEN, N., T. W. HARRIS, I. ANTOSHECHKIN, C. BASTIANI, T. BIERI, D. BLASIAR, K. BRADNAM, P. CANARAN, J. CHAN, C. K. CHEN, W. J. CHEN, F. CUNNINGHAM, P. DAVIS, E. KENNY, R. KISHORE, D. LAWSON, R. LEE, H. M. MULLER, C. NAKAMURA, S. PAI, P. OZERSKY, A. PETCHERSKI, A. ROGERS, A. SABO, E. M. SCHWARZ, K. VAN AUKEN, Q. WANG, R. DURBIN, J. SPIETH, P. W. STERNBERG and L. D. STEIN. 2005a. WormBase: a comprehensive data resource for *Caenorhabditis* biology and genomics. *Nucleic Acids Res*, **33**(Database issue), pp.D383-9.

- CHEN, N., D. LAWSON, K. BRADNAM, T. W. HARRIS and L. D. STEIN. 2004. WormBase as an integrated platform for the *C. elegans* ORFeome. *Genome Res.*, **14**(10B), pp.2155-61.
- CHEN, Q., S. REHMAN, G. SMANT and J. T. JONES. 2005b. Functional analysis of pathogenicity proteins of the potato cyst nematode *Globodera rostochiensis* using RNAi. *Molecular Plant-Microbe Interactions*, **18**(7), pp.621-625.
- CHITWOOD, D. J. 2003. Research on plant-parasitic nematode biology conducted by the United States Department of Agriculture - Agricultural Research Service. *Pest Management Science*, **59**(6-7), pp.748-753.
- CHITWOOD, D. J. and R. N. PERRY. 2009. Reproduction, physiology and biochemistry. *Root-knot nematodes*, pp.182-200.
- CHOI, J. and A. P. NEWMAN. 2006. A two-promoter system of gene expression in *C. elegans*. *Developmental biology*, **296**(2), pp.537-544.
- COBURN, C. and D. GEMS. 2013. The mysterious case of the *C. elegans* gut granule: death fluorescence, anthranilic acid and the kynurenine pathway. *Frontiers in genetics*, **4**.
- COLES, G., J. EAST and S. JENKINS. 1975. The mechanism of action of the anthelmintic levamisole. *General Pharmacology: The Vascular System*, **6**(4), pp.309-313.
- CONSORTIUM, C. E. S. 1998. Genome sequence of the nematode *C. elegans*: A platform for investigating biology. *Science*, **282**(5396), pp.2012-2018.
- CORRINGER, P. J., N. LE NOVERE and J. P. CHANGEUX. 2000. Nicotinic receptors at the amino acid level. *Annu Rev Pharmacol Toxicol*, **40**, pp.431-58.
- COSTA, J. C., C. J. LILLEY, H. J. ATKINSON and P. E. URWIN. 2009. Functional characterisation of a cyst nematode acetylcholinesterase gene using *Caenorhabditis elegans* as a heterologous system. *International Journal for Parasitology*, **39**(7), pp.849-858.
- COTTON, J. A., C. J. LILLEY, L. M. JONES, T. KIKUCHI, A. J. REID, P. THORPE, I. J. TSAI, H. BEASLEY, V. BLOK, P. J. A. COCK, S. EVES-VAN DEN AKKER, N. HOLROYD, M. HUNT, S. MANTELIN, H. NAGHRA, A. PAIN, J. E. PALOMARES-RIUS, M. ZAROWIECKI, M. BERRIMAN, J. T. JONES and P. E. URWIN. 2014. The genome and life-stage specific transcriptomes of *Globodera pallida* elucidate key aspects of plant parasitism by a cyst nematode. *Genome Biology*, **15**(3).
- CROLL, N. 1975. Components and patterns in the behaviour of the nematode *Caenorhabditis elegans*. *Journal of Zoology*, **176**(2), pp.159-176.
- CROOK, M., K. GRANT and W. N. GRANT. 2010. Failure of *Parastrephloides trichosuri* daf-7 to complement a *Caenorhabditis elegans* daf-7 (e1372) mutant: Implications for the evolution of parasitism. *International Journal for Parasitology*, **40**(14), pp.1675-1683.
- CULETTO, E., H. A. BAYLIS, J. E. RICHMOND, A. K. JONES, J. T. FLEMING, M. D. SQUIRE, J. A. LEWIS and D. B. SATTELLE. 2004. The *Caenorhabditis elegans* unc-63 gene encodes a Levamisole-sensitive nicotinic acetylcholine receptor alpha subunit. *Journal of Biological Chemistry*, **279**(41), pp.42476-42483.
- CULLY, D. F., D. K. VASSILATIS, K. K. LIU, P. S. PARESS, L. H. VAN DER PLOEG, J. M. SCHAEFFER and J. P. ARENA. 1994. Cloning of an avermectin-sensitive glutamate-gated chloride channel from *Caenorhabditis elegans*. *Nature*, **371**(6499), pp.707-11.

- DANQUAH, W. B., M. A. BACK, I. G. GROVE and P. P. HAYDOCK. 2011. In vitro nematicidal activity of a garlic extract and salicylaldehyde on the potato cyst nematode, *Globodera pallida*. *Nematology*, **13**(7), pp.869-885.
- DEMPSEY, C. M., S. M. MACKENZIE, A. GARGUS, G. BLANCO and J. Y. SZE. 2005. Serotonin (5HT), fluoxetine, imipramine and dopamine target distinct 5HT receptor signaling to modulate *Caenorhabditis elegans* egg-laying behavior. *Genetics*, **169**(3), pp.1425-1436.
- DEN NIJS, L. and C. LOCK. 1992. Differential hatching of the potato cyst nematodes *Globodera rostochiensis* and *G. pallida* in root diffusates and water of differing ionic composition. *Netherlands Journal of Plant Pathology*, **98**(2), pp.117-128.
- DENT, J. A., M. W. DAVIS and L. AVERY. 1997. avr-15 encodes a chloride channel subunit that mediates inhibitory glutamatergic neurotransmission and ivermectin sensitivity in *Caenorhabditis elegans*. *Embo J*, **16**(19), pp.5867-79.
- DENT, J. A., M. M. SMITH, D. K. VASSILATIS and L. AVERY. 2000. The genetics of ivermectin resistance in *Caenorhabditis elegans*. *Proceedings of the National Academy of Sciences of the United States of America*, **97**(6), pp.2674-2679.
- DIETERICH, C. and R. J. SOMMER. 2009. How to become a parasite - lessons from the genomes of nematodes. *Trends in Genetics*, **25**(5), pp.203-209.
- DOLGIN, E., M. FELIX and A. CUTTER. 2008. Hakuna Nematoda: genetic and phenotypic diversity in African isolates of *Caenorhabditis elegans* and *C. briggsae*. *Heredity*, **100**(3), pp.304-315.
- DONG, L., X. LI, L. HUANG, Y. GAO, L. ZHONG, Y. ZHENG and Y. ZUO. 2013. Lauric acid in crown daisy root exudate potently regulates root-knot nematode chemotaxis and disrupts *Mi-flp-18* expression to block infection. *Journal of Experimental Botany*, pert356.
- DOYLE, E. A. and K. N. LAMBERT. 2003. *Meloidogyne javanica* chorismate mutase 1 alters plant cell development. *Molecular Plant-Microbe Interactions*, **16**(2), pp.123-131.
- DUFOUR, V., R. N. BEECH, C. WEVER, J. A. DENT and T. G. GEARY. 2013. Molecular cloning and characterization of novel glutamate-gated chloride channel subunits from *Schistosoma mansoni*. *Plos Pathogens*, **9**(8), pe1003586.
- DUNCAN, L. W. and M. MOENS. 2013. Migratory Endoparasitic Nematodes. *Plant nematology* CABI.
- DUPUY, D., Q. R. LI, B. DEPLANCKE, M. BOXEM, T. HAO, P. LAMESCH, R. SEQUERRA, S. BOSAK, L. DOUCETTE-STAMM, I. A. HOPE, D. E. HILL, A. J. WALHOUT and M. VIDAL. 2004. A first version of the *Caenorhabditis elegans* Promoterome. *Genome Res*, **14**(10B), pp.2169-75.
- EIMER, S., A. GOTTSCHALK, M. HENGARTNER, H. R. HORVITZ, J. RICHMOND, W. R. SCHAFER and J. L. BESSEREAU. 2007. Regulation of nicotinic receptor trafficking by the transmembrane Golgi protein UNC-50. *The EMBO journal*, **26**(20), pp.4313-4323.
- EKBLOM, R. and J. B. W. WOLF. 2014. A field guide to whole-genome sequencing, assembly and annotation. *Evolutionary Applications*, **7**(9), pp.1026-1042.

- ELLING, A. A., M. MITREVA, J. RECKNOR, X. GAI, J. MARTIN, T. R. MAIER, J. P. McDERMOTT, T. HEWEZI, D. M. BIRD and E. L. DAVIS. 2007. Divergent evolution of arrested development in the dauer stage of *Caenorhabditis elegans* and the infective stage of *Heterodera glycines*. *Genome Biol*, **8**(10), pR211.
- ELSWORTH, B., M. JONES and M. BLAXTER. 2013. Badger—an accessible genome exploration environment. *Bioinformatics*, **29**(21), pp.2788-2789.
- ELSWORTH, B., J. WASMUTH and M. BLAXTER. 2011. NEMBASE4: the nematode transcriptome resource. *International Journal for Parasitology*, **41**(8), pp.881-894.
- ERNST, K., A. KUMAR, D. KRIESELT, D. U. KLOOS, M. S. PHILLIPS and M. W. GANAL. 2002. The broad-spectrum potato cyst nematode resistance gene (Hero) from tomato is the only member of a large gene family of NBS-LRR genes with an unusual amino acid repeat in the LRR region. *The Plant Journal*, **31**(2), pp.127-136.
- FAUVIN, A., C. CHARVET, M. ISSOUF, J. CORRET, J. CABARET and C. NEVEU. 2010. cDNA-AFLP analysis in levamisole-resistant *Haemonchus contortus* reveals alternative splicing in a nicotinic acetylcholine receptor subunit. *Molecular and Biochemical Parasitology*, **170**(2), pp.105-107.
- FENWICK, D. 1940. Methods for the recovery and counting of cysts of *Heterodera schachtii* from soil. *Journal of helminthology*, **18**(04), pp.155-172.
- FIRE, A., S. XU, M. K. MONTGOMERY, S. A. KOSTAS, S. E. DRIVER and C. C. MELLO. 1998. Potent and specific genetic interference by double-stranded RNA in *Caenorhabditis elegans*. *Nature*, **391**(6669), pp.806-811.
- FLEENOR, J., L. TIMMONS, S. XU, K. LIU and B. KELLY. Fire Lab 1999 Vector Supplement-May 1999.
- FLEMING, J. T., M. D. SQUIRE, T. M. BARNES, C. TORNOE, K. MATSUDA, J. AHNN, A. FIRE, J. E. SULSTON, E. A. BARNARD, D. B. SATTELLE and J. A. LEWIS. 1997. *Caenorhabditis elegans* levamisole resistance genes *lev-1*, *unc-29*, and *unc-38* encode functional nicotinic acetylcholine receptor subunits. *Journal of Neuroscience*, **17**(15), pp.5843-5857.
- FRECKMAN, D. W., R. MANKAU and H. FERRIS. 1975. Nematode community structure in desert soils - nematode recovery. *Journal of Nematology*, **7**(4), pp.343-346.
- FRIEDLAND, A. E., Y. B. TZUR, K. M. ESVELT, M. P. COLAIACOVO, G. M. CHURCH and J. A. CALARCO. 2013. Heritable genome editing in *C. elegans* via a CRISPR-Cas9 system. *Nat Meth*, **10**(8), pp.741-743.
- GABALDÓN, T. 2008. Large-scale assignment of orthology: back to phylogenetics? *Genome Biology*, **9**(10), pp.235-235.
- GALLY, C., S. EIMER, J. E. RICHMOND and J.-L. BESSEREAU. 2004. A transmembrane protein required for acetylcholine receptor clustering in *Caenorhabditis elegans*. *Nature*, **431**(7008), pp.578-582.
- GEARY, T. G. 2005. Ivermectin 20 years on: maturation of a wonder drug. *Trends in Parasitology*, **21**(11), pp.530-532.

- GHEDIN, E., S. WANG, D. SPIRO, E. CALER, Q. ZHAO, J. CRABTREE, J. E. ALLEN, A. L. DELCHER, D. B. GUILIANO and D. MIRANDA-SAAVEDRA. 2007. Draft genome of the filarial nematode parasite *Brugia malayi*. *Science*, **317**(5845), pp.1756-1760.
- GILLAN, V., K. MAITLAND, G. MCCORMACK, N. A. N. HIM and E. DEVANEY. 2009. Functional genomics of hsp-90 in parasitic and free-living nematodes. *International Journal for Parasitology*, **39**(10), pp.1071-1081.
- GLENDINNING, S. K., S. D. BUCKINGHAM, D. B. SATTELLE, S. WONNACOTT and A. J. WOLSTENHOLME. 2011. Glutamate-Gated Chloride Channels of *Haemonchus contortus* Restore Drug Sensitivity to Ivermectin Resistant *Caenorhabditis elegans*. *Plos One*, **6**(7), pe22390.
- GODFRAY, H. C. J., T. BLACQUIERE, L. M. FIELD, R. S. HAILS, G. PETROKOFSKY, S. G. POTTS, N. E. RAIN, A. J. VANBERGEN and A. R. MCLEAN. 2014. A restatement of the natural science evidence base concerning neonicotinoid insecticides and insect pollinators. *Proceedings of the Royal Society of London B: Biological Sciences*, **281**(1786), p20140558.
- GOLDEN, J. W. and D. L. RIDDLE. 1984. The *Caenorhabditis elegans* dauer larva: developmental effects of pheromone, food, and temperature. *Developmental biology*, **102**(2), pp.368-378.
- GONZALEZ-SERRICCHIO, A. S. and P. W. STERNBERG. 2006. Visualization of *C. elegans* transgenic arrays by GFP. *BMC genetics*, **7**(1), p36.
- GOODELL, P. and H. FERRIS. 1989. Influence of environmental factors on the hatch and survival of *Meloidogyne incognita*. *Journal of Nematology*, **21**(3), p328.
- GOTTSCHALK, A., R. B. ALMEDOM, T. SCHEDLETZKY, S. D. ANDERSON, J. R. YATES and W. R. SCHAFER. 2005. Identification and characterization of novel nicotinic receptor-associated proteins in *Caenorhabditis elegans*. *Embo Journal*, **24**(14), pp.2566-2578.
- GRANT, W. N., S. J. SKINNER, J. NEWTON-HOWES, K. GRANT, G. SHUTTLEWORTH, D. D. HEATH and C. B. SHOEMAKER. 2006. Heritable transgenesis of *Parastrengyloides trichosuri*: a nematode parasite of mammals. *International Journal for Parasitology*, **36**(4), pp.475-483.
- GRAUSO, M., R. REENAN, E. CUETTO and D. SATTELLE. 2002. Novel putative nicotinic acetylcholine receptor subunit genes, Da5, Da6 and Da7, in *Drosophila melanogaster* identify a new and highly conserved target of adenosine deaminase acting on RNA-mediated A-to-I pre-mRNA editing. *Genetics*, **160**(4), pp.1519-1533.
- GROOMBRIDGE, B. 1992. Nematodes. *Global Biodiversity*. Springer, pp.88-92.
- GRUNDLER, F., M. BETKA and U. WYSS. 1991. Influence of changes in the nurse cell system (syncytium) on sex determination and development of the cyst nematode *Heterodera schachtii*: Total amounts of proteins and amino acids. *Phytopathology*, **81**(1), pp.70-74.
- GUBANOV, N. M. 1951. Giant nematoda from the placenta of Cetacea; *Placentonema gigantissima* nov. gen., nov. sp. *Dokl Akad Nauk SSSR*, **77**(6), pp.1123-5.
- GUNDERSEN, C., R. MILEDI and I. PARKER. 1983. Serotonin receptors induced by exogenous messenger RNA in *Xenopus* oocytes. *Proceedings of the Royal society of London. Series B. Biological sciences*, **219**(1214), pp.103-109.

- GURDON, J. 1971. Use of Frog Eggs and Oocytes for the Study of Messenger RNA and its Translation. *Nature*, **233**, p177.
- HARA, M. and M. HAN. 1995. Ras farnesyltransferase inhibitors suppress the phenotype resulting from an activated ras mutation in *Caenorhabditis elegans*. *Proc Natl Acad Sci U S A*, **92**(8), pp.3333-7.
- HARROW, I. D. and K. A. GRATION. 1985. Mode of action of the anthelmintics morantel, pyrantel and levamisole on muscle cell membrane of the nematode *Ascaris suum*. *Pesticide Science*, **16**(6), pp.662-672.
- HART, A. C., S. SIMS and J. M. KAPLAN. 1995. Synaptic code for sensory modalities revealed by *C. elegans* GLR-1 glutamate receptor. *Nature*, **378**(6552), pp.82-85.
- HASHMI, S., C. BRITTON, J. LIU, D. B. GUILIANO, Y. OKSOV and S. LUSTIGMAN. 2002. Cathepsin L is essential for embryogenesis and development of *Caenorhabditis elegans*. *Journal of Biological Chemistry*, **277**(5), pp.3477-3486.
- HAUGSTETTER, J., T. BLICHER and L. ELLGAARD. 2005. Identification and characterization of a novel thioredoxin-related transmembrane protein of the endoplasmic reticulum. *Journal of Biological Chemistry*, **280**(9), pp.8371-8380.
- HERNANDO, G., I. BERGÉ, D. RAYES and C. BOUZAT. 2012. Contribution of Subunits to *Caenorhabditis elegans* Levamisole-Sensitive Nicotinic Receptor Function. *Molecular Pharmacology*, **82**(3), pp.550-560.
- HEUNGENS, K., D. MUGNIÉRY, M. VAN MONTAGU, G. GHEYSEN and A. NIEBEL. 1996. A method to obtain disinfected *Globodera* infective juveniles directly from cysts. *Fundamental and Applied Nematology*, **19**(1), pp.91-93.
- HEWEZI, T., P. HOWE, T. R. MAIER, R. S. HUSSEY, M. G. MITCHUM, E. L. DAVIS and T. J. BAUM. 2008. Cellulose binding protein from the parasitic nematode *Heterodera schachtii* interacts with *Arabidopsis* pectin methylesterase: cooperative cell wall modification during parasitism. *The Plant Cell*, **20**(11), pp.3080-3093.
- HIBBS, R. E. and E. GOUAUX. 2011. Principles of activation and permeation in an anion-selective Cys-loop receptor. *Nature*, **474**(7349), pp.54-60.
- HILLS, T., P. J. BROCKIE and A. V. MARICQ. 2004. Dopamine and glutamate control area-restricted search behavior in *Caenorhabditis elegans*. *The Journal of Neuroscience*, **24**(5), pp.1217-1225.
- HOBSON, R. J., J. GENG, A. D. GRAY and R. W. KOMUNIECKI. 2003. SER-7b, a constitutively active Gαs coupled 5-HT7-like receptor expressed in the *Caenorhabditis elegans* M4 pharyngeal motorneuron. *Journal of Neurochemistry*, **87**(1), pp.22-29.
- HOBSON, R. J., V. M. HAPIAK, H. XIAO, K. L. BUEHRER, P. R. KOMUNIECKI and R. W. KOMUNIECKI. 2006. SER-7, a *Caenorhabditis elegans* 5-HT7-like receptor, is essential for the 5-HT stimulation of pharyngeal pumping and egg laying. *Genetics*, **172**(1), pp.159-169.
- HOLDEN-DYE, L., M. JOYNER, V. O'CONNOR and R. J. WALKER. 2013. Nicotinic acetylcholine receptors: A comparison of the nAChRs of *Caenorhabditis elegans* and parasitic nematodes. *Parasitology international*, **62**(6), pp.606-615.

- HOLDEN-DYE, L. and R. WALKER. 2011. Neurobiology of plant parasitic nematodes. *Invertebrate Neuroscience*, **11**(1), pp.9-19.
- HOLTERMAN, M., A. VAN DER WURFF, S. VAN DEN ELSEN, H. VAN MEGEN, T. BONGERS, O. HOLOVACHOV, J. BAKKER and J. HELDER. 2006. Phylum-wide analysis of SSU rDNA reveals deep phylogenetic relationships among nematodes and accelerated evolution toward crown clades. *Molecular Biology and Evolution*, **23**(9), pp.1792-1800.
- HOPE, I. A. 1999. *C. elegans: A Practical Approach: A Practical Approach*. Oxford University Press.
- HOROSZOK, L., V. RAYMOND, D. B. SATTELLE and A. J. WOLSTENHOLME. 2001. GLC-3: a novel fipronil and BIDN-sensitive, but picrotoxinin-insensitive, L-glutamate-gated chloride channel subunit from *Caenorhabditis elegans*. *British Journal of Pharmacology*, **132**(6), pp.1247-1254.
- HU, Y., S.-H. XIAO and R. V. AROIAN. 2009. The new anthelmintic tribendimidine is an L-type (levamisole and pyrantel) nicotinic acetylcholine receptor agonist. *PLoS Negl Trop Dis*, **3**(8), pe499.
- HUANG, G., R. DONG, R. ALLEN, E. L. DAVIS, T. J. BAUM and R. S. HUSSEY. 2006. A root-knot nematode secretory peptide functions as a ligand for a plant transcription factor. *Molecular Plant-Microbe Interactions*, **19**(5), pp.463-470.
- HUANG, G., B. GAO, T. MAIER, R. ALLEN, E. L. DAVIS, T. J. BAUM and R. S. HUSSEY. 2003. A profile of putative parasitism genes expressed in the esophageal gland cells of the root-knot nematode *Meloidogyne incognita*. *Molecular Plant-Microbe Interactions*, **16**(5), pp.376-381.
- HUANG, Y., M. S. WILLIAMSON, A. L. DEVONSHIRE, J. D. WINDASS, S. J. LANSDELL and N. S. MILLAR. 1999. Molecular Characterization and Imidacloprid Selectivity of Nicotinic Acetylcholine Receptor Subunits from the Peach-Potato Aphid *Myzus persicae*. *Journal of Neurochemistry*, **73**(1), pp.380-389.
- HUSSEY, R., C. MIMS and S. WESTCOTT III. 1992. Ultrastructure of root cortical cells parasitized by the ring nematode *Criconemella xenoplax*. *Protoplasma*, **167**(1-2), pp.55-65.
- HUSSON, S. J., E. CLYNEN, G. BAGGERMAN, T. JANSSEN and L. SCHOOFS. 2006. Defective processing of neuropeptide precursors in *Caenorhabditis elegans* lacking proprotein convertase 2 (KPC-2/EGL-3): mutant analysis by mass spectrometry. *Journal of Neurochemistry*, **98**(6), pp.1999-2012.
- INOUE, H., H. NOJIMA and H. OKAYAMA. 1990. High efficiency transformation of *Escherichia coli* with plasmids. *Gene*, **96**(1), pp.23-28.
- JACOB, T. C. and J. M. KAPLAN. 2003. The EGL-21 carboxypeptidase E facilitates acetylcholine release at *Caenorhabditis elegans* neuromuscular junctions. *The Journal of Neuroscience*, **23**(6), pp.2122-2130.
- JAOUANNET, M., L. PERFUS-BARBECH, E. DELEURY, M. MAGLIANO, G. ENGLER, P. VIEIRA, E. G. DANCHIN, M. D. ROCHA, P. COQUILLARD and P. ABAD. 2012. A root-knot nematode-secreted protein is injected into giant cells and targeted to the nuclei. *New Phytologist*, **194**(4), pp.924-931.

- JAYANTHI, L. D., S. APPARSUNDARAM, M. D. MALONE, E. WARD, D. M. MILLER, M. EPPLER and R. D. BLAKELY. 1998. The *Caenorhabditis elegans* gene T23G5.5 encodes an antidepressant- and cocaine-sensitive dopamine transporter. *Molecular Pharmacology*, **54**(4), pp.601-609.
- JEX, A. R., S. LIU, B. LI, N. D. YOUNG, R. S. HALL, Y. LI, L. YANG, N. ZENG, X. XU and Z. XIONG. 2011. *Ascaris suum* draft genome. *Nature*, **479**(7374), pp.529-533.
- JIANG, G., L. ZHUANG, S. MIYAUCHI, K. MIYAKE, Y.-J. FEI and V. GANAPATHY. 2005. A Na⁺/Cl⁻ coupled GABA transporter, gat-1, from *Caenorhabditis elegans* structural and functional features, specific expression in GABA-ergic neurons, and involvement in muscle function. *Journal of Biological Chemistry*, **280**(3), pp.2065-2077.
- JIN, Y., E. JORGENSEN, E. HARTWIEG and H. R. HORVITZ. 1999. The *Caenorhabditis elegans* gene unc-25 encodes glutamic acid decarboxylase and is required for synaptic transmission but not synaptic development. *The Journal of Neuroscience*, **19**(2), pp.539-548.
- JIN, Y., N. TIAN, J. CAO, J. LIANG, Z. YANG and J. LV. 2007. RNA editing and alternative splicing of the insect nAChR subunit alpha6 transcript: evolutionary conservation, divergence and regulation. *BMC evolutionary biology*, **7**(1), p98.
- JOHNSTON, M., P. MCVEIGH, S. MCMASTER, C. FLEMING and A. MAULE. 2010. FMRFamide-like peptides in root knot nematodes and their potential role in nematode physiology. *Journal of helminthology*, **84**(03), pp.253-265.
- JONES, A., P. DAVIS, J. HODGKIN and D. SATTELLE. 2007. The nicotinic acetylcholine receptor gene family of the nematode *Caenorhabditis elegans*: an update on nomenclature. *Invertebrate Neuroscience*, **7**, pp.129 - 131.
- JONES, A. K., V. RAYMOND-DELPECH, S. H. THANY, M. GAUTHIER and D. B. SATTELLE. 2006. The nicotinic acetylcholine receptor gene family of the honey bee, *Apis mellifera*. *Genome research*, **16**(11), pp.1422-1430.
- JONES, A. K. and D. B. SATTELLE. 2004. Functional genomics of the nicotinic acetylcholine receptor gene family of the nematode, *Caenorhabditis elegans*. *Bioessays*, **26**(1), pp.39-49.
- JONES, A. K. and D. B. SATTELLE. 2008. The cys-loop ligand-gated ion channel gene superfamily of the nematode, *Caenorhabditis elegans*. *Invertebrate Neuroscience*, **8**(1), pp.41-47.
- JONES, A. K. and D. B. SATTELLE. 2010. Diversity of insect nicotinic acetylcholine receptor subunits. *Insect nicotinic acetylcholine receptors*. Springer, pp.25-43.
- JONES, J. T., C. FURLANETTO, E. BAKKER, B. BANKS, V. BLOK, Q. CHEN, M. PHILLIPS and A. PRIOR. 2003. Characterization of a chorismate mutase from the potato cyst nematode *Globodera pallida*. *Molecular Plant Pathology*, **4**(1), pp.43-50.
- JONES, J. T., A. HAEGERMAN, E. G. DANCHIN, H. S. GAUR, J. HELDER, M. G. JONES, T. KIKUCHI, R. MANZANILLA-LOPEZ, J. E. PALOMARES-RIUS, W. M. WESEMAEL and R. N. PERRY. 2013. Top 10 plant-parasitic nematodes in molecular plant pathology. *Mol Plant Pathol*, **14**(9), pp.946-61.
- JONES, S. J., D. L. RIDDLE, A. T. POUZYREV, V. E. VELCULESCU, L. HILLIER, S. R. EDDY, S. L. STRICKLIN, D. L. BAILLIE, R. WATERSTON and M. A. MARRA. 2001. Changes in gene

expression associated with developmental arrest and longevity in *Caenorhabditis elegans*. *Genome Res.*, **11**(8), pp.1346-52.

JORGENSEN, E. M. 2005. GABA.

JOSPIN, M., Y. B. QI, T. M. STAWICKI, T. BOULIN, K. R. SCHUSKE, H. R. HORVITZ, J. L. BESSEREAU, E. M. JORGENSEN and Y. S. JIN. 2009. A Neuronal Acetylcholine Receptor Regulates the Balance of Muscle Excitation and Inhibition in *Caenorhabditis elegans*. *Plos Biology*, **7**(12).

KALETTA, T. and M. O. HENGARTNER. 2006. Finding function in novel targets: *C. elegans* as a model organism. *Nature Reviews Drug Discovery*, **5**(5), pp.387-399.

KÄLL, L., A. KROGH and E. L. L. SONNHAMMER. 2007. Advantages of combined transmembrane topology and signal peptide prediction—the Phobius web server. *Nucleic Acids Research*, **35**(Web Server issue), pp.W429-W432.

KAMATH, R. S., A. G. FRASER, Y. DONG, G. POULIN, R. DURBIN, M. GOTTA, A. KANAPIN, N. LE BOT, S. MORENO, M. SOHRMANN, D. P. WELCHMAN, P. ZIPPERLEN and J. AHRINGER. 2003. Systematic functional analysis of the *Caenorhabditis elegans* genome using RNAi. *Nature*, **421**(6920), pp.231-237.

KAMINSKY, R., P. DUCRAY, M. JUNG, R. CLOVER, L. RUFENER, J. BOUVIER, S. S. WEBER, A. WENGER, S. WIELAND-BERGHAUSEN, T. GOEBEL, N. GAUVRY, F. PAUTRAT, T. SKRIPSKY, O. FROELICH, C. KOMOIN-OKA, B. WESTLUND, A. SLUDER and P. MASER. 2008. A new class of anthelmintics effective against drug-resistant nematodes. *Nature*, **452**(7184), pp.176-180.

KAO, P. N., A. J. DWORK, R. R. KALDANY, M. L. SILVER, J. WIDEMAN, S. STEIN and A. KARLIN. 1984. Identification of the alpha subunit half-cystine specifically labeled by an affinity reagent for the acetylcholine receptor binding site. *J Biol Chem*, **259**(19), pp.11662-5.

KAPLAN, R. M. 2004. Drug resistance in nematodes of veterinary importance: a status report. *Trends in Parasitology*, **20**(10), pp.477-481.

KARCZMAREK, A., S. FUDALI, M. LICHOCKA, M. SOBCZAK, W. KUREK, S. JANAKOWSKI, J. ROOSIEN, W. GOLINOWSKI, J. BAKKER and A. GOVERSE. 2008. Expression of two functionally distinct plant endo- β -1, 4-glucanases is essential for the compatible interaction between potato cyst nematode and its hosts. *Molecular Plant-Microbe Interactions*, **21**(6), pp.791-798.

KASS, J., T. C. JACOB, P. KIM and J. M. KAPLAN. 2001. The EGL-3 proprotein convertase regulates mechanosensory responses of *Caenorhabditis elegans*. *The Journal of Neuroscience*, **21**(23), pp.9265-9272.

KATIKI, L. M., J. F. FERREIRA, A. M. ZAJAC, C. MASLER, D. S. LINDSAY, A. C. S. CHAGAS and A. F. AMARANTE. 2011. *Caenorhabditis elegans* as a model to screen plant extracts and compounds as natural anthelmintics for veterinary use. *Veterinary parasitology*, **182**(2), pp.264-268.

KEARN, J., E. LUDLOW, J. DILLON, V. O'CONNOR and L. HOLDEN-DYE. 2014. Fluensulfone is a nematicide with a mode of action distinct from anticholinesterases and macrocyclic lactones. *Pesticide Biochemistry and Physiology*, **109**(0), pp.44-57.

- KERAMIDAS, A., A. J. MOORHOUSE, P. R. SCHOFIELD and P. H. BARRY. 2004. Ligand-gated ion channels: mechanisms underlying ion selectivity. *Progress in biophysics and molecular biology*, **86**(2), pp.161-204.
- KERRY, B., A. BARKER and K. EVANS. 2002. Investigation of potato cyst nematode control. *DEFRA report*.
- KIM, J., D. S. POOLE, L. E. WAGGONER, A. KEMPF, D. S. RAMIREZ, P. A. TRESCHOW and W. R. SCHAFER. 2001a. Genes affecting the activity of nicotinic receptors involved in *Caenorhabditis elegans* egg-laying behavior. *Genetics*, **157**(4), pp.1599-1610.
- KIM, S. K., J. LUND, M. KIRALY, K. DUKE, M. JIANG, J. M. STUART, A. EIZINGER, B. N. WYLIE and G. S. DAVIDSON. 2001b. A gene expression map for *Caenorhabditis elegans*. *Science*, **293**(5537), pp.2087-92.
- KIMBER, M. and C. FLEMING. 2005. Neuromuscular function in plant parasitic nematodes: a target for novel control strategies? *Parasitology*, **131**(S1), pp.S129-S142.
- KIMBER, M. J., C. C. FLEMING, A. J. BLOURSON, D. W. HALTON and A. G. MAULE. 2001. FMRFamide-related peptides in potato cyst nematodes. *Molecular and Biochemical Parasitology*, **116**(2), pp.199-208.
- KOPP, S. R., A. C. KOTZE, J. S. MCCARTHY, R. J. TRAUB and G. T. COLEMAN. 2008. Pyrantel in small animal medicine: 30 years on. *The Veterinary Journal*, **178**(2), pp.177-184.
- KRACUN, S., P. C. HARKNESS, A. J. GIBB and N. S. MILLAR. 2008. Influence of the M3–M4 intracellular domain upon nicotinic acetylcholine receptor assembly, targeting and function. *British Journal of Pharmacology*, **153**(7), pp.1474-1484.
- KROGH, A., B. LARSSON, G. VON HEIJNE and E. L. L. SONNHAMMER. 2001. Predicting transmembrane protein topology with a hidden Markov model: Application to complete genomes. *Journal of Molecular Biology*, **305**(3), pp.567-580.
- KUMAR, S., P. H. SCHIFFER and M. BLAXTER. 2012. 959 Nematode Genomes: a semantic wiki for coordinating sequencing projects. *Nucleic Acids Research*, **40**(D1), pp.D1295-D1300.
- KWA, M. S., J. G. VEENSTRA, M. VAN DIJK and M. H. ROOS. 1995. β -Tubulin Genes from the Parasitic Nematode *Haemonchus contortus* Modulate Drug Resistance in *Caenorhabditis elegans*. *Journal of Molecular Biology*, **246**(4), pp.500-510.
- LAFFAIRE, J.-B., S. JAUBERT, P. ABAD and M.-N. ROSSO. 2003. Molecular cloning and life stage expression pattern of a new acetylcholinesterase gene from the plant-parasitic nematode *Meloidogyne incognita*. *Nematology*, **5**(2), pp.213-217.
- LAING, R., T. KIKUCHI, A. MARTINELLI, I. TSAI, R. BEECH, E. REDMAN, N. HOLROYD, D. BARTLEY, H. BEASLEY, C. BRITTON, D. CURRAN, E. DEVANEY, A. GILABERT, M. HUNT, F. JACKSON, S. JOHNSTON, I. KRYUKOV, K. LI, A. MORRISON, A. REID, N. SARGISON, G. SAUNDERS, J. WASMUTH, A. WOLSTENHOLME, M. BERRIMAN, J. GILLEARD and J. COTTON. 2013. The genome and transcriptome of *Haemonchus contortus*, a key model parasite for drug and vaccine discovery. *Genome Biology*, **14**(8), pR88.
- LAMBSHEAD, P. J. D. and G. BOUCHER. 2003. Marine nematode deep-sea biodiversity - hyperdiverse or hype? *Journal of Biogeography*, **30**(4), pp.475-485.

- LANSDELL, S. J. and N. S. MILLAR. 2000. Cloning and heterologous expression of D α 4, a *Drosophila* neuronal nicotinic acetylcholine receptor subunit: identification of an alternative exon influencing the efficiency of subunit assembly. *Neuropharmacology*, **39**(13), pp.2604-2614.
- LAUGHTON, D. L., G. G. LUNT and A. J. WOLSTENHOLME. 1997. Reporter gene constructs suggest that the *Caenorhabditis elegans* avermectin receptor beta-subunit is expressed solely in the pharynx. *Journal of Experimental Biology*, **200**(10), pp.1509-1514.
- LEE, R. Y. N., E. R. SAWIN, M. CHALFIE, H. R. HORVITZ and L. AVERY. 1999. EAT-4, a homolog of a mammalian sodium-dependent inorganic phosphate cotransporter, is necessary for glutamatergic neurotransmission in *Caenorhabditis elegans*. *Journal of Neuroscience*, **19**(1), pp.159-167.
- LEWIS, J. A., J. S. ELMER, J. SKIMMING, S. MCLAFFERTY, J. FLEMING and T. MCGEE. 1987. Cholinergic receptor mutants of the nematode *Caenorhabditis elegans*. *The Journal of Neuroscience*, **7**(10), pp.3059-3071.
- LEWIS, J. A., C. H. WU, H. BERG and J. H. LEVINE. 1980. The genetics of levamisole resistance in the nematode *Caenorhabditis elegans*. *Genetics*, **95**(4), pp.905-28.
- LEWIS, S. E., S. M. J. SEARLE, N. HARRIS, M. GIBSON, V. IYER, J. RICHTER, C. WIEL, L. BAYRAKTAROGLU, E. BIRNEY, M. A. CROSBY, J. S. KAMINKER, B. B. MATTHEWS, S. E. PROCHNIK, C. D. SMITH, J. L. TUPY, G. M. RUBIN, S. MISRA, C. J. MUNGALL and M. E. CLAMP. 2002. Apollo: a sequence annotation editor. *Genome Biology*, **3**(12), pp.research0082.1-82.14.
- LI, C. 2005. The ever-expanding neuropeptide gene families in the nematode *Caenorhabditis elegans*. *Parasitology*, **131**(Suppl), pp.S109-127.
- LI, S., C. M. ARMSTRONG, N. BERTIN, H. GE, S. MILSTEIN, M. BOXEM, P. O. VIDALAIN, J. D. HAN, A. CHESNEAU, T. HAO, D. S. GOLDBERG, N. LI, M. MARTINEZ, J. F. RUAL, P. LAMESCH, L. XU, M. TEWARI, S. L. WONG, L. V. ZHANG, G. F. BERRIZ, L. JACOTOT, P. VAGLIO, J. REBOUL, T. HIROZANE-KISHIKAWA, Q. LI, H. W. GABEL, A. ELEWA, B. BAUMGARTNER, D. J. ROSE, H. YU, S. BOSAK, R. SEQUERRA, A. FRASER, S. E. MANGO, W. M. SAXTON, S. STROME, S. VAN DEN HEUVEL, F. PIANO, J. VANDENHAUTE, C. SARDET, M. GERSTEIN, L. DOUCETTE-STAMM, K. C. GUNSALES, J. W. HARPER, M. E. CUSICK, F. P. ROTH, D. E. HILL and M. VIDAL. 2004. A map of the interactome network of the metazoan *C. elegans*. *Science*, **303**(5657), pp.540-3.
- LI, X., H. C. MASSEY, T. J. NOLAN, G. A. SCHAD, K. KRAUS, M. SUNDARAM and J. B. LOK. 2006. Successful transgenesis of the parasitic nematode *Strongyloides stercoralis* requires endogenous non-coding control elements. *International Journal for Parasitology*, **36**(6), pp.671-679.
- LILLEY, C. J., H. J. ATKINSON and P. E. URWIN. 2005. Molecular aspects of cyst nematodes. *Molecular Plant Pathology*, **6**(6), pp.577-588.
- LITTLE, P. R., A. HODGE, S. J. MAEDER, N. C. WIRTHERLE, D. R. NICHOLAS, G. G. COX and G. A. CONDER. 2011. Efficacy of a combined oral formulation of derquantel-abamectin against the adult and larval stages of nematodes in sheep, including anthelmintic-resistant strains. *Vet Parasitol*, **181**(2-4), pp.180-93.

- LIU, B., J. K. HIBBARD, P. E. URWIN and H. J. ATKINSON. 2005. The production of synthetic chemodisruptive peptides in planta disrupts the establishment of cyst nematodes. *Plant biotechnology journal*, **3**(5), pp.487-496.
- LO, W. Y., E. J. BOTZOLAKIS, X. TANG and R. L. MACDONALD. 2008. A Conserved Cys-loop Receptor Aspartate Residue in the M3-M4 Cytoplasmic Loop Is Required for GABA(A) Receptor Assembly. *Journal of Biological Chemistry*, **283**(44), pp.29740-29752.
- LUKAS, R. J., J. P. CHANGEUX, N. LE NOVERE, E. X. ALBUQUERQUE, D. J. K. BALFOUR, D. K. BERG, D. BERTRAND, V. A. CHIAPPINELLI, P. B. S. CLARKE, A. C. COLLINS, J. A. DANI, S. R. GRADY, K. J. KELLAR, J. M. LINDSTROM, M. J. MARKS, M. QUIK, P. W. TAYLOR and S. WONNACOTT. 1999. International Union of Pharmacology. XX. Current status of the nomenclature for nicotinic acetylcholine receptors and their subunits. *Pharmacological Reviews*, **51**(2), pp.397-401.
- LYNAGH, T., R. N. BEECH, M. J. LALANDE, K. KELLER, B. A. CROMER, A. J. WOLSTENHOLME and B. LAUBE. 2015. Molecular basis for convergent evolution of glutamate recognition by pentameric ligand-gated ion channels. *Sci. Rep.*, **5**.
- MADURO, M. and D. PILGRIM. 1995. Identification and cloning of *unc-119*, a gene expressed in the *Caenorhabditis elegans* nervous system. *Genetics*, **141**(3), pp.977-88.
- MARTIN, R. J. and A. P. ROBERTSON. 2007. Mode of action of levamisole and pyrantel, anthelmintic resistance, E153 and Q57. *Parasitology*, **134**(Pt 8), pp.1093-104.
- MARTIN, R. J., A. P. ROBERTSON, S. K. BUXTON, R. N. BEECH, C. L. CHARVET and C. NEVEU. 2012. Levamisole receptors: a second awakening. *Trends Parasitol*, **28**(7), pp.289-96.
- MARYON, E. B., R. CORONADO and P. ANDERSON. 1996. *unc-68* encodes a ryanodine receptor involved in regulating *C. elegans* body-wall muscle contraction. *The Journal of cell biology*, **134**(4), pp.885-893.
- MASLER, E. 2007. Responses of *Heterodera glycines* and *Meloidogyne incognita* to exogenously applied neuromodulators. *Journal of helminthology*, **81**(04), pp.421-427.
- MASLER, E. P. 2008. Responses of *Heterodera glycines* and *Meloidogyne incognita* to exogenously applied biogenic amines. *Nematology*, **10**, pp.911-917.
- MCDONALD, P. W., S. L. HARDIE, T. N. JESSEN, L. CARVELLI, D. S. MATTHIES and R. D. BLAKELY. 2007. Vigorous motor activity in *Caenorhabditis elegans* requires efficient clearance of dopamine mediated by synaptic localization of the dopamine transporter DAT-1. *The Journal of Neuroscience*, **27**(51), pp.14216-14227.
- MCINTIRE, S. L., E. JORGENSEN and H. R. HORVITZ. 1993. Genes required for GABA function in *Caenorhabditis elegans*. *Nature*, **364**(6435), pp.334-7.
- MCINTIRE, S. L., R. J. REIMER, K. SCHUSKE, R. H. EDWARDS and E. M. JORGENSEN. 1997. Identification and characterization of the vesicular GABA transporter. *Nature*, **389**(6653), pp.870-876.
- MCKAY, J. P., D. M. RAIZEN, A. GOTTSCHALK, W. R. SCHAFER and L. AVERY. 2004. *eat-2* and *eat-18* are required for nicotinic neurotransmission in the *Caenorhabditis elegans* pharynx. *Genetics*, **166**(1), pp.161-169.

- MCLNTIRE, S. L., E. JORGENSEN, J. KAPLAN and H. R. HORVITZ. 1993. The GABAergic nervous system of *Caenorhabditis elegans*.
- MELAKEBERHAN, H., A. XU, A. KRAVCHENKO, S. MENNAN and E. RIGA. 2006. Potential use of arugula (*Eruca sativa* L.) as a trap crop for *Meloidogyne hapla*. *Nematology*, **8**(5), pp.793-799.
- MELLO, C. and A. FIRE. 1995. DNA transformation. *Methods Cell Biol*, **48**(48), pp.451-482.
- MELLO, C. C., J. M. KRAMER, D. STINCHCOMB and V. AMBROS. 1991. Efficient gene transfer in *C. elegans*: extrachromosomal maintenance and integration of transforming sequences. *The EMBO journal*, **10**(12), p3959.
- MILEDI, R., I. PARKER and K. SUMIKAWA. 1982. Properties of acetylcholine receptors translated by cat muscle mRNA in *Xenopus* oocytes. *The EMBO journal*, **1**(11), p1307.
- MILLAR, N. 2008. RIC-3: a nicotinic acetylcholine receptor chaperone. *British Journal of Pharmacology*, **153**(S1), pp.S177-S183.
- MILLAR, N. S. and C. GOTTI. 2009. Diversity of vertebrate nicotinic acetylcholine receptors. *Neuropharmacology*, **56**(1), pp.237-246.
- MILLS, H., R. WRAGG, V. HAPIAK, M. CASTELLETTO, J. ZAHRATKA, G. HARRIS, P. SUMMERS, A. KORCHNAK, W. LAW and B. BAMBER. 2012. Monoamines and neuropeptides interact to inhibit aversive behaviour in *Caenorhabditis elegans*. *The EMBO journal*, **31**(3), pp.667-678.
- MILNE, I., D. LINDNER, M. BAYER, D. HUSMEIER, G. MCGUIRE, D. F. MARSHALL and F. WRIGHT. 2009. TOPALi v2: a rich graphical interface for evolutionary analyses of multiple alignments on HPC clusters and multi-core desktops. *Bioinformatics*, **25**(1), pp.126-127.
- MINNIS, S. T., P. P. J. HAYDOCK, S. K. IBRAHIM, I. G. GROVE, K. EVANS and M. D. RUSSELL. 2002. Potato cyst nematodes in England and Wales - occurrence and distribution. *Annals of Applied Biology*, **140**(2), pp.187-195.
- MISHINA, M., T. TOBIMATSU, K. IMOTO, K. TANAKA, Y. FUJITA, K. FUKUDA, M. KURASAKI, H. TAKAHASHI, Y. MORIMOTO, T. HIROSE, S. INAYAMA, T. TAKAHASHI, M. KUNO and S. NUMA. 1985. Location of functional regions of acetylcholine-receptor alpha-subunit by site-directed mutagenesis. *Nature*, **313**(6001), pp.364-369.
- MOENS, M., R. N. PERRY and J. L. STARR. 2009. *Meloidogyne* species—a diverse group of novel and important plant parasites. *Root-knot nematodes*, **1**, p483.
- MOERMAN, D. G., G. M. BENIAN, R. J. BARSTEAD, L. A. SCHRIEFER and R. H. WATERSTON. 1988. Identification and intracellular localization of the *unc-22* gene product of *Caenorhabditis elegans*. *Genes & development*, **2**(1), pp.93-105.
- MONGAN, N. P., H. A. BAYLIS, C. ADCOCK, G. R. SMITH, M. S. P. SANSOM and D. B. SATTELLE. 1998. An extensive and diverse gene family of nicotinic acetylcholine receptor alpha subunits in *Caenorhabditis elegans*. *Receptors & Channels*, **6**(3), pp.213-+.
- MONGAN, N. P., A. K. JONES, G. R. SMITH, M. S. P. SANSOM and D. B. SATTELLE. 2002. Novel $\alpha 7$ -like nicotinic acetylcholine receptor subunits in the nematode *Caenorhabditis elegans*. *Protein Science : A Publication of the Protein Society*, **11**(5), pp.1162-1171.

- MULCAHY, B., L. HOLDEN-DYE and V. O'CONNOR. 2013. Pharmacological assays reveal age-related changes in synaptic transmission at the *Caenorhabditis elegans* neuromuscular junction that are modified by reduced insulin signalling. *Journal of Experimental Biology*, **216**(3), pp.492-501.
- NELSON, L. S., M. L. ROSOFF and C. LI. 1998. Disruption of a neuropeptide gene, *flp-1*, causes multiple behavioral defects in *Caenorhabditis elegans*. *Science*, **281**(5383), pp.1686-1690.
- NEVEU, C., C. L. CHARVET, A. FAUVIN, J. CORRET, R. N. BEECH and J. CABARET. 2010. Genetic diversity of levamisole receptor subunits in parasitic nematode species and abbreviated transcripts associated with resistance. *Pharmacogenetics and genomics*, **20**(7), pp.414-425.
- NICOL, J. M., S. J. TURNER, D. COYNE, L. DEN NIJS, S. HOCKLAND and Z. T. MAAFI. 2011. Current nematode threats to world agriculture. *Genomics and molecular genetics of plant-nematode interactions*. Springer, pp.21-43.
- NOBLE, T., J. STIEGLITZ and S. SRINIVASAN. 2013. An integrated serotonin and octopamine neuronal circuit directs the release of an endocrine signal to control *C. elegans* body fat. *Cell metabolism*, **18**(5), pp.672-684.
- OKKEMA, P. G., S. W. HARRISON, V. PLUNGER, A. ARYANA and A. FIRE. 1993. Sequence requirements for myosin gene expression and regulation in *Caenorhabditis elegans*. *Genetics*, **135**(2), p385.
- OKUDA, T., T. HAGA, Y. KANAI, H. ENDOU, T. ISHIHARA and I. KATSURA. 2000. Identification and characterization of the high-affinity choline transporter. *Nature neuroscience*, **3**(2), pp.120-125.
- OPPERMAN, C. H., D. M. BIRD, V. M. WILLIAMSON, D. S. ROKHSAR, M. BURKE, J. COHN, J. CROMER, S. DIENER, J. GAJAN, S. GRAHAM, T. D. HOUFEK, Q. LIU, T. MITROS, J. SCHAFF, R. SCHAFFER, E. SCHOLL, B. R. SOSINSKI, V. P. THOMAS and E. WINDHAM. 2008. Sequence and genetic map of *Meloidogyne hapla*: A compact nematode genome for plant parasitism. *Proceedings of the National Academy of Sciences of the United States of America*, **105**(39), pp.14802-14807.
- PATEL, N., N. HAMAMOUCH, C. LI, T. HEWEZI, R. S. HUSSEY, T. J. BAUM, M. G. MITCHUM and E. L. DAVIS. 2010. A nematode effector protein similar to annexins in host plants. *Journal of Experimental Botany*, **61**(1), pp.235-248.
- PEDERSEN, J. S. 2010. *C. elegans* motility analysis in ImageJ - A practical approach.
- PENG, J. and J. XU. 2011. RaptorX: exploiting structure information for protein alignment by statistical inference. *Proteins*, **79**(Suppl 10), pp.161-171.
- PERRY, R. N. and M. MOENS. 2013. *Plant nematology*. CABI.
- PETERSEN, T. N., S. BRUNAK, G. VON HEIJNE and H. NIELSEN. 2011. SignalP 4.0: discriminating signal peptides from transmembrane regions. *Nature Methods*, **8**(10), pp.785-786.
- PETRASH, H. A., A. PHILBROOK, M. HABURCAK, B. BARBAGALLO and M. M. FRANCIS. 2013. ACR-12 ionotropic acetylcholine receptor complexes regulate inhibitory motor neuron activity in *Caenorhabditis elegans*. *The Journal of Neuroscience*, **33**(13), pp.5524-5532.

- PHILBROOK, A., B. BARBAGALLO and M. M. FRANCIS. 2013. A tale of two receptors: Dual roles for ionotropic acetylcholine receptors in regulating motor neuron excitation and inhibition. *Worm*, **2**(3), pe25765.
- PIOTTE, C., L. ARTHAUD, P. ABAD and M. N. ROSSO. 1999. Molecular cloning of an acetylcholinesterase gene from the plant parasitic nematodes, *Meloidogyne incognita* and *Meloidogyne javanica*. *Molecular and Biochemical Parasitology*, **99**(2), pp.247-256.
- PRAITIS, V., E. CASEY, D. COLLAR and J. AUSTIN. 2001. Creation of low-copy integrated transgenic lines in *Caenorhabditis elegans*. *Genetics*, **157**(3), pp.1217-26.
- QI, Y. B., M. D. PO, P. MAC, T. KAWANO, E. M. JORGENSEN, M. ZHEN and Y. JIN. 2013. Hyperactivation of B-type motor neurons results in aberrant synchrony of the *Caenorhabditis elegans* motor circuit. *The Journal of Neuroscience*, **33**(12), pp.5319-5325.
- QIAN, H., A. P. ROBERTSON, J. A. POWELL-COFFMAN and R. J. MARTIN. 2008. Levamisole resistance resolved at the single-channel level in *Caenorhabditis elegans*. *Faseb Journal*, **22**(9), pp.3247-3254.
- QIAN, W. and J. ZHANG. 2008. Evolutionary dynamics of nematode operons: easy come, slow go. *Genome research*, **18**(3), pp.412-421.
- QIN, L., G. SMANT, J. STOKKERMANS, J. BAKKER, A. SCHOTS and J. HELDER. 1998. Cloning of a trans-spliced glyceraldehyde-3-phosphate-dehydrogenase gene from the potato cyst nematode *Globodera rostochiensis* and expression of its putative promoter region in *Caenorhabditis elegans*. *Mol Biochem Parasitol*, **96**(1-2), pp.59-67.
- RAMBAUT, A. 2009. *FigTree v.1.3.1* [online]. [Accessed]. Available from: <http://tree.bio.ed.ac.uk/software/figtree/>.
- RAND, J. 2006. Acetylcholine. *WormBook: the online review of C. elegans biology*, pp.1-21.
- RAND, J. B. 1989. Genetic analysis of the cha-1-unc-17 gene complex in *Caenorhabditis*. *Genetics*, **122**(1), pp.73-80.
- RAND, J. B. and R. L. RUSSELL. 1985. Properties and partial purification of choline acetyltransferase from the nematode *Caenorhabditis elegans*. *J Neurochem*, **44**(1), pp.189-200.
- RANGANATHAN, R., E. R. SAWIN, C. TRENT and H. R. HORVITZ. 2001. Mutations in the *Caenorhabditis elegans* serotonin reuptake transporter MOD-5 reveal serotonin-independent and -independent activities of fluoxetine. *Journal of Neuroscience*, **21**(16), pp.5871-5884.
- RAPTI, G., J. RICHMOND and J. L. BESSEREAU. 2011. A single immunoglobulin-domain protein required for clustering acetylcholine receptors in *C. elegans*. *The EMBO journal*, **30**(4), pp.706-718.
- RASMANN, S., J. G. ALI, J. HELDER and W. H. VAN DER PUTTEN. 2012. Ecology and evolution of soil nematode chemotaxis. *Journal of chemical ecology*, **38**(6), pp.615-628.
- RAYES, D., M. J. DE ROSA, M. BARTOS and C. BOUZAT. 2004. Molecular basis of the differential sensitivity of nematode and mammalian muscle to the anthelmintic agent levamisole. *J Biol Chem*, **279**(35), pp.36372-81.

- RAYES, D., M. J. DE ROSA, S. M. SINE and C. BOUZAT. 2009. Number and locations of agonist binding sites required to activate homomeric Cys-loop receptors. *The Journal of Neuroscience*, **29**(18), pp.6022-6032.
- RAYMOND, V., N. MONGAN and D. SATTELLE. 2000. Anthelmintic actions on homomer-forming nicotinic acetylcholine receptor subunits: chicken α 7 and ACR-16 from the nematode *Caenorhabditis elegans*. *Neuroscience*, **101**(3), pp.785-791.
- RAYMOND, V. and D. B. SATTELLE. 2002. Novel animal-health drug targets from ligand-gated chloride channels. *Nature Reviews Drug Discovery*, **1**(6), pp.427-436.
- REX, E. and R. W. KOMUNIECKI. 2002. Characterization of a tyramine receptor from *Caenorhabditis elegans*. *Journal of Neurochemistry*, **82**(6), pp.1352-1359.
- REYNOLDS, A. M., T. K. DUTTA, R. H. CURTIS, S. J. POWERS, H. S. GAUR and B. R. KERRY. 2011. Chemotaxis can take plant-parasitic nematodes to the source of a chemo-attractant via the shortest possible routes. *Journal of The Royal Society Interface*, **8**(57), pp.568-577.
- RICHMOND, J. E. and E. M. JORGENSEN. 1999. One GABA and two acetylcholine receptors function at the *C. elegans* neuromuscular junction. *Nature neuroscience*, **2**(9), pp.791-797.
- RIGA, E., R. PERRY, J. BARRETT and M. JOHNSTON. 1996. Electrophysiological responses of males of the potato cyst nematodes, *Globodera rostochiensis* and *G. pallida*, to their sex pheromones. *Parasitology*, **112**(02), pp.239-246.
- RISTAINO, J. B. and W. THOMAS. 1997. Agriculture, methyl bromide, and the ozone hole: can we fill the gaps? *Plant Disease*, **81**(9), pp.964-977.
- ROBERTS, B., A. ANTONOPOULOS, S. M. HASLAM, A. J. DICKER, T. N. MCNEILLY, S. L. JOHNSTON, A. DELL, D. P. KNOX and C. BRITTON. 2013. Novel expression of *Haemonchus contortus* vaccine candidate aminopeptidase H11 using the free-living nematode *Caenorhabditis elegans*. *Veterinary research*, **44**(1), pp.1-15.
- ROBERTSON, A. P., H. E. BJORN and R. J. MARTIN. 1999. Resistance to levamisole resolved at the single-channel level. *The FASEB journal*, **13**(6), pp.749-760.
- ROBINSON, A., R. INSERRA, E. CASWELL-CHEN, N. VOVLAS and A. TROCCOLI. 1997. *Rotylenchulus* species: Identification, distribution, host ranges, and crop plant resistance. *Nematropica*, **27**(2), pp.127-180.
- RÖDELSPERGER, C., A. STREIT and R. J. SOMMER. 2013. Structure, Function and Evolution of The Nematode Genome. *eLS*.
- ROMINE, N. M., R. J. MARTIN and J. K. BEETHAM. 2013. Computational cloning of drug target genes of a parasitic nematode, *Oesophagostomum dentatum*. *BMC genetics*, **14**(1), p55.
- ROMINE, N. M., R. J. MARTIN and J. K. BEETHAM. 2014. Transcriptomic evaluation of the nicotinic acetylcholine receptor pathway in levamisole-resistant and-sensitive *Oesophagostomum dentatum*. *Molecular and Biochemical Parasitology*, **193**(1), pp.66-70.

- RUFENER, L., R. BAUR, R. KAMINSKY, P. MÄSER and E. SIGEL. 2010. Monepantel allosterically activates DEG-3/DES-2 channels of the gastrointestinal nematode *Haemonchus contortus*. *Molecular Pharmacology*, **78**(5), pp.895-902.
- RUFENER, L., N. BEDONI, R. BAUR, S. REY, D. A. GLAUSER, J. BOUVIER, R. BEECH, E. SIGEL and A. PUOTI. 2013. *acr-23* Encodes a Monepantel-Sensitive Channel in *Caenorhabditis elegans*. *Plos Pathogens*, **9**(8).
- SAGER, H., B. HOSKING, B. BAPST, P. STEIN, K. VANHOFF and R. KAMINSKY. 2009. Efficacy of the amino-acetonitrile derivative, monepantel, against experimental and natural adult stage gastro-intestinal nematode infections in sheep. *Veterinary parasitology*, **159**(1), pp.49-54.
- SANGER, F., S. NICKLEN and A. R. COULSON. 1977. DNA sequencing with chain-terminating inhibitors. *Proc Natl Acad Sci U S A*, **74**(12), pp.5463-7.
- SARAI, R. S., S. R. KOPP, G. T. COLEMAN and A. C. KOTZE. 2013. Acetylcholine receptor subunit and P-glycoprotein transcription patterns in levamisole-susceptible and -resistant *Haemonchus contortus*. *International Journal for Parasitology: Drugs and Drug Resistance*, **3**, pp.51-58.
- SASSER, J. 1980. Root-Knot Nematodes: A Globe. *Plant Disease*, **64**(1), p37.
- SAUR, T., S. E. DEMARCO, A. ORTIZ, G. R. SLIWOSKI, L. HAO, X. WANG, B. M. COHEN and E. A. BUTTNER. 2013. A Genome-Wide RNAi Screen in *Caenorhabditis elegans* Identifies the Nicotinic Acetylcholine Receptor Subunit ACR-7 as an Antipsychotic Drug Target. *Plos Genetics*, **9**(2).
- SAWIN, E. R., R. RANGANATHAN and H. R. HORVITZ. 2000. *C. elegans* locomotory rate is modulated by the environment through a dopaminergic pathway and by experience through a serotonergic pathway. *Neuron*, **26**(3), pp.619-631.
- SCHUSKE, K., A. A. BEG and E. M. JORGENSEN. 2004. The GABA nervous system in *C. elegans*. *Trends in neurosciences*, **27**(7), pp.407-414.
- SEEBURG, P. H. 2002. A-to-I editing: new and old sites, functions and speculations. *Neuron*, **35**(1), pp.17-20.
- SELLINGS, L., S. PEREIRA, C. QIAN, T. DIXON-MCDougall, C. NOWAK, B. ZHAO, R. F. TYNDALE and D. KOORY. 2013. Nicotine-motivated behavior in *Caenorhabditis elegans* requires the nicotinic acetylcholine receptor subunits *acr-5* and *acr-15*. *European Journal of Neuroscience*, **37**(5), pp.743-756.
- SHARPE, M. J. and H. J. ATKINSON. 1980. Improved visualization of dopaminergic-neurons in nematodes using the glyoxylic-acid fluorescence method. *Journal of Zoology*, **190**(Feb), pp.273-284.
- SHIMOMURA, M., H. SATOH, M. YOKOTA, M. IHARA, K. MATSUDA and D. B. SATTELLE. 2005. Insect-vertebrate chimeric nicotinic acetylcholine receptors identify a region, loop B to the N-terminus of the *Drosophila* Da2 subunit, which contributes to neonicotinoid sensitivity. *Neuroscience letters*, **385**(2), pp.168-172.
- SIEVERS, F., A. WILM, D. DINEEN, T. J. GIBSON, K. KARPLUS, W. LI, R. LOPEZ, H. MCWILLIAM, M. REMMERT, J. SÖDING, J. D. THOMPSON and D. G. HIGGINS. 2011. Fast, scalable

generation of high-quality protein multiple sequence alignments using Clustal Omega. *Molecular systems biology*, 539(7).

- SINE, S. M., K. OHNO, C. BOUZAT, A. AUERBACH, M. MILONE, J. N. PRUITT and A. G. ENGEL. 1995. Mutation of the acetylcholine-receptor alpha-subunit causes a slow-channel myasthenic syndrome by enhancing agonist binding-affinity. *Neuron*, **15**(1), pp.229-239.
- SINE, S. M., P. QUIRAM, F. PAPANIKOLAOU, H. J. KREIENKAMP and P. TAYLOR. 1994. Conserved tyrosines in the alpha-subunit of the nicotinic acetylcholine-receptor stabilize quaternary ammonium groups of agonists and curariform antagonists. *Journal of Biological Chemistry*, **269**(12), pp.8808-8816.
- SMIT, A. B., N. I. SYED, D. SCHAAP, J. VAN MINNEN, J. KLUMPERMAN, K. S. KITS, H. LODDER, R. C. VAN DER SCHORS, R. VAN ELK, B. SORGEDRAGER, K. BREJC, T. K. SIXMA and W. P. GERAERTS. 2001. A glia-derived acetylcholine-binding protein that modulates synaptic transmission. *Nature*, **411**(6835), pp.261-8.
- SOBCZAK, M., A. AVROVA, J. JUPOWICZ, M. S. PHILLIPS, K. ERNST and A. KUMAR. 2005. Characterization of susceptibility and resistance responses to potato cyst nematode (*Globodera* spp.) infection of tomato lines in the absence and presence of the broad-spectrum nematode resistance *Hero* gene. *Molecular Plant-Microbe Interactions*, **18**(2), pp.158-168.
- SOMMER, R. J. and A. STREIT. 2011. Comparative genetics and genomics of nematodes: genome structure, development, and lifestyle. *Annual review of genetics*, **45**, pp.1-20.
- SQUIRE, M. D., C. TORNOE, H. A. BAYLIS, J. T. FLEMING, E. A. BARNARD and D. B. SATTELLE. 1995. Molecular cloning and functional co-expression of a *Caenorhabditis elegans* nicotinic acetylcholine receptor subunit (*acr-2*). *Receptors Channels*, **3**(2), pp.107-15.
- STEWART, G. R., R. N. PERRY and D. J. WRIGHT. 2001. Occurrence of dopamine in *Panagrellus redivivus* and *Meloidogyne incognita*. *Nematology*, **3**, pp.843-848.
- STINCHCOMB, D., J. SHAW, S. H. CARR and D. HIRSH. 1985. Extrachromosomal DNA transformation of *Caenorhabditis elegans*. *Molecular and cellular biology*, **5**(12), pp.3484-3496.
- STOREY, R. M. J. 1984. The relationship between neutral lipid reserves and infectivity for hatched and dormant juveniles of *Globodera* spp. *Annals of Applied Biology*, **104**(3), pp.511-520.
- SUO, S., Y. KIMURA and H. H. VAN TOL. 2006. Starvation induces cAMP response element-binding protein-dependent gene expression through octopamine-Gq Signaling in *Caenorhabditis elegans*. *The Journal of Neuroscience*, **26**(40), pp.10082-10090.
- SUO, S., N. SASAGAWA and S. ISHIURA. 2002. Identification of a dopamine receptor from *Caenorhabditis elegans*. *Neuroscience letters*, **319**(1), pp.13-16.
- SUO, S., N. SASAGAWA and S. ISHIURA. 2003. Cloning and characterization of a *Caenorhabditis elegans* D2-like dopamine receptor. *Journal of Neurochemistry*, **86**(4), pp.869-878.
- SZE, J. Y., M. VICTOR, C. LOER, Y. SHI and G. RUVKUN. 2000. Food and metabolic signalling defects in a *Caenorhabditis elegans* serotonin-synthesis mutant. *Nature*, **403**(6769), pp.560-564.

- TAMURA, K., G. STECHER, D. PETERSON, A. FILIPSKI and S. KUMAR. 2013. MEGA6: molecular evolutionary genetics analysis version 6.0. *Molecular Biology and Evolution*, **30**(12), pp.2725-2729.
- TASNEEM, A., L. M. IYER, E. JAKOBSSON and L. ARAVIND. 2004. Identification of the prokaryotic ligand-gated ion channels and their implications for the mechanisms and origins of animal Cys-loop ion channels. *Genome Biology*, **6**(1), pR4.
- TAYLOR, C. M., Q. WANG, B. A. ROSA, S. C.-C. HUANG, K. POWELL, T. SCHIDL, E. J. PEARCE, S. ABUBUCKER and M. MITREVA. 2013. Discovery of anthelmintic drug targets and drugs using chokepoints in nematode metabolic pathways. *Plos Pathogens*, **9**(8), pe1003505.
- THACKER, C. and A. M. ROSE. 2000. A look at the *Caenorhabditis elegans* Kex2/Subtilisin-like proprotein convertase family. *Bioessays*, **22**(6), pp.545-553.
- THANY, S. H., G. LENAERS, V. RAYMOND-DELPECH, D. B. SATTELLE and B. LAPIED. 2007. Exploring the pharmacological properties of insect nicotinic acetylcholine receptors. *Trends in pharmacological sciences*, **28**(1), pp.14-22.
- THOMPSON, A. J., H. A. LESTER and S. C. R. LUMMIS. 2010. The structural basis of function in Cys-loop receptors. *Quarterly Reviews of Biophysics*, **43**(4), pp.449-499.
- THORPE, P., S. MANTELIN, P. J. COCK, V. C. BLOK, M. C. COKE, S. EVES-VAN DEN AKKER, E. GUZEEVA, C. J. LILLEY, G. SMANT and A. J. REID. 2014. Genomic characterisation of the effector complement of the potato cyst nematode *Globodera pallida*. *BMC genomics*, **15**(1), p923.
- TOMASELLI, G. F., J. T. MC LAUGHLIN, M. E. JURMAN, E. HAWROT and G. YELLEN. 1991. Mutations affecting agonist sensitivity of the nicotinic acetylcholine receptor. *Biophysical Journal*, **60**(3), pp.721-727.
- TONKIN, L. A., L. SACCOMANNO, D. P. MORSE, T. BRODIGAN, M. KRAUSE and B. L. BASS. 2002. RNA editing by ADARs is important for normal behavior in *Caenorhabditis elegans*. *The EMBO journal*, **21**(22), pp.6025-6035.
- TOROUTINE, D., R. M. FOX, S. E. VON STETINA, A. BURDINA, D. M. MILLER, 3RD and J. E. RICHMOND. 2005. *acr-16* encodes an essential subunit of the levamisole-resistant nicotinic receptor at the *Caenorhabditis elegans* neuromuscular junction. *J Biol Chem*, **280**(29), pp.27013-21.
- TOWERS, P. R., B. EDWARDS, J. E. RICHMOND and D. B. SATTELLE. 2005. The *Caenorhabditis elegans* *lev-8* gene encodes a novel type of nicotinic acetylcholine receptor alpha subunit. *Journal of Neurochemistry*, **93**(1), pp.1-9.
- TREININ, M. and M. CHALFIE. 1995. A mutated acetylcholine receptor subunit causes neuronal degeneration in *C. elegans*. *Neuron*, **14**(4), pp.871-877.
- TREININ, M., B. GILLO, L. LIEBMAN and M. CHALFIE. 1998. Two functionally dependent acetylcholine subunits are encoded in a single *Caenorhabditis elegans* operon. *Proc Natl Acad Sci U S A*, **95**(26), pp.15492-5.
- TRENT, C., N. TSUNG and H. R. HORVITZ. 1983. Egg-laying defective mutants of the nematode *Caenorhabditis elegans*. *Genetics*, **104**(4), pp.619-647.

- TRIPATHI, L., A. BABIRYE, H. RODERICK, J. N. TRIPATHI, C. CHANGA, P. E. URWIN, W. K. TUSHEMEREIRWE, D. COYNE and H. J. ATKINSON. 2015. Field resistance of transgenic plantain to nematodes has potential for future African food security. *Scientific Reports*, **5**(8127)
- TRUDGILL, D. 1967. The effect of environment on sex determination in *Heterodera rostochiensis*. *Nematologica*, **13**(2), pp.263-272.
- TRUDGILL, D. 1997. Parthenogenetic root-knot nematodes (*Meloidogyne* spp.); how can these biotrophic endoparasites have such an enormous host range? *Plant Pathology*, **46**(1), pp.26-32.
- TRUDGILL, D., M. ELLIOTT, K. EVANS and M. PHILLIPS. 2003. The white potato cyst nematode (*Globodera pallida*)—a critical analysis of the threat in Britain. *Annals of Applied Biology*, **143**(1), pp.73-80.
- TURNER, S. J. and S. A. SUBBOTIN. 2013. Cyst Nematodes. *Plant nematology Ed2*, pp.109-143.
- UNIPROT, C. 2015. UniProt: a hub for protein information. *Nucleic Acids Research*, **43**(Database issue), pp.D204-12.
- URWIN, P. E., C. J. LILLEY and H. J. ATKINSON. 2002. Ingestion of double-stranded RNA by pre-parasitic juvenile cyst nematodes leads to RNA interference. *Molecular Plant-Microbe Interactions*, **15**(8), pp.747-752.
- VAN MEGEN, H., S. VAN DEN ELSEN, M. HOLTERMAN, G. KARSSSEN, P. MOOYMAN, T. BONGERS, O. HOLOVACHOV, J. BAKKER and J. HELDER. 2009. A phylogenetic tree of nematodes based on about 1200 full-length small subunit ribosomal DNA sequences. *Nematology*, **11**(6), pp.927-950.
- VASHLISHAN, A. B., J. M. MADISON, M. DYBBS, J. BAI, D. SIEBURTH, Q. CH'NG, M. TAVAZOIE and J. M. KAPLAN. 2008. An RNAi screen identifies genes that regulate GABA synapses. *Neuron*, **58**(3), pp.346-361.
- VOS, P., G. SIMONS, T. JESSE, J. WIJBRANDI, L. HEINEN, R. HOGERS, A. FRIJTERS, J. GROENENDIJK, P. DIERGAARDE and M. REIJANS. 1998. The tomato *Mi-1* gene confers resistance to both root-knot nematodes and potato aphids. *Nature Biotechnology*, **16**(13), pp.1365-1369.
- WAGGONER, L. E., K. A. DICKINSON, D. S. POOLE, Y. TABUSE, J. MIWA and W. R. SCHAFER. 2000. Long-term nicotine adaptation in *Caenorhabditis elegans* involves PKC-dependent changes in nicotinic receptor abundance. *The Journal of Neuroscience*, **20**(23), pp.8802-8811.
- WANG, C., G. BRUENING and V. M. WILLIAMSON. 2009. Determination of preferred pH for root-knot nematode aggregation using pluronic F-127 gel. *Journal of chemical ecology*, **35**(10), pp.1242-1251.
- WANG, H. L., F. GAO, N. BREN and S. M. SINE. 2003. Curariform antagonists bind in different orientations to the nicotinic receptor ligand binding domain. *J Biol Chem*, **278**(34), pp.32284-91.
- WARD, S. and J. S. CARREL. 1979. Fertilization and sperm competition in the nematode *Caenorhabditis elegans*. *Developmental biology*, **73**(2), pp.304-321.

- WATERHOUSE, A. M., J. B. PROCTER, D. M. A. MARTIN, M. CLAMP and G. J. BARTON. 2009. Jalview Version 2—a multiple sequence alignment editor and analysis workbench. *Bioinformatics*, **25**(9), pp.1189-1191.
- WESEMAEL, W. M., R. N. PERRY and M. MOENS. 2006. The influence of root diffusate and host age on hatching of the root-knot nematodes, *Meloidogyne chitwoodi* and *M. fallax*. *Nematology*, **8**(6), pp.895-902.
- WHARTON, D. A. and W. BLOCK. 1993. Freezing tolerance in some antarctic nematodes. *Functional Ecology*, **7**(5), pp.578-584.
- WHITE, J., E. SOUTHGATE, J. THOMSON and S. BRENNER. 1986. The structure of the nervous system of the nematode *Caenorhabditis elegans*: the mind of a worm. *Phil. Trans. R. Soc. Lond*, **314**, pp.1-340.
- WHITEHORN, P. R., S. O'CONNOR, F. L. WACKERS and D. GOULSON. 2012. Neonicotinoid pesticide reduces bumble bee colony growth and queen production. *Science*, **336**(6079), pp.351-352.
- WIECZOREK, K., B. GOLECKI, L. GERDES, P. HEINEN, D. SZAKASITS, D. M. DURACHKO, D. J. COSGROVE, D. P. KREIL, P. S. PUZIO and H. BOHLMANN. 2006. Expansins are involved in the formation of nematode-induced syncytia in roots of *Arabidopsis thaliana*. *The Plant Journal*, **48**(1), pp.98-112.
- WILLIAMS, B. D. and R. H. WATERSTON. 1994. Genes critical for muscle development and function in *Caenorhabditis elegans* identified through lethal mutations. *The Journal of cell biology*, **124**(4), pp.475-490.
- WILLIAMSON, S. M., A. P. ROBERTSON, L. BROWN, T. WILLIAMS, D. J. WOODS, R. J. MARTIN, D. B. SATTELLE and A. J. WOLSTENHOLME. 2009. The Nicotinic Acetylcholine Receptors of the Parasitic Nematode *Ascaris suum*: Formation of Two Distinct Drug Targets by Varying the Relative Expression Levels of Two Subunits. *Plos Pathogens*, **5**(7).
- WILLIAMSON, S. M., T. K. WALSH and A. J. WOLSTENHOLME. 2007. The cys-loop ligand-gated ion channel gene family of *Brugia malayi* and *Trichinella spiralis*: a comparison with *Caenorhabditis elegans*. *Invertebrate Neuroscience*, **7**(4), pp.219-226.
- WINTER, M., M. MCPHERSON and H. ATKINSON. 2002. Neuronal uptake of pesticides disrupts chemosensory cells of nematodes. *Parasitology*, **125**(06), pp.561-565.
- WORMBASE. 2009. release WS204.
- WRIGHT, D., A. BIRTLE and I. ROBERTS. 1984. Triphasic locomotor response of a plant-parasitic nematode to avermectin: inhibition by the GABA antagonists bicuculline and picrotoxin. *Parasitology*, **88**(02), pp.375-382.
- WYSS, U. and F. GRUNDLER. 1992. Feeding behavior of sedentary plant parasitic nematodes. *Netherlands Journal of Plant Pathology*, **98**(2), pp.165-173.
- WYSS, U., F. M. GRUNDLER and A. MUNCH. 1992. The parasitic behaviour of second-stage juveniles of *Meloidogyne incognita* in roots of *Arabidopsis thaliana*. *Nematologica*, **38**(1), pp.98-111.
- WYSS, U. and U. ZUNKE. 1986. Observations on the behaviour of second stage juveniles of *Heterodera schachtii* inside host roots. *Revue Nematol*, **9**(2), pp.153-165.

- YASSIN, L., B. GILLO, T. KAHAN, S. HALEVI, M. ESHEL and M. TREININ. 2001. Characterization of the *deg-3/des-2* receptor: a nicotinic acetylcholine receptor that mutates to cause neuronal degeneration. *Molecular and Cellular Neuroscience*, **17**(3), pp.589-599.
- YATES, D. M., V. PORTILLO and A. J. WOLSTENHOLME. 2003. The avermectin receptors of *Haemonchus contortus* and *Caenorhabditis elegans*. *International Journal for Parasitology*, **33**(11), pp.1183-1193.